Facing Hypoxia and Ischemia - Cell-Specific Signaling and Metabolism at the Blood-Brain Barrier

Dissertation

zur

Erlangung der naturwissenschaftlichen Doktorwürde
(Dr. sc. nat.)

vorgelegt der

Mathematisch-naturwissenschaftlichen Fakultät

der

Universität Zürich

von

Sabrina Engelhardt

aus

Deutschland

Promotionskomitee

Prof. Dr. Max Gassmann (Vorsitz der Dissertation)
Dr. Omolara O. Ogunshola (Leitung der Dissertation)
Prof. Dr. François Verrey
Prof. Dr. Pierre-Olivier Couraud
Dr. Ignacio A. Romero (Externer Gutachter)

Zürich 2014

ZUSAMMENFASSUNG

Obwohl es nur circa 1-2% der Köpermasse ausmacht, verbraucht das Gehirn im Ruhezustand 20% des gesamten Sauerstoffes und 25% aller Glucose im Körper. Dieser außerordentliche Nährstoffverbrauch erfordert eine ständige Wiederauffüllung der Nährstoffreserven und eine strikte Kontrolle der Homöostase im Gehirn, was in erster Linie durch die Zellen der Bluthirnschranke (BHS) gewährleistet wird. Die BHS befindet sich auf der Ebene der Kapillaren und postkapillaren Venolen und setzt sich aus Endothelzellen, benachbarten perivaskulären Perizyten und Astrozyten sowie einer Basallamina zusammen. Aufgrund seines hohen Nährstoffverbrauches reagiert das Gehirn besonders empfindlich auf Hypoxie und Ischämie, welche sich durch eine unzureichende Sauerstoffversorgung beziehungsweise eine kombinierte Sauerstoff- und Nährstoffknappheit auszeichnen. Sowohl Hypoxie als auch Ischämie beeinträchtigen die Integrität der BHS und sind eng mit verschiedenen neurologischen Erkrankungen wie Schlaganfall, Alzheimer und Multipler Sklerose verknüpft. Ziel dieser Arbeit war es die molekularen Zusammenhänge einer Dysfunktion der BHS in Bezug auf Hypoxie und Ischämie besser zu verstehen, wobei hier vor allem die individuellen Reaktionen der verschiedenen Zelltypen im Vordergrund standen.

Der Transkriptionsfaktor HIF-1 (Hypoxie induzierbarer Faktor 1) ist der zentrale Regulator Hypoxie vermittelter Antworten, seine Rolle bezüglich der Beeinträchtigung der BHS unter diesen Bedingungen ist allerdings weitgehend unklar. Aus diesem Grund haben wir die direkte Auswirkung von HIF-1 auf die Integrität der BHS untersucht. Als *in vitro* Modell wurde die Ratten Endothelzelllinie RBE4 auf Transwellplatten kultiviert. Unsere Ergebnisse zeigten, dass die Stabilisierung von HIF-1 unter normalen Sauerstoffbedingungen eine vergleichbare Beeinträchtigung der BHS zur Folge hat wie unter Hypoxie. Wenn hingegen die Aktivität von HIF-1 unter Hypoxie gehemmt wurde, hatte dies einen protektiven Effekt auf die Integrität der BHS. Interessanterweise wurde der negative Effekt des HIF-1 Signalweges hauptsächlich durch eine Zerstörung der Schlussleiste (tight junctions) vermittelt, insbesondere einer Verlagerung der assoziierten Proteine weg von der Zellmembran, wobei eine Verminderung der Proteinexpression nur eine untergeordnete Rolle spielte. Zusätzlich sprechen unsere Ergebnisse dafür, dass die erhöhte Phosphorylierung von Tyrosinresten von Occludin und in geringerem Maße auch Claudin-5 durch HIF-1 und wahrscheinlich auch VEGF (Vascular

endothelial growth factor) verursacht wird und zu der beobachteten Dysfunktion der BHS führt.

Unter hypoxischen und ischämischen Stressbedingungen spielen die generelle Toleranz der einzelnen Zelltypen sowie ihre spezifischen Antworten eine entscheidende Rolle für die Regulierung der BHS. In einer früheren Studie konnte unsere Gruppe die Bedeutsamkeit der Astrozyten und Perizyten für die Aufrechterhaltung der BHS unter mildem (1% O_2) sowie erheblichem (0.1%O_2) Sauerstoffentzug aufzeigen. Abhängig vom Schweregrad der Hypoxie beeinflussten die Zelltypen die BHS in unterschiedlicher Weise - Perizyten waren in der Lage die BHS unter akuter Hypoxie aufrecht zu erhalten was Astrozyten nicht gelang. Diese Ergebnisse legen nahe, dass die individuellen Antworten der BHS Zellen eine zentrale Rolle in ihrer Regulierung erfüllen. Aus diesem Grund hat sich der zweite Teil dieser Arbeit mit einer vergleichenden Studie befasst, in der die Hypoxie und Ischämie vermittelten Antworten von RBE4 Zellen, Perizyten und Astrozyten charakterisiert wurden. Indem generelle zelluläre Parameter wie Expression von Hypoxie gesteuerten Genen und Proteinen, die Dynamik des Zytoskeletts, Zellteilung und Zellviabilität untersucht wurden, konnten Endothelzellen klar als derjenige Zelltyp charakterisiert werden, der am stärksten reagierte und am sensibelsten war; Astrozyten hingegen waren am tolerantesten. Endothelzellen zeigten schon bei Hypoxie eine hohe Verletzlichkeit, wobei Astrozyten und Perizyten hier kaum reagierten und eine vergleichbare Toleranz zeigten. Ischämie hingegen tolerierten Astrozyten interessanterweise sehr viel besser als Perizyten. Diese Unterschiede in Bezug auf die Sensitivität sowie Genexpression untermauern die besondere Relevanz der resistenten perivaskulären Zellen für die Unterstützung der Endothelzellenfunktion. Die Tatsache, dass im Generellen die zellspezifischen Antworten sehr unterschiedlich sind, wirft die Frage auf, wie Hypoxie-regulierte Genexpression gesteuert wird.

Mit Hilfe von Flüssigchromatographie gekoppelter Massenspektrometrie haben wir die Frage weiterverfolgt, ob eine differentielle Aktivität metabolischer Stoffwechselwege die unterschiedliche Toleranz von Endothelzellen und Astrozyten gegenüber Hypoxie und Ischämie erklären kann. In der Tat haben wir tiefgreifende Unterschiede im basalen sowie ischämischen Stoffwechsel zwischen Astrozyten und Endothelzellen beobachtet, welche sehr wahrscheinlich entscheidend dazu beitragen in Zeiten von Nährstoffmangel zu überleben. Wir

konnten den Schluss ziehen, dass der basale Stoffwechsel von Astrozyten darauf programmiert ist Metaboliten anzureichern, die unter Stressbedingungen helfen den Energie- und Redoxhaushalt aufrecht zu erhalten, wie zum Beispiel Glykogen, Phosphokreatin oder Glutathion. Endothelzellen hingegen schienen diese Stoffe nicht zu speichern. Die Folgen dieser Unterschiede konnten wir vor allem unter ischämischen Bedingungen im Kohlenhydratstoffwechsel beobachten. In Astrozyten war dieser Stoffwechselweg nach 24 Stunden nur geringfügig beeinträchtigt, wohingegen in Endothelzellen sehr viele Metaboliten stark erniedrigt waren, was nahelegt, dass sie bereits die meisten ihrer Zuckerreserven verbraucht haben. Solchen zellspezifischen und charakteristischen Anpassungen wie diesen liegen komplexe Antworten zugrunde, die maßgeblich zur Regulierung der BHS Stabilität beitragen. Zusammenfassend beleuchtet diese Arbeit die vielschichtigen Reaktionen und unterschiedliche Toleranz der verschieden BHS Zellen in Bezug auf hypoxische Stresssituationen. Aufgrund der komplexen Struktur der BHS beleuchtet diese Arbeit, dass der Erkenntnisgewinn in Bezug auf die individuellen zellulären Antworten uns eine zentrale Grundlage bietet, um die Regulation der BHS unter Normalsituationen sowie Stressbedingungen besser zu verstehen.

SUMMARY

Of the whole body expenditure the brain consumes about 20% of oxygen (O_2) and 25% of glucose although it accounts for only 1-2% of the total body mass. This extraordinary nutrient demand requires continuous replenishment and very well coordinated regulation of brain homeostasis - that is primarily mediated by the cells of the blood-brain barrier (BBB). The BBB is located at the level of brain capillaries and postcapillary venules being composed of endothelial cells, surrounded by perivascular pericytes and astrocytes as well as basement membranes. Due to its high nutrient demand, the brain is particularly vulnerable to insults like hypoxia or ischemia that are characterized by insufficient O_2 supply or combined O_2 and nutrient shortage, respectively. Hypoxia and ischemia both disturb BBB integrity, and are closely associated with various neurological disorders such as stroke, Alzheimer's disease and multiple sclerosis. This work was directed towards a better understanding of the molecular relationships of hypoxic/ischemic BBB impairment with a special focus on the individual responses of the different barrier cells.

Hypoxia-inducible factor-1 (HIF-1) transcription factor is the predominant regulator of hypoxic responses but its impact on hypoxia-mediated barrier impairment remains poorly defined, thus we investigated the direct consequence of HIF-1 induction on barrier function. Using the rat brain endothelial cell line RBE4 cultured on transwells as *in vitro* model our data demonstrated that normoxic HIF-1 stabilization results in similar disturbance of BBB function like hypoxic exposure, whereas hypoxic HIF-1 inhibition had a positive effect on barrier integrity. Interestingly the barrier compromising effects of HIF-1 were predominantly regulated via tight junction disruption and translocation of tight junction proteins from the plasma membrane and only to a minor extent through reduction of tight junction protein expression. In addition our data advocates that increased tyrosine phosphorylation of occludin and to a lesser extent claudin-5, likely induced through vascular endothelial growth factor (VEGF), is a mechanism by which HIF-1 mediates BBB dysfunction.

During hypoxic and ischemic stress the general tolerance of the individual cell types and the adaptive responses initiated are very important for barrier outcome. Previously our group was able to highlight the importance of astrocytes and pericytes for barrier function maintenance under mild (1% O_2) and severe (0.1% O_2) hypoxia. Importantly depending on the severity of

the insult the cell types differentially modulated barrier function - showing that pericytes were able to maintain barrier function under severe O_2 deprivation whereas astrocytes could not. These data suggested that the individual hypoxic responses of the BBB cells crucially regulate barrier function. As a consequence the second part of this thesis focused on performing a comprehensive study to better characterize the hypoxic/ischemic responses of RBE4 cells, primary astrocytes and pericytes. Comparing general cellular parameters like hypoxic target gene/protein induction, cytoskeletal rearrangements, proliferation and cell survival, endothelial cells were clearly defined as the most responsive and sensitive cell type amongst the three, whereas astrocytes proved to be the most tolerant. Importantly the endothelial cells were vulnerable during O_2 deprivation alone, whereas astrocytes and pericytes were hardly affected and exhibited quite similar responses. However astrocytes resisted extended severe oxygen-glucose deprivation much better than pericytes. These differences in terms of overall sensitivity and target gene induction corroborate the importance of support of endothelial function by the more resistant perivascular cells. With their overall responses being quite different raises an important and intriguing question of how hypoxic cell-specific gene induction is regulated.

Using liquid chromatography-mass spectrometry (LC-MS) we pursued the question whether different activity of metabolic pathways could account for differential tolerance of endothelial cells and astrocytes to hypoxic and ischemic treatment. Indeed profound differences in the basal and ischemic metabolism of astrocytes and endothelial cells were identified that are likely crucial to survive periods of nutrient depletion. We concluded that basal astrocyte metabolism is programmed to accumulate metabolites that help maintain energy and redox state in times of distress including glycogen, phosphocreatine and glutathione, whereas in contrast endothelial cells do not seem to accumulate these compounds. During ischemia the consequences of these differences were particularly seen in central carbohydrate metabolism, wherein the pathway appeared to be only mildly affected after 24h of treatment in astrocytes, while in endothelial cells a large number of metabolites were reduced suggesting that the latter have consumed most of their sugar stores. Specific and differential characteristics of adaptation such as these can clearly underlie the complex responses of the different cells and modulate their contribution to BBB stability.

Taken together this work highlights the diverse reaction and tolerance of the individual barrier cell types to stress conditions. Due to the complex structure of the BBB this work emphasizes that an increase of our knowledge about the individual cell responses will provide a foundation to understand barrier regulation under normal and injury conditions.

TABLE OF CONTENTS

1 INTRODUCTION 11

1.1 The blood-brain barrier (BBB) - general considerations 11

1.1.1 Function and anatomy of the BBB 11

1.1.2 Contribution of perivascular cells to BBB regulation* 16

1.1.2.1 Astrocytes 16*

1.1.2.2 Pericytes 18*

1.2 Hypoxia and ischemia 20

1.2.1 The HIF-1 signaling pathway* 21

1.2.2 Consequences of hypoxic injury on cell state 24

1.2.2.1 Adaptive hypoxic responses 24

1.2.2.2 Detrimental hypoxic responses 28

1.2.3 Normoxic versus hypoxic/ischemic cellular metabolism 29

1.3 Hypoxic/ischemic BBB modulation 33

1.3.1 Mechanisms of hypoxic barrier disruption* 33

1.3.2 HIF-1 regulates BBB permeability* 34

1.3.3 Contribution of astrocytes and pericytes to hypoxic BBB regulation* 35

1.3.3.1 Astrocytes 35*

1.3.3.2 Pericytes 38*

2 AIM OF THE THESIS 40

3 RESULTS 42

3.1 Hypoxia selectively disrupts brain microvascular endothelial tight junction complexes trough a hypoxia-inducible factor-1 (HIF-1) dependent mechanism (published manuscript) 43

3.2 Differential responses of blood-brain barrier cells to hypoxia and ischemia - a comparative study (submitted manuscript) 54

3.3 Differential metabolic adaptation of astrocytes and endothelial cells to hypoxic and ischemic injury (additional, unpublished data) 86

3.3.1 Introduction 86
3.3.2 Material and Methods 86
3.3.3 Results 90
3.3.4 Discussion 107

4 CONCLUSIONS AND PERSPECTIVES 112

5 APPENDIX 118

6 REFERENCES 126

7 REVIEW ARTICLE 138

8 ABBREVIATIONS 160

9 ACKNOWLEDGEMENTS 161

10 CURRICULUM VITAE 162

* Sections adapted from our review (Engelhardt *et al.*, 2014b).

1 INTRODUCTION

Note: Sections marked with * have been adapted from our very recent review (Engelhardt *et al.*, 2014b) and were originally written by S. Engelhardt. The sections have been updated with additional recent information where required.

1.1 THE BLOOD-BRAIN BARRIER (BBB) - GENERAL CONSIDERATIONS

1.1.1 Function and anatomy of the BBB

In 1885 Paul Ehrlich discovered the presence of a specialized anatomical barrier between the brain and the blood circulation when dyes injected into the peripheral blood stream stained all organs except the brain and the spinal cord (Ehrlich, 1885). 15 years later Lewandowsky first introduced the term Bluthirnschranke (blood-brain barrier) (Lewandowsky, 1900). The blood-brain barrier (BBB) crucially supports brain function by maintaining brain homeostasis, controlling cerebral nutrient uptake and molecular traffic, excluding potentially harmful substances from the brain, and strictly regulating immune surveillance (Abbott, 2013). In addition the BBB is also implicated in regulation of local blood flow and neuronal development (Iadecola and Nedergaard, 2007; Stenman *et al.*, 2008; Takano *et al.*, 2006).

Brain capillary endothelial cells form the core of the BBB and are supported by surrounding pericytes, perivascular astrocytes and the basal lamina to fulfill their unique function (Abbott *et al.*, 2006; Engelhardt *et al.*, 2014b). Subsequently, the importance of intercellular signaling between the BBB and neurons, microglia and immune cells led to a more integrated view of cellular interactions within the brain and its vascular beds, referred to as the neurovascular unit (NVU) (Abbott, 2013; Neuwelt *et al.*, 2011) (Fig. 1.1). Importantly the barrier function of the BBB acts on various levels, firstly as a physical barrier via expression of tight junction proteins and low pinocytic activity, secondly as a transport barrier by strictly limiting transport from the blood into the brain and *vice versa* through expression of specialized transporter systems, and finally as a metabolic barrier that converts molecules in transit through expression of specialized enzyme systems (Abbott *et al.*, 2010).

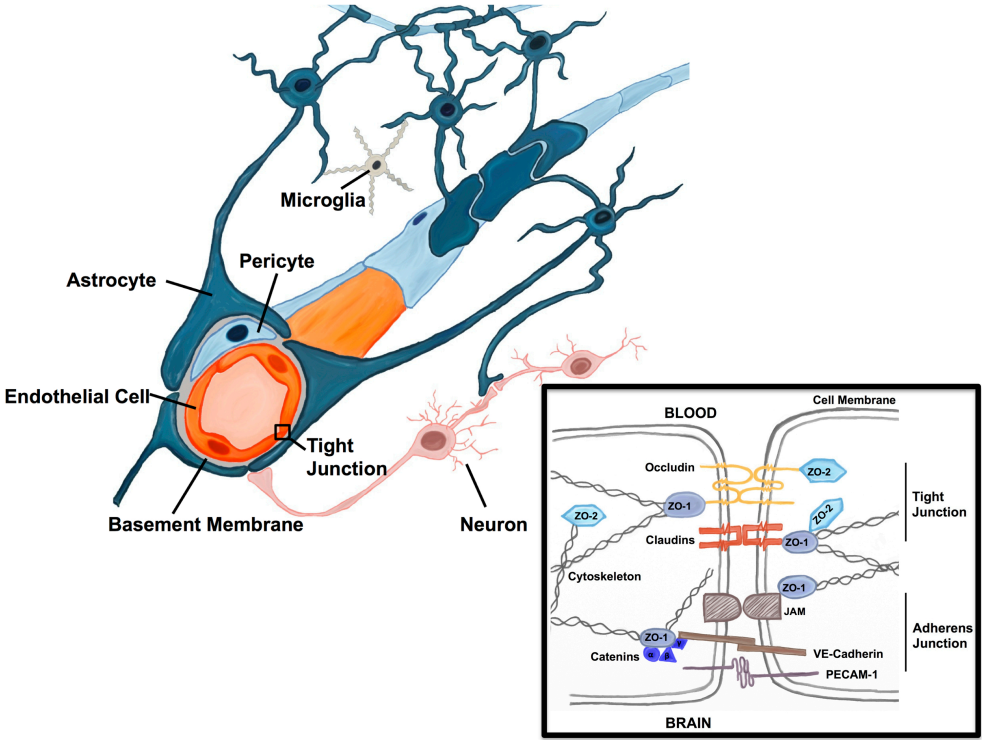

Figure 1.1: The BBB protects neurons and glial cells from systemically circulating agents as brain microvessels form a very tight barrier clearly distinct from vessels in other organs. The barrier is formed by ECs (red), that line the blood vessels, surrounded by pericytes (light blue), basement membrane (grey) and astrocytic (dark blue) end-feet. Astrocytes provide the cellular link to the adjacent neurons (pink). The illustration also shows microglial cells (grey) in contact with astrocytes. Inset (black box) shows the cell–cell contact that takes place between two adjacent ECs at the BBB and demonstrates the basic organization of the BBB tight and adherens junctional proteins. Note the interactions of the junctional proteins with the cytoskeleton. Adapted from (Engelhardt *et al.*, 2014b).

Endothelial junctions - tight and adherens junction complexes

At the junctional complex of polarized epithelia and endothelia three different structures are found: the tight junction (TJ) and adherens junction (AJ) complexes and desmosomes (Niessen, 2007). TJ and AJ together physically connect neighboring cells, participate in endothelial cell polarization and mechanotransduction and provide intercellular signaling platforms (Baum and Georgiou, 2011; Gulino-Debrac, 2013) (Fig 1.1 box). Although AJ participate in limiting paracellular passage between the adjacent cells, TJ are the major structures according for paracellular tightness, which is one of the most, if not the single most important feature of a tight BBB (Luissint *et al.*, 2012). Both TJ and AJ complexes are composed of transmembrane proteins, cytoplasmic scaffold proteins associated with the

cytoskeleton and signaling/polarity molecules (Niessen, 2007). The nectin-afadin and cadherin-catenin complexes represent the central structures of the AJ. In addition PECAM-1 (platelet endothelial cell adhesion molecule), a member of the immunoglobulin (Ig) superfamily of cell adhesion molecules localizes to endothelial AJ and participates in cell-cell adhesion and signal transmission (Ilan and Madri, 2003; Niessen, 2007). Nectins are members of the Ig-like adhesion receptor family forming lateral homodimers that interact either homophilically or heterophilically with the extracellular domains of neighboring cells. Nectins connect to the actin cytoskeleton via the actin-binding protein afadin (AF-6) (Niessen, 2007) and represent the first scaffold for formation of AJ and TJ (Takai *et al.*, 2003; Takai and Nakanishi, 2003). The cadherins constitute a family of roughly 20 members that homophilically interact with each other between adjacent cells in a Ca^{2+}-dependent manner (Meng and Takeichi, 2009). The different cadherin family members are expressed in a tissue and cell specific manner, with VE-cadherin (vascular endothelial) being specific for endothelial cells (Vestweber, 2008). In addition to its adhesive functions VE-cadherin has been implemented in regulation of proliferation, apoptosis and paracellular permeability via regulation of TJ proteins, like claudin-5 and occludin (Taddei *et al.*, 2008; Walsh *et al.*, 2011). The cytoplasmic adaptor proteins of the catenin family, like β-catenin or p120-catenin connect cadherins to the actin cytoskeleton and microtubules (Baum and Georgiou, 2011; Meng and Takeichi, 2009). More than just functioning as linker molecules catenins fulfill important roles in cellular signaling. β-catenin binds to EGF receptor and tyrosine phosphatases but also is a central modulator of the *wnt* signaling pathway thus linking cellular adhesion to cell fate determination signaling, whereas p120-catenin has been implemented in regulation of endocytosis (Niessen, 2007).

At the TJ at least three different types of transmembrane proteins are located that mediate cell-cell adhesion: the proteins of the claudin, occludin and junctional adhesion molecules family (JAMs) (Bauer *et al.*, 2011; Luissint *et al.*, 2012). Claudins and the members of the occludin family belong to the superfamily of MARVEL (Mal and related proteins for vesicle trafficking and membrane link) proteins that contain a conserved four-transmembrane MARVEL domain (Sanchez-Pulido *et al.*, 2002). The claudins constitute a family of more than 24 members and are separated by sequence homology into classical (Claudins 1-10, 14, 15,

17, 19) and non-classical claudins (Claudins 11-13, 16, 18, 20-24) (Krause *et al.*, 2008). All claudins share the common function of paracellular sealing, which is tissue-, size- and charge selective (Krause *et al.*, 2008). Indeed the tightness of a tissue appears to be crucially dependent on the combination of expressed claudin isoforms and as such tightening claudins (claudins 1, 5, 11, 14) and pore forming (claudins 2, 7, 15, 16) claudins have been identified (Krause *et al.*, 2008). Both homo- and heterophilic interactions have been observed for claudins. Endothelial cells at the BBB express the claudin isoforms 1, 3, 5 and 12 (Goncalves *et al.*, 2013). Knockout studies using transgenic mouse models have revealed the particular importance of TJ proteins for BBB function. C*laudin-5*$^{-/-}$ mice showed normal development and morphology of the vasculature, but exhibited increased BBB permeability to molecules smaller than 800 Da and died within 10h after birth (Nitta *et al.*, 2003). In contrast, the occludin knockout did not cause vascular impairment or disturbed tight junction morphology, but resulted in increased calcification of the cerebellum and basal ganglia (Saitou *et al.*, 2000). However a complex histological phenotype with chronic inflammation and poor TJ integrity in various epithelial tissues suggests a role for occludin in TJ stability rather than TJ assembly (Cummins, 2012; Saitou *et al.*, 2000).

The integral membrane proteins of the TJ interact with adaptor/scaffolding proteins, signaling molecules and transcriptional regulators (Bauer *et al.*, 2011). Scaffolding proteins such as zonula occludens (ZO-1) proteins 1-3, AF-6 or cingulin provide the physical link between the TJ transmembrane proteins and the actin cytoskeleton and confer stability (Bauer *et al.*, 2011; Gonzalez-Mariscal *et al.*, 2003).

Regulation and posttranslational modifications of tight junction complexes

Through interaction with kinases and small GTPases, TJ directly participate in cell signaling events and are able to transmit extracellular information into the cells (Gonzalez-Mariscal *et al.*, 2003). Particularly the small GTPases of the Rho family, RhoA, Rac1 and Cdc42 and protein kinases like PI3K, PKC and MAPK have been attributed an important function in signaling events at the TJ and similarly TJ regulation (Bauer *et al.*, 2011; Gonzalez-Mariscal *et al.*, 2008). Importantly TJ are not rigid structures but constantly undergo dynamic changes (Niessen, 2007; Steed *et al.*, 2010). A study by Shen and co-workers used fluorescently-

tagged tight junction proteins to follow their dynamics by fluorescence recovery after photobleaching (FRAP) and showed that claudin-1 stably localized to the tight junctions, whereas about 70% of the occludin diffused rapidly within the cellular membranes and about 70% of ZO-1 molecules translocated between a membrane associated state and the cytoplasm (Shen *et al.*, 2008). Besides diffusion and translocation, tight junctions also undergo degradation and posttranslational alterations that affect overall barrier tightness (Luissint *et al.*, 2012). Indeed many TJ-associated proteins can be phosphorylated at serine, threonine and tyrosine residues (Luissint *et al.*, 2012). The phosphorylation pattern in the end affects TJ protein conformation and their interaction with each other and thus crucially regulates BBB tightness (Gonzalez-Mariscal *et al.*, 2008; Luissint *et al.*, 2012). In MDCK cells strong Ser/Thr-phosphorylation of occludin triggers its localization to TJ whereas non or weakly phosphorylated occludin is mainly distributed across basolateral membranes (Sakakibara *et al.*, 1997). However in brain cells Ser/Thr phosphorylation of occludin and claudin-5 by Rho/ROCK has been correlated to BBB breakdown (Persidsky *et al.*, 2006). Similarly increased Tyr-phosphorylation of occludin has been observed during BBB impairment (Cummins, 2012; Engelhardt *et al.*, 2014a; Gonzalez-Mariscal *et al.*, 2008). These studies show that the effect of phosphorylation on barrier function cannot be generalized because depending on the tissue, cell type, the kinase involved and on the type of stimulus the outcome on barrier integrity can be very distinct (Cummins, 2012; Gonzalez-Mariscal *et al.*, 2008). Importantly proteins localized at the AJ have also been implicated in TJ control. AJ facilitate formation of TJ by recruitment of ZO-1 to cadherin complexes, which then forms a scaffold for TJ formation (Itoh *et al.*, 1997; Niessen, 2007). β-catenin has been shown to regulate maintenance of BBB phenotype during embryonic and postnatal development *in vivo* and its inactivation causes decreased claudin-3 expression coincidentally with BBB breakdown (Liebner *et al.*, 2008). Similarly VE-cadherin was shown increase barrier tightness via upregulation of claudin-5 expression and suppression of occludin phosphorylation (Taddei *et al.*, 2008; Walsh *et al.*, 2011).

Overall these studies highlight the highly dynamic nature of the TJ and the multifaceted possibilities of TJ regulation through signaling cascades as well as cellular structures like the cytoskeleton or AJ.

1.1.2 Contribution of perivascular cells to BBB regulation*

Endothelial cells certainly represent the core of the BBB. However it has become very evident that the inductive environment of the brain crucially contributes to the tightness of brain endothelial cells (Ballabh *et al.*, 2004). Many *in vitro* studies revealed that upon co-culture with perivascular cells, particularly astrocytes and pericytes, endothelial cells exhibit a state of significant tightness and tight junction expression (Abbott *et al.*, 2006; Ballabh *et al.*, 2004; Ogunshola, 2011). In the following two chapters the current state of research on the impact of astrocytes and pericytes on physiological BBB function will be discussed.

1.1.2.1 Astrocytes*

Similar to neurons and other glial cells, astrocytes originate from the neuroectoderm (Allen and Barres, 2009). To date 11 different types of astrocytes are classified based on their structural and functional interaction with their environment, of which 8 are specifically associated with blood vessels (Abbott *et al.*, 2006). Astrocytes are crucially involved in control of neuronal function through regulation of brain homeostasis, supply of neurons with energy and substrates for neurotransmission and recycling of neurotransmitters. Furthermore they represent the connection between neurons and the brain vasculature, which they cover with their end-feet. Almost 50 years ago the close proximity of the astrocytic end-feet to the brain endothelium raised the hypothesis that astrocytes contribute to BBB regulation (Davson and Oldendorf, 1967). Since then a number of *in vivo* (Janzer and Raff, 1987; Stewart and Wiley, 1981; Willis *et al.*, 2004b) and particularly *in vitro* studies have demonstrated the importance of astrocytes to BBB induction and regulation. Deletion of astrocytes *in vivo* using 3-chloropropandiol results in increased vascular permeability to 10 kDa dextran and 300 kDa fibrinogen, implying a major disruption of the BBB. Moreover a loss of claudin-5, occludin and ZO-1 from the cellular junctions is observed, whereas astrocytic repopulation reverses tight junction protein loss and restored BBB function (Willis, 2011; Willis *et al.*, 2004a). Studying the contribution of astrocytes to BBB function *in viv*o is highly complex due to technical challenges and as such *in vitro* studies have crucially contributed to our understanding about astrocytic modulation of BBB tightness. Model systems using astrocyte-endothelial co-cultures (Al Ahmad *et al.*, 2009; Dehouck *et al.*, 1990; Fischer *et al.*, 2000; Rist *et al.*, 1997)

as well as astrocyte-conditioned media (Raub *et al.*, 1992; Rubin *et al.*, 1991) demonstrated the inductive potential of astrocytes on barrier tightness by increased transendothelial electrical resistance (TEER) and reduced permeability to low molecular weight tracers (for detailed review refer to the excellent article by (Deli *et al.*, 2005)). There is now good evidence that barrier induction through astrocytes is mainly mediated via changes in the number, length and complexity of endothelial TJs (Tao-Cheng *et al.*, 1987), expression levels of TJ and associated-proteins like occludin and ZO-1 (Colgan *et al.*, 2008; Siddharthan *et al.*, 2007) and the redistribution of junctional proteins such as platelet endothelial cell adhesion molecule-1 (PECAM-1), ZO-1 and claudin-5 at endothelial junctions (Al Ahmad *et al.*, 2011; Colgan *et al.*, 2008). In addition astrocytes modulate expression and polarized localization of endothelial transporters, such as P-glycoprotein (P-gp) or multi drug resistance protein (MRP) (Al Ahmad *et al.*, 2011; Berezowski *et al.*, 2004) as well as BBB-specific enzyme-systems such as γ-glutamyl transpeptidase (Hayashi *et al.*, 1997; Meyer *et al.*, 1991) and thus crucially regulate EC function. Major efforts have been made to unravel how astrocytes modulate TJs, transporters and enzyme systems. Astrocytes are known to secrete a large number of substances including peptides, growth factors and chemokines (Nico and Ribatti, 2012) several of which modulate barrier function, such as basic fibroblast growth factor (bFGF), transforming growth factor-β1 (TGF-β1), glial cell-derived neurotrophic factor and src-suppressed C-kinase substrate (SSeCKS) (Dohgu *et al.*, 2004; Igarashi *et al.*, 1999; Lee *et al.*, 2003; Reuss *et al.*, 2003; Shimizu *et al.*, 2012; Sobue *et al.*, 1999; Walshe *et al.*, 2009). For instance bFGF has demonstrated barrier-tightening effects *in vitro* by reducing barrier permeability (Sobue *et al.*, 1999) and increasing endothelial γ-glutamyl-transpeptidase and alkaline phosphatase activity (el Hafny *et al.*, 1996). *In vivo* bFGF knockout increases BBB permeability to albumin and reduces expression of ZO-1 and occludin, and coincides with reduced astrocyte differentiation (Reuss *et al.*, 2003). The effect of astrocyte-secreted TGF-β1 on barrier function is discussed controversially. While some studies observed reduced BBB permeability and increased TJ expression in presence of TGF-β1/TGF-β (Dohgu *et al.*, 2005; Dohgu *et al.*, 2004; Walshe *et al.*, 2009) others reported adverse effects (Shen *et al.*, 2011). This discrepancy may be explained by the fact that TGF-β effects on the endothelium are highly dependent on the endothelial activation state and the tissue environment,

especially the extracellular matrix as it mediates TGF-β activation (Cambier *et al.*, 2005). Table 1.1 summarizes the discussed barrier inducing properties of astrocytes.

Over the past 20 years our understanding of the importance of astrocytes as regulators of BBB physiology and how they modulate barrier characteristics has dramatically increased but, realistically, unraveling of the complex pathways has just begun.

Inductive effects of perivascular cells on normal BBB function	
Astrocytes	• **tight junction (TJ) integrity**
	• increased number and length of TJ • elevated TJ protein expression • stabilized localization of TJ proteins at the cellular junctions
	• **polarized expression of endothelial transporter and enzyme systems**
	• p-glycoprotein • γ-glutamyl transpeptidase
	• **secreted factors increasing BBB function**
	• basic fibroblast growth factor (bFGF) • transforming growth factor-β (TGF-β) • glial cell-derived neurotrophic factor (GDNF) • src-suppressed C-kinase substrate (SSeCKS)
Pericytes	• **increased tight junction protein expression**
	• **inhibition of endothelial transcytosis** (via Mfsd2a)
	• **secreted factors increasing BBB function**
	• angiopoietin-1 (ANG-1) • transforming growth factor-β (TGF-β)

Table 1.1: Stabilizing effects of astrocytes and pericytes during physiological BBB regulation.

1.1.2.2 Pericytes*

The origin of CNS pericytes remains unclear with derivation from the mesoderm and neuroectoderm as well as from the monocyte lineage under general discussion (Sa-Pereira *et al.*, 2012). Diverse functions within the brain have been attributed to pericytes including regulation of brain homeostasis, angiogenesis, blood flow, immune and phagocytic activity, as well as being a source of pluripotent stem cells (Sa-Pereira *et al.*, 2012). The impact of pericytes on BBB induction and maintenance is less well characterized than astrocyte-induced responses. During development pericytes fulfill central roles in vessel stabilization through inhibition of EC proliferation and migration as well as regulation of vessel maturation

(Al Ahmad *et al.*, 2011; Antonelli-Orlidge *et al.*, 1989; Hellstrom *et al.*, 2001; Sa-Pereira *et al.*, 2012). Recent *in vivo* studies using platelet-derived growth factor receptor β (PDGF-Rβ) knockout mice have significantly improved our understanding. During embryonic angiogenesis pericytes are recruited to the vessels via EC-derived platelet-derived growth factor β (PDGF-β). The impaired recruitment of pericytes to the brain microvasculature through abrogation of PDGF-β signaling either by PDGF-β or PDGF-Rβ knockout resulted in severe vascular consequences such as increased vessel diameter, formation of microaneurysms, endothelial hyperplasia and increased vessel permeability (Daneman *et al.*, 2010; Hellstrom *et al.*, 2001; Lindahl *et al.*, 1997). These alterations in vessel tightness were attributed to enhanced caveolae formation and transcytosis, abnormal TJ alignment and increased expression of permeability inducing factors like vascular endothelial growth factor (VEGF) and angiopoietin (ANG)-2 (Daneman *et al.*, 2010; Hellstrom *et al.*, 2001). Corresponding studies in adult mice revealed that pericytes are also crucial for adult BBB maintenance as reduced pericytic vessel coverage resulted in increased BBB permeability, altered endothelial gene expression and loss of astrocyte end-feet polarization (Armulik *et al.*, 2010). Age-dependent pericyte-loss in PDGF-R$\beta^{+/-}$ mice elevated parenchymal accumulation of blood proteins and leakage of neurotoxic and vasculotoxic substances into the brain parenchyma and reduction of ZO-1 and occludin protein expression (Bell *et al.*, 2010). A very recent study by Ben-Zvi and co-workers demonstrated the importance of pericyte-mediated signaling on BBB tightness (Ben-Zvi *et al.*, 2014). *Mfsd2a* (major facilitator super family domain containing 2a) is selectively expressed in BBB endothelial cells and its ablation results in increased BBB permeability due to increased transcytotic activity. Interestingly pericyte-deficient mice similarly showed increased transcytotic activity and reduced vascular Mfsd2a expression, suggesting a crucial role in pericyte-mediated signaling in regulating Mfsd2a expression and reducing endothelial transcytotic activity.

In vitro studies using cells of human, murine, bovine, and porcine origin further underlined the positive effect of pericytes on BBB tightness (Al Ahmad *et al.*, 2009; Daneman *et al.*, 2010; Dohgu *et al.*, 2005; Hayashi *et al.*, 2004; Nakagawa *et al.*, 2007). Similar to astrocytes, pericytes are capable of secreting factors that modulate BBB permeability under normal conditions, like ANG-1 (Hori *et al.*, 2004; Wang *et al.*, 2007), TGF-β1 (Dohgu *et al.*, 2005) and

GDNF (Shimizu *et al.*, 2012) that increase ZO-1, claudin-5 or occludin *in vitro* (Hori *et al.*, 2004; Shimizu *et al.*, 2011; Wang *et al.*, 2007). Therefore similar to astrocytes, pericytes seem capable of modulating TJs. In contrast a few *in vitro* studies report that co-culture of ECs with pericytes reduces TEER via induction of matrix metalloproteinases (MMP) -2 and -9 activity and activation of VEGF-mediated signaling (Thanabalasundaram *et al.*, 2010; Zozulya *et al.*, 2008). Interestingly this negative impact of pericytes seems to be dependent on their differentiation state (Thanabalasundaram *et al.*, 2011). The discussed effects of pericytes on barrier function are shown in Table 1.1.

1.2 HYPOXIA AND ISCHEMIA

Hypoxia develops when the blood stream fails to supply the oxygen demand of tissues and often acts as an initial trigger for pathophysiological changes at the BBB (Zepeda *et al.*, 2013). Hypoxic events can be divided into two major groups: non-vascular mechanisms, like high altitude, anemia, carbon monoxide poisoning or suffocation and pathologies affecting the vasculature either acutely or chronically. Atherosclerosis, and hypertension are important pathologies associated with reduced blood supply through vascular defects, which ultimately result in tissue hypoxia (Stanimirovic and Friedman, 2012). Ischemia is characterized by impaired blood supply ultimately resulting in combined tissue hypoxia and impaired nutrient supply, thus representing a more severe injury than hypoxia alone and is a hallmark of pathologies like ischemic and hemorrhagic stroke, traumatic brain injury, severe hypotension or cardiac arrest (Hawkins and Davis, 2005; Zoppo and Hallenbeck, 2000). Overall similar effects on cellular function like metabolic dysregulation, oxidative stress, inflammatory responses and BBB impairment are observed in both hypoxia and ischemia (Stanimirovic and Friedman, 2012) and responses to both injuries are regulated via hypoxic transcription factors, such as the HIF-1 pathway (Singh *et al.*, 2012).

1.2.1 The HIF-1 signaling pathway*

Hypoxia requires an immediate response of the affected tissues/cells to sustain their function and prevent cell death. The most important tasks of the adaptation process are to decrease energy consumption and increase oxygenation. This is mainly achieved through metabolic adaptation and temporal cell cycle arrest as well as induction of angiogenic and erythropoietic genes (Wenger *et al.*, 2005). Different signaling pathways are involved in these events including the unfolded protein response, mTOR (mammalian target of rapamycin) signaling and hypoxia-inducible factor (HIF)-mediated gene regulation (Majmundar *et al.*, 2010). HIFs are considered master regulators of the hypoxic response and are heterodimeric transcription factors composed of an oxygen sensitive α-subunit and a constitutively expressed β-subunit. Under normoxia the HIFα subunits are constitutively transcribed but constantly targeted for proteasomal degradation through a cascade of hydroxylation of conserved proline residues via prolyl hydroxylases (PHDs), subsequent recognition by the Von Hippel Lindau (VHL) protein, ubiquitination and degradation by the proteasome. As oxygen tension drops, the PHD enzymes are inhibited and the lack of hydroxylation results in cytoplasmic stabilization of the α-subunits. After phosphorylation HIFαs translocate to the nucleus and dimerize with ARNT (Aryl hydrocarbon receptor nuclear translocator, also known as HIF-β) and co-activators forming a functional HIF transcription factor (Fandrey and Gassmann, 2009; Wenger *et al.*, 2005). By binding to hypoxia responsive elements in promoter regions HIFs induce expression of target genes involved in cellular adaptation to hypoxic stress regulating erythropoiesis, angiogenesis, proliferation, and cellular metabolism (Ogunshola and Al-Ahmad, 2012) (Fig. 1.2).

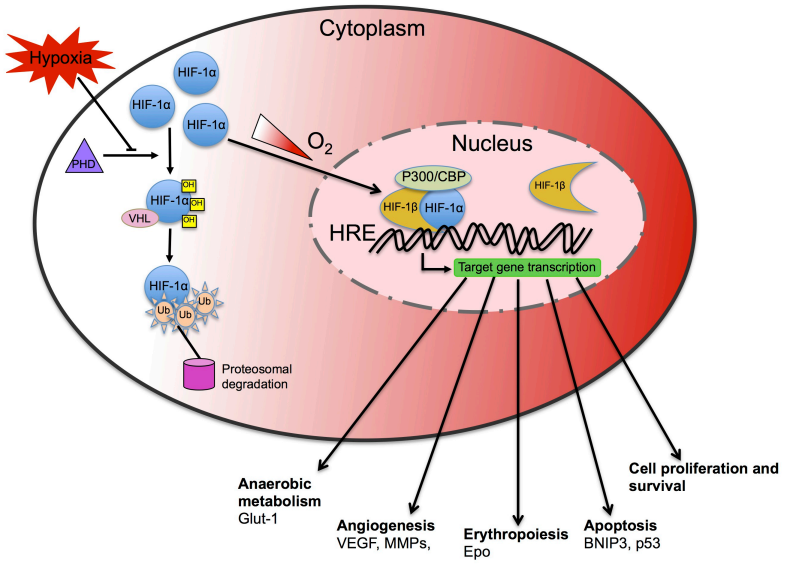

Figure 1.2: Schematic diagram illustrating the mechanism of HIF-1 regulation under normoxic and hypoxic conditions. HIFs are heterodimeric transcription factors composed of an oxygen-sensitive α-subunit and a constitutively expressed β-subunit (also known as ARNT). Under normoxia (white gradient), the HIF-1α subunit is constitutively transcribed but constantly targeted degradation through hydroxylation of conserved proline residues by PHDs leading to recognition by VHL protein, ubiquitination and subsequent degradation by proteasome. As oxygen tension drops (red gradient), the PHD enzymes are inhibited and the lack of hydroxylation results in cytoplasmic stabilization of the α-subunits. After phosphorylation, HIF-1α translocates to the nucleus and dimerizes with HIF-1β and co-activators such as p300/CBP forming a functional HIF-1 transcription factor. HIF-1 then binds to hypoxia-responsive elements (HREs) in the promoter regions of its many targets inducing expression of genes involved in cellular adaptation to hypoxic stress by regulating erythropoiesis, angiogenesis, proliferation and cellular metabolism in order to reduce O_2 consumption and increase O_2 delivery to tissues. Adapted from (Engelhardt *et al.*, 2014b).

Three different HIFs have been identified namely HIF-1, -2 and -3 of which HIF-1 is the most widely studied. More than 100 HIF-1 target genes are known to date (Semenza, 2003) and as a consequence HIF-1 signaling is considered essential for cellular adaptation and survival during acute hypoxia. Mice with constitutive HIF-1α $^{-/-}$ die at E11 due to vascular and cardiac defects (Iyer *et al.*, 1998; Ryan *et al.*, 1998). Underlining the crucial contribution of HIF-1 in brain development it was further reported that HIF-1α knockout causes a lack of cerebral vessel formation (Ryan *et al.*, 1998)

Several HIF-1 target genes are neuroprotective and act as pro-survival factors such as erythropoietin and VEGF. Moreover HIF-1 signaling regulates the expression of several proteins implicated in glycolysis such as phosphofructokinase or enolase-1 and glucose

transporter 1 (GLUT-1) thus regulating metabolic adaptation to low oxygenation. Besides its positive effects HIF-1 also accounts for detrimental effects observed during hypoxia/ischemia by activation of pro-death genes, such as BNIP3 (BCL2/adenovirus E1B 19 kDa protein-interacting protein 3), COX2, or p53 stabilization (Singh *et al.*, 2012). The potential dual outcome of HIF-1 signaling has also been documented in various *in vivo* disease studies. A study by Helton and colleagues reported that late-stage brain deletion of HIF-1α in adult mice protects from ischemic cell death and that decreased HIF-1 levels are neuroprotective (Helton *et al.*, 2005). Similarly in neonatal hypoxic-ischemic injury in rats it was shown that inhibition of HIF-1 signaling using 2-methoxyestradiol (2ME2) exerts a neuroprotective effect through reduction of infarct volume and brain edema, whereas HIF-1 stabilization via PHD inhibition using dimethyloxalylglycine (DMOG) had opposite effects (Chen *et al.*, 2008b). In contrast two other studies observed positive effects of HIF-1 signaling on injury outcome. Using a rat middle cerebral artery occlusion ischemic stroke model Yan *et al.* showed that inhibition of HIF-1 signaling using 3-(5'-hydroxymethyl-2'-furyl)-1-benzylindazole (YC-1) results in increased infarct volumes and mortality rates albeit reduced permeability to Evans blue was observed (Yan *et al.*, 2011). Neuronal-specific HIF-1α depletion in a mouse model transient focal ischemia led to increased tissue damage and cell death (Baranova *et al.*, 2007). At present it is not clear what determines whether the initiated HIF-1 mediated response is protective or detrimental. However it is likely that the severity of the insult and its duration, as well as cell type-specific differences and paracrine signaling play a critical role. Thus HIF-1 signaling is a key determinant of functional outcome. In contrast less is known about HIF-2 signaling. HIF-2α knock down in mice is lethal around day E16.5 due to complications including bradycardia and incomplete lung maturation (Compernolle *et al.*, 2002; Tian *et al.*, 1998). In contrast to HIF-1α, that is expressed constitutively in all tissues, HIF-2α shows a tissue-specific restricted expression pattern, which is limited to the endothelium, brain, kidney, lung, heart and small intestine (Loboda *et al.*, 2010; Zepeda *et al.*, 2013). Structurally HIF-1α and HIF-2α are very closely related, have an amino acid sequence homology of 48% and similar protein structures (Koh and Powis, 2012). Although they activate common target genes, both HIF-α isoforms also activate individual, specific genes due to disparities in their transactivation domains (Loboda *et al.*, 2010). In contrast to HIF-1α, HIF-2α does not induce

glycolytic enzymes but instead specifically controls erythropoietin and oct4 (transcription factor regulating stem cell proliferation) expression. HIF-2α also predominantly regulates cyclin D4 and transforming growth factor α induction, whereas HIF-1α does not (Loboda *et al.*, 2010). Generally HIF-1α is considered to particularly mediate acute adaptation to hypoxia, whereas HIF-2α is predominantly involved in chronic adaptation (van Patot and Gassmann, 2011).

HIF-2α is highly expressed in embryonic vasculature controlling target genes involved in regulation of vascular function and angiogenesis (Skuli *et al.*, 2009). Indeed endothelial cell-specific HIF-2α knockdown causes severe vascular defects including increased vessel permeability, abnormal vessel ultrastructure and pulmonary hypertension (Skuli *et al.*, 2009), implicating its crucial role in vessel function. Unfortunately the role of HIF-2 signaling on BBB function has been largely neglected so far and therefore will not be further discussed.

1.2.2 Consequences of hypoxic injury on cell state

1.2.2.1 Adaptive hypoxic responses

As discussed above hypoxic and ischemic signaling leads to the up-regulation of a large number of genes that critically modulate cellular adaptation and determine functional outcome. With regard to an entire organism adaptive responses include adaptation of metabolism, increase of local blood flow, induction of erythropoiesis and angiogenesis in order to decrease reduce O_2 consumption and increase O_2 delivery to the issues (Fandrey and Gassmann, 2009; Ogunshola and Al-Ahmad, 2012). At the cellular level the major requirement for survival is to reach a balance between energy consumption and energy production, as depletion of ATP ultimately results in bioenergetic collapse, and to keep oxidative stress levels low in order to reduce damage (Wheaton and Chandel, 2011). The cellular responses mediating these adaptations are discussed in detail below.

Adaptations to maintain cellular energy balance

Hypoxia decreases mitochondrial electron transport chain through HIF-1 mediated gene regulation leading to a reduction of ATP production (Wheaton and Chandel, 2011), thus an

adaptation of cell metabolism is indispensable in order to enable sufficient production of ATP (discussed in detail in Section 1.2.2.3).

Another important mechanism used by cells to maintain energy balance is the reduction of energy and O_2 consumption via inhibition of highly energy demanding processes like protein synthesis, Na-K-ATPase activity and proliferation (Semenza, 2011; Tracy and Macleod, 2007; Wheaton and Chandel, 2011). Indeed mRNA translation is a major consumer of cellular energy and many studies have shown that during hypoxia mRNA translation is inhibited via mTOR and PERK (pancreatic eIF2α kinase) signaling (Arsham *et al.*, 2003; Bi *et al.*, 2005; Koritzinsky *et al.*, 2006; Wheaton and Chandel, 2011). It is note-worthy however that many HIF-1 target genes are translated in a cap-independent manner and thus continue to be translated even if general translation is inhibited. (Tracy and Macleod, 2007). Inhibition of the Na-K-ATPase during hypoxia is another very efficient way to reduce cellular energy consumption as this pump has been reported to consume between 30-50% of total cellular energy demand (Murphy and Crewther, 2013; Wheaton and Chandel, 2011). Indeed hypoxic phosphorylation of the Na-K-ATPase results in its internalization in an AMPK/PKC ς dependent manner (Gusarova *et al.*, 2009) and chronic hypoxia triggers HIF-1 induced degradation of the Na-K-ATPase by the proteasome (Zhou *et al.*, 2008). Appropriate regulation of cell cycle similarly represents a fundamental characteristic to adapt to altered O_2 levels (Semenza, 2011). Most cell types reduce their proliferative rate through a hypoxia-mediated arrest in the G1 phase in an HIF-1 dependent fashion, although some specialized cells like endothelial cells undergo mitosis in hypoxia as an adaptive mechanism (Semenza, 2011). A significant reduction of proliferation has been measured by BrdU incorporation in primary mouse fibroblasts and B-lymphocytes after 24h of hypoxic exposure (0.5% O_2) (Goda *et al.*, 2003). Importantly the reduction in proliferation was abolished in HIF-1α knock out fibroblasts, thus implying a HIF-1α- dependent regulation of cell cycle. A similar observation has also been made for embryonic mouse stem cells (Carmeliet *et al.*, 1998). Interestingly both studies observed a correlation between HIF-1α stabilization and increased mRNA expression of cyclin dependent kinase (CDK) inhibitor p21 (Carmeliet *et al.*, 1998; Goda *et al.*, 2003).

A correlation between HIF-1α, c-myc - that has been shown to promote proliferation via inhibition of p21 - and p21 was also demonstrated. Under normoxic conditions c-myc binds the p21 promoter, inhibits its transcription and consequently promotes proliferation, whereas under hypoxic conditions HIF-1α directly interacts with c-myc and displaces it from p21 promoter, thus allowing its transcription and inhibition of cell proliferation (Koshiji *et al.*, 2004; Semenza, 2011). In addition HIF-1α regulates proliferation through interaction with the mini-chromosome maintenance (MCM) helicase. MCM assembles at the replication origin and is essential for DNA replication. Two of its subunits MCM7 and MCM3 have been shown to crucially affect HIF-1 signaling by targeting HIF-1α for degradation via promoting its hydroxylation and inhibiting its transactivation domain in an asparaginyl-dependent manner, respectively (Hubbi *et al.*, 2011). However during prolonged hypoxia MCM mRNA decreases in a HIF-1α dependent manner implying a mutual regulation between MCM helicases and HIF-1α in control of cell proliferation (Semenza, 2011).

Induction of autophagy was considered for a long time as a cell death preceding mechanism, however growing experimental evidence suggests a survival promoting action by clearing of damaged organelles and proteins, energy generation through catabolism of macromolecules and reduction of oxidative stress (Balduini *et al.*, 2012; Tracy and Macleod, 2007; Zhang *et al.*, 2008). A study by Bellot and coworkers demonstrated the survival-promoting role of hypoxia-induced autophagy as knock-down of BNIP3/BNIP3L (Nix, a closely related protein of BNIP3) and Beclin-1 results in increased hypoxic cell death rates (Bellot *et al.*, 2009). Furthermore their data shows that double knockdown of BNIP3 and BNIP3L leads to a significant reduction of hypoxia-induced autophagy, whereas its ectopic overexpression under normoxic conditions stimulates autophagy (Bellot *et al.*, 2009). They propose a model in which BNIP3 acts as initiator of Beclin-1 and LC3 mediated autophagy via displacement of Beclin-1 from its inhibitory interaction with Bcl-2 (B-cell lymphoma 2) (Bellot *et al.*, 2009).

Reduction of oxidative stress

Due to its high O_2 consumption and oxidative metabolism the brain is prone to accumulate reactive oxygen species (ROS) and experience oxidative stress (Chong *et al.*, 2005; Warner *et al.*, 2004). In addition some particular anatomical features, like high amounts of unsaturated fatty acids, high iron levels and a relatively low catalase activity similarly account for the high vulnerability of the brain to oxidative damage (Chong *et al.*, 2005). Cells constantly generate ROS. A major ROS source is electron leak in the electron transport chain but also certain enzymes such as nitric oxide synthases, cyclooxygenase, lipooxygenase, or L-amino acid oxidase account for ROS production (Chong *et al.*, 2005; Erecinska and Silver, 2001). Oxidative stress only develops when ROS outbalance the cellular anti-oxidative capacity (Warner *et al.*, 2004). Indeed low levels of ROS may have a positive effect on initiation of adaptive responses and contribute to initiation of hypoxic signaling via HIF stabilization (Hamanaka and Chandel, 2010). However excessive ROS generation causes lipid peroxidation, protein, nucleic acid and carbohydrate damage ultimately resulting in irreversible cellular injury (Erecinska and Silver, 2001; Hamanaka and Chandel, 2010). Hypoxia and ischemia are characterized by increased ROS production and reduction of oxidative stress represents another crucial parameter modulating survival or cell death in these injuries (Chandel *et al.*, 2000; Guzy *et al.*, 2005; Hamanaka and Chandel, 2010; Warner *et al.*, 2004; Zepeda *et al.*, 2013). Superoxide is the major factor causing oxidative stress (Warner *et al.*, 2004) and brain cells have developed different scavenging mechanisms. Enzymatic antioxidants like superoxide dismutase, peroxidases and catalase, convert superoxide to H_2O_2, water and water and oxygen, respectively (Warner *et al.*, 2004). In addition dietary and endogenous antioxidants like glutathione, ascorbate or α-tocopherol function as potent superoxide scavengers (Warner *et al.*, 2004). However the most important direct adaptation of cells experiencing oxidative stress is probably the inhibition of the mitochondrial electron transport chain to actively reduce ROS formation *per se* (Erecinska and Silver, 2001; Wheaton and Chandel, 2011). Interestingly it was shown that in mouse embryonic fibroblasts BNIP3-mediated autophagy via Beclin-1 and autophagy protein 5 (Atg5) functions as an adaptive mechanism by reduction of ROS formation and inhibition of cell death during prolonged hypoxia (Zhang *et al.*, 2008).

1.2.2.2 Detrimental hypoxic responses

Besides numerous positive adaptation mechanisms, adverse responses are similarly observed during hypoxia/ischemia when a sufficient adaptation cannot be achieved. Due to their importance for this project the adverse effects of hypoxia on BBB function are discussed in a separate chapter (see Section 1.3). On a cellular level insufficient adaptation or too severe injury conditions ultimately results in initiation of cell death due to depletion of energy stores or irreversible cellular damage, e.g. through ROS as discussed above.

Induction of apoptosis in response to hypoxic exposure is quite well characterized. Apoptosis represents an energy dependent process thus a combination of severe hypoxia and presence of ATP is required for its induction (Greijer and van der Wall, 2004). In contrast hypoxia combined with nutrient depletion prevents apoptosis and provokes necrosis (Greijer and van der Wall, 2004). Hypoxia has been shown to trigger apoptosis via three different mechanisms:

1. Inhibition of the mitochondrial electron transport chain causes a reduction in membrane potential leading to reduced mitochondrial ATP production resulting in activation of the pro-apoptotic proteins Bak and Bax (Altman and Rathmell, 2012; Greijer and van der Wall, 2004). These trigger increased release of cytochrome C from the mitochondria, which in the end activates the caspase signaling cascade and ultimately results in apoptosis (Greijer and van der Wall, 2004; Wei *et al.*, 2001).

2. Elevated ROS levels trigger cytochrome C independent activation of caspase-3 and -12 finally resulting in activation of the initiator caspase-9 that mediates apoptosis (Greijer and van der Wall, 2004). In addition ROS have also been shown to mediate apoptosis via p53 induced cytochrome C release in a number of different tissues (Altman and Rathmell, 2012).

3. Hypoxic activation of the c-Jun NH_2 terminal kinase (JNK) has been reported to mediate cell death in melanoma cells, as its depletion protected the cells from hypoxia-induced cell death (Greijer and van der Wall, 2004; Kunz *et al.*, 2001).

Importantly HIF-1 signaling has been shown to promote hypoxia-induced apoptosis by two different mechanisms - p53 stabilization that results in Bak/Bax activation triggering mitochondrial cytochrome C release (Altman and Rathmell, 2012; Greijer and van der Wall, 2004) and via BNIP3/BNIP3L mediated inhibition of the anti-apoptotic proteins Bcl-2 and Bcl-xL (Kubli *et al.*, 2007; Renault and Manon, 2011).

Necrotic cell death primarily occurs when cells cannot meet their minimal energy demand to maintain electrochemical potential resulting in osmotic stress, cell swelling and cell rupture (Altman and Rathmell, 2012; Zong and Thompson, 2006). Ischemia/reperfusion, which is characterized by nutrient depletion with subsequent excessive ROS production, is frequently associated with necrosis (Altman and Rathmell, 2012; Zong and Thompson, 2006). Induction of necrosis has been further observed in various cells types, including neurons, particularly after anoxic or near anoxic events (O_2<0.1%) (Lenihan and Taylor, 2013; Niquet *et al.*, 2003; Steinbach *et al.*, 2003).

1.2.3 Normoxic versus hypoxic/ischemic cellular metabolism

Normoxic energy metabolism - a focus on brain cells

Under normal conditions the major energy source of the brain is glucose, that is transported from the blood stream via the BBB into the brain parenchyma (Duelli and Kuschinsky, 2001; Hertz, 2008; Hertz *et al.*, 2007; Wiesinger *et al.*, 1997). Glucose can be metabolized via various metabolic pathways including glycolysis, pentose phosphate pathway (PPP), the glucuronic acid pathway and glycogen synthesis (Wamelink *et al.*, 2008; Wiesinger *et al.*, 1997). Importantly glycolysis and its further metabolism represents the major pathway for ATP generation. Under normoxic conditions glycolysis produces pyruvate, which then is transported to the mitochondria, converted to acetyl coenzyme A (acetyl-CoA) and further metabolized in via oxidative metabolism in the TCA (Tricarboxylic acid) cycle (Fig. 1.3) (Wheaton and Chandel, 2011). The TCA cycle intermediates are then further used for biosynthetic processes, e.g. lipid synthesis, whereas the produced reducing equivalents NADH and $FADH_2$ are used in the electron transport chain to generate large amounts of ATP (Wheaton and Chandel, 2011). Importantly complete mitochondrial oxidation of glucose feeding the electron transport chain yields about 17 times more ATP than glycolysis alone (30-34 ATP versus 2 ATP respectively) (Belanger *et al.*, 2011). In the brain particularly the energy metabolism of neurons and astrocytes has been a focus of research. Astrocytes appear to have a very efficient and versatile metabolism for oxidative metabolism as well as aerobic glycolysis (Bouzier-Sore and Pellerin, 2013). Although under normal conditions oxidative metabolism accounts for major energy production in astrocytes and in conditions of

high energy demand astrocytes strongly induce aerobic glycolysis and glycogenolysis to compensate the increased energy demand (Hertz *et al.*, 2007).

Based on estimated energy expenditures neurons have been predicted to account for about 70% of cerebral glucose consumption, whereas astrocyte metabolism would only account for 30% (Bouzier-Sore and Pellerin, 2013). However astrocytes have a higher glycolytic activity than neurons and glucose transport/utilization studies have revealed that they also consume more glucose than neurons (Bouzier-Sore and Pellerin, 2013). It has been shown that as a result of their high glycolytic activity astrocytes predominantly convert pyruvate to lactate via lactate dehydrogenase (LDH) that is then released to serve as a neuronal energy source, explaining the relatively high rate of glucose consumption (Bouzier-Sore and Pellerin, 2013). Neurons in general exhibit a high rate of oxidative metabolism and a low glycolytic rate compared to astrocytes (Belanger *et al.*, 2011). Interestingly increased induction of neuronal glycolysis under normal conditions induces cell death and oxidative stress (Belanger *et al.*, 2011), which clarifies why they prefer lactate as energy substrate over glucose (Bouzier-Sore *et al.*, 2006). In neurons lactate is converted back to pyruvate and directly metabolized via in the TCA cycle to generate NADH/$FADH_2$ for efficient ATP generation via the mitochondrial electron transport chain (Dienel, 2012; Pellerin, 2010). In total contrast data on the cellular metabolism of endothelial cells information is very rare. However cultured HUVECs were shown to display a preference for glycolytic metabolism (Harjes *et al.*, 2012) and additionally glutamine utilization and fatty acid oxidation capacity was reported for endothelial cells, particularly during stress conditions (Harjes *et al.*, 2012).

In summary brain cells have clear dispositions towards particular substrates and pathways for energy production. Whereas neurons clearly prefer oxidative metabolism, endothelial cells appear to be mainly glycolytic and astrocytes exhibit a versatile metabolism efficiently using both pathways.

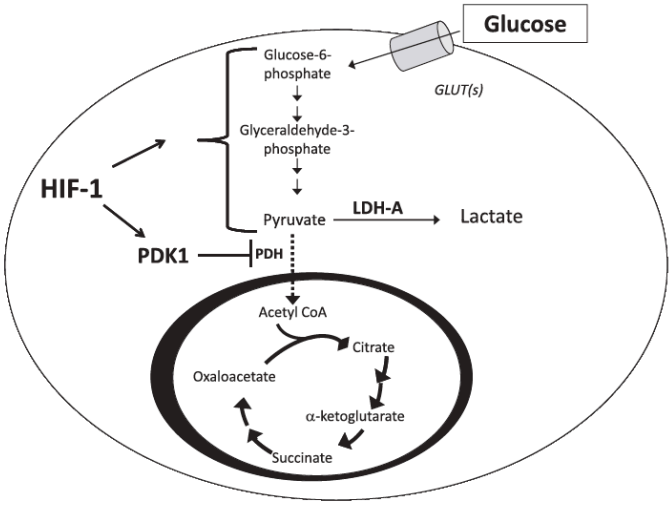

Figure 1.3: Overview of glycolysis and oxidative glucose metabolism. Under normoxic conditions glucose is transported via glucose transporters (GLUTs) into the cell and converted to pyruvate during glycolysis. Pyruvate is transported into the mitochondria and converted to Acetyl-CoA. In the tricarboxylic acid cycle acetyl-CoA gets further metabolized finally yielding NADH and $FADH_2$ for electron transport chain. HIF-1 promotes a metabolic shift from oxidative metabolism to glycolysis through induction of lactate dehydrogenase A, which produces lactate from pyruvate and up-regulation of pyruvate dehydrogenase kinase 1 (PDK1) inhibiting conversion of pyruvate into acetyl-CoA. Adapted from (Wheaton and Chandel, 2011).

Hypoxic/ischemic modulation of energy metabolism

As discussed previously hypoxic conditions significantly influence cellular metabolism, mainly because oxidative metabolism is reduced (Wheaton and Chandel, 2011). After prolonged hypoxia carbon flux into the TCA cycle diminishes because of reduced conversion of pyruvate into acetyl-CoA (Wheaton and Chandel, 2011). HIF-1 signaling directly affects pyruvate conversion via induction of lactate dehydrogenase A (LDH-A) and pyruvate dehydrogenase kinase 1 (PDK1) (Wheaton and Chandel, 2011) (Fig. 1.3). PDK1 inactivates pyruvate dehydrogenase (PDH), the enzyme that mediates conversion of pyruvate into acetyl-CoA (Kim *et al.*, 2006; Papandreou *et al.*, 2006). LDH-A directly converts pyruvate into lactate using NADH (Wheaton and Chandel, 2011). In consequence the lack of acetyl-CoA reduces TCA cycle activity and the mitochondrial electron transport chain because of NADH and $FADH_2$ reduction and ultimately inhibits oxidative glucose metabolism (Wheaton and Chandel, 2011). As a consequence the cells need to find a way to feed their energy needs through other metabolic pathways. During hypoxia/ischemia lactate accumulates in the brain (Dienel, 2012) indicating that glycolysis increases. It has been well reported that HIF-1 up-regulates

glycolysis associated genes, such as glucose transporters and glycolytic enzymes including aldolase A, LDH, endolase 1 and others (Wenger *et al.*, 2005).

Astrocytes are particularly resistant to hypoxia and ischemia (Hertz, 2008) because their metabolism exhibits some particular features: 1. Astrocytes are well-known to rapidly switch from oxidative metabolism to increase their glycolytic rate under hypoxia as well as ischemia (Hertz, 2008; Prebil *et al.*, 2011), likely accounting for the increase in brain lactate concentrations. 2. Astrocytes are the major stores of glycogen in the brain (Cataldo and Broadwell, 1986a; Cataldo and Broadwell, 1986b), that is utilized during hypoxic but particularly ischemic conditions to replenish cellular energy stores (Kahlert and Reiser, 2004; Niitsu *et al.*, 1999). Importantly glycogen can be more rapidly degraded than glucose during anoxic conditions, as here initiation of glycolysis does not require ATP (Belanger *et al.*, 2011; Hertz, 2008).

Cultured neurons adapt their energy metabolism in response to hypoxia by up-regulation of glycolysis and inhibition of oxidative metabolism (Malthankar-Phatak *et al.*, 2008). However they only possess minor amounts of glycogen and their preferred pathway, oxidative metabolism, is less active during hypoxia (Cataldo and Broadwell, 1986a; Cataldo and Broadwell, 1986b; Wheaton and Chandel, 2011) thus they suffer much more from hypoxic and ischemic injuries than astrocytes.

1.3 HYPOXIC/ISCHEMIC BBB MODULATION

1.3.1 Mechanisms of hypoxic barrier disruption*

Hypoxia, when the oxygen demand of tissues is not met, acts as an initial trigger for pathophysiological changes at the BBB such as altered distribution of water and ions, inflammatory events and oxidative stress, edema formation, infiltration of peripheral immune cells and leakage of blood proteins into the brain. In addition, hypoxia induces major alterations in vessel structure as it stimulates proliferation of ECs leading to formation of new blood vessels and furthermore promotes activation and proliferation of astrocytes (Ogunshola and Al-Ahmad, 2012; Stanimirovic and Friedman, 2012). A large number of *in vivo* and *in vitro* studies have demonstrated that hypoxia is a major stress factor inducing BBB disruption (Al Ahmad *et al.*, 2009; Kaur *et al.*, 2006; Lochhead *et al.*, 2010; Schoch *et al.*, 2002). Regarding the temporal course of hypoxic barrier opening detailed *in vivo* studies are rare. Increased BBB permeability to evans blue has been observed in mice already 6h after onset of hypoxia (7% O_2) (Li *et al.*, 2011). Also after 24 and 48h of hypoxic exposure to 8% O_2 an increased BBB leakage to sodium fluorescein was demonstrated in mice (Bauer *et al.*, 2010; Schoch *et al.*, 2002). An interesting study by Witt and colleagues demonstrated in a rat model that exposure to 6% O_2 for 1h with subsequent re-oxygenation results in a biphasic opening of the BBB within the first hour and again after 6-24h of re-oxygenation (Witt *et al.*, 2008). *In vitro* a decrease in endothelial tightness has been observed between the first 30 min of hypoxic exposure for up to 48h (Abbruscato and Davis, 1999b; Al Ahmad *et al.*, 2009; Fischer *et al.*, 1999; Fleegal *et al.*, 2005; Kuhlmann *et al.*, 2007; Yamagata *et al.*, 2004). Hypoxic exposure of rat brain microvascular endothelial cell line RBE4 to 1% O_2 only induced significant reduction of transendothelial electrical resistance (TEER) after 48h, in contrast in near anoxic conditions (0.1% O_2) a rapid loss of TEER was observed after 4-8h (Al Ahmad *et al.*, 2009). Similarly a study using primary bovine microvascular endothelial cells showed increased permeability to radiolabeled sucrose only after 48h of hypoxic exposure (Abbruscato and Davis, 1999a). In porcine brain endothelial cells TEER was significantly impaired already at 8h of hypoxic exposure (1% O_2) (Yamagata *et al.*, 2004). Overall these results demonstrate

that the time point of barrier impairment *in vitro* is highly dependent on severity of O_2 deprivation, cell sources and culture systems used as well on the read out applied.

The mechanisms of hypoxic barrier disruption have been studied intensively *in vitro* and *in vivo* and it is evident that disruption of the BBB occurs on many different molecular levels. TJ complexes are major targets of hypoxic BBB disruption. At the molecular level hypoxia modulates protein expression levels and subcellular redistribution of occludin, ZO-1 and claudin-5 (Bauer *et al.*, 2010; Fischer *et al.*, 2002; Koto *et al.*, 2007; Mark and Davis, 2002; Willis *et al.*, 2010) that determines their localization at the plasma membrane and interaction with other proteins at the TJ (Luissint *et al.*, 2012). This redistribution critically compromises TJ integrity and is likely mediated via phosphorylation changes at serine, threonine and tyrosine residues and by caveolae-mediated endocytosis. Protein kinase C enzymes, myosin light chain kinase, and RhoA alter TJ protein phosphorylation and contribute to hypoxic or inflammatory barrier disruption (Luissint *et al.*, 2012). Increased transcellular and pinocytic activity of brain ECs are additional events that contribute to augmented barrier permeability during hypoxia (Cipolla *et al.*, 2004; Plateel *et al.*, 1997). Hypoxia-mediated alterations and breakdown of the basement membrane also aggravate BBB opening and are particularly important during ischemic events (Candelario-Jalil *et al.*, 2009; Stanimirovic and Friedman, 2012). Direct and indirect contribution of pericytes and astrocytes to hypoxic-mediated BBB permeability is discussed below.

1.3.2 HIF-1 regulates BBB permeability*

Growing evidence suggests that HIF-1 could play a pivotal role in the changes that occur at the BBB during hypoxia. Good insights have been obtained from cerebral ischemia and reperfusion studies as well as *in vitro* work (Ogunshola and Al-Ahmad, 2012). The HIF-1 inhibitors 2ME2 and YC-1 reduce edema formation (directly correlating to BBB permeability) and infarct volumes in rat models of ischemia/reperfusion and neonatal hypoxic-ischemic brain injury (Chen *et al.*, 2008a; Yeh *et al.*, 2007) whereas rapid DMOG-induced HIF-1α stabilization increased edema formation. In both studies these effects were attributed to modulation in VEGF production (Chen *et al.*, 2008a). In a rat model of cerebral ischemia using middle cerebral artery occlusion, HIF-1 inhibition using YC-1 remarkably reduced BBB impairment as indicated by reduced evans blue extravasation, nonetheless overall a negative

outcome of HIF-1 inhibition on infarct volume and mortality was observed (Yan *et al.*, 2011). Our own *in vitro* work using brain ECs also suggests that HIF-1 stabilization is directly linked with barrier disruption and that inhibition of HIF-1 can significantly improve barrier stability (Engelhardt *et al.*, 2014a) (see Section 3.1). We were able to correlate HIF-1 induced barrier permeability to translocation of claudin-5 and ZO-1 from the plasma membrane, whereas total expression of tight junction proteins was only slightly affected. Importantly we also observed increased tyrosine phosphorylation of occludin and to a minor extent of claudin-5. Overall this implicates that rearrangements at the TJ and posttranslational modifications primarily account for HIF-1 mediated barrier impairment. Likewise HIF-1 inhibition using siRNA in a rat focal ischemia model showed less BBB disruption and a better outcome for the animals in correlation with decreased VEGF levels, as well as reduction of caspase-3 and p53 expression (Chen *et al.*, 2009). These studies highlight that HIF-1 stabilization likely triggers increased BBB permeability through activation of its multiple target genes and signaling cascade.

1.3.3 Contribution of astrocytes and pericytes to hypoxic BBB regulation*

The next section discusses the response of BBB cells to hypoxia/ischemia and their subsequent impact on BBB function.

1.3.3.1 Astrocytes*

Knowledge of the basal responses of astrocytes to reduced oxygenation is limited and far from complete. We know that astrocytes are more resistant to hypoxia and ischemia than neurons. As discussed above this is likely due to their higher capacity to metabolically adapt to hypoxia/ischemia by using alternate energy sources and switching to anaerobic glycolysis thereby ensuring maintenance of the ATP levels (Schmid-Brunclik *et al.*, 2008; Turner and Adamson, 2011). Astrocytes are activated *in vivo* (Kaur *et al.*, 2006) and *in vitro* (Schmid-Brunclik *et al.*, 2008) following hypoxic/ischemic injury and secrete elevated levels of a large number of factors that can be neurotoxic as well as neuroprotective (Trendelenburg and Dirnagl, 2005; Vangeison and Rempe, 2009). Modulation of a variety of proteins by these cells suggests a highly complex tempering of their function and subsequent barrier status.

Indeed a microarray study recorded more than 1100 hypoxia-responsive genes in human astrocytes with 5 times more genes up-regulated than suppressed. Notably many of the up-regulated genes were glycolytic enzymes and angiogenic molecules (Mense *et al.*, 2006). Astrocyte co-culture with ECs results in mutual up-regulation and preservation of anti-oxidant enzymatic activity and reduced radical-induced endothelial cell injury (lipid peroxidation) compared to endothelial monocultures (Ogunshola and Al-Ahmad, 2012; Schroeter *et al.*, 1999). Different *in vitro* studies have shown that astrocyte co-culture or treatment of ECs with astrocyte-conditioned media improves endothelial cell performance and maintenance of barrier function during hypoxic insults (Al Ahmad *et al.*, 2009; Brown *et al.*, 2003; Fischer *et al.*, 2000). Coinciding with these observations astrocytes/astrocyte-conditioned media preserve the junctional localization of TJ proteins, like ZO-1 or claudin-5 (Al Ahmad *et al.*, 2011; Fischer *et al.*, 2000) and hypoxia/glycaemia-dependent down-regulation of the adherens junction protein VE-cadherin is partially reversed in the presence of astrocytes (Abbruscato and Davis, 1999b). Media from hypoxic and re-oxygenated astrocytes contains ANG-1 that increases occludin expression and reduces endothelial proliferation thereby stabilizing the vasculature (Song *et al.*, 2002). In addition co-culture with astrocytes abrogates endothelial caspase-3 activation during hypoxia (Al Ahmad *et al.*, 2009) thereby reducing cell death and caspase-3 mediated TJ disruption (Zehendner *et al.*, 2011).

Astrocytes are also the major source of VEGF in the brain and respond to hypoxic stimuli with increased induction and secretion of VEGF that acts as an endothelial survival factor (Chow *et al.*, 2001; Kaur *et al.*, 2006; Mense *et al.*, 2006; Schmid-Brunclik *et al.*, 2008). However VEGF is also a prominent angiogenic molecule and thus a strong inducer of vascular permeability *in vitro* and *in vivo* (Fischer *et al.*, 1999; Schoch *et al.*, 2002). Our group has shown that despite a beneficial effect of astrocyte co-cultures on hypoxic barrier maintenance, inhibition of VEGF signaling (with the VEGF receptor inhibitor SU1498) further improved maintenance of barrier characteristics (Al Ahmad *et al.*, 2011). In agreement, astrocyte-derived VEGF was also shown to drive BBB disruption after hypoxic exposure (Kaur *et al.*, 2006) and in CNS inflammatory disease (Argaw *et al.*, 2012). Thus the impact of VEGF secretion during insult is multi-faceted. VEGF binds and activates two tyrosine kinase receptors namely VEGFR-1 (Flt-1) and VEGFR-2 (KDR/Flk-1). Hypoxia-induced endothelial

hyper permeability seems to be mediated predominantly by activation of Flt-1 (Vogel *et al.*, 2007) in agreement with the finding that hypoxia up-regulates both the expression of Flt-1 and binding of VEGF to Flt-1 (Fischer *et al.*, 1999). Excellent reviews on hypoxia- and HIF-1-mediated VEGF permeability have been published (Fan *et al.*, 2009; Nakayama and Berger, 2013). However it has also been shown that VEGF splicing can occur in the terminal exon resulting in variants, termed VEGFxxxb, that act as anti-angiogenic dominant negative splice isoforms (Ladomery *et al.*, 2007; Nowak *et al.*, 2008). Notably, high homology means these anti-angiogenic isoforms may have been mistakenly identified as the more canonical species in many studies. Although the ratio of the b-isoforms to the canonical species could be highly relevant, investigations on the effects of stimuli such as hypoxia on these splice variants are yet to be performed.

Astrocytic secretion of MMPs during hypoxia also causes BM reorganization and weakens barrier function. Increased activity of MMP-2, MMP-9 and MMP-13 was detected in hypoxic astrocyte supernatants and treatment of ECs with those supernatants led to MMP-13-dependent delocalization and proteolysis of ZO-1 and disruption of VE-Cadherin (Lu *et al.*, 2009). Astrocytes additionally express various cytokines in response to hypoxic stimulation. For example IL-1β is a HIF-1 target gene (Zhang *et al.*, 2006) that can in a feedback loop activate HIF-1α and VEGF expression in an NFκB-dependent manner in astrocytes and cause down-regulation of the vessel-stabilizing factor SSeCKs (Argaw *et al.*, 2006). Also large amounts of chemokine ligand 2 (CCL2, also referred to as monocyte chemoattractant protein 1 (MCP-1)) and CCL12 (MCP-5) are produced by hypoxic astrocytes in a HIF-1 dependent manner (Mojsilovic-Petrovic *et al.*, 2007). Apart from its main function of recruiting leukocytes at sites of inflammation, CCL2 was shown to increase the paracellular permeability of endothelial monolayers via TJ redistribution mediated by Rho signaling (Stamatovic *et al.*, 2003) and is involved in formation of vasogenic edema *in vivo* (Stamatovic *et al.*, 2005). Altogether, these studies suggest that the hypoxic responses of astrocytes are critical during injury and disease and particularly impact on the stability of the BBB. A summary of the discussed effects of astrocytes on hypoxic barrier function is presented in Table 1.2.

Inductive effects of perivascular cells on BBB function during hypoxia	
Astrocytes	
BBB protective	**BBB permeabilizing**
• reduction of endothelial oxidative stress and radical-induced injury	• vascular endothelial growth factor (VEGF) secretion
• preservation of TJ and AJ structure	• increased matrix metalloproteinase (MMP) activity
• reduction of cell death	• pro-inflammatory cytokines
Pericytes	
BBB protective	**BBB permeabilizing**
• preservation of TJ	• vascular endothelial growth factor (VEGF) secretion
• reduction of cell death	• increased matrix metalloproteinase (MMP) activity
	• pro-inflammatory cytokines

Table 1.2: Summary of astrocytic and pericytic signaling on hypoxic barrier tightness

1.3.3.2 Pericytes*

Only few studies have investigated the survival of pericytes after hypoxic and ischemic insults. Our *in vitro* data suggests that pericytes have comparable sensitivity to astrocytes (see Section 3.2). We did not observe any impairment of mitochondrial activity in pericytes exposed for up to 48h in 0.2% oxygen reflecting no loss of viability, whereas ischemic conditions reduced mitochondrial function only after 24h of exposure (see Section 3.2). Likewise it was shown that ECs are much more susceptible to ischemia than astrocytes and pericytes *in vitro* (Ceruti *et al.*, 2011). I*n vivo* pericytes were observed to migrate away from microvessels in response to traumatic brain injury (Dore-Duffy *et al.*, 2000) and hypoxic stimuli already 2h after onset of the insult and preceding any changes in vessel structure (Gonul *et al.*, 2002). Furthermore a reduction of pericyte-to-endothelial cell ratio was reported after 1 week of hypobaric hypoxia (Dore-Duffy and LaManna, 2007). Although the cell status during these events remains unclear, the fact that the changes occurred during pathologies associated with increased BBB permeability suggest that pericyte loss *per se* could augment barrier leakage. Indeed *in vitro* models highlight that pericyte presence protects endothelial monolayers from hypoxic barrier disruption particularly during prolonged and severe oxygen

deprivation by maintaining TJ protein localization (Al Ahmad *et al.*, 2009; Hayashi *et al.*, 2004) and reducing endothelial caspase-3 activation (Al Ahmad *et al.*, 2009; Al Ahmad *et al.*, 2011). Interestingly, under severe conditions co-culture of pericytes with ECs maintained TEER and reduced paracellular flux of labeled substances better than astrocyte co-cultures (Al Ahmad *et al.*, 2009).

Like astrocytes, pericytes respond to hypoxia with up-regulation of various growth factors. Park *et al*. demonstrated that in retinal pericytes ANG-1, but not ANG-2 mRNA is significantly elevated (Park et al., 2003) again suggesting a vessel stabilizing effect. Interestingly the induction of ANG-1 could be mimicked through treatment of the pericytes with recombinant VEGF (Park *et al.*, 2003). An *in vivo* study suggested that hypoxic pericytes rapidly increase VEGF levels within 24h, whereas astrocytic VEGF production was observed after 4 days (Dore-Duffy and LaManna, 2007). In our studies we observed differential outcome when inhibiting VEGF signaling using SU1498 wherein beneficial effects were observed in endothelial cell pericyte co-cultures during 1% O_2 but not during more severe oxygen deprivation (0.1% O_2) (Al Ahmad *et al.*, 2009). Although temporal-spatial VEGF-mediated induction of ANG-1 may be a plausible explanation for some of the barrier stabilizing effects of pericytes during hypoxia it is unlikely that elevated VEGF expression does not largely contribute to hypoxic barrier disruption, indeed VEGF signaling by other brain cells may also have an impact. Like astrocytes pericytes also secrete MMPs and their expression is augmented through pro-inflammatory cytokines like tumor necrosis factor (TNF) -α (Takata *et al.*, 2011). Additionally pericytes can induce MMP expression in ECs although the link between pericyte MMP expression and hypoxic barrier disruption is still to be properly demonstrated.

Taken together however the data highlights that timing, severity and cellular crosstalk is likely to be very complex. Overall despite limited information, similar to astrocytes, pericytes appear to fulfill important barrier-stabilizing functions but in response to stress also secrete molecules that can cause BBB remodeling and increased permeability. Thus more studies are required to understand the multiple roles of this elusive perivascular cell. A summary of the discussed effects of pericytes on hypoxic barrier function is presented in Table 1.2.

2 AIM OF THE THESIS

The BBB fulfills a fundamental role in controlling brain function during health and disease. Hypoxic and ischemic injuries represent a state of increased BBB permeability and thus disturbance of brain homeostasis. Therefore pathological disruption of BBB stability can have dire consequences. Although a physiologically tight and intact BBB is a required for normal brain function, it inhibits drug delivery and retention in the brain and therefore is often considered a bane in such contexts. Researchers are desperately looking for ways of modulating BBB integrity and increasing drug delivery into the brain. As such better understanding of the mechanisms contributing to barrier opening are valuable in two different ways. Firstly a profound knowledge of the molecular mechanisms of BBB impairment is indispensable to develop novel counteracting therapies for disease treatment; secondly this knowledge can be applied to develop new strategies by which the barrier could be transiently opened for drug delivery.

This work addressed three major questions to deepen our knowledge of hypoxic/ischemic BBB regulation and to better understand how the different cells at the BBB function together in order to control its tightness, as follows:

1. **DOES HIF-1 MEDIATED SIGNALING CONTRIBUTE TO HYPOXIC BBB DISRUPTION AT THE LEVEL OF ENDOTHELIAL TIGHT AND ADHERENS JUNCTIONS?**

   The rat brain microvascular endothelial cell line RBE4 was used to determine the outcome of HIF-1 signaling on BBB function. As such the effects of normoxic HIF-1α stabilization and hypoxic HIF-1 inhibition, on barrier tightness as well as tight and adherens junction modulation were compared to events that occur during hypoxic BBB impairment.

2. **HOW COMPARATIVELY RESISTANT ARE THE DIFFERENT BBB CELL TYPES TO HYPOXIC AND ISCHEMIC INSULTS? DO INDIVIDUAL RESPONSES IN THESE INJURY MODELS CORRELATE TO THEIR ROLES IN BARRIER MODULATION?**

   A comparative study of the hypoxic and ischemic response of RBE4 cells, primary rat brain astrocytes and pericytes was performed. A number of characteristics were assessed including HIF-1α stabilization, hypoxia-induced gene and protein expression, proliferation and cell survival.

3. **WHAT DETERMINES THE SENSITIVITY OF CELLS TO HYPOXIC AND ISCHEMIC INJURIES? IS THERE A GENERAL DIFFERENCE IN CELLULAR METABOLISM BETWEEN ENDOTHELIAL CELLS AND ASTROCYTES?**

   An untargeted liquid-chromatography-mass spectrometry (LC-MS) approach was used to investigate the metabolic changes occurring during O_2 deprivation and ischemia in primary rat brain microvascular endothelial cells and astrocytes. The subsequent analysis focused on identifying pathways and metabolites that confer increased tolerance to astrocytes compared to endothelial cells during such injury conditions.

3 RESULTS

3.1 HYPOXIA SELECTIVELY DISRUPTS BRAIN MICROVASCULAR ENDOTHELIAL TIGHT JUNCTION COMPLEXES TROUGH A HYPOXIA-INDUCIBLE FACTOR-1 (HIF-1) DEPENDENT MECHANISM

Sabrina Engelhardt, Abraham J. Al-Ahmad*, Max Gassmann and Omolara O. Ogunshola*

* Authors contributed equally to manuscript

Journal of Cellular Physiology, Volume 229, Issue 8, pages 1096-1105

Sabrina Engelhardt and Abraham J. Al-Ahmad equally contributed to study experimental design and realization, performed the data analysis and wrote the manuscript. Omolara O. Ogunshola provided funds, designed and supervised the study and wrote the manuscript. Max Gassmann provided financial support and was involved in project discussion.

Journal of Cellular Physiology

Hypoxia Selectively Disrupts Brain Microvascular Endothelial Tight Junction Complexes Through a Hypoxia-Inducible Factor-1 (HIF-1) Dependent Mechanism

SABRINA ENGELHARDT,[1] ABRAHAM J. AL-AHMAD,[2] MAX GASSMANN,[1] AND OMOLARA O. OGUNSHOLA[1]*

[1]*Vetsuisse Faculty, Institute of Veterinary Physiology & Zurich Center Integrative Physiology (ZIHP), University of Zurich, Zurich, Switzerland*

[2]*Department of Chemical & Biological Engineering, College of Engineering, University of Wisconsin-Madison, Wisconsin*

The blood–brain barrier (BBB) constitutes a critical barrier for the maintenance of central nervous system homeostasis. Brain microvascular endothelial cells line the vessel walls and express tight junction (TJ) complexes that restrict paracellular passage across the BBB, thereby fulfilling a crucial role in ensuring brain function. Hypoxia, an impaired O_2 delivery, is known to cause BBB dysfunction but the mechanisms that drive this disruption remain unclear. This study discloses the relevance of the master regulator of the hypoxic response, hypoxia-inducible factor-1 (HIF-1), in hypoxia-induced barrier disruption using the rat brain endothelial cell line RBE4. Hypoxic exposure rapidly induced stabilization of the HIF-1 oxygen-dependent alpha subunit (HIF-1α) concomitantly with BBB impairment and TJ disruption mainly through delocalization and increased tyrosine phosphorylation of TJ proteins. Similar observations were obtained by normoxic stabilization of HIF-1α using $CoCl_2$, deferoxamine, and dimethyloxalylglycine underlining the involvement of HIF-1 in barrier dysfunction particularly via TJ alterations. In agreement inhibition of HIF-1 stabilization by 2-methoxyestradiol and YC-1 improved barrier function in hypoxic cells. Overall our data suggests that activation of HIF-1-mediated signaling disrupts TJ resulting in increased BBB permeability.
J. Cell. Physiol. 229: 1096–1105, 2014. © 2013 Wiley Periodicals, Inc.

The blood–brain barrier (BBB) constitutes a pivotal structure of the neurovascular unit and is primarily formed of specialized brain microvascular endothelial cells that are surrounded and supported by cerebral astrocytes, pericytes, microglia, neurons, and a defined extracellular matrix (Hawkins and Davis, 2005; Daneman, 2012). Microvascular endothelial cells are "gatekeepers" controlling transport of substances between the blood and brain tissue via formation of tight junction (TJ) complexes (Wolburg and Lippoldt, 2002). Notably, proper arrangement and function of TJ complexes is critical for maintenance of BBB integrity.

At least three different types of transmembrane proteins are located at the TJ namely proteins of the claudin family, occludin, and junctional adhesion molecules (Wolburg and Lippoldt, 2002). Integral TJ proteins are linked to each other as well as to the cytoskeleton by cytoplasmic adaptor proteins, such as zonula occludens (ZO), that provide structural stability for the TJ (Gonzalez-Mariscal et al., 2003). All endothelial cells also express adherens junction proteins (AJ), such as VE-Cadherin, PECAM-1, and the cytoplasmic adaptor protein β-catenin, which similarly to TJ physically connect neighboring cells and participate in defining the apical–basal axis of cells (Baum and Georgiou, 2011). Data suggests that AJs can influence TJ organization and function and particularly VE-Cadherin was shown to modulate paracellular permeability via regulation of claudin-5 expression (Taddei et al., 2008) and suppression of occludin phosphorylation (Walsh et al., 2011). As the structural and functional integrity of TJs is a prerequisite for an intact BBB it is not surprising that alterations in these components is a key event in barrier impairment. During the last decades it has become increasingly apparent that BBB disruption contributes to the pathophysiology of many neurological diseases including AIDS, Alzheimer's disease, chronic pain, multiple sclerosis, Parkinson's disease, and stroke (Rosenberg, 2012) although the mechanisms involved remain largely unknown. Hypoxia characterizes many of these diseases and is a major stress factor that induces BBB disruption in vivo and in vitro (Witt et al., 2008; Al Ahmad et al., 2009; McCaffrey et al., 2009; Lochhead et al., 2010; Kimura et al., 2011). The cellular response to hypoxia is predominantly driven through the activation of the hypoxia-induced factor-1 (HIF-1) pathway (Fandrey and Gassmann,

The authors declare no conflict of interest.

Sabrina Engelhardt and Abraham J. Al-Ahmad contributed equally to this work.

Contract grant sponsor: Swiss National Science Foundation; Contract grant number: 31003A-A133016.

*Correspondence to: Omolara O. Ogunshola, Vetsuisse Faculty, Institute of Veterinary Physiology & Zurich Center of Integrative Human Physiology (ZIHP), University of Zurich, Winterthurerstrasse 260, Zurich CH-8057, Switzerland.
E-mail: larao@access.uzh.ch

Manuscript Received: 27 June 2013
Manuscript Accepted: 17 December 2013

Accepted manuscript online in Wiley Online Library (wileyonlinelibrary.com): 25 December 2013.
DOI: 10.1002/jcp.24544

2009). Under normal conditions, the oxygen regulated HIF-1α subunit is rapidly degraded via prolyl hydroxylation that targets its degradation in the proteasome. Hypoxia inhibits prolyl hydroxylase activity resulting in HIF-1α subunit stabilization in the cytoplasm and translocation to the nucleus, where it dimerizes with the aryl-hydrocarbon receptor nuclear translocator (ARNT) to form HIF-1. HIF-1 then binds to hypoxia responsive elements in promotor regions of target genes involved in cellular adaptation to hypoxic stress and induces their expression. To date about 100 HIF-1 target genes have been identified that participate in the control of a variety of different cellular processes such as erythropoiesis, angiogenesis, proliferation, cellular metabolism, survival, and apoptosis (Wenger et al., 2005).

Since HIF-1 is a key determinant for adaptation to oxygen deprivation and is thus crucial for cell survival, it seems likely that this key transcription factor also plays a central role in hypoxia-mediated barrier permeability. This study aimed to directly assess the consequence of HIF-1 induction on barrier integrity using an in vitro model of the BBB. We show that stabilization of HIF-1 rapidly compromises barrier stability predominantly through the disruption of TJ complexes.

Materials and Methods

Materials

Cell culture media and reagents were purchased from Gibco® (Life Technologies, Zug, Switzerland). Basic fibroblast growth factor was obtained from Pepro Tech (Rocky Hill, NJ). 2-methoxyestadiol (2ME2) was ordered from Tocris (Bristol, UK), cobalt chloride ($CoCl_2$), dimethyloxalylglycine (DMOG), and deferoxamine mesylate salt (DFO) from Sigma–Aldrich (Buchs, Switzerland). YC-1 was purchased from Cayman Chemicals (Tallinn, Estonia) and Transwells™ from Corning (Schiphol, The Netherlands). Radiolabeled ^{14}C-Sucrose was purchased from Hartmann Analytic GmbH (Braunschweig, Germany) and 40 kDa FITC-Dextran from Sigma–Aldrich. RIPA lysis buffer was obtained from Cell Signaling Technology (Danvers, MA), protease inhibitor cocktail Set III from Calbiochem (Merck, Darmstadt, Germany). Membrane protein extraction kit was obtained from BioChain (Newark, NJ). Pierce BCA Protein Assay was from Thermo Fisher Scientific Inc. (Rockford, IL). For protein detection by Western blotting and immunofluorescence antibodies directed against occludin, claudin-5, and ZO-1 from Invitrogen (Basel, Switzerland), β-actin antibody from Sigma–Aldrich (Buchs, Switzerland), HIF-1α antibody from Novus Biologicals (Littleton, CO), and β-catenin antibody was from Chemicon (Millipore, Billerica, MA) were used. The PECAM-1 antibody was a gift from Dr. P.J. Newman (BloodCenter of Wisconsin, Milwaukee, WI). Anti-phosphotyrosine antibody agarose conjugate was purchased from Milipore. Secondary antibodies for Western blotting were obtained from Jackson ImmunoResearch (Suffolk, UK) and Alexa-488 conjugated antibodies from Invitrogen were used for immunofluorescence. Quantikine VEGF ELISA kits were from R&D Systems Europe (Abingdon, UK).

Cell culture & reagents

The rat brain endothelial cell line RBE4 was used for all experiments (Roux et al., 1994). Cells were cultivated in 50:50 α-MEM/Ham's F-10 medium mixture supplemented with 10% FBS, 300 μg/ml Geneticin, and 1 ng/ml basic fibroblast growth factor on rat tail collagen coated petri dishes and coverslips. Rat tail collagen was isolated as described (Roll et al., 1980). $CoCl_2$ and DFO were dissolved directly in RBE4 media. All other solutions were made up in DMSO. Diluted working concentrations did not exceed a maximal concentration of 0.1% DMSO.

Barrier function assessment

Barrier function of RBE4 monolayers was assessed by real-time measurement of transendothelial electrical resistance (TEER) as well as paracellular permeability to radiolabeled sucrose and 40 kDa FITC-dextran. Experiments were performed using RBE4 monolayers grown on rat tail collagen-coated Transwells™ as previously described (Al Ahmad et al., 2009). All measurements were normalized to the 0 h time point of the corresponding treatment.

Hypoxic exposures

Hypoxic experiments were carried out in a purpose-built hypoxic glove-box chamber (InVivo$_2$ 400, Ruskinn Technologies, Pencoed, UK) maintained at 37°C with 5% CO_2. O_2 concentration was constantly monitored internally with an O_2 sensor. In all experiments cells were exposed to hypoxia (1% O_2).

Immunoblots

Confluent monolayers were washed with ice-cold PBS and homogenized in RIPA lysis buffer supplemented with protease inhibitor cocktail. Fractionation of membrane and cytoplasmic proteins was performed using the membrane protein extraction kit from BioChain according to the manufacturer's protocol. Accurate protein concentration was determined using Pierce BCA Protein Assay. Twenty-five microgram of total protein were separated by denaturing SDS–Page and subsequently transferred onto nitrocellulose membranes. Membranes were blocked in 5% non-fat dry milk dissolved in TBS or PBS followed by incubation at 4°C overnight in the presence of antibodies directed against β-actin (1:5,000), β-catenin (1:1,000), PECAM-1 (1:7,000) HIF-1α (1:1,000), occludin (1:500), claudin-5 (1:300), or ZO-1 (1:250). Membranes were washed with 0.1% Tween-20 in TBS or PBS and incubated in presence of horseradish peroxidase (HRP) conjugated secondary antibody. Band detection was performed by enhanced chemiluminescent substrate and visualized using luminescent image analyzer LAS-3000 (Fujifilm, Dielsdorf, Switzerland). Blot quantification was performed using ImageJ software (ImageJ, NIH, Bethesda, MD).

Immunoprecipitation (IP)

Cell cultures were washed with cold phosphate-buffered saline containing 1 mM sodium orthovanadate and 50 mM NaF then scraped into lysis buffer (see above). One milligram of protein was suspended in IP buffer (50 mM Tris–HCl pH 7.4, 150 mM EDTA and 0.5% NP-40, 1 mM $NaVO_3$, 1 mM PMSF) and 30 μl of anti-phosphotyrosine antibody agarose conjugate (4G10, Millipore) was added. Samples were then incubated at 4°C in a circular rotator for 3 h prior to centrifugation at 800*g* for 1 min. Supernatant was removed and beads were washed 3× with IP buffer. Captured proteins were eluted from the beads by adding 2× Laemmli buffer, boiling at 80°C for 2 min and centrifugation at 16,000*g* for 2 min. Samples were then run on 15% SDS–Page gel as above.

Cell viability

Cell viability was assayed using a propidium iodide automated cell counter (ADAM, Digital Bio, Witec AG, Littau, Switzerland) according to the manufacturers protocol.

Microscopy and immunofluorescence

Cells were cultured on rat tail collagen coated glass coverslips. After treatments cells were briefly washed with ice-cold PBS, fixed with 4% paraformaldehyde solution then permeabilized

using 0.1% Triton-X100. After blocking with 10% normal goat serum the cells were incubated with primary antibodies against claudin-5 (1:100), ZO-1 (1:100), and β-catenin (1:100) at 4°C overnight. Cells were washed with PBS and incubated in presence of Alexa488-conjugated secondary antibody (1:500). Coverslips were mounted on microscopic slides and micrograph pictures were taken using an inverted fluorescence microscope coupled to an 8-bit CCD camera (Axiocam HR, Carl Zeiss, Feldbach, Switzerland).

Vascular endothelial growth factor Enzyme-Linked Immunosorbent Assay (ELISA)

Intracellular vascular endothelial growth factor (VEGF) measurements in 50 μg of total protein were performed using Quantikine VEGF ELISA kits according to the manufacturers instructions. Optical density was measured at 450 nm, with wavelength correction at 570 nm (Muliskan RC; Thermo Labsystems, Helsinki, Finnland).

Statistical analysis

All results are expressed as mean ± SD from three or more independent experiments. Statistical significance was assessed by one-way ANOVA for comparison of different time points within a group, two-way ANOVA for comparison between different groups. A *P*-value below 0.05 was considered significant.

Results

Hypoxia-driven HIF-1α protein stabilization correlates with barrier disruption in endothelial cells

To observe the effect of hypoxic exposure on HIF-1 stabilization in RBE4 monolayers, we investigated time-dependent changes in HIF-1α protein levels by immunoblot (Fig. 1A). As expected under normoxic conditions HIF-1α was hardly detected, however hypoxia induced significant stabilization within 2 h. HIF-1α levels peaked at 8 h of hypoxic exposure and subsequently declined. Next, we assessed changes in RBE4 monolayer barrier function by TEER (Fig. 1B). Interestingly, we noted a significant decrease in electrical resistance at 8 h, when HIF-1α stabilization was maximal, that remained stable for up to 24 h. Further exposure to hypoxia resulted in complete loss of resistance indicating major barrier disturbance. To further confirm this readout, we measured paracellular permeability to sucrose (342 Da) and 40 kDa FITC-dextran (Fig. 1C). After 24 h we noted a significant increase in sucrose permeability but not of the higher molecular weight FITC-dextran, whereas both molecules showed a significant increase at 48 h.

Hypoxia induces barrier disruption by tight junction rearrangement

Next we investigated the effect of hypoxic exposure on TJ proteins by immunoblotting and immunofluorescence (Fig. 2). Surprisingly no significant change in claudin-5 or occludin protein expression was noted (Fig. 2A,B), although ZO-1 protein levels were significantly down-regulated after prolonged hypoxic exposure (Fig. 2C). Similarly expression of the adherens junction protein VE-cadherin as well as associated proteins β-catenin and PECAM-1 were not significantly affected by hypoxic exposure although a trend for increased protein expression of PECAM-1 was observed (Supplementary Fig. 1A–C). It is well documented that not only absolute TJ protein levels but also their organization and localization is of particular relevance for barrier function (Harhaj and Antonetti, 2004; Johnson et al., 2008). To further investigate these changes we performed immunofluorescence staining after 48 h

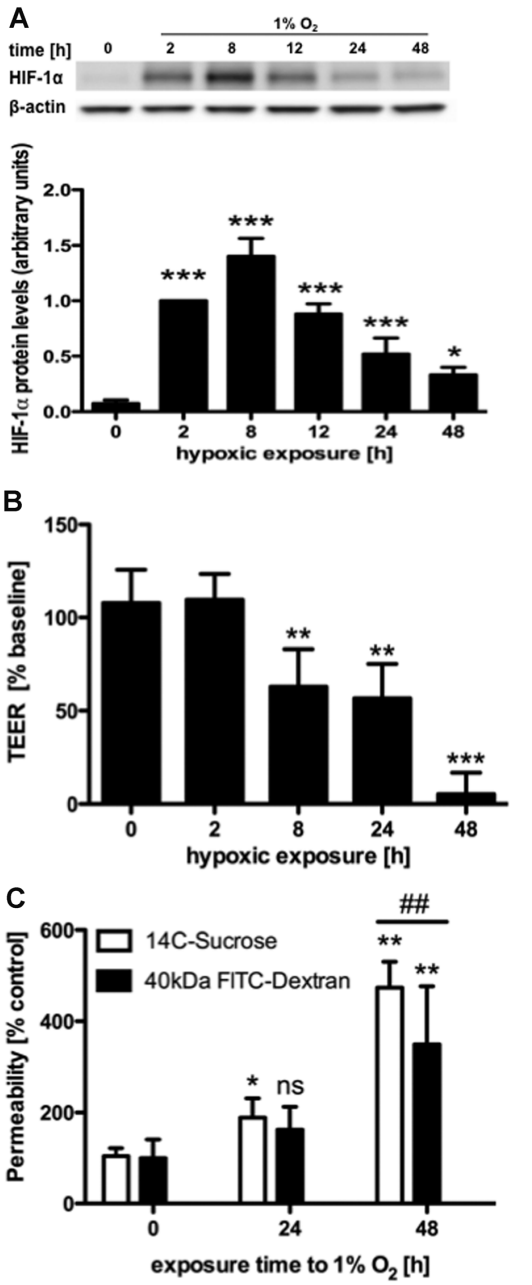

Fig. 1. Hypoxia induces HIF-1α stabilization and barrier disruption in RBE4 monolayers. (A) Upper panel: representative HIF-1α immunoblot of RBE4 cells exposed to 1% O_2 at different time points. Lower panel: Densitometric quantification of HIF-1α protein levels. N = 3; $^{*}P < 0.05$ and $^{***}P < 0.001$ compared to 0 h time point. (B) TEER measurements of RBE4 monolayers exposed to hypoxia. Resistance values were normalized to normoxic control (0 h time point). N = 6, $^{**}P < 0.01$ and $^{***}P < 0.001$. (C) Permeability measurements of normoxic and hypoxic monolayers to ^{14}C-sucrose (342 Da) and FITC-dextran (40 kDa). Values were normalized to normoxic control (0 h time point). N = 4, $^{*}P < 0.05$ and $^{**}P < 0.01$ versus normoxic group, $^{\#\#}P < 0.01$ in comparison between sucrose and FITC-dextran.

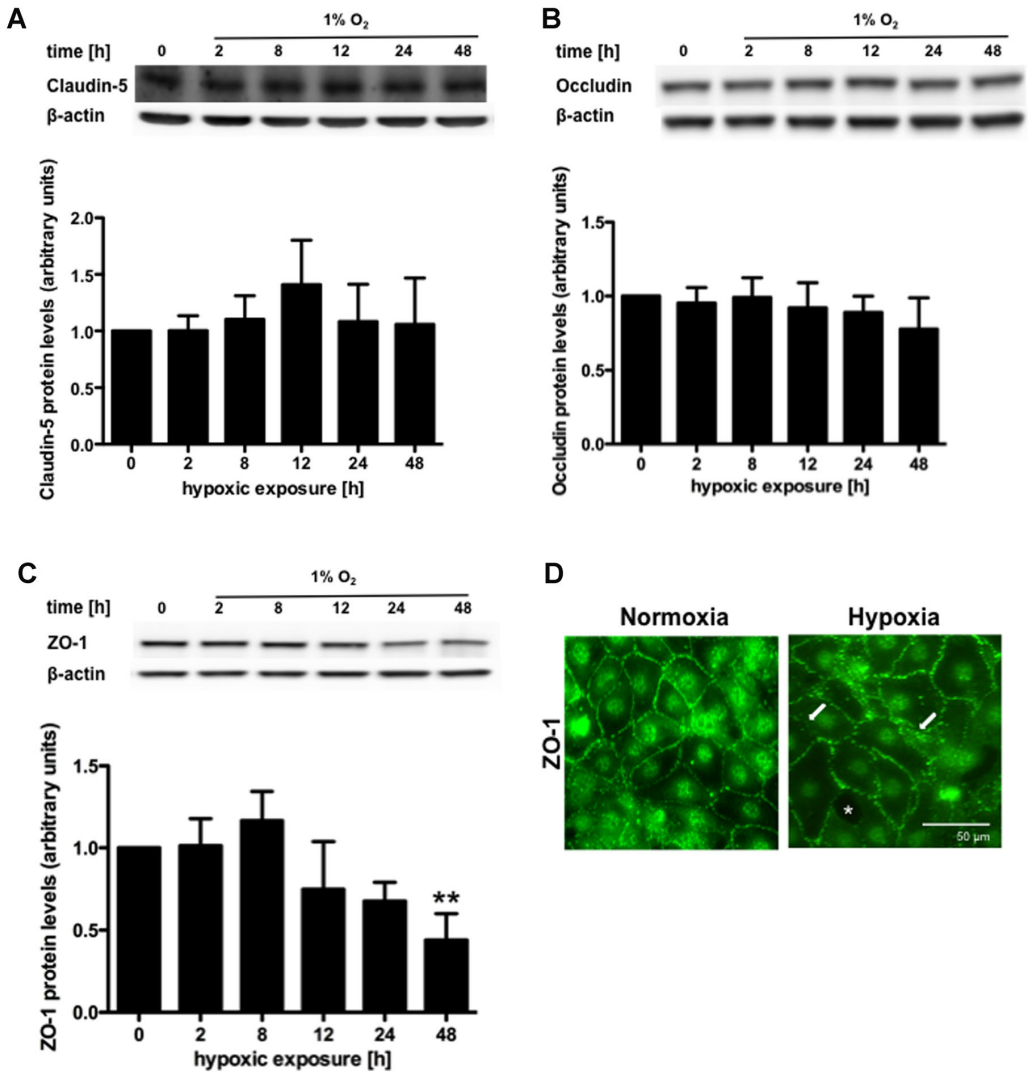

Fig. 2. Effect of hypoxia on TJ protein expression and localization. In all experiments, confluent RBE4 cells were exposed for up to 48 h to 1% O_2. Immunoblots for claudin-5 (A), occludin (B) and ZO-1 (C) (upper panels) were performed and protein levels were quantified by densitometry (lower panels). N = 3, $^{**}P < 0.01$ compared to 0 h time point. (D) Representative micrograph pictures of ZO-1 immunostaining of RBE4 monolayers during normoxia and after 48 h of hypoxic exposure. White arrows highlight disrupted protein localization and asterisk indicates gap formation.

of hypoxic exposure. In hypoxic cells ZO-1 immunoreactivity was discontinuous and heterogeneous (arrows, Fig. 2D) compared to the normoxic control and at some areas we observed formation of intercellular gaps (asterisk, Fig. 2D). Although hypoxic exposure did not affect the localization of either β-catenin or PECAM-1 disruption of VE-cadherin localization was observed (Supplementary Fig. 1D).

HIF-1α stabilization alters TJ protein integrity and barrier function

To determine the direct impact of HIF-1 on barrier disruption we stabilized HIF-1α in normoxic RBE4 cells by treating them with cobalt chloride ($CoCl_2$, 100 μM), dimethyloxalylglycine (DMOG, 100 μM) or deferoxamine (DFO, 100 μM). Firstly, we confirmed HIF-1α stabilization by performing immunoblot of RBE4 cell lysates (Fig. 3A). DFO was the strongest inducer producing the highest HIF-1α levels, followed by $CoCl_2$. Interestingly, DMOG only modestly stabilized HIF-1α compared to the other inhibitors. Similar to results from hypoxic exposure (Fig. 1A) HIF-1α protein levels were strongly elevated at early time points for up to 8 h and then decreased (Fig. 3A). As seen under hypoxic conditions no differences were observed in protein levels for either TJ proteins (claudin-5 and occludin) or AJ proteins (β-catenin and VE-cadherin) after 24 h although DFO did down regulate AJ proteins after

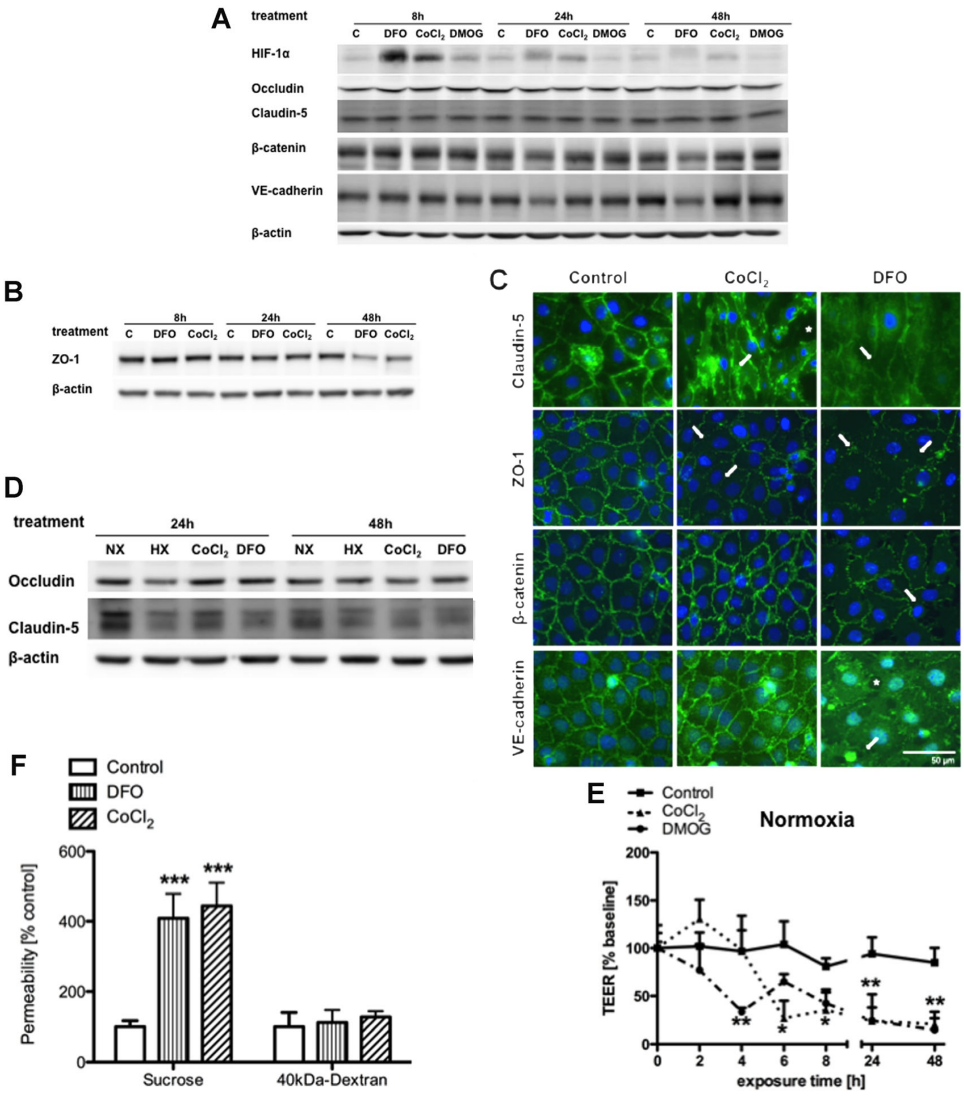

Fig. 3. Pharmacological HIF-1α stabilization disrupts tight junction complexes and impairs barrier function. Immunoblots of RBE4 cell monolayers treated at normoxia with 100 μM $CoCl_2$, 100 μM DFO, or 100 μM DMOG for 8, 24, and 48 h, untreated cells were used as control C (A,B). Western blot analysis of ZO-1 protein expression (B) shows reduced levels after 48 h of DFO and $CoCl_2$ treatment. (C) Representative micrograph pictures of claudin-5, ZO-1, β-catenin, and VE-cadherin localization (green) in endothelial monolayers either untreated or following treatment with either 100 μM $CoCl_2$ or 100 μM DFO for 48 h. Note the disruption of staining in areas marked by arrows. Asterisk indicates gap formation. Blue: DAPI. (D) Western blot was performed after membrane fractionation of monolayers exposed to normoxia (NX), hypoxia (HX), 100 μM $CoCl_2$ or 100 μM DFO (both at normoxia) for 24 and 48 h. Note reduced claudin-5 protein levels in the plasma membrane fraction after 24 and 48 h, whereas occludin levels remain largely unaffected. (E) Barrier function of monolayers exposed to 100 μM $CoCl_2$ or 100 μM DMOG was assessed by TEER, $^{*}P < 0.05$ and $^{**}P < 0.01$ compared to untreated control of corresponding time point. (F) Measurement of paracellular permeability to ^{14}C-sucrose and 40 kDa FITC-dextran in RBE4 monolayers treated for 48 h with 100 μM $CoCl_2$ or 100 μM DFO. N = 3, $^{***}P < 0.001$ compared to untreated control of corresponding time point.

48 h (Fig. 3A). No changes in ZO-1 at 8 and 24 h were observed despite strong HIF-1α induction but decreased levels were observed after 48 h (Fig. 3B) again correlating nicely with the hypoxic treatments suggesting a delayed action between HIF-1α stabilization and ZO-1 down-regulation.

As normoxic HIF-1α stabilization did not induce major changes in TJ protein levels we investigated changes in cell junction localization (Fig. 3C). Treatment with $CoCl_2$ did not significantly alter β-catenin or VE-cadherin but DFO had a stronger effect causing noticeable delocalization. In contrast dramatic changes in claudin-5 and ZO-1 localization were observed using all stabilizers such as stretched appearance of the staining, gap formation (asterisk), increased cytoplasmic localization as well as loss of continuous staining at cell–cell

borders (Fig. 3C, arrows). These changes suggest that the TJ proteins might be trafficked away from the plasma membrane in response to HIF-1α stabilization. To further corroborate this hypothesis we monitored protein levels of claudin-5 and occludin at the plasma membrane following hypoxic exposure and normoxic HIF-1α stabilization by performing membrane fractionation (Fig. 3D). In both cases decreased abundance of claudin-5 was detected in membrane fractions confirming that HIF-1 stabilization reduces claudin-5 retention at TJ complexes validating the immunofluorescence data (Fig. 3C). Surprisingly, we did not observe significant changes in occludin protein levels in the membrane fraction, suggesting that HIF-1 signaling does not appreciably impact occludin localization (Fig. 3D). To underline the relevance of the observed tight junction rearrangements we assessed barrier integrity by TEER and paracellular permeability (Fig. 3E,F). Both DMOG and $CoCl_2$ treatment rapidly decreased barrier resistance within 4–6 h and the disruption remained steady for up to 48 h (Fig. 3E). These data were further confirmed by increased sucrose permeability in cells treated with stabilizers for 48 h although no significant increase in 40 kDa FITC-dextran permeability was detected (Fig. 3F). Notably, neither drug affected cell survival compared to control suggesting that loss of barrier function is unlikely due to increased cell death (Supplementary Fig. 2A). In conclusion the effects of normoxic HIF-1α stabilization on TJ localization and barrier integrity mimicked hypoxia-induced barrier opening.

Inhibition of hypoxic HIF-1α stabilization improves barrier function

To further support our hypothesis that activation of HIF-1 *per se* mediates hypoxic barrier disruption, we pharmacologically inhibited HIF-1 signaling during hypoxic stress to test whether loss of HIF-1 activity can improve barrier function. To this aim we pretreated cells with 1 μM methoxyestradiol (2ME2) or 10 μM YC-1 [frequently used HIF-1 inhibitors (Yeh et al., 2007; Chen et al., 2010; Yan et al., 2011)] prior to hypoxia (Fig. 4A). HIF-1α stabilization was impaired in cells treated with either inhibitor compared to hypoxic treatment only, especially after 8 h (Fig. 4A). Importantly neither 2ME2 nor YC-1 altered expression of claudin-5, occludin, ZO-1, VE-cadherin, or β-catenin protein levels compared to control underlining that HIF-1 does not modulate TJ or AJ at the protein level (Fig. 4A). Next immunofluorescence was used to investigate ZO-1, β-catenin, and VE-cadherin localization in hypoxic cells treated with 2ME2 or YC-1 for 48 h (Fig. 4B). A significant improvement in ZO-1 protein localization compared to control cells was noted by continuous staining at the cell-cell borders and a decrease in frayed junctions. An improvement in VE-cadherin staining was also seen, particularly with 2ME2 treatment, but in contrast no changes in β-catenin localization were observed. We again assessed the relevance of these observations for barrier function and although no improvement in TEER was measured during early time points, a clear beneficial effect was observed after 48 h of exposure (Fig. 4C). Interestingly a differential inhibitor effect was observed as 2ME2-treated cells had better barrier function than those treated with YC-1, displaying higher TEER at 48 h (Fig. 4C) that correlated with decreased permeability to sucrose and 40 kDa FITC-dextran (Fig. 4D). This differential effect was explained by the fact that whereas 2ME2 treatment did not induce cell death YC-1 had a tendency to impair cell survival, although not significantly (Supplementary Fig. 2B).

HIF-1 modulates tight junction protein phosphorylation

Since alterations in BBB integrity are closely associated with TJ phosphorylation, we monitored the tyrosine phosphorylation

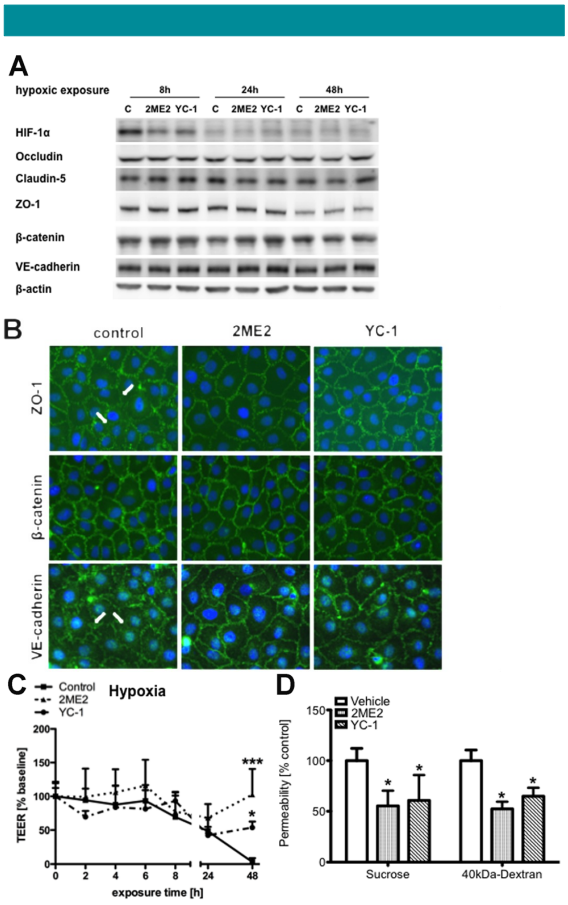

Fig. 4. Inhibition of hypoxia-induced HIF-1α stabilization by 2ME2 and YC-1 partially restores barrier function. (A) Representative immunoblot of HIF-1α, occludin, claudin-5, ZO-1, β-catenin, and VE-cadherin in hypoxic cells treated with 1 μM 2ME2, 10 μM YC-1, and 0.05% DMSO as control C. (B) Representative immunofluorescence of ZO-1, β-catenin, and VE-cadherin (green) in hypoxic RBE4 monolayers treated with 2ME2 or YC-1. Cells were exposed to hypoxia for 48 h, 0.05% DMSO served as control. Arrows denote loss of continuous cell border staining. Blue: DAPI. (C) TEER measurements of hypoxic endothelial monolayers following treatment with 2ME2 or YC-1, compared to control. N = 3, $^{*}P < 0.05$ and $^{***}P < 0.001$ compared to control at corresponding time point. (D) Paracellular permeability of ^{14}C-sucrose and FITC-dextran in cells exposed to hypoxia for 48 h. N = 3, $^{*}P < 0.05$ compared to control at corresponding time point.

status of claudin-5 and occludin proteins by immunoprecipitation. Hypoxia strongly and rapidly increased phosphorylation of both proteins (Fig. 5A). Increased occludin phosphorylation was also strongly mimicked during normoxic HIF-1 induction whereas claudin-5 phosphorylation was only moderately affected (Fig. 5B). In contrast preventing hypoxic HIF-1 stabilization via 2ME2 or YC1 had little effect on phosphorylation status (Fig. 5B and data not shown).

Activation of HIF-1 signaling increases VEGF production in RBE4 cells

VEGF is a well-documented HIF-1 target gene (Wenger et al., 2005) mediating TJ alterations and hypoxic BBB disruption

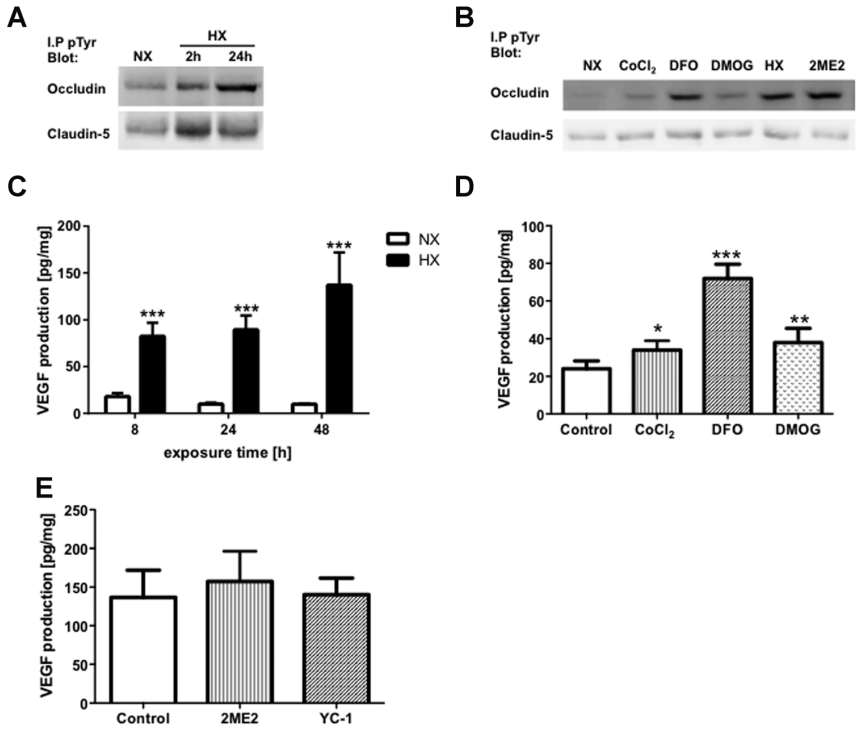

Fig. 5. HIF-1 stabilization increases tight junction protein tyrosine phosphorylation and modulates VEGF levels. (A) Representative immunoblot of proteins immunoprecipitated with phosphotyrosine-specific beads after normoxic (NX) and hypoxic (HX) exposure. (B) Representative immunoblot of occludin and claudin-5 immunoprecipitated with phosphotyrosine-specific beads after 24 h of treatment with HIF-1 stabilizers and inhibitors under normoxia and hypoxia, respectively. ELISA of intracellular VEGF induction of RBE4 cells (C) exposed to normoxia and hypoxia for 8, 24, and 48 h. N = 5, $^{***}P < 0.001$; (D) treated with 100 μM $CoCl_2$, 100 μM DFO, and 100 μM DMOG for 8 h. N = 6 $^{*}P < 0.05$, $^{**}P < 0.01$, $^{***}P < 0.001$ and (E) exposed to hypoxia and treated with 1 μM 2ME2, 10 μM YC-1, and 0.05% DMSO as control. N = 5.

(Fischer et al., 2002). For this reason we investigated whether the normoxic barrier impairment through HIF-1α stabilizers and hypoxic barrier maintenance through HIF-1 inhibitors was mediated via modulation of VEGF levels. As expected hypoxic exposure of RBE4 cells for up to 48 h resulted in robust and sustained up-regulation of intracellular VEGF levels (Fig. 5C) that correlated well with the observed onset of hypoxic barrier disruption after 8 h (Fig. 1B,C). VEGF levels were also elevated upon normoxic HIF-1 stabilization after 8 h of treatment (Fig. 5D) correlating with previous observations (Fig. 3E). In contrast 8 and 24 h of hypoxic exposure with 2ME2 or YC-1 treatment did not alter VEGF levels (data not shown). Unexpectedly, no down-regulation of VEGF levels was observed even after 48 h of HIF-1 inhibition (Fig. 5E) despite a significant improvement of barrier function at this time point (Fig. 4C).

Discussion

O_2 deprivation compromises cerebral tissue integrity and greatly disrupts neuronal function. Although changes in barrier function during hypoxic and ischemic conditions have been documented (Abbruscato and Davis, 1999; Witt et al., 2003; Brown and Davis, 2005; Al Ahmad et al., 2009), until now the relationship between activation of the HIF-1 pathway and barrier function in brain endothelial cells has not been thoroughly investigated. This study provides evidence that HIF-1 signaling participates in hypoxia-driven BBB opening.

HIF-1α stabilization constitutes the key event in the activation of the HIF-1 pathway. Under our experimental conditions, endothelial monolayers demonstrated significant stabilization of HIF-1α after 2 h of hypoxia similar to results in primary rat brain endothelial cells as reported by Luo et al. (2012) that decreased after 12 h of hypoxia suggesting the presence of a negative feedback loop as already proposed for other cells (Stiehl et al., 2006). HIF-1 stabilization is regulated by activity of prolyl hydroxylase (PHD) enzymes that use molecular oxygen to hydroxylate the α subunit and target it for proteasomal degradation (Fandrey and Gassmann, 2009). Inhibition of PHD activity by chelating Fe^{2+} and/or using 2-oxoglutarate competitive substrate analogs (dimethyl-2-oxoglutarate or dimethyloxalylglycine), is a common mechanism for forcing HIF-1α stabilization in a normoxic environment. We used three different HIF-1α stabilizers: deferoxamine (DFO, an iron chelator), cobalt chloride ($CoCl_2$, a substrate analog to iron) and dimethyloxalylglycine (DMOG, a 2-oxoglutarate competitor). Interestingly DFO and $CoCl_2$ were very effective in producing robust HIF-1α stabilization, whereas DMOG effects were more discrete but still induced changes in barrier integrity comparable to $CoCl_2$. Additionally we used 2ME2 and YC-1 to inhibit HIF-1α activity in hypoxia. We again noted differential effects of the inhibitors

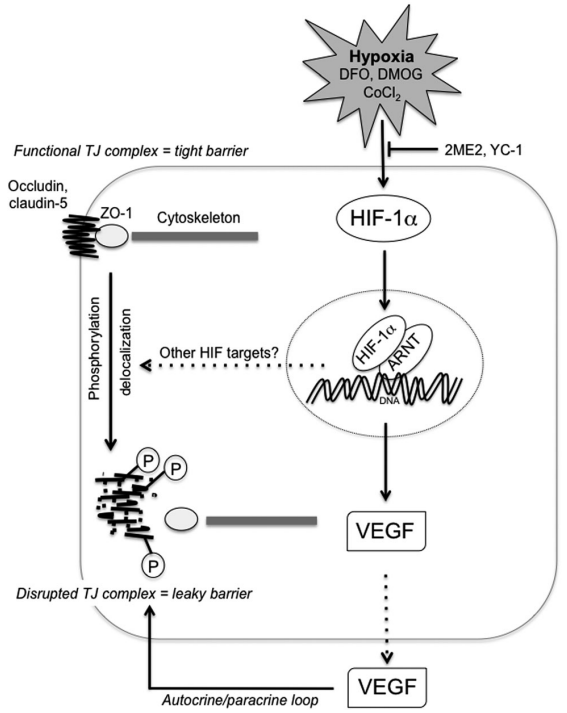

Fig. 6. Proposed mechanism of HIF-1 action on barrier function. Hypoxia (as well as chemical stabilization) stabilizes of HIF-1α and its nuclear translocation where the functional HIF-1 binds target genes and induces VEGF expression. VEGF is then secreted and, by either autocrine or paracrine signaling, participates in disruption of tight junction stability via increased tyrosine phosphorylation and delocalization of tight junction proteins. Direct effects of other HIF-1 targets on tight junction stability cannot be excluded.

likely due to their modes of action (Mabjeesh et al., 2003; Xia et al., 2012).

Both hypoxic HIF-1 induction and normoxic stabilization induced endothelial barrier opening whereas HIF-1 inhibition protected against hypoxic barrier disruption. Delayed opening of the barrier, that is, only after HIF-1α was already stabilized, suggested barrier stability is mediated via one or more HIF-1 effectors. VEGF, an important HIF-1 target gene and well-known vascular permeabilizing factor (Minchenko et al., 1994; Fischer et al., 1999) would be a prominent candidate. Hypoxia-induced VEGF levels were shown to decrease ZO-1 protein expression and induce ZO-1 rearrangements in brain endothelial cells (Fischer et al., 2002; Yeh et al., 2007). Moreover our previous study showed that the VEGF receptor inhibitor SU1498 significantly improves barrier maintenance under hypoxia (Al Ahmad et al., 2009). Thus the delay between HIF-1α stabilization and decreased barrier function may represent the lag time from induction of VEGF expression until its biological efficacy, although other factors are also likely to contribute. Indeed VEGF levels after normoxic HIF-1α stabilization correlated well with VEGF levels during hypoxic exposure, supporting our hypothesis. Although HIF-1 inhibition partially reversed the negative effects of hypoxia by maintaining TJs and decreasing barrier permeability the inhibitors surprisingly failed to reduce VEGF levels. Thus, 2ME2 and YC-1 likely protect BBB integrity by an as yet unidentified mechanism. Of note YC-1 has been shown to prevent $CoCl_2$-induced VEGF expression in vitro (Yeh et al., 2007; Chen et al., 2010; Yan et al., 2011) however we did not detect similar changes in our system.

Structural and functional integrity of TJs is a prerequisite for an intact BBB (Hawkins and Davis, 2005; Luissint et al., 2012). Hypoxic and normoxic HIF-1α stabilization preferentially caused TJ complex rearrangement rather than protein down-regulation, with the exception of ZO-1. Reduced ZO-1 levels following hypoxic exposure nicely correlates with previous literature (Fischer et al., 2002; Koto et al., 2007). In contrast AJ protein expression (VE-cadherin, PECAM-1, and β-catenin) was altered only by DFO treatment although the reasons for this remain largely unclear. A study on hypoxic human corneal epithelial cells also demonstrated very similar effects of hypoxia with decreased barrier function associated with ZO-1 down-regulation whereas protein expression of occludin and the AJ proteins E-cadherin and β-catenin were unaffected (Kimura et al., 2010). In our model ZO-1 and claudin-5 were delocalized from the plasma membrane upon hypoxia and normoxic HIF-1 activation, whereas occludin was unaffected correlating with in vivo studies highlighting the importance of ZO-1 and claudin-5 for normal vascular development and barrier maintenance (Nitta et al., 2003; Katsuno et al., 2008). Similarly, Liu et al. (2012) observed that combined oxygen and glucose deprivation (OGD) did not affect total claudin-5 levels in a mouse endothelial cell line (bEND3) but caused a caveolin-1-mediated redistribution away from cell borders. Interestingly, OGD-induced relocation of ZO-1 and claudin-5 was shown to be partially mediated by caspase-3 activation independently of apoptotic events (Zehendner et al., 2011) and our previous study also revealed a significant contribution of caspase-3 activation to barrier disruption in hypoxic RBE4 cells (Al Ahmad et al., 2009). However, whether these mechanisms are regulated directly by HIF-1 remains to be experimentally addressed. Remarkably organization of the AJ protein VE-cadherin was also disturbed by oxygen deprivation suggesting it may also play a role in maintaining BBB stability in agreement with other studies (Taddei et al., 2008; Walsh et al., 2011). Although the disturbance in our system required a more chronic exposure it is important that the previous studies were not performed on brain microvascular cells and in most cases involved OGD, a very severe insult that would expectedly give rise to more rapid alterations. Transient inhibition of HIF-1 improved barrier function during hypoxic stress, by better maintenance of TJ complexes as well as somewhat improved AJ localization rather than protein up-regulation agreeing with other stress models (Yan et al., 2011, 2012; Yeh et al., 2007). This beneficial response was again observed after prolonged exposure.

Generally post-translational modifications, and particularly phosphorylation of TJ proteins control the biological function of cellular junctions by determining their localization, association with each other and interactions with regulatory proteins (Fischer et al., 2002; Harhaj and Antonetti, 2004; Krause et al., 2008; Blasig et al., 2011). In particular, increased tyrosine phosphorylation of ZO-1 (Fischer et al., 2002) and occludin (Kale et al., 2003; Takenaga et al., 2009; Du et al., 2010) are suggested to participate in hypoxia-mediated barrier breakdown as well as glutamate-mediated disruption (Andras et al., 2007). Moreover, VEGF was also shown to promote tyrosine phosphorylation of ZO-1 and occludin resulting in TJ destabilization and increased permeability (Fischer et al., 2002; Luissint et al., 2012). Although we did not investigate ZO-1 phosphorylation our data advocates that HIF-1, perhaps partially via VEGF induction, mediates increased tyrosine phosphorylation of occludin resulting in barrier dysfunction whereas effects on claudin-5 are less significant. As the

inhibitors failed to prevent hypoxia-induced TJ tyrosine phosphorylation or suppress VEGF levels our data suggests that phosphorylation occurs prior to delocalization since the inhibitors prevent the latter but not the former. Clearly more studies need to be performed to fully answer this intriguing finding.

It must not be overlooked that long-term inhibition of HIF-1α may have a detrimental effect as a tendency to decreased cell viability was seen in cells treated with YC-1. Indeed being a central driving force of cellular adaptation it may be important not to completely block such a beneficial pathway. This raises the dual nature of HIF-1 modulation—clearly its inhibition is essential for minimizing barrier disruption however an exacerbated and extended suppression of its activity may also reduce cell survival and thereby compromise recovery. Thus temporal suppression of HIF-1 activity may be essential to preserve barrier function during injury but basal activity may also be necessary to augment endothelial survival after insult. In this regard it is worth noting that development and future use of small molecule HIF-1 stabilizers (mainly PHD inhibitors) as therapeutics to improve neuronal/cell survival after injury is swiftly gaining widespread attention (Harten et al., 2010; Miyata et al., 2011; Ogunshola and Al-Ahmad, 2012). However, indications that HIF-1 may disturb barrier function means the use of such therapeutics must be treated with caution. Enhanced edema and influx of other blood-borne molecules as a result of increased BBB permeability will increase intracranial pressure and the transport of potentially detrimental substances into the brain parenchyma thereby exacerbating injury. Possible adverse effects of reduced barrier integrity must be carefully assessed when administering HIF-1 stabilizing drugs, and duration of HIF-1 stabilization and the regions being targeted must also be taken into consideration since both will highly influence the outcome of treatment (Miyata et al., 2011; Ogunshola and Al-Ahmad, 2012). Indeed the development of pharmacological agents that limit TJ alterations could selectively target and prevent detrimental effects of HIF-1 on barrier function.

In conclusion, we demonstrate that activation of the HIF-1 pathway mediates hypoxia-induced barrier dysfunction by delocalization and phosphorylation of TJ proteins and VEGF secretion (Fig. 6). Our data also suggests that changes in VE-cadherin may also contribute to BBB alterations. Although this study focused on the endothelial component of the BBB we previously highlighted the importance of astrocytes and pericytes in modulating endothelial cell responses to hypoxia (Al Ahmad et al., 2009, 2011, 2012). Further investigation of how temporal–spatial paracrine signaling between these cells modulates the HIF-1 pathway in brain endothelial cells is essential to provide information not only on the possible outcome of HIF-1 stabilizers on barrier function but also identify new targets to fight injury-induced barrier disruption.

Acknowledgments

This work was supported by SNSF grant number 31003A-A133016 to O.O. Ogunshola.

Literature Cited

Abbruscato TJ, Davis TP. 1999. Combination of hypoxia/aglycemia compromises in vitro blood-brain barrier integrity. J Pharmacol Exp Ther 289:668–675.
Al Ahmad A, Gassmann M, Ogunshola OO. 2009. Maintaining blood-brain barrier integrity: Pericytes perform better than astrocytes during prolonged oxygen deprivation. J Cell Physiol 218:612–622.
Al Ahmad A, Gassmann M, Ogunshola OO. 2012. Involvement of oxidative stress in hypoxia-induced blood-brain barrier breakdown. Microvasc Res 84:222–225.
Al Ahmad A, Taboada CB, Gassmann M, Ogunshola OO. 2011. Astrocytes and pericytes differentially modulate blood-brain barrier characteristics during development and hypoxic insult. J Cereb Blood Flow Metab 31:693–705.
Andras IE, Deli MA, Veszelka S, Hayashi K, Hennig B, Toborek M. 2007. The NMDA and AMPA/KA receptors are involved in glutamate-induced alterations of occludin expression and phosphorylation in brain endothelial cells. J Cereb Blood Flow Metab 27:1431–1443.
Baum B, Georgiou M. 2011. Dynamics of adherens junctions in epithelial establishment, maintenance, and remodeling. J Cell Biol 192:907–917.
Blasig IE, Bellmann C, Cording J, Del Vecchio G, Zwanziger D, Huber O, Haseloff RF. 2011. Occludin protein family: Oxidative stress and reducing conditions. Antioxid Redox Signal 15:1195–1219.
Brown RC, Davis TP. 2005. Hypoxia/aglycemia alters expression of occludin and actin in brain endothelial cells. Biochem Biophys Res Commun 327:1114–1123.
Chen C, Ostrowski RP, Zhou C, Tang J, Zhang JH. 2010. Suppression of hypoxia-inducible factor-1alpha and its downstream genes reduces acute hyperglycemia-enhanced hemorrhagic transformation in a rat model of cerebral ischemia. J Neurosci Res 88:2046–2055.
Daneman R. 2012. The blood–brain barrier in health and disease. Ann Neurol 72:648–672.
Du D, Xu F, Yu L, Zhang C, Lu X, Yuan H, Huang Q, Zhang F, Bao H, Jia L, Wu X, Zhu X, Zhang X, Zhang Z, Chen Z. 2010. The tight junction protein, occludin, regulates the directional migration of epithelial cells. Dev Cell 18:52–63.
Fandrey J, Gassmann M. 2009. Oxygen sensing and the activation of the hypoxia inducible factor 1 (HIF-1)–invited article. Adv Exp Med Biol 648:197–206.
Fischer S, Clauss M, Wiesnet M, Renz D, Schaper W, Karliczek GF. 1999. Hypoxia induces permeability in brain microvessel endothelial cells via VEGF and NO. Am J Physiol 276: C812–C820.
Fischer S, Wobben M, Marti HH, Renz D, Schaper W. 2002. Hypoxia-induced hyperpermeability in brain microvessel endothelial cells involves VEGF-mediated changes in the expression of zonula occludens-1. Microvasc Res 63:70–80.
Gonzalez-Mariscal L, Betanzos A, Nava P, Jaramillo BE. 2003. Tight junction proteins. Prog Biophys Mol Biol 81:1–44.
Harhaj NS, Antonetti DA. 2004. Regulation of tight junctions and loss of barrier function in pathophysiology. Int J Biochem Cell Biol 36:1206–1237.
Harten SK, Ashcroft M, Maxwell PH. 2010. Prolyl hydroxylase domain inhibitors: A route to HIF activation and neuroprotection. Antioxid Redox Signal 12:459–480.
Hawkins BT, Davis TP. 2005. The blood–brain barrier/neurovascular unit in health and disease. Pharmacol Rev 57:173–185.
Johnson PH, Frank D, Costantino HR. 2008. Discovery of tight junction modulators: Significance for drug development and delivery. Drug Discov Today 13:261–267.
Kale G, Naren AP, Sheth P, Rao RK. 2003. Tyrosine phosphorylation of occludin attenuates its interactions with ZO-1, ZO-2, and ZO-3. Biochem Biophys Res Commun 302:324–329.
Katsuno T, Umeda K, Matsui T, Hata M, Tamura A, Itoh M, Takeuchi K, Fujimori T, Nabeshima Y, Noda T, Tsukita S. 2008. Deficiency of zonula occludens-1 causes embryonic lethal phenotype associated with defected yolk sac angiogenesis and apoptosis of embryonic cells. Mol Biol Cell 19:2465–2475.
Kimura K, Teranishi S, Kawamoto K, Nishida T. 2010. Protection of human corneal epithelial cells from hypoxia-induced disruption of barrier function by hepatocyte growth factor. Exp Eye Res 90:337–343.
Kimura K, Teranishi S, Kawamoto K, Nishida T. 2011. Protective effect of dexamethasone against hypoxia-induced disruption of barrier function in human corneal epithelial cells. Exp Eye Res 92:388–393.
Koto T, Takubo K, Ishida S, Shinoda H, Inoue M, Tsubota K, Okada Y, Ikeda E. 2007. Hypoxia disrupts the barrier function of neural blood vessels through changes in the expression of claudin-5 in endothelial cells. Am J Pathol 170:1389–1397.
Krause G, Winkler L, Mueller SL, Haseloff RF, Piontek J, Blasig IE. 2008. Structure and function of claudins. Biochim Biophys Acta 1778:631–645.
Liu J, Jin X, Liu KJ, Liu W. 2012. Matrix metalloproteinase-2-mediated occludin degradation and caveolin-1-mediated claudin-5 redistribution contribute to blood-brain barrier damage in early ischemic stroke stage. J Neurosci 32:3044–3057.
Lochhead JJ, McCaffrey G, Quigley CE, Finch J, DeMarco KM, Nametz N, Davis TP. 2010. Oxidative stress increases blood-brain barrier permeability and induces alterations in occludin during hypoxia-reoxygenation. J Cereb Blood Flow Metab 30:1625–1636.
Luissint AC, Artus C, Glacial F, Ganeshamoorthy K, Couraud PO. 2012. Tight junctions at the blood brain barrier: Physiological architecture and disease-associated dysregulation. Fluids Barriers CNS 9:23.
Luo J, Martinez J, Yin X, Sanchez A, Tripathy D, Grammas P. 2012. Hypoxia induces angiogenic factors in brain microvascular endothelial cells. Microvasc Res 83:138–145.
Mabjeesh NJ, Escuin D, LaVallee TM, Pribluda VS, Swartz GM, Johnson MS, Willard MT, Zhong H, Simons JW, Giannakakou P. 2003. 2ME2 inhibits tumor growth and angiogenesis by disrupting microtubules and dysregulating HIF. Cancer Cell 3:363–375.
McCaffrey G, Willis CL, Staatz WD, Nametz N, Quigley CA, Hom S, Lochhead JJ, Davis TP. 2009. Occludin oligomeric assemblies at tight junctions of the blood-brain barrier are altered by hypoxia and reoxygenation stress. J Neurochem 110:58–71.
Minchenko A, Bauer T, Salceda S, Caro J. 1994. Hypoxic stimulation of vascular endothelial growth factor expression in vitro and in vivo. Lab Invest 71:374–379.
Miyata T, Takizawa S, van Ypersele de Strihou C. 2011. Hypoxia. 1. Intracellular sensors for oxygen and oxidative stress: Novel therapeutic targets. Am J Physiol Cell Physiol 300: C226–C231.
Nitta T, Hata M, Gotoh S, Seo Y, Sasaki H, Hashimoto N, Furuse M, Tsukita S. 2003. Size-selective loosening of the blood-brain barrier in claudin-5-deficient mice. J Cell Biol 161:653–660.
Ogunshola OO, Al-Ahmad A. 2012. HIF-1 at the blood-brain barrier: A mediator of permeability? High Alt Med Biol 13:153–161.
Roll FJ, Madri JA, Albert J, Furthmayr H. 1980. Codistribution of collagen types IV and AB2 in basement membranes and mesangium of the kidney. an immunoferritin study of ultrathin frozen sections. J Cell Biol 85:597–616.
Rosenberg GA. 2012. Neurological diseases in relation to the blood-brain barrier. J Cereb Blood Flow Metab 32:1139–1151.
Roux F, Durieu-Trautmann O, Chaverot N, Claire M, Mailly P, Bourre JM, Strosberg AD, Couraud PO. 1994. Regulation of gamma-glutamyl transpeptidase and alkaline phosphatase activities in immortalized rat brain microvessel endothelial cells. J Cell Physiol 159:101–113.
Stiehl DP, Wirthner R, Koditz J, Spielmann P, Camenisch G, Wenger RH. 2006. Increased prolyl 4-hydroxylase domain proteins compensate for decreased oxygen levels. Evidence for an autoregulatory oxygen-sensing system. J Biol Chem 281:23482–23491.
Taddei A, Giampietro C, Conti A, Orsenigo F, Breviario F, Pirazzoli V, Potente M, Daly C, Dimmeler S, Dejana E. 2008. Endothelial adherens junctions control tight junctions by VE-cadherin-mediated upregulation of claudin-5. Nat Cell Biol 10:923–934.
Takenaga Y, Takagi N, Murotomi K, Tanonaka K, Takeo S. 2009. Inhibition of Src activity decreases tyrosine phosphorylation of occludin in brain capillaries and attenuates increase

in permeability of the blood-brain barrier after transient focal cerebral ischemia. J Cereb Blood Flow Metab 29:1099–1108.
Walsh TG, Murphy RP, Fitzpatrick P, Rochfort KD, Guinan AF, Murphy A, Cummins PM. 2011. Stabilization of brain microvascular endothelial barrier function by shear stress involves VE-cadherin signaling leading to modulation of pTyr-occludin levels. J Cell Physiol 226:3053–3063.
Wenger RH, Stiehl DP, Camenisch G. 2005. Integration of oxygen signaling at the consensus HRE. Sci STKE 2005:re12.
Witt KA, Mark KS, Hom S, Davis TP. 2003. Effects of hypoxia-reoxygenation on rat blood-brain barrier permeability and tight junctional protein expression. Am J Physiol Heart Circ Physiol 285:H2820–H2831.
Witt KA, Mark KS, Sandoval KE, Davis TP. 2008. Reoxygenation stress on blood-brain barrier paracellular permeability and edema in the rat. Microvasc Res 75:91–96.
Wolburg H, Lippoldt A. 2002. Tight junctions of the blood-brain barrier: Development, composition and regulation. Vascul Pharmacol 38:323–337.
Xia Y, Choi HK, Lee K. 2012. Recent advances in hypoxia-inducible factor (HIF)-1 inhibitors. Eur J Med Chem 49:24–40.
Yan J, Zhang Z, Shi H. 2012. HIF-1 is involved in high glucose-induced paracellular permeability of brain endothelial cells. Cell Mol Life Sci 69:115–128.
Yan J, Zhou B, Taheri S, Shi H. 2011. Differential effects of HIF-1 inhibition by YC-1 on the overall outcome and blood-brain barrier damage in a rat model of ischemic stroke. PLoS ONE 6:e27798.
Yeh WL, Lu DY, Lin CJ, Liou HC, Fu WM. 2007. Inhibition of hypoxia-induced increase of blood-brain barrier permeability by YC-1 through the antagonism of HIF-1alpha accumulation and VEGF expression. Mol Pharmacol 72:440–449.
Zehendner CM, Librizzi L, de Curtis M, Kuhlmann CR, Luhmann HJ. 2011. Caspase-3 contributes to ZO-1 and Cl-5 tight-junction disruption in rapid anoxic neurovascular unit damage. PLoS ONE 6:e16760.

Supporting Information

Additional supporting information may be found in the online version of this article at the publisher's web-site.

3.2 DIFFERENTIAL RESPONSES OF BLOOD-BRAIN BARRIER CELLS TO HYPOXIA AND ISCHEMIA - A COMPARATIVE STUDY

Sabrina Engelhardt, Sheng-Fu Huang, Max Gassmann and Omolara O. Ogunshola

submitted to Fluids and Barriers of the CNS, September 2014

Sabrina Engelhardt contributed to experimental design and realization of the study, performed the data analysis and wrote the manuscript. Sheng-Fu Huang contributed to experimental realization of the project. Omolara O. Ogunshola provided funds, designed and supervised the study and wrote the manuscript. Max Gassmann provided financial support and was involved in project discussion.

DIFFERENTIAL RESPONSES OF BLOOD-BRAIN BARRIER CELLS TO HYPOXIA AND ISCHEMIA- A COMPARATIVE STUDY

Sabrina Engelhardt[1], Sheng-Fu Huang[1], Max Gassmann[1], Omolara O. Ogunshola[1]*

[1] Institute of Veterinary Physiology & Zurich Center for Integrative Human Physiology (ZIHP), Vetsuisse Faculty, University of Zurich, Zurich, Switzerland.

Keywords: endothelial cells, astrocytes, pericytes, cell death, HIF-1, in vitro

* Corresponding author:

Omolara O. Ogunshola, PhD

Institute of Veterinary Physiology & Zurich Center for Integrative Human Physiology (ZIHP), Vetsuisse Faculty, University of Zurich, Winterthurerstrasse 260, CH-8057 Zurich, Switzerland.

Tel: +41 44 635 8805, Fax: +41 44 635 8, Email: larao@access.uzh.ch

Total number of figures: 6, total number of tables: 0, supplementary figures: 0

Contract grant sponsor: Swiss National Science Foundation, Contract grant number: 31003A-A133016

ABSTRACT

Undisturbed functioning of the blood-brain barrier (BBB) crucially depends on paracellular signaling between its associated cells namely endothelial cells, pericytes and astrocytes. Hypoxia and ischemia are well-known factors causing BBB impairment and the contribution of the perivascular cells to hypoxic/ischemic barrier regulation has gained increased attention. However, detailed information on hypoxic/ischemic responses of the associated BBB cells is rare. We show that the endothelial cell line RBE4 has greater responsiveness and sensitivity to oxygen deprivation than astrocytes and pericytes. This higher sensitivity coincided with significant stabilization of HIF-1α, early disruption of the actin cytoskeleton and strong metabolic impairment at conditions where the other cell types remained largely unaffected. Moreover, unlike astrocytes and pericytes RBE4 cells were incapable of inducing autophagy as protective mechanism. Both perivascular cells tolerated ischemic conditions well, but importantly astrocytes proved to be most resistant. Our data shows that appropriate adaptation of proliferation and induction of survival-promoting autophagy likely contribute to astrocytic and pericytic tolerance under injury conditions. Thus this study provides important information for a better understanding of the cell-specific hypoxic/ischemic responses of BBB cells, which is fundamental to unravel the complex cellular interaction between the cells in an injury-related context *in vivo.*

INTRODUCTION

Brain neurons require a stable environment and high nutrient supply for proper functioning (Turner and Adamson, 2011). In this regard the well-coordinated teamwork of the cells at the blood-brain barrier (BBB) is indispensable. Endothelial cells (EC) that line barrier vessels have intimate contact with supporting pericytes (PC) and astrocytes (AC), as well as microglia, neurons and a well-defined extracellular matrix to fulfill their gatekeeper function at the BBB, crucially controlling nutrient supply and homeostatic balance (Engelhardt *et al.*, 2014a; Ronaldson and Davis, 2012). It has become very apparent that EC depend on inductive signaling of the surrounding cell types to fully develop and maintain their unique barrier phenotype (Abbott *et al.*, 2006; Ogunshola, 2011). Recently the important contribution of AC and PC to BBB induction and maintenance has received increasing attention (for review see (Engelhardt *et al.*, 2014b)).

Hypoxia (reduced tissue oxygenation) severely impairs BBB function *in vivo* and *in vitro* (Al Ahmad *et al.*, 2009; Kaur *et al.*, 2006; Lochhead *et al.*; Schoch *et al.*, 2002) causing pathophysiological changes including disturbed energy balance and water/ion homeostasis, inflammatory events and leakage of blood-proteins into the brain (Engelhardt *et al.*, 2014b). Similarly ischemia, being characterized by impaired nutrient and O_2 supply, also results in significant BBB breakdown (Liu *et al.*, 2012; Nico and Ribatti, 2012). Clearly, during injury conditions specific responses of AC and PC impact BBB maintenance and brain function. Both AC and PC have been shown to support barrier function via tight junction retention and reduction of endothelial cell death under hypoxic conditions (Al Ahmad *et al.*, 2009; Al Ahmad *et al.*, 2011; Brown *et al.*, 2003; Fischer *et al.*, 2000; Hayashi *et al.*, 2004; Zehendner *et al.*, 2011). On the contrary both cell types up-regulate barrier permeabilizing factors in response to hypoxia/ischemia such as vascular endothelial growth factor (VEGF), cytokines, and matrix metalloproteinases (MMPs) (Mojsilovic-Petrovic *et al.*, 2007; Nomura *et al.*, 1995; Stamatovic *et al.*, 2006; Takata *et al.*, 2011). Currently we do not understand well how, or from where, the differential signals that alter BBB characteristics originate, although some evidence suggests that injury severity and duration determines the functional outcome of hypoxic/ischemic insults on BBB tightness (Chen *et al.*, 2009; Engelhardt *et al.*, 2014b; Halterman and Federoff, 1999). In this regard hypoxia-inducible factor 1 (HIF-1), a central regulator of

hypoxic/ischemic responses, is of particular importance. HIF-1 constitutes a heterodimeric transcription factor composed of the hypoxia-inducible HIF-1α subunit and the constitutively expressed HIF-1β subunit (Fandrey and Gassmann, 2009). HIF-1 mediates hypoxic adaptation through transcriptional control of more than 100 genes participating in angiogenesis, proliferation and cellular metabolism to reduce O_2 consumption and increase O_2 supply but can also trigger cell death (Fandrey and Gassmann, 2009; Ogunshola and Al-Ahmad, 2012; Wenger *et al.*, 2005). The ability of different cell types to adapt to hypoxic/ischemic stress varies considerably. Neurons for example are very sensitive to such insults, whereas other brain cells like astrocytes are far more resistant (Turner and Adamson, 2011). Our previous study showed that AC and PC differentially modulate BBB permeability at varying severities of hypoxic insults (Al Ahmad *et al.*, 2009), implying that insult severity likely triggers individual cell-specific responses with subsequent consequences on barrier modulation.

To gain better knowledge of cell-specific behavior in terms of overall tolerance as well as potential signaling to surrounding cells, we directly compared basal responses of the individual BBB cells (brain microvascular endothelial cell line RBE4, primary rat pericytes and astrocytes) to hypoxic and ischemic insults *in vitro*. We analyzed different parameters that influence hypoxic and ischemic responses including HIF-1α stabilization and HIF-1 target gene expression, actin cytoskeletal alterations, proliferation, and cell survival. Notably the responsiveness and tolerance of the three cell types differed considerably and likely underlies their ability to maintain and/or modulate BBB integrity.

MATERIAL AND METHODS

Cell culture and isolation of primary cells

All cell culture media and reagents were obtained from Gibco® (Life Technologies, Zug, Switzerland). The rat brain endothelial cell line RBE4 (Roux *et al.*, 1994) was cultivated in 1:1 α-MEM/Ham's F-10 medium mixture supplemented with 10% FBS, 300 µg/ml geneticin, and 1 ng/ml basic fibroblast growth factor (Pepro Tech, Rocky Hill, NJ) on rat tail collagen-coated petri dishes. Rat tail collagen was isolated as described in Roll *et al.* (Roll *et al.*, 1980). Primary rat astrocytes were isolated from neonatal pups as described previously (Chow *et al.*, 2001) and cultured in DMEM supplemented with 10% FBS and 50 µg/ml gentamycin sulfate. Primary rat brain pericytes were isolated from male adult rats following an established protocol (Asashima *et al.*, 2002) with slight modifications. Briefly, cortices were homogenized after removal of meninges. Subsequently microvessels were isolated by centrifugation (20 min at 3000 g at 4°C) using dextran (final concentration 16%) and digested in DMEM + 0.1% Collagenase/Dispase + 125 ug/ml DNAse I (both Roche Diagnostics, Rotkreuz, Switzerland) in a water bath for 2h at 37°C. After centrifugation (700 g, 5 min) freshly isolated pericytes were plated on rat tail collagen coated dishes and cultured in DMEM supplemented with 20% FBS, 50 µg/ml gentamycin sulfate and 2.5 µg/ml amphotericin B until confluency. Subsequent passages were maintained on uncoated dishes in astrocyte medium. For all experiments astrocytes and pericytes were used at passage 2.

Hypoxic and ischemic exposures

O_2 deprivation experiments were carried out in purpose-built hypoxic glove-box chambers (In$Vivo_2$ 400, Ruskinn Technologies, Pencoed, UK) maintained at 37°C with 5% CO_2. O_2 concentration was constantly monitored with an internal O_2 sensor. Cells were exposed to hypoxia (1% O_2) and near anoxia (0.2% O_2) for up to 48h. Normoxic controls were maintained at 21% O_2, 5% CO_2 at 37°C. Ischemia was simulated *in vitro* by oxygen-glucose deprivation (OGD). OGD exposures were carried out for astrocytes and pericytes in glucose-free media under hypoxia and near anoxia.

Western blotting

Cells were washed with ice-cold PBS and homogenized in cell lysis buffer (50 mM Tris, 150 mM NaCl, 1% Triton X-100, 1% NP-40) supplemented with protease inhibitor cocktail (Calbiochem, Darmstadt, Germany), 1 mM sodium orthovanadate, 1 mM dithiothreitol, 0.5 mM phenylmethansulfonyl fluoride and 1 mM EDTA. Protein concentration was determined with Pierce BCA protein assay (Thermo Fisher Scientific Inc., Rockford, IL). 20 µg of total protein were separated on denaturing SDS-Page and transferred onto a nitrocellulose membrane. Membranes were blocked at room temperature in 5% non-fat dry milk or 5% BSA dissolved in Tris-buffered saline containing 0.1% Tween-20 and subsequently incubated overnight at 4°C with primary antibodies against β-actin (1:5000, Sigma–Aldrich, Buchs, Switzerland), α-tubulin (1:2000, Sigma–Aldrich), HIF-1α (1:1000, Novus Biologicals, Littleton, CO), LC3 (1:2000, Novus Biologicals), Beclin-1 (1:250, Santa Cruz Biotech, Heidelberg, Germany), Bax (1:1000, Merck Milipore, Darmstadt, Germany) or BNIP3 (1:1000, Cell Signaling Technology, Leiden, The Netherlands). Membranes were washed with 0.1% Tween-20 in TBS and incubated with of horseradish peroxidase conjugated secondary antibody (ImmunoResearch, Suffolk, UK). Band detection was performed using enhanced chemiluminescent substrate and visualized using luminescent image analyzer *LAS-3000* (Fujifilm, Dielsdorf, Switzerland). Blot quantification was performed using ImageJ software (ImageJ, NIH, Bethesda, USA).

Quantitative Real-time PCR

Total RNA was isolated directly from culture dishes using TRIzol® Reagent (Life Technologies, Zug, Switzerland) according to the manufacturer`s description. For cDNA conversion 1 µg of RNA per sample was reverse transcribed using the ImProm-II ReverseTranscriptase kit (Promega, Dübendorf, Switzerland) according to the manufacturer's instructions. Quantitative real-time PCR was performed with an ABI 7500 Fast Real-Time PCR System (Applied Biosystems, Zug, Switzerland) using Power Sybr® Green PCR Master Mix (Applied Biosystems, Zug, Switzerland). The following primers were used: PHD2 5`-AAGCCATGGTCGCCTGTTAC-3` and 5`-TGCGTACCTTGTGGCGTATG-3`, VEGF 5`-CGCAAGAAATCCCGGTTTAA-3` and 5`-CAAATGCTTTCTCCGCTCTGA-3`, GLUT-1 5`-

GGGCATGATTGGTTCCTTCTC-3` and 5`-CAGGTTCATCATCAGCATGGA-3`, MMP-9 5`-GGGAACGTATCTGGAAATTCGAC-3` and 5`-CCGGTTGTGGAAACTCACAC-3`, BNIP3 5`-GCTCCCAGACACCACAAGA-3` and 5`-GCTGAGAAAATTCCCCCTTT-3` and β-actin 5`-CTGGCTCCTAGCACCATGAAG-3` and 5`-GCCACCGATCCACACAGAGT-3`. All data were normalized to β-actin. Fold changes were calculated by the comparative ΔΔCt method.

F-actin staining and microscopy

RBE4 cells were grown on rat tail collagen-coated coverslips, astrocytes on gelatin-coated coverslips and pericytes on uncoated coverslips until confluency. After hypoxic and ischemic exposure cells were fixed in 4% paraformaldehyde, permeabilized in 0.1% Triton X-100 in PBS and stained for filamentous actin (F-actin) using rhodamine-conjugated phalloidin (Life Technologies, Zug, Switzerland). Cell nuclei were counterstained with DAPI (4′,6-Diamidin-2-phenylindol). Pictures were taken using an inverted fluorescence microscope coupled to an 8-bit CCD camera (Axiocam HR, Carl Zeiss, Feldbach, Switzerland) and processed using ImageJ software (ImageJ, NIH, Bethesda, USA).

BrdU incorporation assay

Cell proliferation was measured via BrdU incorporation using the colorimetric BrdU Cell Proliferation ELISA (Roche Diagnostics, Rotkreuz, Switzerland) according to the manufacturer`s instructions. Briefly, 80-90% confluent astrocytes and pericytes were subjected to OGD and O_2 deprivation for 24h and 48h. For 24h treatments BrdU reagent was added simultaneously with onset of OGD/O_2 deprivation, whereas for 48h exposures BrdU was added 24h before the end of the treatment. After exposure cells were fixed for 30 min and incubated for 1.5h at 37°C with a peroxidase conjugated BrdU antibody (anti-BrdU-POD). After three PBS washes, peroxidase substrate was added and plates incubated to reach an $OD_{405/520}$ of 0.4-0.5. The colorimetric reaction was stopped by adding 1M H_2SO_4 and absorbance was read at 450/620 nm using a Multiskan RC Microplate Photometer (Thermo Labsystems, Helsinki, Finnland).

MTT assay

Cell viability was measured using MTT (3-(4,5-dimethylthiazol-2-yl)-2,5-diphenyltetrazolium bromide) assay. All cells were cultured in 96-well plates. After ischemic and hypoxic exposures a 5 mg/ml MTT solution (Sigma-Aldrich, Buchs, Switzerland) was added to the medium to obtain a final concentration 0.5 mg/ml and plates were incubated for 1h at 37°C. Subsequently the media was removed, cells were lysed by adding 100 µl dimethyl sulfoxide and optical density was measured at 560/670 nm using a Multiskan RC Microplate Photometer (Thermo Labsystems, Helsinki, Finnland).

Statistical analysis

All results are expressed as mean ± SD of three or more independent experiments. Statistical significance was assessed by one-way ANOVA for comparison within one group or two-way ANOVA for comparison between different groups using GraphPad Prism 5 software (La Jolla, CA). Bonferroni`s post hoc test was used for all analyses. A *P*-value below 0.05 was considered significant.

RESULTS

HIF-1α induction profiles in BBB cells

Stabilization of HIF-1α protein levels in response to O_2 deprivation represents a central mechanism of cells to adapt to reduced oxygenation (Semenza, 2011; Wenger *et al.*, 2005). HIF-1α expression profiles of the rat endothelial cell line RBE4 (EC), primary rat astrocytes (AC) and pericytes (PC) were analyzed after exposure to hypoxia (HX, 1% O_2) or near anoxia (AX, 0.2% O_2) for up to 24h and compared to normoxic baseline expression (NX+Glc) indicated by the dashed line (Fig. 1A). In addition AC and PC were subjected to oxygen-glucose deprivation (OGD) at 1% and 0.2% O_2. Since EC were extremely sensitive to O_2 deprivation alone already they did not receive additional OGD treatment. In all cell types HIF-1α protein was rapidly stabilized within 2 to 6h after onset of exposure and then reduced again after 24h (Fig. 1A). However the actual induction profiles differed across the cell types; in EC HIF-1α levels reached their plateau already after 2h and remained stable until 6h, whereas in AC HIF-1α stabilization peaked at 6h. PC had an intermediate profile showing already high HIF-1α expression after 2h that tended to increase after 6h. Moreover, AC and PC HIF-1α levels remained elevated after 24h for most exposures, whereas expression levels in RBE4 cells had already returned to baseline. Importantly EC and PC did not show any difference in total HIF-1α expression between HX and AX at any time point. Similarly OGD did not further increase HIF-1α stabilization in PC compared to O_2 deprivation alone. AC, in contrast showed a clear trend of increased HIF-1α expression depending on the severity of the insult (HX versus AX and O_2 deprivation versus OGD) (Fig. 1A).

To directly compare the amount of HIF-1α protein across the three cell types, equal amounts of whole cell lysates exposed to HX (Fig.1B) or AX (Fig.1C) in the presence of glucose were simultaneously analyzed on the same Western blot membrane. Intriguingly EC showed for both O_2 concentrations 3-5 times higher HIF-1α expression than AC and PC. Overall these results imply that RBE4 cells sense low O_2 very rapidly and respond with a strong but short lasting HIF-1α stabilization suggesting a greater responsiveness to O_2 deprivation than AC and PC. The “stereotype” HIF-1α response of EC and PC to mild (HX) and more severe (AX) insults indicates an inability to respond in a more fine-tuned manner as observed in AC.

Differential regulation of HIF-1 and ischemia-inducible gene expression in BBB cells

To further characterize the individual BBB cell responses to reduced oxygenation mRNA expression profiles of the HIF-1 targets PHD2, VEGF and GLUT-1 as well as the hypoxia/ischemia-inducible MMP-9 (Bauer *et al.*, 2010; Wenger *et al.*, 2005) were analyzed by qPCR after 24 and 48h of treatment (Fig. 2B-E). A table of the basal normoxic threshold cycles (CT) for the individual cell types and analyzed genes is presented in Figure 2A. EC had the highest basal expression of PHD2 with a CT of 26.7 compared to AC and PC with a CT of about 28 (Fig. 2A). EC showed only weak induction during O_2 deprivation of maximal 3-fold after 24h, whereas the perivascular cells showed an induction of 5 and10-fold after 24h HX and AX respectively (Fig. 2B). Interestingly exposure to HX-Glc led to a further very pronounced increase in PHD2 mRNA in AC and PC, whereas increased expression after 24h AX-Glc was only observed in PC. The PHD2 profiles of 48h exposures were similar to 24h, although in general the induction levels were slightly lower and the strong PC induction under AX-Glc was lost.

A different behavior of the cell types was observed for VEGF induction (Fig. 2C). Here PC had the highest basal expression during NX with a CT of 26.8, whereas EC and AC had a value of about 29 (Fig. 2A). After 24h of HX EC showed a much stronger induction than AC and PC, whereas during AX the VEGF expression change was comparable between all cell types (Fig. 2C), again suggesting that EC react very strongly to O_2 deprivation compared to AC and PC. After OGD we detected a very strong increase in VEGF induction in AC and PC similarly to PHD2 expression previously. Expression patterns at 48h were similar to 24h with the exception that AX levels were much lower in EC than in AC and PC.

A gradual increase from EC (CT 23) over PC (CT 22) to AC (CT 20) was observed for basal GLUT-1 expression (Fig. 2A). For all cell types we observed a good correlation of increased GLUT-1 mRNA expression with increased severity and duration of the insult (Fig. 2D). Again EC showed the strongest induction (up to 20 fold) during O_2 deprivation followed by PC with the lowest increase in AC (Fig. 2D). Moreover OGD elevated GLUT-1 mRNA in AC and PC compared to O_2 deprivation alone.

Interestingly, basal expression of MMP9 mRNA (CT 33, Fig. 2A) was very low in EC, not altered after 24h of O_2 deprivation and even decreased after 48h (Fig. 2E). AC and PC

showed comparable severity-dependent up-regulation of MMP9 mRNA after 24 and 48h in presence of glucose and OGD differed only in HX-Glc where AC showed a remarkable increase of MMP-9 compared to PC.

In conclusion these findings highlight the differential regulation of hypoxic/barrier-modulating genes in BBB cells and the consequence of cell-specific responses.

Injury induced actin cytoskeletal rearrangements in BBB cells

Reduced oxygenation causes a dynamic regulation of the actin cytoskeleton resulting in changes of cell contractility, shape and motility (Zieseniss, 2014) thereby providing important information on cell state and activation. Changes in F-actin structures were visualized after injury using phalloidin staining (Fig. 3). Under normoxic conditions parallel bundles of F-actin were observed in EC that localized to cell-cell borders and formed a cortical actin rim, a structure being crucial for maintaining endothelial tightness (Prasain and Stevens, 2009) (Fig. 3A). Already within 6h HX- and AX-mediated disruption of the cortical actin rim was observed and characterized by formation of stress fibers (white arrow) while appearance of disassembled F-actin (asterisk, Fig. 3A) occurred within 24h. Furthermore large inter-endothelial gaps were observed after 24h of AX (red arrows, Fig. 3A) and by 48h of AX a large number of cells were detached or dead (data not shown). AC and PC present a different architecture of F-actin with parallel bundles arranged across the cells so called stress fibers (Prasain and Stevens, 2009). In contrast to EC both AC and PC proved to be very insensitive to O_2 deprivation in presence of glucose as no alterations in F-actin organization were observed after 24h in either HX (data not shown) or AX (Fig. 3B) and even prolonged treatment for 48h had no effect (data not shown). Although hypoxic OGD was ineffective, near anoxic OGD caused appearance of condensed and disorganized stress fibers in both cell types after 24h of treatment (Fig. 3B) that was further pronounced after 48h (data not shown). Importantly, the effects on AC were less severe as only a small fraction were affected and cell shape was largely conserved after 24h AX-Glc, whereas nearly all PC displayed significant F-actin disruption and chaotic cell shape changes resulting in very long and thin processes (Fig. 3B). These results underline our previous observation that EC are very

sensitive to O_2 deprivation even in hypoxic conditions, whereas AC and PC tolerate prolonged and severe O_2 deprivation.

AC and PC adapt their proliferation during O_2 deprivation and ischemia

In addition to cytoskeletal changes controlling cell shape and motility, modulation of proliferation represents a crucial factor for survival of hypoxic/ischemic events (Wong *et al.*, 2013). Proliferation of AC and PC was measured using a BrdU incorporation ELISA. RBE4 cells were excluded from the proliferation assays, as the immortalized line is characterized by excessive proliferative rates. Exposure for 24h in presence or absence of glucose did not alter proliferation of AC or PC (Fig. 4A) although a trend towards reduced BrdU incorporation under AX-Glc was measured, albeit slightly stronger in PC (Fig. 4A). Prolonged hypoxic treatment for 48h significantly reduced proliferation in both cell types and was further aggravated by OGD (Fig. 4B). Again a trend of PC being more affected in glucose-free conditions than AC was observed, although not significant. For both cell types BrdU incorporation was severity dependent resulting in virtually complete proliferation inhibition in glucose-free conditions after 48h of treatment (Fig. 4B).

Hypoxic/ischemic exposure differentially affects metabolic activity of BBB cells

To assess BBB cell viability we performed MTT assays that allow overall evaluation of the degree of cellular impairment. After 24h of HX and AX exposure the metabolic activity of EC was already severely reduced by about 40%, whereas AC and PC did not show any change (Fig. 5A). Notably, glucose withdrawal at normal and hypoxic O_2 levels slightly lowered metabolic activity of AC and PC. Interestingly AC were able to maintain this activity even in AX-Glc, whereas the metabolic rate of PC was significantly reduced. Prolonged treatment for 48h delineated further important differences (Fig. 5B) with EC showing only 30% of initial activity during HX, whereas AC and PC remained largely unaffected (Fig. 5B). AX almost completely abolished EC metabolic activity whereas AC were about 30% impaired. Surprisingly, during prolonged normoxic glucose withdrawal PC were less affected than AC that lost more than 50% of their initial activity. However by 48h of HX-Glc similar degrees of AC and PC metabolic impairment that was further accentuated in AX-Glc were observed. In

summary EC exhibit severe and early metabolic impairment during O_2 deprivation even in presence of glucose, whereas both AC and PC remained largely unaffected and tolerate periods of up to 24h OGD in HX or AX very well.

Differential regulation of autophagy and cell death in BBB cells

The effects seen in the MTT assay highlighted interesting differences in cell status and thus cell viability during different injury paradigms. However since this assay does not allow direct conclusion of survival and cell death pathway activation, prominent apoptotic and autophagy markers were analyzed (Fig. 6). Since BNIP3 is a HIF-1 target gene (Wenger *et al.*, 2005) and an important signaling molecule at the interface between autophagy and apoptosis (Kubli *et al.*, 2007; Tracy and Macleod, 2007) its mRNA and protein expression levels were analyzed by qPCR and Western blot respectively (Fig. 6A&B). All three cells upregulated BNIP3 transcription in response to O_2 deprivation, however their fold induction and temporal expression profiles differed strongly (Fig. 6A). An 8-10 fold increase in EC mRNA after 24h of HX and AX was measured, whereas prolonged exposure resulted in only 3-fold induction (Fig. 6A). In total contrast, the induction range for PC and AC was 50-fold and 150-fold respectively with strongly elevated levels of BNIP3 occurring particularly during HX-Glc (Fig. 6A). Unexpectedly BNIP3 protein levels did not reflect the qPCR data for EC at any time point, but instead a significant reduction after 48h of AX was observed (Fig. 6B). In contrast AC and PC protein levels correlated well with the induction seen in the qPCR. Moreover the reduced fold-change induction of BNIP3 protein in PC compared to AC also correlated well with mRNA expression.

The consequences of increased hypoxic BNIP3 expression are discussed very controversially as both cell death/apoptosis promoting (Azad *et al.*, 2008; Kubli *et al.*, 2007) and survival-promoting functions via induction of autophagy have been reported (Bellot *et al.*, 2009; Tracy and Macleod, 2007). The cell death promoting function of BNIP3 has been attributed to Bax activation (Kubli *et al.*, 2007). Bax (Bcl-2 associated protein X) is a crucial regulator of mitochondria-dependent apoptosis, as it forms pores in the outer mitochondrial membrane allowing release of apoptotic proteins such as cytochrome C (Renault and Manon, 2011). We did not observe Bax upregulation in any of the BBB cells (Fig. 7A) and levels stayed constant

up to 24h of O_2 deprivation and/or OGD with prolonged treatment for 48h leading to a significant reduction in all cell types. These results suggest that in our model BNIP3 does not induce Bax-mediated cell death.

BNIP3 also regulates autophagy via the activation of Beclin-1 with subsequent formation of LC3-II (Bellot *et al.*, 2009). Beclin-1 participates in early autophagosome formation by coordinating localization of autophagic proteins and membrane trafficking (Kang *et al.*, 2011). Surprisingly, similar to Bax we did not observe increased Beclin-1 expression in any of the cell types during injury, but a reduction in total protein levels particularly at AX-Glc treatments for AC and PC and at all hypoxic/anoxic for RBE4 cells (Fig. 7B).

To further investigate this intriguing observation we measured levels of LC3 (microtubule-associated protein light chain 3), a central protein of the canonical autophagy machinery and a down-stream target of Beclin-1 (Kang *et al.*, 2011). LC3 exists in 2 isoforms with LC3-I having a cytoplasmic localization whereas LC3-II, though conjugation with phosphatidylethanolamine (PE), localizes at membranes of autophagosomes and therefore its protein levels reflect formation of autophagosomes (Mizushima and Yoshimori, 2007). In all cell types LC3-I levels were only significantly affected after prolonged exposure and severe insults (Fig. 8A) although PC already showed a clear trend of reduced levels after 24h (Fig. 8A). In complete contrast interesting cell-type specific LC3-II profiles were observed. Correlating well with the effects observed for BNIP3 expression EC did not upregulate LC3-II but significantly downregulated its expression suggesting no ongoing autophagy (Fig. 8B). In presence of glucose AC and PC only showed minor changes in LC3-II levels during O_2 deprivation with a mild but significant reduction observed at 48h in both cell types (Fig. 8B). However a glucose-dependent increase in LC3-II levels was observed in both AC and PC. AC showed a strong increase in LC3-II after 24h at NX-Glc and AX-Glc that were even more pronounced after 48h. PC exhibited a significant rise in LC3-II after 24h at all OGD conditions, which were also evident after 48h although slightly reduced (Fig. 8B).

DISCUSSION

The BBB represents a central component for regulation of proper brain function and therefore requires a very tight regulation that depends on signaling inputs of surrounding AC and PC to maintain its unique properties and function (Abbott *et al.*, 2006; Engelhardt *et al.*, 2014b; Ogunshola and Al-Ahmad, 2012). Similarly AC and PC also modulate BBB tightness during hypoxic and ischemic insults, however the critical factors mediating cell-specific responses as well as their functional consequences on BBB integrity remain a topic of debate (Al Ahmad *et al.*, 2009; Engelhardt *et al.*, 2014b; Hayashi *et al.*, 2004; Kaur *et al.*, 2006; Lu *et al.*, 2009; Schroeter *et al.*, 1999). One reason for this is that our understanding about the individual responses of the BBB cellular components in terms of proliferation, survival, target gene induction and barrier modulation during injury is very limited. This study is the first to directly compare hypoxic and ischemic responses of all three major cells types at the BBB and to address various aspects of cellular adaptation and survival. We show that the BBB cells differ considerably in sensitivity to hypoxic and ischemic insults. All our data points to the fact that endothelial cells experience O_2 deprivation much more severely than the other cell types and show a higher susceptibility. Two publications by Ceruti *et al.* and Redzic *et al.* recently compared survival of primary rat endothelial cells, AC and PC under OGD (0% O_2) and similarly concluded that EC are much more susceptible than AC and PC (Ceruti *et al.*, 2011; Redzic *et al.*, 2013). Importantly our data further shows that AC tolerate ischemic injury better than PC. In this regard it is note worthy that the tolerance of the different BBB cells correlates well with the degree of O_2 they experience under physiological conditions *in vivo*. Indeed in brain capillaries an O_2 content of roughly 8% (pO_2 58 mm Hg) has been recorded (Vovenko, 1999), whereas O_2 concentrations in the brain parenchyma are about 4% (pO_2 35 mm Hg) (Koh and Powis, 2012) thus based on their localization EC are accustomed to higher physiological O_2 concentrations than PC and AC.

The HIF-1 signaling pathway crucially controls hypoxic/ischemic gene expression for cell survival and energy metabolism but also expression of genes regulating apoptosis and autophagy (Bagnall *et al.*, 2014; Fandrey and Gassmann, 2009; Ogunshola and Al-Ahmad, 2012). Growing evidence suggests that the severity as well as the duration of an insult play a crucial role in determination of the pathways becoming activated (Al Ahmad *et al.*, 2009;

Chen *et al.*, 2009; Engelhardt *et al.*, 2014b; Halterman and Federoff, 1999). Indeed we observed the more sensitive EC stabilize 3-5 times more HIF-1α protein than the relatively resistant AC and PC, suggesting that HIF-1 induction correlates to sensitivity and may determine functional outcome for the different cells. In addition rapid stabilization of HIF-1α and the observation that O_2 deprivation severity did not alter the amount of HIF-1α stabilized in either EC or PC points to their greater responsiveness towards hypoxia/ischemia, but a less finely tuned response, compared to AC. Other studies have also shown that HIF-1α induction is strongly cell-type dependent. A study by Bracken and colleagues showed that whereas some cells readily stabilize HIF-1α at 5% O_2 others require O_2 levels below 1% and that HIF-1α transactivation, is also dependent on the severity of hypoxic insults in different cell types (Bracken *et al.*, 2006). A direct consequence of HIF-1α stabilization is the induction of HIF-1 target genes and accordingly mRNA levels of such HIF-1 target genes revealed a cell-specific regulation. Pronounced induction of VEGF (particularly during mild hypoxia) and GLUT-1 in EC compared to the other cell types correlated well with their massive HIF-1α stabilization, again underlining their strong responsiveness to hypoxic events. Interestingly despite an early HIF-1α stabilization similar to EC, PC did not induce VEGF expression in comparable strength. As the total levels of HIF-1α stabilization are much lower in PC than in EC this suggests that the amount of HIF-1 accounts for the differential regulation of target genes. In contrast PHD2 and BNIP3 induction levels were much lower in EC than in AC and PC although both are HIF-1 target genes, again suggesting that there is either a cell type-specific regulation/activation or a severity-dependent regulation of HIF-1 target gene expression. Indeed it was shown previously, that mRNA expression of hypoxia-inducible genes varies considerably amongst cell types and that cell-type specific induction of target genes occurs (Chi *et al.*, 2006). Intriguingly the authors could correlate the amount of HIF-1α transcripts and protein abundance to the fold induction of hypoxia responsive genes and most importantly to the susceptibility to the cells to hypoxic injury (Chi *et al.*, 2006). Indeed we herein present very similar correlations.

Appropriate adaptation of energy metabolism is a crucial factor for surviving injurious events like O_2 deprivation and ischemia, thus the transcriptional regulation of the glucose transporter GLUT-1 is of particular interest as glucose represents the major brain energy source (Hertz,

2008). During O_2 deprivation glycolysis becomes crucial for ATP production (Serkova *et al.*, 2008) and strong induction of GLUT-1 in EC during O_2 deprivation agrees with literature showing that in EC and cerebral microvessels glucose consumption as well as transport increases in response to hypoxia (Loike *et al.*, 1992; Mann *et al.*, 2003). This raises the question whether EC are more dependent on glucose uptake to feed their ATP consumption during O_2 deprivation than AC and PC. A possible reason for this can either be that PC and AC exhibit different energy metabolism or that they do not rely as much as EC on glucose *per se* because they can more efficiently use alternate energy sources such as glycogen or glutamate. Interestingly GLUT-1 induction in AC was lower than PC. Indeed their versatile metabolism i.e. ability to exhibit both high rates of oxidative metabolism but also glycolysis as well as to use alternate energy fuels apart from glucose seems to make AC particularly resistant to hypoxic/ischemic injuries (Belanger *et al.*, 2011; Bouzier-Sore and Pellerin, 2013; Prebil *et al.*, 2011; Turner and Adamson, 2011). In addition it has been long known that AC are the major glycogen store within the brain, whereas capillary endothelial cells and PC only possess minor reserves (Cataldo and Broadwell, 1986a; Cataldo and Broadwell, 1986b).

A more global interpretation about the well being of the BBB cells was obtained looking at the actin cytoskeletal architecture and metabolic activity using MTT assay. The results of both experiments accentuated the rapid impairment of RBE4 cells on different levels of cellular function. Firstly the rapid cytoskeletal impairment coincides with loss of BBB function under similar conditions (Al Ahmad *et al.*, 2009; Engelhardt *et al.*, 2014a). And EC metabolic function rapidly decreased at low O_2 concentrations at time points where AC and PC remained completely unaffected. Interestingly, changes in cytoskeleton structure preceded metabolic suppression in all cell types. AC and PC only showed breakdown of their stress fibers and severe inhibition only in severe OGD and prolonged treatments highlighting that both cell types are able to cope well with hypoxia/ischemia. Importantly the results obtained strongly suggested that AC were more resistant to ischemic conditions than PC. Similarly the BrdU proliferation assay suggested higher tolerance of AC to ischemia, as their proliferation rate was better maintained compared to PC although not significantly. Importantly both AC and PC adapted their proliferative rate depending on duration as well as insult severity, likely a crucial reaction to reduce energy consumption and foster cell survival. In line with this a

microarray study showed that hypoxia down-regulated genes were mainly linked to proliferation (Chi *et al.*, 2006). In contrast increased AC proliferation during hypoxia and ischemia has also been reported *in vivo* and *in vitro* during acute (6h) OGD and hypoxic exposure (Fan *et al.*, 2013; Li *et al.*, 2010; Schmid-Brunclik *et al.*, 2008; Zaidi *et al.*, 2004). In our study we did not observe increased proliferation of AC after ischemic treatment, which is probably due to the chronic time point selected suggesting differential effects with different severities.

The changes observed in metabolic activity using MTT assay indicated that a crucial difference between viability of EC versus PC and AC exists. Particularly the HIF-1 target gene BNIP3 represents a point of intersection in regulation of cell viability during O_2 deprivation. For BNIP3 both pro-apoptotic/cell death promoting functions, via Bax activation (Azad *et al.*, 2008; Kubli *et al.*, 2007) and survival-promoting functions via autophagy-related proteins including Beclin-1 and LC3-II (Bellot *et al.*, 2009) have been observed. We did not detect increased Bax levels suggesting that BNIP3 does not promote Bax-mediated cell death in our model system. As indicated by the increase in LC3-II expression our data more points towards BNIP3-mediated induction of autophagy. This observation is further supported by our previous findings, as the resistant AC and PC showed strong BNIP3 expression, whereas the susceptible RBE4 cells did not. Unexpectedly the expression profile of LC3-II did not match the profile observed for BNIP3, indeed we frequently observed low LC3-II when BNIP3 levels were very high. It has been shown that LC3-II represents a good indicator for the number of autophagosomes formed, but does not necessarily indicate autophagic flux, as LC3-II itself is degraded during the maturation of autophagosomes (Mizushima and Yoshimori, 2007). For this reason, a strong activation of autophagy can lead to low LC3-II levels because of its rapid degradation, which then may be misinterpreted as lack of autophagy. To combat this problem drugs inhibiting autophagosome and lysosome fusion can be used, as well as correlation of p62 levels to LC3-II (Mizushima and Yoshimori, 2007). Although our results point towards activation of autophagy by AC and PC to modulate their cell survival additional experiments would be required to fully understand the underlying mechanism, however this was beyond the scope of the current study. In conclusion we can hypothesize that activation of autophagy in our model system represents an adaptive mechanism of AC and PC to cope with

hypoxic/ischemic injuries, potentially by removing damaged mitochondria and regeneration of ATP by catabolism of existing cytoplasmic precursors (Balduini *et al.*, 2012), whereas RBE4 cells do not seem to be able to profit from similar responses. Whether the lack of autophagy induction in RBE4 cells represents a cell line artifact or whether autophagy induction in brain microvascular endothelial cells is not activated in response to hypoxia remains unclear. However for peripheral endothelial cells activation of autophagy in response to hypoxia has been demonstrated (Chen *et al.*, 2013). Interestingly it has been shown that survival-promoting BNIP3-mediated mitochondrial autophagy represents a HIF-1 dependent mechanism (Zhang *et al.*, 2008)

In conclusion this study highlights that the BBB cell types vary considerably in their sensitivity to O_2 deprivation and ischemia. We show on different levels of cellular responses that EC are highly susceptible to O_2 deprivation, whereas AC and PC are very tolerant to sole O_2 deprivation and even ischemic conditions, although AC tolerate extreme ischemic exposure (0.2% O_2) better than PC. We advocate that the physiological oxygen concentration that cells experience plays a significant role in their sensitivity to insult. Clearly, since differential susceptibility underlies BBB alterations better understanding of such causative relationships is crucial to combat BBB disturbance during injury.

REFERENCES

Abbott, N. J., L. Ronnback and E. Hansson. 2006. Astrocyte-endothelial interactions at the blood-brain barrier. *Nat Rev Neurosci.* 7:41-53.

Al Ahmad, A., M. Gassmann and O. O. Ogunshola. 2009. Maintaining blood-brain barrier integrity: pericytes perform better than astrocytes during prolonged oxygen deprivation. *J Cell Physiol.* 218:612-622.

Al Ahmad, A., C. B. Taboada, M. Gassmann and O. O. Ogunshola. 2011. Astrocytes and pericytes differentially modulate blood-brain barrier characteristics during development and hypoxic insult. *J Cereb Blood Flow Metab.* 31:693-705.

Asashima, T., H. Iizasa, T. Terasaki, K. Hosoya, K. Tetsuka, M. Ueda, M. Obinata and E. Nakashima. 2002. Newly developed rat brain pericyte cell line, TR-PCT1, responds to transforming growth factor-beta1 and beta-glycerophosphate. *Eur J Cell Biol.* 81:145-152.

Azad, M. B., Y. Chen, E. S. Henson, J. Cizeau, E. McMillan-Ward, S. J. Israels and S. B. Gibson. 2008. Hypoxia induces autophagic cell death in apoptosis-competent cells through a mechanism involving BNIP3. *Autophagy.* 4:195-204.

Bagnall, J., J. Leedale, S. E. Taylor, D. G. Spiller, M. R. White, K. J. Sharkey, R. N. Bearon and V. See. 2014. Tight control of hypoxia-inducible factor-alpha transient dynamics is essential for cell survival in hypoxia. *J Biol Chem.* 289:5549-5564.

Balduini, W., S. Carloni and G. Buonocore. 2012. Autophagy in hypoxia-ischemia induced brain injury. *J Matern Fetal Neonatal Med.* 25 Suppl 1:30-34.

Bauer, A. T., H. F. Burgers, T. Rabie and H. H. Marti. 2010. Matrix metalloproteinase-9 mediates hypoxia-induced vascular leakage in the brain via tight junction rearrangement. *Journal of cerebral blood flow and metabolism : official journal of the International Society of Cerebral Blood Flow and Metabolism.* 30:837-848.

Belanger, M., I. Allaman and P. J. Magistretti. 2011. Brain energy metabolism: focus on astrocyte-neuron metabolic cooperation. *Cell Metab.* 14:724-738.

Bellot, G., R. Garcia-Medina, P. Gounon, J. Chiche, D. Roux, J. Pouyssegur and N. M. Mazure. 2009. Hypoxia-induced autophagy is mediated through hypoxia-inducible factor induction of BNIP3 and BNIP3L via their BH3 domains. *Mol Cell Biol.* 29:2570-2581.

Bouzier-Sore, A. K. and L. Pellerin. 2013. Unraveling the complex metabolic nature of astrocytes. *Front Cell Neurosci.* 7:179.

Bracken, C. P., A. O. Fedele, S. Linke, W. Balrak, K. Lisy, M. L. Whitelaw and D. J. Peet. 2006. Cell-specific regulation of hypoxia-inducible factor (HIF)-1alpha and HIF-2alpha stabilization and transactivation in a graded oxygen environment. *J Biol Chem.* 281:22575-22585.

Brown, R. C., K. S. Mark, R. D. Egleton, J. D. Huber, A. R. Burroughs and T. P. Davis. 2003. Protection against hypoxia-induced increase in blood-brain barrier permeability: role of tight junction proteins and NFkappaB. *Journal of cell science.* 116:693-700.

Cataldo, A. M. and R. D. Broadwell. 1986a. Cytochemical identification of cerebral glycogen and glucose-6-phosphatase activity under normal and experimental conditions: I. Neurons and glia. *Journal of Electron Microscopy Technique.* 3:413-437.

Cataldo, A. M. and R. D. Broadwell. 1986b. Cytochemical identification of cerebral glycogen and glucose-6-phosphatase activity under normal and experimental conditions. II. Choroid plexus and ependymal epithelia, endothelia and pericytes. *J Neurocytol.* 15:511-524.

Ceruti, S., L. Colombo, G. Magni, F. Vigano, M. Boccazzi, M. A. Deli, B. Sperlagh, M. P. Abbracchio and A. Kittel. 2011. Oxygen-glucose deprivation increases the enzymatic activity and the microvesicle-mediated release of ectonucleotidases in the cells composing the blood-brain barrier. *Neurochemistry international.*

Chen, G., W. Zhang, Y. P. Li, J. G. Ren, N. Xu, H. Liu, F. Q. Wang, Z. J. Sun, J. Jia and Y. F. Zhao. 2013. Hypoxia-induced autophagy in endothelial cells: a double-edged sword in the progression of infantile haemangioma? *Cardiovasc Res.* 98:437-448.

Chen, W., R. Hartman, R. Ayer, S. Marcantonio, J. Kamper, J. Tang and J. H. Zhang. 2009. Matrix metalloproteinases inhibition provides neuroprotection against hypoxia-ischemia in the developing brain. *J Neurochem.* 111:726-736.

Chi, J. T., Z. Wang, D. S. Nuyten, E. H. Rodriguez, M. E. Schaner, A. Salim, Y. Wang, G. B. Kristensen, A. Helland, A. L. Borresen-Dale, A. Giaccia, M. T. Longaker, T.

Hastie, G. P. Yang, M. J. van de Vijver and P. O. Brown. 2006. Gene expression programs in response to hypoxia: cell type specificity and prognostic significance in human cancers. *PLoS Med.* 3:e47.

Chow, J., O. Ogunshola, S. Y. Fan, Y. Li, L. R. Ment and J. A. Madri. 2001. Astrocyte-derived VEGF mediates survival and tube stabilization of hypoxic brain microvascular endothelial cells in vitro. *Brain research. Developmental brain research.* 130:123-132.

Engelhardt, S., A. J. Al-Ahmad, M. Gassmann and O. O. Ogunshola. 2014a. Hypoxia selectively disrupts brain microvascular endothelial tight junction complexes through a hypoxia-inducible factor-1 (HIF-1) dependent mechanism. *J Cell Physiol.* 229:1096-1105.

Engelhardt, S., S. Patkar and O. O. Ogunshola. 2014b. Cell-specific blood-brain barrier regulation in health and disease: a focus on hypoxia. *Br J Pharmacol.* 171:1210-1230.

Fan, Y. Y., J. M. Zhang, H. Wang, X. Y. Liu and F. H. Yang. 2013. Leukemia inhibitory factor inhibits the proliferation of primary rat astrocytes induced by oxygen-glucose deprivation. *Acta Neurobiol Exp (Wars).* 73:485-494.

Fandrey, J. and M. Gassmann. 2009. Oxygen sensing and the activation of the hypoxia inducible factor 1 (HIF-1)--invited article. *Adv Exp Med Biol.* 648:197-206.

Fischer, S., M. Wobben, J. Kleinstuck, D. Renz and W. Schaper. 2000. Effect of astroglial cells on hypoxia-induced permeability in PBMEC cells. *American journal of physiology. Cell physiology.* 279:C935-944.

Halterman, M. W. and H. J. Federoff. 1999. HIF-1alpha and p53 promote hypoxia-induced delayed neuronal death in models of CNS ischemia. *Exp Neurol.* 159:65-72.

Hayashi, K., S. Nakao, R. Nakaoke, S. Nakagawa, N. Kitagawa and M. Niwa. 2004. Effects of hypoxia on endothelial/pericytic co-culture model of the blood-brain barrier. *Regulatory peptides.* 123:77-83.

Hertz, L. 2008. Bioenergetics of cerebral ischemia: a cellular perspective. *Neuropharmacology.* 55:289-309.

Kang, R., H. J. Zeh, M. T. Lotze and D. Tang. 2011. The Beclin 1 network regulates autophagy and apoptosis. *Cell Death Differ.* 18:571-580.

Kaur, C., V. Sivakumar, Y. Zhang and E. A. Ling. 2006. Hypoxia-induced astrocytic reaction and increased vascular permeability in the rat cerebellum. *Glia.* 54:826-839.

Koh, M. Y. and G. Powis. 2012. Passing the baton: the HIF switch. *Trends Biochem Sci.* 37:364-372.

Kubli, D. A., J. E. Ycaza and A. B. Gustafsson. 2007. Bnip3 mediates mitochondrial dysfunction and cell death through Bax and Bak. *Biochem J.* 405:407-415.

Li, L., J. V. Welser, P. Dore-Duffy, G. J. del Zoppo, J. C. Lamanna and R. Milner. 2010. In the hypoxic central nervous system, endothelial cell proliferation is followed by astrocyte activation, proliferation, and increased expression of the alpha 6 beta 4 integrin and dystroglycan. *Glia.* 58:1157-1167.

Liu, J., X. Jin, K. J. Liu and W. Liu. 2012. Matrix metalloproteinase-2-mediated occludin degradation and caveolin-1-mediated claudin-5 redistribution contribute to blood-brain barrier damage in early ischemic stroke stage. *The Journal of neuroscience : the official journal of the Society for Neuroscience.* 32:3044-3057.

Lochhead, J. J., G. McCaffrey, C. E. Quigley, J. Finch, K. M. DeMarco, N. Nametz and T. P. Davis. Oxidative stress increases blood-brain barrier permeability and induces alterations in occludin during hypoxia-reoxygenation. *J Cereb Blood Flow Metab.* 30:1625-1636.

Loike, J. D., L. Cao, J. Brett, S. Ogawa, S. C. Silverstein and D. Stern. 1992. Hypoxia induces glucose transporter expression in endothelial cells. *Am J Physiol.* 263:C326-333.

Lu, D. Y., W. H. Yu, W. L. Yeh, C. H. Tang, Y. M. Leung, K. L. Wong, Y. F. Chen, C. H. Lai and W. M. Fu. 2009. Hypoxia-induced matrix metalloproteinase-13 expression in astrocytes enhances permeability of brain endothelial cells. *Journal of cellular physiology.* 220:163-173.

Mann, G. E., D. L. Yudilevich and L. Sobrevia. 2003. Regulation of amino acid and glucose transporters in endothelial and smooth muscle cells. *Physiol Rev.* 83:183-252.

Mizushima, N. and T. Yoshimori. 2007. How to interpret LC3 immunoblotting. *Autophagy.* 3:542-545.

Mojsilovic-Petrovic, J., D. Callaghan, H. Cui, C. Dean, D. B. Stanimirovic and W. Zhang. 2007. Hypoxia-inducible factor-1 (HIF-1) is involved in the regulation of hypoxia-stimulated expression of monocyte chemoattractant protein-1 (MCP-1/CCL2) and MCP-5 (Ccl12) in astrocytes. *Journal of neuroinflammation.* 4:12.

Nico, B. and D. Ribatti. 2012. Morphofunctional aspects of the blood-brain barrier. *Curr Drug Metab.* 13:50-60.

Nomura, M., S. Yamagishi, S. Harada, Y. Hayashi, T. Yamashima, J. Yamashita and H. Yamamoto. 1995. Possible participation of autocrine and paracrine vascular endothelial growth factors in hypoxia-induced proliferation of endothelial cells and pericytes. *J Biol Chem.* 270:28316-28324.

Ogunshola, O. O. 2011. In vitro modeling of the blood-brain barrier: simplicity versus complexity. *Curr Pharm Des.* 17:2755-2761.

Ogunshola, O. O. and A. Al-Ahmad. 2012. HIF-1 at the blood-brain barrier: a mediator of permeability? *High altitude medicine & biology.* 13:153-161.

Prasain, N. and T. Stevens. 2009. The actin cytoskeleton in endothelial cell phenotypes. *Microvascular research.* 77:53-63.

Prebil, M., J. Jensen, R. Zorec and M. Kreft. 2011. Astrocytes and energy metabolism. *Arch Physiol Biochem.* 117:64-69.

Redzic, Z. B., T. Rabie, B. A. Sutherland and A. M. Buchan. 2013. Differential effects of paracrine factors on the survival of cells of the neurovascular unit during oxygen glucose deprivation. *International journal of stroke : official journal of the International Stroke Society.*

Renault, T. T. and S. Manon. 2011. Bax: Addressed to kill. *Biochimie.* 93:1379-1391.

Roll, F. J., J. A. Madri, J. Albert and H. Furthmayr. 1980. Codistribution of collagen types IV and AB2 in basement membranes and mesangium of the kidney. an immunoferritin study of ultrathin frozen sections. *J Cell Biol.* 85:597-616.

Ronaldson, P. T. and T. P. Davis. 2012. Blood-brain barrier integrity and glial support: mechanisms that can be targeted for novel therapeutic approaches in stroke. *Curr Pharm Des.* 18:3624-3644.

Roux, F., O. Durieu-Trautmann, N. Chaverot, M. Claire, P. Mailly, J. M. Bourre, A. D. Strosberg and P. O. Couraud. 1994. Regulation of gamma-glutamyl transpeptidase and alkaline phosphatase activities in immortalized rat brain microvessel endothelial cells. *J Cell Physiol.* 159:101-113.

Schmid-Brunclik, N., C. Burgi-Taboada, X. Antoniou, M. Gassmann and O. O. Ogunshola. 2008. Astrocyte responses to injury: VEGF simultaneously modulates cell death and proliferation. *Am J Physiol Regul Integr Comp Physiol.* 295:R864-873.

Schoch, H. J., S. Fischer and H. H. Marti. 2002. Hypoxia-induced vascular endothelial growth factor expression causes vascular leakage in the brain. *Brain.* 125:2549-2557.

Schroeter, M. L., K. Mertsch, H. Giese, S. Muller, A. Sporbert, B. Hickel and I. E. Blasig. 1999. Astrocytes enhance radical defence in capillary endothelial cells constituting the blood-brain barrier. *FEBS Lett.* 449:241-244.

Semenza, G. L. 2011. Hypoxia-inducible factor 1: regulator of mitochondrial metabolism and mediator of ischemic preconditioning. *Biochim Biophys Acta.* 1813:1263-1268.

Serkova, N. J., N. A. Reisdorph and M. C. Patot. 2008. Metabolic Markers of Hypoxia: Systems Biology Application in Biomedicine. *Toxicology Mechanisms and Methods.* 18:81-95.

Stamatovic, S. M., O. B. Dimitrijevic, R. F. Keep and A. V. Andjelkovic. 2006. Protein kinase Calpha-RhoA cross-talk in CCL2-induced alterations in brain endothelial permeability. *The Journal of biological chemistry.* 281:8379-8388.

Takata, F., S. Dohgu, J. Matsumoto, H. Takahashi, T. Machida, T. Wakigawa, E. Harada, H. Miyaji, M. Koga, T. Nishioku, A. Yamauchi and Y. Kataoka. 2011. Brain pericytes among cells constituting the blood-brain barrier are highly sensitive to tumor necrosis factor-alpha, releasing matrix metalloproteinase-9 and migrating in vitro. *J Neuroinflammation.* 8:106.

Tracy, K. and K. F. Macleod. 2007. Regulation of mitochondrial integrity, autophagy and cell survival by BNIP3. *Autophagy.* 3:616-619.

Turner, D. A. and D. C. Adamson. 2011. Neuronal-Astrocyte Metabolic Interactions. *Journal of Neuropathology and Experimental Neurology.* 70:167-176.

Vovenko, E. 1999. Distribution of oxygen tension on the surface of arterioles, capillaries and venules of brain cortex and in tissue in normoxia: an experimental study on rats. *Pflugers Arch.* 437:617-623.

Wenger, R. H., D. P. Stiehl and G. Camenisch. 2005. Integration of oxygen signaling at the consensus HRE. *Science's STKE : signal transduction knowledge environment.* 2005:re12.

Wong, W. J., B. Qiu, M. S. Nakazawa, G. Qing and M. C. Simon. 2013. MYC degradation under low O2 tension promotes survival by evading hypoxia-induced cell death. *Mol Cell Biol.* 33:3494-3504.

Zaidi, A. U., D. A. Bessert, J. E. Ong, H. Xu, J. D. Barks, F. S. Silverstein and R. P. Skoff. 2004. New oligodendrocytes are generated after neonatal hypoxic-ischemic brain injury in rodents. *Glia.* 46:380-390.

Zehendner, C. M., L. Librizzi, M. de Curtis, C. R. Kuhlmann and H. J. Luhmann. 2011. Caspase-3 contributes to ZO-1 and Cl-5 tight-junction disruption in rapid anoxic neurovascular unit damage. *PloS one.* 6:e16760.

Zhang, H., M. Bosch-Marce, L. A. Shimoda, Y. S. Tan, J. H. Baek, J. B. Wesley, F. J. Gonzalez and G. L. Semenza. 2008. Mitochondrial autophagy is an HIF-1-dependent adaptive metabolic response to hypoxia. *J Biol Chem.* 283:10892-10903.

Zieseniss, A. 2014. Hypoxia and the modulation of the actin cytoskeleton - emerging interrelations. *Hypoxia.* 2:11-21.

Figure 1

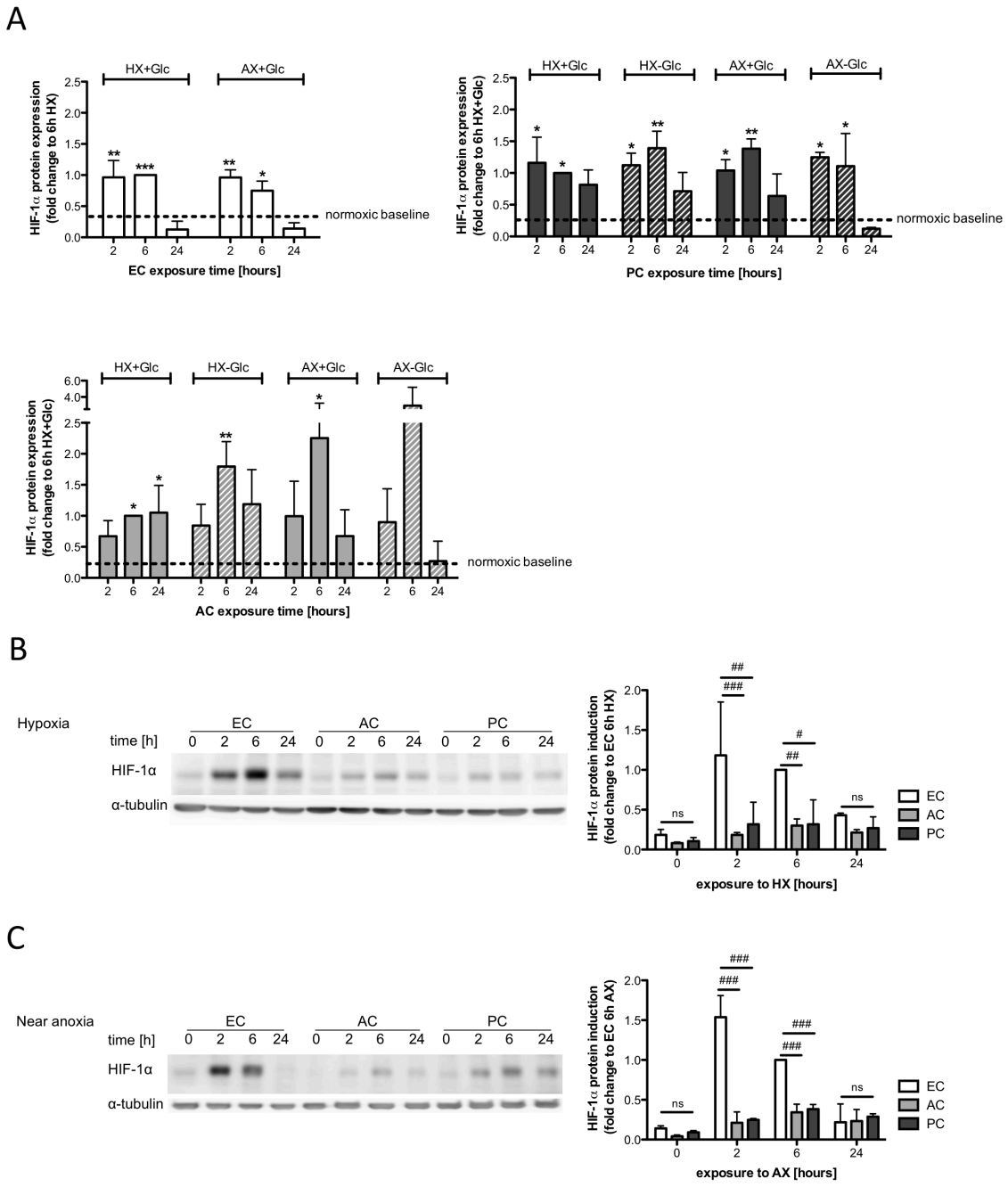

Figure 1: HIF-1α induction profiles in BBB cells. Western blot analysis of HIF-1α protein expression in RBE4 cells (EC), pericytes (PC) and astrocytes (AC) exposed to hypoxia (HX) and near anoxia (AX) in presence (+) or absence (-) of glucose (Glc) for up to 24h. **(A)** Densitometric quantification of HIF-1α protein expression in EC (upper left panel), PC (upper right panel) and AC (lower left panel). N=3; *P<0.05, **P<0.01, ***P<0.001; 1-way ANOVA compared to normoxic baseline. Representative Western blots of comparative HIF-1α expression of the different cell types and their densitometric quantifications exposed to hypoxia **(B)** and near anoxia **(C)**. N=3. $^{\#}$P<0.05, $^{\#\#}$P<0.01, $^{\#\#\#}$P<0.001; 2-way ANOVA compared to EC.

Figure 2

A

	PHD2	VEGF	GLUT-1	MMP-9	β-actin
EC	26.70±0.42	29.23±0.67	23.24±0.12	33.13±1.71	15.98±0.26
AC	28.00±0.39	29.55±1.04	20.13±0.80	32.01±1.12	15.33±0.81
PC	28.42±0.25	26.81±0.51	22.43±0.28	29.55±0.72	15.45±0.15

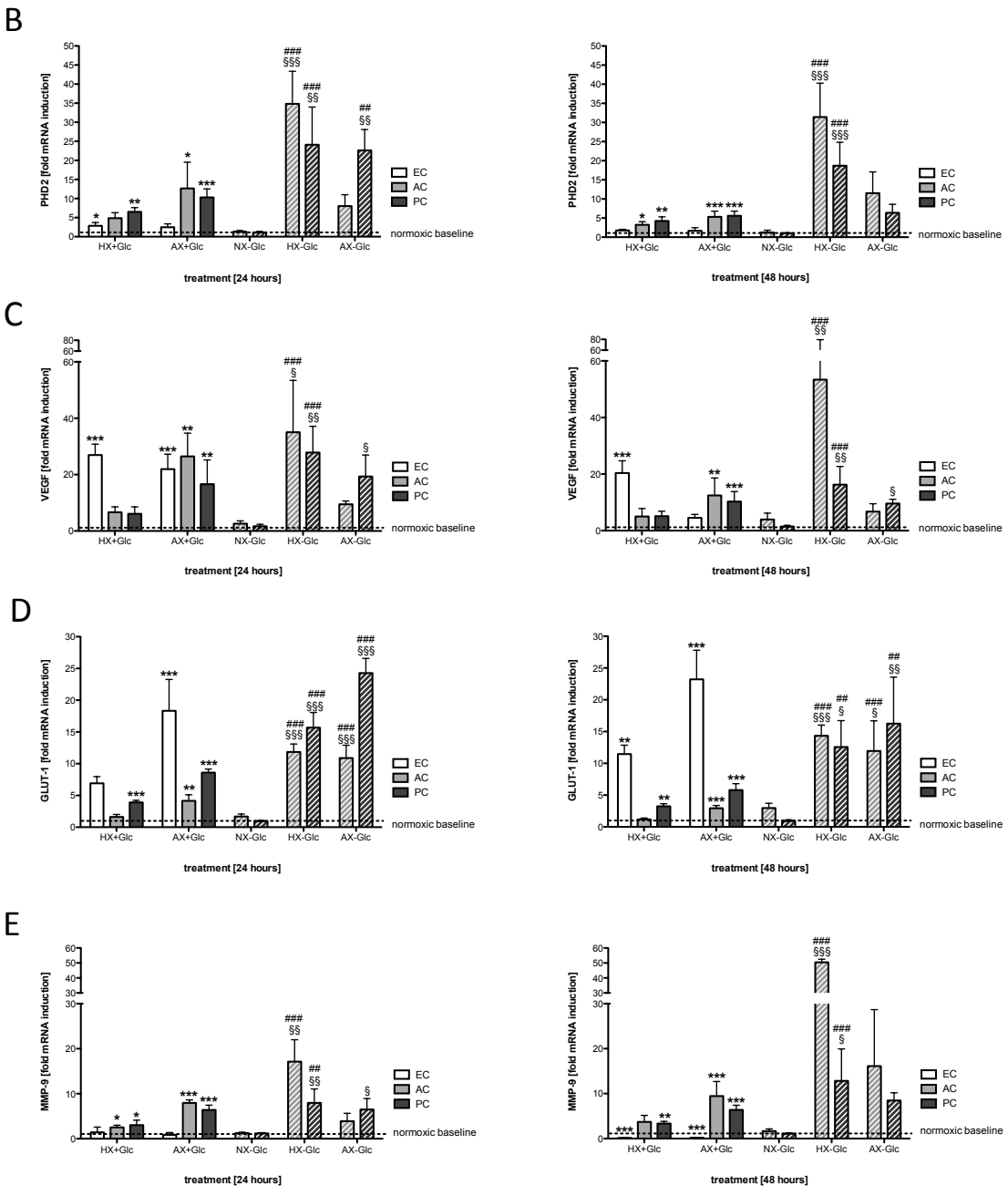

Figure 2: Differential regulation of HIF-1 and ischemia inducible gene expression in BBB cells by quantitative PCR. (A) Table of basal normoxic expression of the analyzed genes showing threshold cycles (CT) ± standard deviation. mRNA expression profiles of PHD2 **(B)**, VEGF **(C)**, GLUT-1**(D)** and MMP-9 **(E)** after 24h (left panel) and 48h (right panel) of O_2 deprivation (solid bars) and oxygen glucose deprivation (hatched bars). N=3-4. *P<0.05, **P<0.01, ***P<0.001; 1-way ANOVA compared to normoxic baseline. §P<0.05, §§P<0.01, §§§P<0.001; 1-way ANOVA compared to normoxia-glucose. $^{\#}$P<0.05, $^{\#\#}$P<0.01, $^{\#\#\#}$P<0.001; 2-way ANOVA comparing + to - glucose treatments.

Figure 3

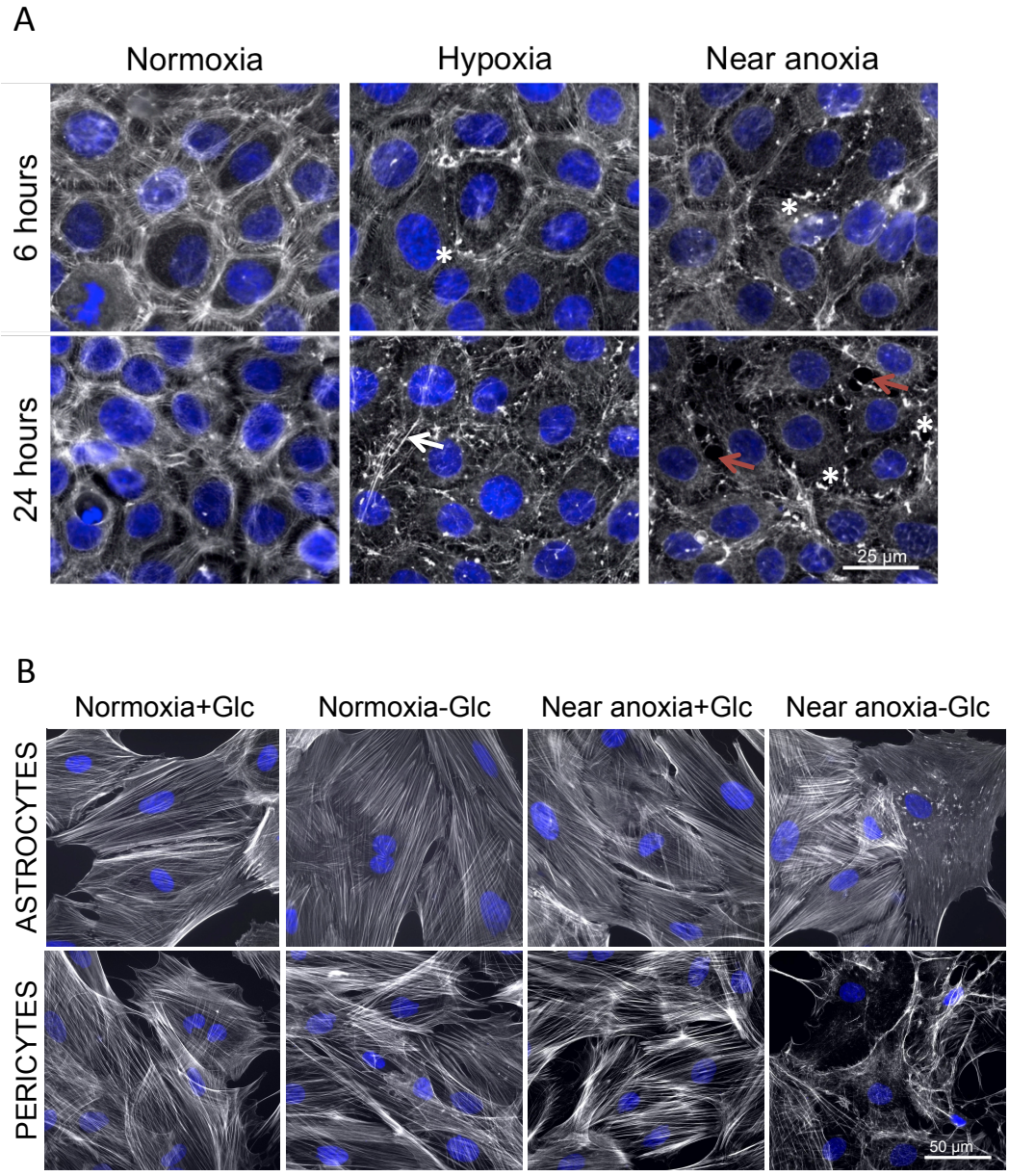

Figure 3: O_2 deprivation and ischemia induce actin cytoskeleton rearrangements in BBB cells. F-actin fibers stained with phalloidin (white) and cell nuclei with DAPI (blue). **(A)** Monolayers of endothelial cells exposed to normoxia, hypoxia and near anoxia for 6 and 24h. White arrow shows stress fiber formation; red arrows indicate interendothelial gap formation. Asterisk highlights breakdown of F-actin resulting in punctuate staining. N=2-3. **(B)** F-actin staining of stress fibers of astrocytes (upper panel) and pericytes (lower panel) exposed to normoxia and near anoxia in presence and absence of glucose for 24h. N= 3.

Figure 4

A

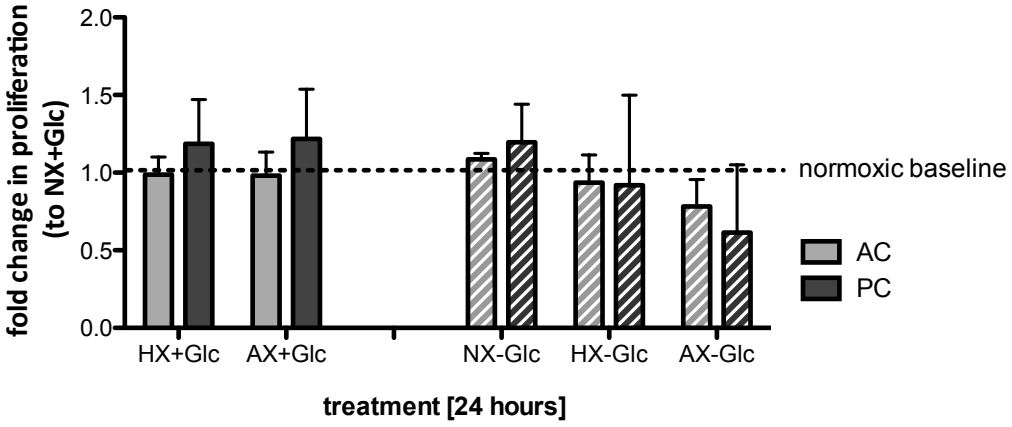

B

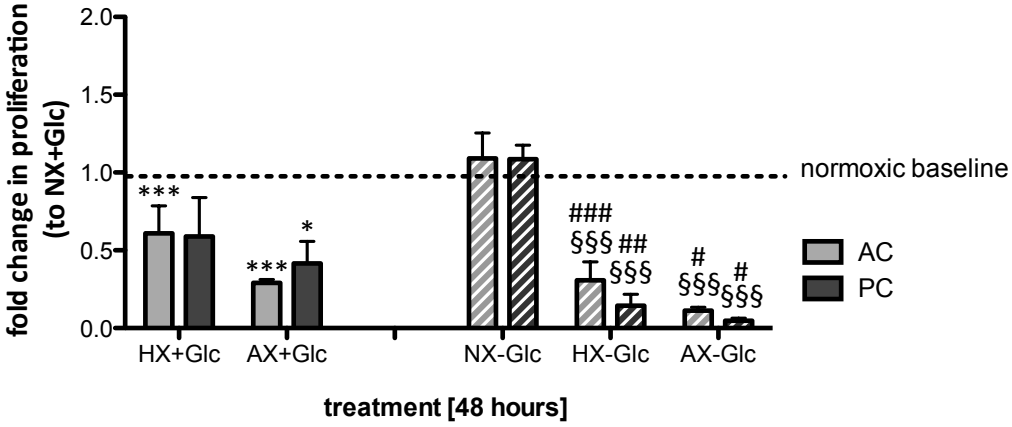

Figure 4: Adaptation of proliferation by astrocytes and pericytes during hypoxic and ischemic insults. Proliferation of astrocytes (AC) and pericytes (PC) was analyzed using BrdU incorporation assay. Proliferation of cells exposed to normoxia, hypoxia and near anoxia in presence (solid bars) and absence (hatched bars) of glucose for 24h **(A)** and 48h **(B)** was measured and normalized to normoxic baseline (NX+Glc). N=3-5. *P<0.05, **P<0.01, ***P<0.001; 1-way ANOVA compared to normoxia+glucose. §§§P<0.001; 1-way ANOVA compared to normoxia-glucose. $^{#}$P<0.05, $^{##}$P<0.01, $^{###}$P<0.001; 2-way ANOVA comparing + to - glucose.

Figure 5

A

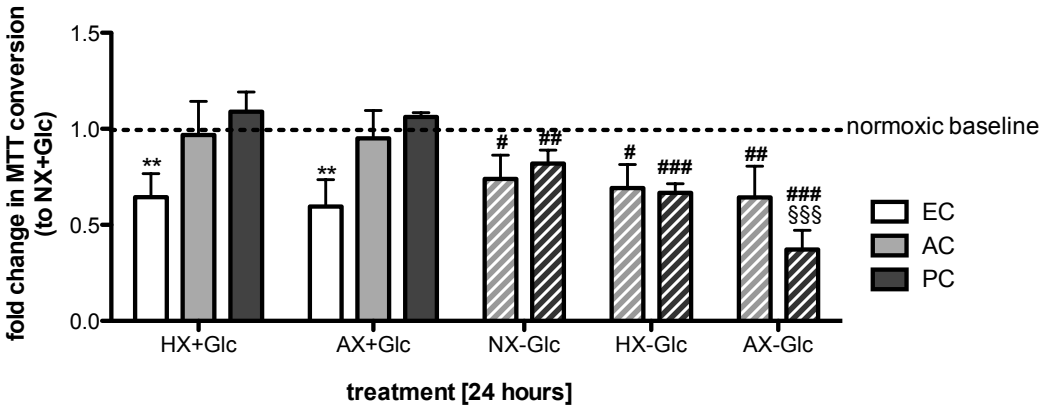

B

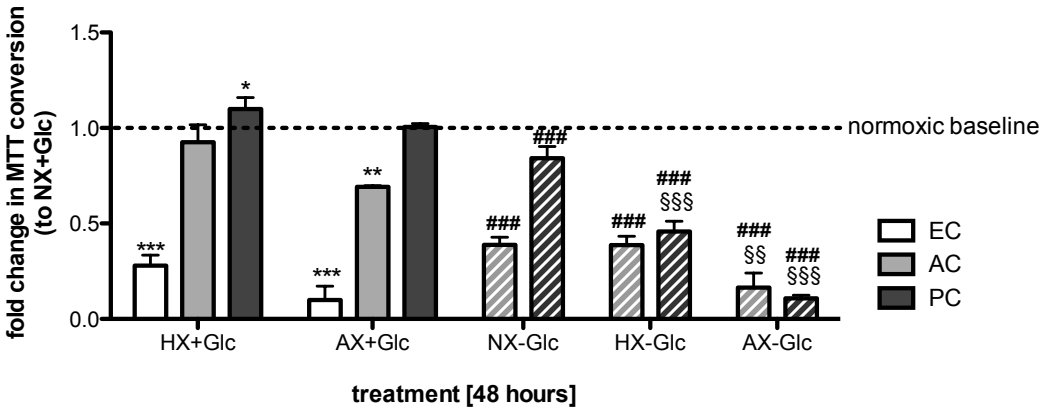

Figure 5: Hypoxic/ischemic exposure differentially modulates metabolic activity of BBB cells. Viability of endothelial cells (EC), astrocytes (AC) and pericytes (PC) was measured by MTT conversion after exposure to normoxia, hypoxia and near anoxia in presence and absence of glucose for 24h **(A)** and 48h **(B)** and normalized to normoxic baseline (NX+Glc). N=3-5. *P<0.05, **P<0.01, ***P<0.001; 1-way ANOVA compared to normoxia+glucose. §§P<0.01, §§§P<0.001; 1-way ANOVA compared to normoxia-glucose. $^{#}$P<0.05, $^{##}$P<0.01, $^{###}$P<0.001; 2-way ANOVA comparing + to - glucose.

Figure 6

A

	BNIP3	β-actin
EC	35.12±1.61	15.98±0.26
AC	36.02±1.81	15.33±0.81
PC	34.04±0.70	15.45±0.15

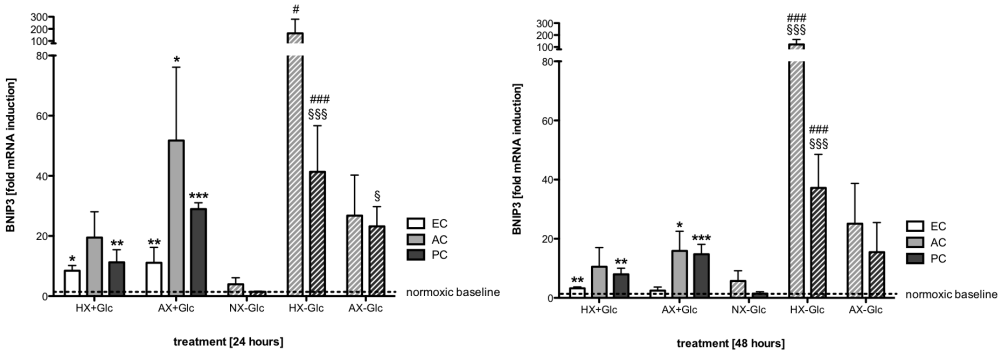

B

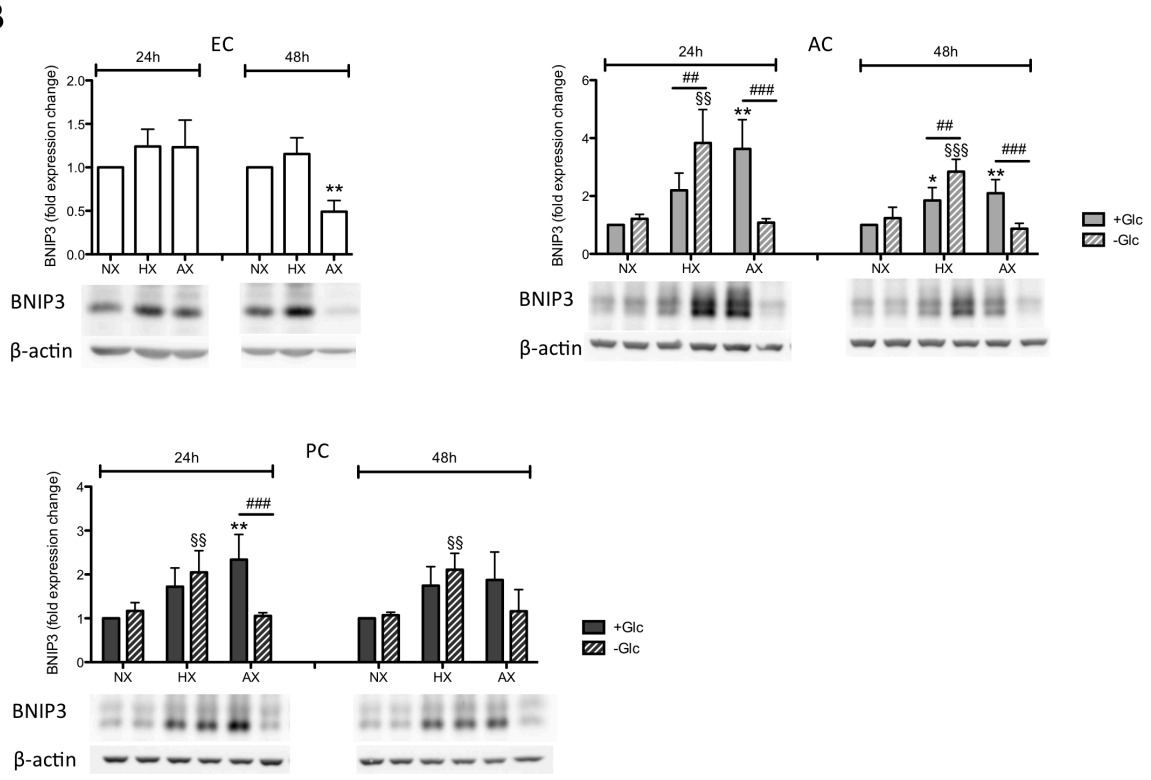

Figure 6: Differential regulation of autophagy and cell death in BBB cells. Expression of autophagy and cell death-related genes was investigated after 24h and 48h exposure to hypoxia (HX), near anoxia (AX) and OGD and compared to normoxia (NX). N=4. **(A)** Table of basal normoxic expression of BNIP3 showing threshold cycles (CT) ± standard deviation (upper panel). BNIP3 mRNA expression after 24h (lower left panel) and 48h (lower right panel) of treatment. Densitometric quantification of protein expression (upper panel) and representative Western blots (lower panels) of BNIP3 **(B)** in endothelial cells (EC), astrocytes (AC) and pericytes (PC). N=4. *P<0.05, **P<0.01, ***P<0.001; 1-way ANOVA compared to normoxia+glucose. §P<0.05, §§P<0.01, §§§P<0.001; 1-way ANOVA compared to normoxia-glucose. $^{\#}$P<0.05, $^{\#\#}$P<0.01, $^{\#\#\#}$P<0.001; 2-way ANOVA comparing + to - glucose treatment.

Figure 7

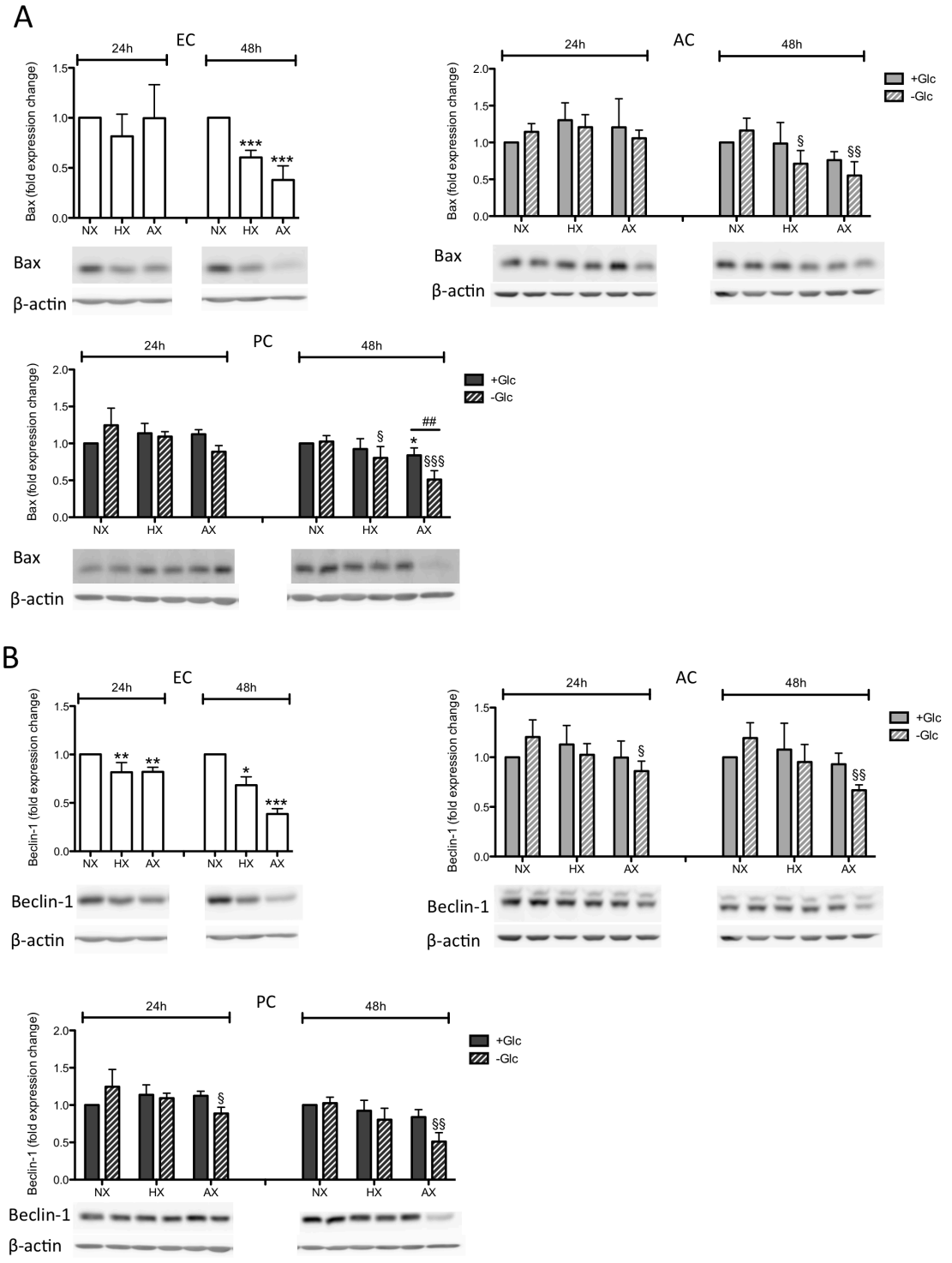

Figure 7: Differential regulation of autophagy and cell death in BBB cells. Densitometric quantification of protein expression (upper panel) and representative Western blots (lower panels) of Bax **(C)**, Beclin-1 **(D)** in endothelial cells (EC), astrocytes (AC) and pericytes (PC). N=4. *P<0.05, **P<0.01, ***P<0.001; 1-way ANOVA compared to normoxia+glucose. §P<0.05, §§P<0.01, §§§P<0.001; 1-way ANOVA compared to normoxia-glucose. $^{\#}$P<0.05, $^{\#\#}$P<0.01, $^{\#\#\#}$P<0.001; 2-way ANOVA comparing + to - glucose treatment.

Figure 8

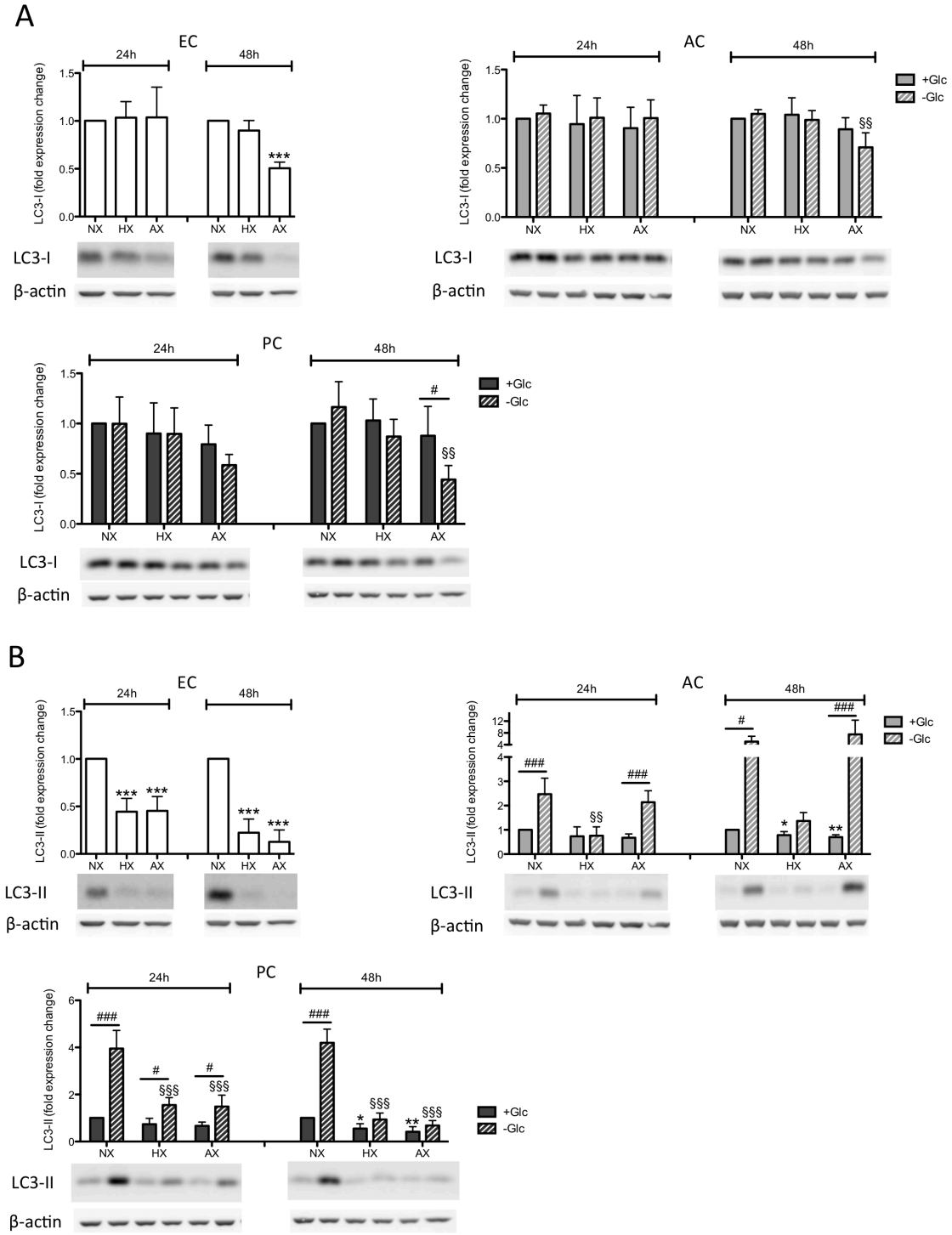

Figure 8: Differential regulation of autophagy and cell death in BBB cells. Densitometric quantification of protein expression (upper panel) and representative Western blots (lower panels) of LC3-I **(E)** and LC3-II **(F)** in endothelial cells (EC), astrocytes (AC) and pericytes (PC). N=4. *P<0.05, **P<0.01, ***P<0.001; 1-way ANOVA compared to normoxia+glucose. §P<0.05, §§P<0.01, §§§P<0.001; 1-way ANOVA compared to normoxia-glucose. $^{\#}$P<0.05, $^{\#\#}$P<0.01, $^{\#\#\#}$P<0.001; 2-way ANOVA comparing + to - glucose treatment.

3.3 DIFFERENTIAL METABOLIC ADAPTATION OF ASTROCYTES AND ENDOTHELIAL CELLS TO HYPOXIC AND ISCHEMIC INJURY

(additional, unpublished results)

3.3.1 Introduction

In my previous work I observed that sensitivity to hypoxic and ischemic insults differs considerably between the different cell types at the BBB (Section 3.2). As both hypoxia and ischemia require profound metabolic adaptation we hypothesized that differences in cellular energy metabolism pathways likely account for these astonishing disparities. To address this question experimentally we compared the hypoxic and ischemic metabolic profiles of primary rat brain microvascular endothelial cells (RBMEC) and astrocytes (AC) - representing hypoxia/ischemia sensitive and tolerant cell types, respectively. To study their metabolic adaptation in a global and untargeted way a liquid chromatography-mass spectrometry (LC-MS) approach was chosen.

3.3.2 Material and Methods

Primary cell isolation

All cell culture media and reagents were obtained from Gibco® (Life Technologies, Zug, Switzerland) and Sigma-Aldrich (Buchs, Switzerland). Primary rat astrocytes were isolated from neonatal pups as described previously (Chow *et al.*, 2001) and cultured in DMEM supplemented with 10% FBS and 50 µg/ml gentamycin sulfate. Primary rat brain microvascular endothelial cells (RBMEC) were isolated from 8-10 weeks old male Wistar rats according to (Coisne *et al.*, 2005) with slight modifications. Briefly, isolated cortices were homogenized after removal of meninges in a 40 ml Dounce homogenizer. Microvessels were isolated from the homogenate adding an equal volume of 30% Dextran solution and subsequent centrifugation at 3000 g for 25 min at 4°C. Then the microvessels were filtered through a 60 µm nylon mesh to remove larger vessels and digested in HBSS buffer supplemented with 10 mM HEPES, 0.1% BSA, 2 mg/ml collagenase-dispase, 10 µg/ml DNAse I and 147 ng/ml TLCK for 45 min at 37°C in a water bath. Digested microvessels were

resuspended in endothelial media (DMEM supplemented with 20% calf serum, BME amino acids, vitamin solution, 2 mM L-glutamine, 1 ng/ml bFGF, 50 µg/ml gentamycin sulfate) and plated on collagen-IV coated culture vessels. 1 day after isolation RBMEC were treated with 3 µg/ml puromycin-containing media for 24h to reduced pericyte contamination.

O_2 deprivation and ischemic treatment

O_2 deprivation experiments were carried out in purpose-built hypoxic glove-box chambers (In$Viv O_2$ 400, Ruskinn Technologies, Pencoed, UK) maintained at 37°C with 5% CO_2. O_2 concentration was constantly monitored with an internal O_2 sensor. Cells were exposed to hypoxia (1% O_2) and near anoxia (0.2% O_2) for 24h. Normoxic controls were maintained at ambient O_2 levels, 37°C, 5% CO_2. Ischemia was simulated *in vitro* by oxygen-glucose deprivation (OGD). OGD was carried out in glucose-free media at hypoxia and near anoxia.

MTT assay

Cell viability was measured using MTT (3-(4,5-dimethylthiazol-2-yl)-2,5-diphenyltetrazolium bromide) assay. All cells were cultured in 96-well plates. After hypoxic/ischemic exposures a 5 mg/ml MTT solution (Sigma-Aldrich, Buchs, Switzerland) was added to the medium to obtain a final concentration 0.5 mg/ml and incubated for 1h at 37°C. Subsequently the media was removed, cells were lysed by adding 100 µl dimethyl sulfoxide and optical density was measured at 560/670 nm using a Multiskan RC Microplate Photometer (Thermo Labsystems, Helsinki, Finnland).

Metabolite extraction

For LC-MS metabolite extractions astrocytes (passage 1) and freshly isolated RBMEC (passage 0) were cultivated until confluence in 3.5 cm dishes in their respective media. After an acclimatization phase of 6h in MS (mass spectrometry) media (DMEM + 10% calf serum + BME amino acids, vitamin solution, 2 mM L-glutamine, 1 ng/ml bFGF and 50 µg/ml gentamycin sulfate) cells were subjected for 24h to O_2 deprivation and OGD as described above. Subsequently cells were washed twice with ice-cold 5 mM NH_4HCO_3 solution and any residual liquid was removed. Cells were immediately quenched in 100 µl 80% methanol (-20°C) containing 20 µg/ml C13/N15 labeled amino acid mixture (Cortecnet, Voisins-Le-

Bretonneux, France) as internal standard, scraped off the dish using a metal spatula and incubated for 10 min on ice for metabolite extraction. After centrifugation (6000 g for 5 min at 4°C) the supernatant containing the metabolites was lyophilized and stored at -80°C until LC-MS measurement. All experiments and exposures were carried out four times independently.

LC-MS measurements

All mass spectrometry measurements and analyses were conducted in cooperation with the Functional Genomics Center Zurich (FGCZ), University of Zurich. Lyophilized metabolite pellets were resuspended in 20 µl ddH_2O and transferred to 96-well plates. Subsequently samples were diluted 1:5 in injection solution (90% acetonitrile, 10% methanol, 50 mM ammonium acetate, pH 9) and centrifuged. 30 µl of the supernatant were transferred to a fresh 96-well plate and directly analyzed on a nanoACQUITY system coupled to a Synapt G2HD mass spectrometer (Waters Corp., Milford, USA). The chromatographic separation of metabolites was performed on a 0.2 µm x 150 mm BEH amide column using a 10 min linear gradient of 90% to 50% acetonitrile. A concentration of 0.5 mM ammonium acetate, pH 9 was kept during the whole chromatographic run. All analyses were done in negative mode using 1.2 kV capillary voltage, 30 V sampling cone voltage and 3 V extraction cone voltage. Source temperature was set to 100°C and Nano Flow Gas was applied.

Data analysis and processing

Data processing and analysis of the LC-MS measurements were carried out by the FGCZ. Waters raw data were first converted to centroid mode and further processed into vendor independent netCDF format. Mass/retention time peak lists including peak intensities for each sample were calculated using the data processing tool cosmiq (Fischer *et al.*, 2014). Signal-to-noise ratio (SNR) of mass peak detection was set to 3, SNR for chromatographic peak detection was set to 10 and a m/z bin size of 0.003 Da was chosen as parameters for cosmiq. For metabolite annotation the resulting list was first matched to a list of metabolites with known retention time and mass. For additional annotation of unknown metabolites, the list of accurate masses was matched to the KEGG database assuming [M-H]- adducts (Ogata *et al.*, 1999). Database hits within a mass window of 0.01 Da were considered.

Data normalization strategy

In order to compare the relative metabolite quantities between the different treatments and cell types, we performed a normalization approach according to the sum of all detected metabolite ion intensities, as previously reported by Katajamaa *et al.* with slight modifications (Katajamaa and Oresic, 2007). This strategy is based on the assumption that the total number of cells, which were used for extraction, is reflected by their total amount of metabolites and hence can be estimated by the sum of measured ion intensities. One NX+Glc RBMEC sample was chosen as reference. The ion intensity for each metabolite was divided by the factor Σis/ Σir, where Σis is the summed ion intensity for each individual sample and Σir is the summed ion intensity of the reference sample.

Pathway analyses

Statistically significant metabolites from four independent experiments were analyzed in a metabolic pathway context using the Kyoto Encyclopedia of Genes and Genomes (KEGG) metabolic pathway map (Ogata *et al.*, 1999) and MetaboAnalyst (Xia *et al.*, 2012). The KEGG pathway map was retrieved in the KGML data format and imported into cytoscape using the KGMLReader tool (Shannon *et al.*, 2003). Fold changes and significance values of the annotated metabolites were mapped on this global pathway map. A list of KEGG IDs was uploaded to the pathway analysis tool of MetaboAnalyst (Xia *et al.*, 2012; Xia and Wishart, 2010) and a list of significant pathways was retrieved using following parameters: *Rattus norvegicus* pathway library, hypergeometric test and relative-betweenness centrality. MetaboAnalyst2.0 is a web-based free tool and can be accessed via http://www.metaboanalyst.ca.

Statistics

All results are expressed as mean ± SD. Statistical significance was either assessed using unpaired student`s t-test or one-way ANOVA for comparison within one group and two-way ANOVA for comparison between different groups using GraphPad Prism 5 software (La Jolla, CA). Bonferroni`s post hoc test was used for all ANOVA analyses. A *P*-value below 0.05 was considered significant.

3.3.3 Results

Pilot experiments

Primary cultures of rat brain astrocytes (AC) and microvascular endothelial cells (RBMEC) were isolated as described above. Astrocytic cultures were characterized by high expression of the astrocyte marker glial fibrillary acidic protein (GFAP), whereas α-smooth muscle actin (α-SMA) and PECAM-1 reactivity was absent, implying no contamination with pericytes or endothelial cells, respectively (Fig. 3.1A). The phenotype of the RBMEC cultures was confirmed by expression of the tight junction proteins occludin, ZO-1 and claudin-5 (Fig. 3.1B). Only minor contamination with pericytes (less than 5%) was observed, as indicated by α-SMA reactivity. Astrocyte contamination was ruled out by complete lack of GFAP expression (Fig. 3.1B).

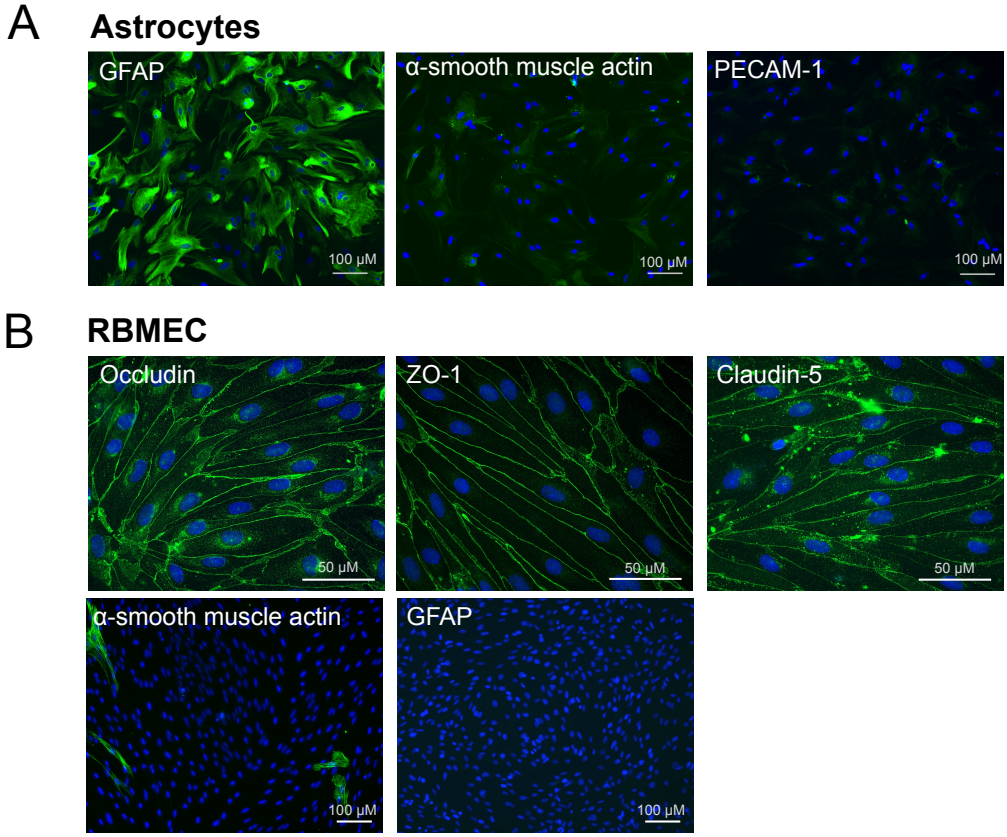

Figure 3.1: Characterization of primary astrocytes and RBMEC cultures. (A) Astrocyte cultures were characterized by strong expression of glial cell marker GFAP (glial fibrillary acidic protein) and absence of pericyte and endothelial cell contamination as shown by α-smooth muscle actin and PECAM-1 staining, respectively. (B) Rat brain microvascular endothelial cell (RBMEC) phenotype was verified by strong expression of the tight junction proteins occludin, ZO-1 and claudin-5 and absence of astrocytic GFAP. A pericyte contamination of below 5% was indicated by α-smooth muscle actin immunoreactivity. Cell nuclei are shown in blue (DAPI).

In order to be able to compare differences in metabolic adaptation between AC and RBMEC during O_2 deprivation and ischemia the use of an identical culture media was indispensable. Typically RBMEC receive a very rich media containing 20% calf serum (CS) and a number of additives, such as vitamins, L-Glutamine, amino acids and basic fibroblast growth factor (bFGF) (RBMEC media). The astrocyte media (AC media) in contrast consists of DMEM and 10% fetal bovine serum (FBS) only. However since media composition can strongly influence cellular metabolism selection of a media suitable for both cell types, which did not contain too rich nutrient conditions but reproduced previous observed effects. The effect of different media on metabolic activity/cell viability was measured using MTT assay after 24h of O_2 deprivation and ischemic treatment. AC and RBMEC were exposed for 24h to normoxia (NX), hypoxia (HX, 1% O_2) and near anoxia (AX, 0.2% O_2) in presence and absence of glucose (+Glc/-Glc). For each cell type its standard media was compared to two other media namely minimal media (DMEM + 10% calf serum + 50 µg/ml gentamycin sulfate) and minimal media + 1 ng/ml bFGF (Fig. 3.2A and Fig. 3.2B). In RBMEC media the endothelial cells hardly responded to O_2 deprivation and oxygen glucose deprivation (OGD) suggesting the media likely contains too much serum and nutrients to observe any major effects of the treatments (Fig. 3.2A). For both minimal media with and without bFGF we observed an increase in MTT conversion in hypoxic (HX) and near anoxic (AX) exposure compared to normoxic baseline. Glucose deprivation during NX led to a reduction of MTT conversion of 30-40%, which was further aggravated upon simultaneous OGD during HX and AX (Fig. 3.2A). Importantly the presence of bFGF in the minimal media did not have any effect on MTT conversion. Culture of AC in either minimal media did not alter metabolic activity under HX or AX compared to the conventional AC media (Fig. 3.2B). However during OGD the rate of MTT conversion was higher when the minimal media were used. This initial effect of the higher tolerance of AC is likely due to the different serum composition in the minimal media, which contains calf serum instead of FBS and thus likely different growth factors. The serum effect was however abolished after prolonged OGD for 48h, as here all media again showed similar response (data not shown). As previously observed for RBMEC the presence of bFGF did not cause any alterations in MTT reduction.

Figure 3.2C depicts the comparison between the response of AC and RBMEC in minimal media without bFGF. Showing the increased activity of RBMEC upon O_2 deprivation, which may be due to increased proliferation, whereas AC remain unaffected. Similarly in OGD AC did not show any dramatic changes in MTT conversion implying their great tolerance for the given exposures, in contrast metabolic activity of RBMEC was decreased in a severity-dependent manner, resulting in about 60% loss of initial activity under AX-Glc (Fig. 3.2C).

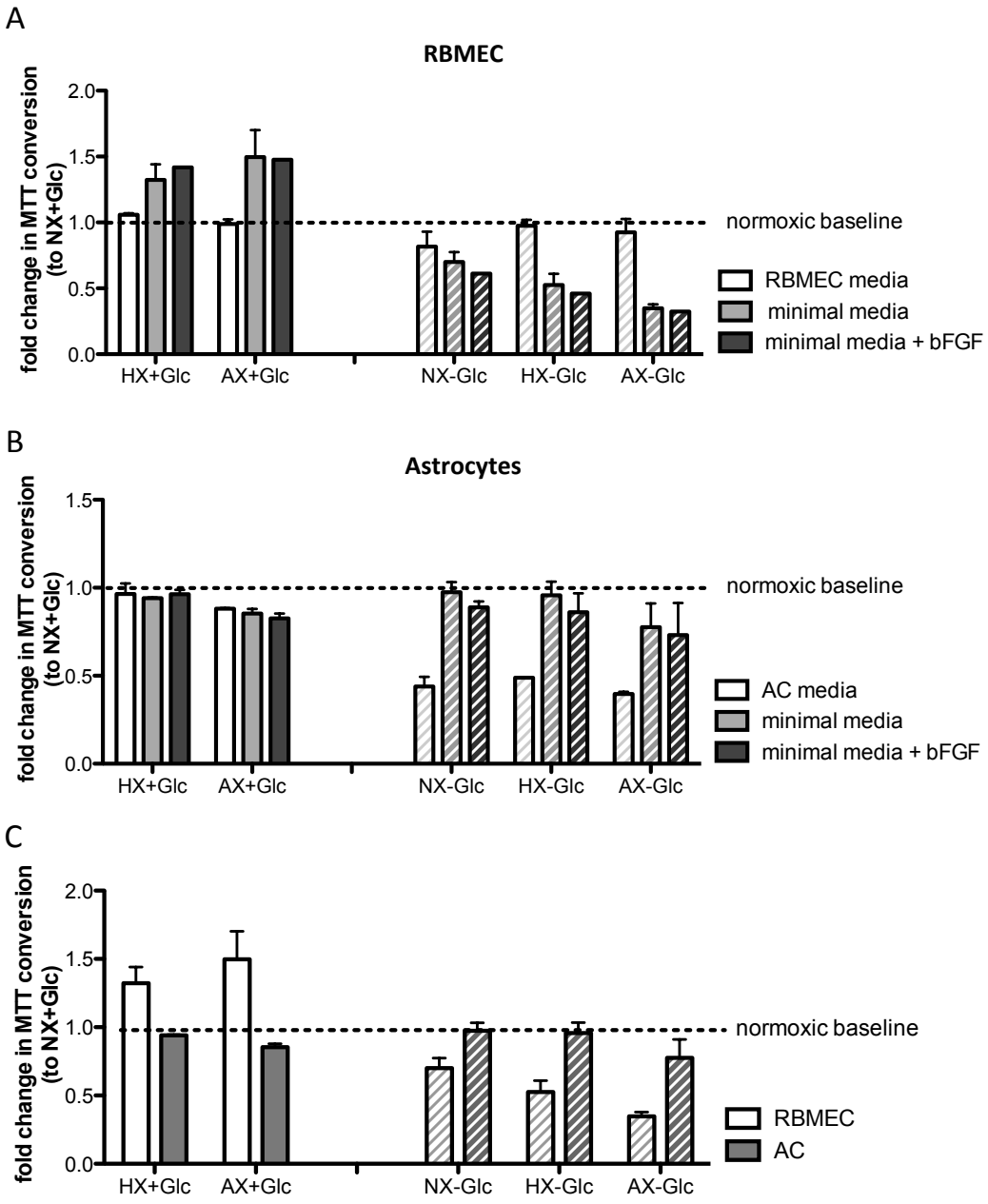

Figure 3.2: Culture media composition affects astrocyte and RBMEC viability. Cell viability of RBMEC **(A)** and astrocytes (AC) **(B)** cultured in their usual media (RBMEC/AC media), minimal media and minimal media + bFGF was measured using MTT assay. Cells were exposed for 24h to normoxia (NX), hypoxia (HX) and near anoxia (AX) in presence (+, solid bars) and absence (-, hatched bars) of glucose (Glc) and compared to normoxic baseline (NX+Glc). **(C)** Comparison of RBMEC and AC viability in minimal media. N=1-3.

Based on these pilot experiments we decided to use the minimal media without bFGF for future metabolomics measurements as this gave the closest responses expected from previous data as well as avoided the additional complication of bFGF-mediated effects.

In spite of carefully testing the media in the MTT assay, we encountered difficulties culturing the RBMEC in the minimal media over longer periods of time. Although cultivation in 96 well plates for the MTT assay did not result in any visual or functional impairment, RBMEC cultured in 3.5 cm petri dishes for the metabolite extractions, started to lift off during the normoxic incubations. Thus ultimately the media composition for the mass spectrometry measurements had to be refined and a media containing similar additives to that of RBMEC media with 10% instead of 20% calf serum was used (mass spectrometry/MS media), which was tolerated well by both cell types. Prior to the actual exposure RBMEC and AC were acclimatized for 6h in the MS media.

Novel insights into cell-specific metabolism of AC and RBMEC during O_2 deprivation and ischemic stress

Using a LC-MS based approach we compared the metabolic profiles of primary rat brain microvascular endothelial cells (RBMEC) and astrocytes (AC). We could annotate about 500 metabolites by accurate mass allowing a global overview of cellular metabolism. Due to the high complexity of the data set a principal component analysis (PCA) was performed. The PCA allows conclusions to be drawn regarding the reproducibility of the data (replicates) and importantly gives information about the difference of the metabolome amongst the treatment groups. Similarly to the pilot experiments AC and RBMEC were subjected for 24h to NX, HX, and AX in presence and absence of glucose. Figure 3.3 is a graphical representation of the PCA for all treatments (colors) of AC (stars) and RBMEC (circles). The plot shows that the four replicates of similar treatments cluster closely together implying a good reproducibility of the observed changes (Fig. 3.3). The three axes represent the major principal components (PC) of the data set. The principal components define the directions of the highest variance/difference in the data set i.e. where the metabolome is most different. The larger the distance between two points the bigger the difference for a certain parameter and the percentage of a given axis is the percentage of total variance that this principal component

accounts for. On the first axis (PC1) a separation of AC versus RBMEC data points is observed showing that the cell type makes the largest contribution to metabolome composition whereas the insult severity, shown on the PC2 axis, is the second most important parameter affecting metabolome composition. The distribution of the data points on the second axis further shows a close clustering of the O_2 deprivation groups for both AC and RBMEC revealing only minor changes in the metabolome due to O_2 deprivation. OGD in contrast induces a spread of the different exposures along the second axis and thus demonstrates more profound changes induced by ischemic treatment (Fig. 3.3).

Next we aimed to determine the main metabolites accounting for cell-type specific differences presented on the first PC axis to identify differential active metabolic pathways between AC

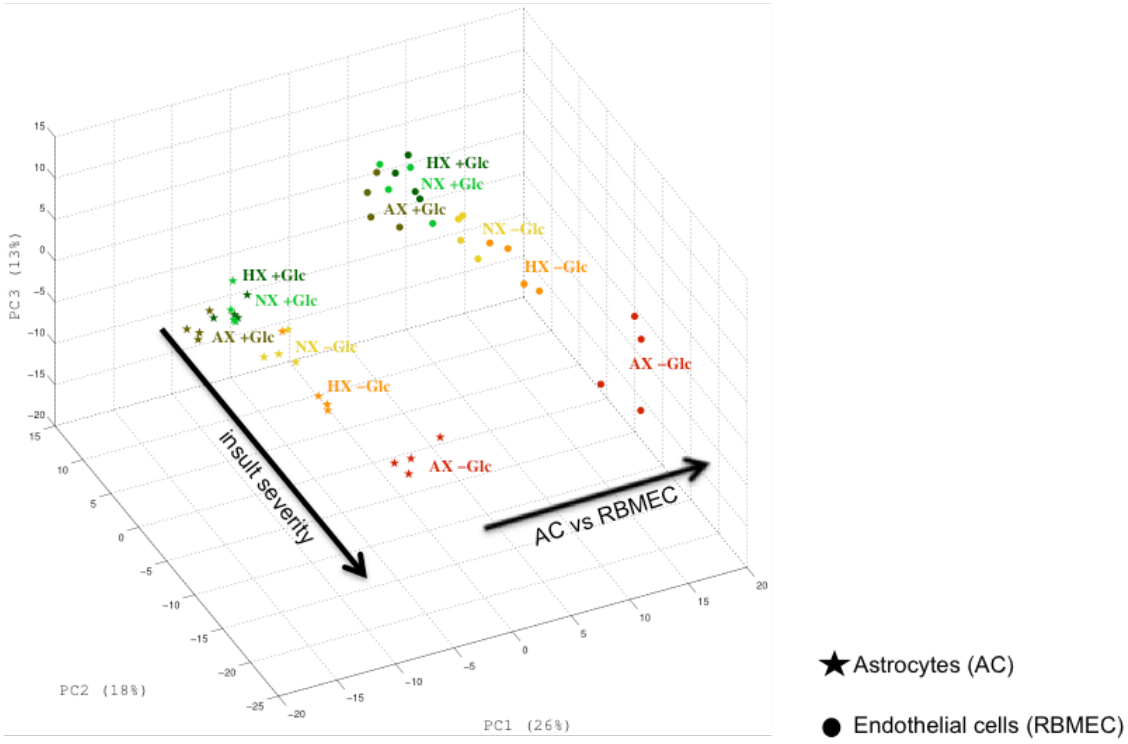

Figure 3.3: Cell type and insult severity chiefly affect metabolome composition. Principal component analysis of the metabolomes of AC (stars) and RBMEC (circles) exposed to normoxia (NX), hypoxia (HX) and near anoxia (AX) in presence and absence of glucose (+/- Glc). Axes represent the principal components (PC) and their contribution to overall metabolome variance in percent (%). As indicated by the arrows PC1 reflects the difference between AC and RBMEC, whereas on PC2 the different treatment groups separate based on insult severity. N=4.

and RBMEC, as these pathways likely account for the differences in hypoxic/ischemic sensitivity between the cell types. To do so a list of all detected metabolites was generated in which the ratio of metabolite abundance of AC to RBMEC was calculated for physiological conditions (NX+Glc). This list was first used for a pathway analysis using the KEGG metabolic pathways tool to generate the map presented in Figure 3.4 that depicts an overview of all metabolic pathways and the involved metabolites. Metabolites increased in AC, compared to RBMEC, are shown in red circles whereas metabolites that are higher in RBMEC are blue. The circle size reflects the fold-change with dark colors indicating significant changes whereas light colored ones are not significant. It is apparent from the map that in AC many metabolites are significantly higher expressed than in RBMEC, particularly in pathways that account for carbohydrate metabolism and TCA cycle (purple box). In addition metabolites involved in glutathione metabolism (orange box) and creatine metabolism (blue box) were strongly elevated in AC. RBMEC in contrast showed an accumulation of metabolites involved in nucleotide (red lines) and lipid metabolism (dark green lines). Appendix Table A.1 shows fold changes and statistics of the top altered metabolites presented in Fig. 3.4. To further characterize the pathways with differential activity in the two cell types, an analysis using the MetaboAnalyst tool was performed (Fig. 3.5). The Table depicts the major active pathways in AC (upper Table) and RBMEC (lower Table) in relation to each other, showing the number of total metabolites involved in the pathway (total), the metabolites found in a pathway just by chance (expected), the number of up-regulated metabolites detected in the sample (hits) and the calculated p-value (raw p). Correlating well with the results obtained from the KEGG analysis we again identified pathways linked to carbohydrate metabolism from top hits for AC including galactose, starch and sucrose, amino sugar and nucleotide sugar and fructose metabolism, as well as glycolysis and citrate cycle (highlighted in red). It is however noteworthy that detection of compounds with similar molecular formula cannot be distinguished by the mass spectrometry measurements, which applies for example for the hexoses (glucose, fructose and galactose) or D- and L-isomers, like amino acids. For this reason the interpretation of glycolysis, fructose and galactose metabolism is difficult as a definite metabolite assignation is not possible.

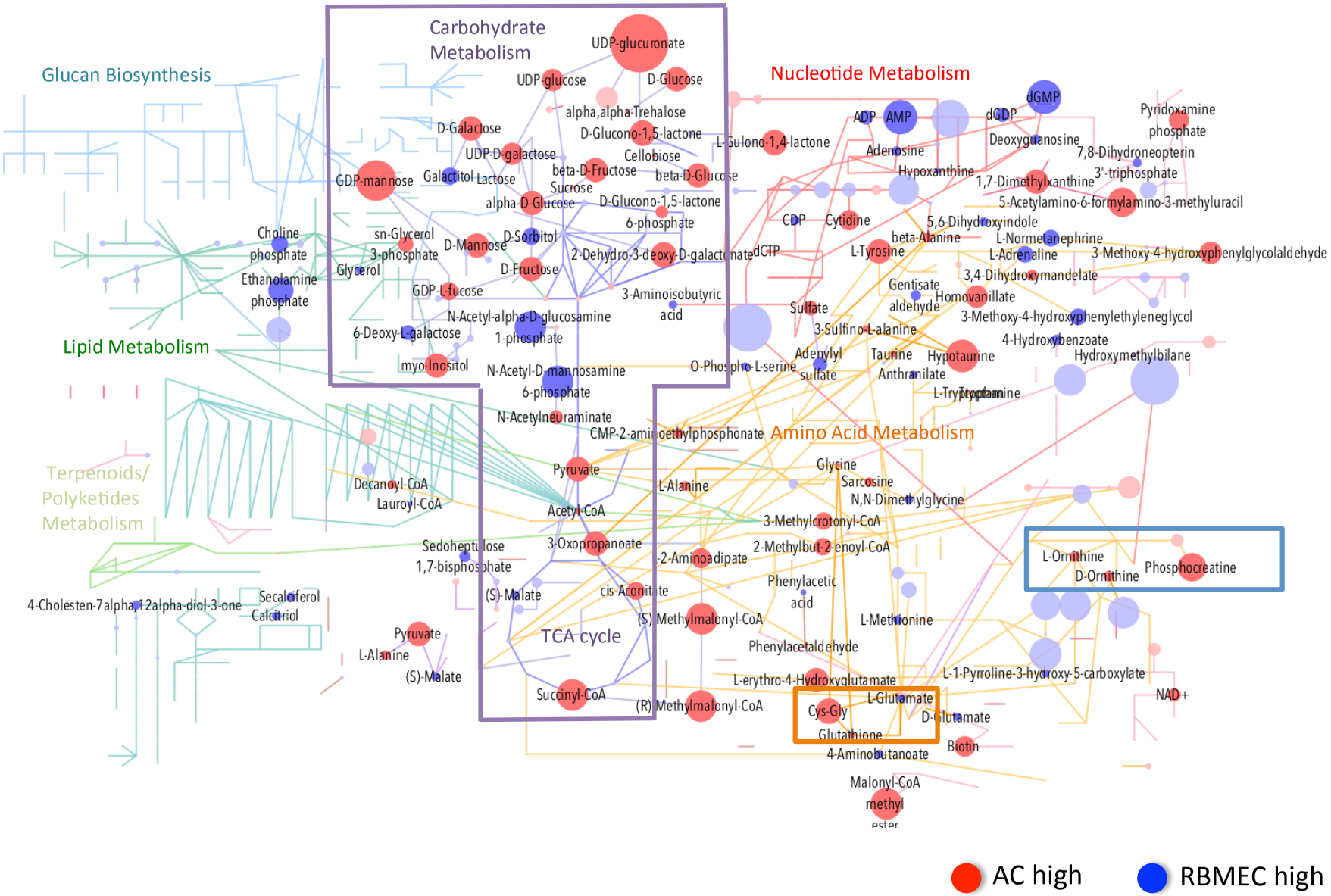
Carbohydrate Metabolism
Glucan Biosynthesis
Nucleotide Metabolism
Lipid Metabolism
Amino Acid Metabolism
Terpenoids/ Polyketides Metabolism
TCA cycle
UDP-glucuronate
UDP-glucose
D-Glucose
alpha,alpha-Trehalose
D-Galactose
D-Glucono-1,5-lactone
UDP-D-galactose
Cellobiose
GDP-mannose
Galactitol
Lactose
beta-D-Fructose
beta-D-Glucose
Sucrose
alpha-D-Glucose
D-Glucono-1,5-lactone
6-phosphate
Choline phosphate
sn-Glycerol 3-phosphate
D-Mannose
D-Sorbitol
2-Dehydro-3-deoxy-D-galactonate
Glycerol
D-Fructose
Ethanolamine phosphate
GDP-L-fucose
3-Aminoisobutyric acid
N-Acetyl-alpha-D-glucosamine 1-phosphate
6-Deoxy-L-galactose
myo-Inositol
N-Acetyl-D-mannosamine 6-phosphate
N-Acetylneuraminate
CMP-2-aminoethylphosphonate
L-Gulono-1,4-lactone
ADP
AMP
dGMP
dGDP
Deoxyguanosine
Adenosine
Hypoxanthine
Pyridoxamine phosphate
7,8-Dihydroneopterin 3'-triphosphate
1,7-Dimethylxanthine
5-Acetylamino-6-formylamino-3-methyluracil
CDP
Cytidine
5,6-Dihydroxyindole
beta-Alanine
L-Normetanephrine
dCTP
L-Tyrosine
L-Adrenaline
3-Methoxy-4-hydroxyphenylglycolaldehyde
3,4-Dihydroxymandelate
Gentisate aldehyde
Homovanillate
Sulfate
3-Methoxy-4-hydroxyphenylethyleneglycol
3-Sulfino-L-alanine
4-Hydroxybenzoate
Adenylyl sulfate
Taurine
Hypotaurine
Hydroxymethylbilane
O-Phospho-L-serine
Anthranilate
L-Tryptophan
Pyruvate
L-Alanine
Glycine
Sarcosine
N,N-Dimethylglycine
Decanoyl-CoA
Lauroyl-CoA
Acetyl-CoA
3-Methylcrotonyl-CoA
Sedoheptulose 1,7-bisphosphate
3-Oxopropanoate
2-Aminoadipate
2-Methylbut-2-enoyl-CoA
L-Ornithine
D-Ornithine
Phosphocreatine
(S)-Malate
cis-Aconitate
Phenylacetic acid
4-Cholesten-7alpha,12alpha-diol-3-one
Secalciferol
Calcitriol
(S)-Methylmalonyl-CoA
L-Methionine
Pyruvate
L-Alanine
(S)-Malate
Phenylacetaldehyde
L-erythro-4-Hydroxyglutamate
L-1-Pyrroline-3-hydroxy-5-carboxylate
NAD+
Succinyl-CoA
(R)-Methylmalonyl-CoA
L-Glutamate
Cys-Gly
D-Glutamate
Glutathione
Biotin
4-Aminobutanoate
Malonyl-CoA methyl ester
AC high
RBMEC high

Figure 3.4: AC and RBMEC exhibit differential activity of metabolic pathways under physiological conditions. The relationship of metabolite abundance between AC and RBMEC under physiological conditions (NX+Glc, N=4) was analyzed using the KEGG metabolic pathway tool shown as overview of metabolites highly abundant in AC (red) and RBMEC (blue) embedded in their metabolic pathways. The size of the circles represents the fold change with dark color depicting significant and light color non-significant differences. Purple box: carbohydrate metabolism pathway, red lines: nucleotide metabolism, dark green lines: lipid metabolism, orange lines: amino acid metabolism, light green lines: terpenoids and polyketides metabolism, light blue lines: glucan biosynthesis blue box: creatine metabolism, orange box: glutathione metabolism.

Since our media did not contain any fructose or galactose but only glucose it seems likely that the hits we get for these pathways in the pathway analysis might be caused by false identification of isomers. Glutathione metabolism was also identified to be very active in AC (highlighted in red). In RBMEC however metabolites of the purine metabolism pathway (a branch of the nucleotide metabolism) as well as different amino acid pathways, including like tyrosine, D-glutamine/D-glutamate and arginine/proline metabolism, were accumulated compared to AC (Fig. 3.5 lower panel, highlighted in blue).

Astrocytes

Pathway	Total	Expected	Hits	Raw p
Galactose Metabolism	26	1.50	11	4.65E-08
Starch and sucrose metabolism	23	1.33	10	1.48E-07
Amino sugar and nucleotide sugar metabolism	37	2.14	10	2.31E-05
Ascorbate and aldarate metabolism	9	0.52	4	1.04E-03
Caffeine metabolism	12	0.69	4	3.59E-04
Propanoate metabolism	20	1.16	5	4.44E-03
Taurine and hypotaurine metabolism	8	0.46	3	8.43E-03
Frutose and mannose metabolism	19	1.10	4	2.06E-02
Citrate cycle (TCA cycle)	20	1.16	4	2.46E-02
Cyanoamino acid metabolism	6	0.35	2	4.25E-02
Glycolysis and Gluconeogenesis	26	1.50	4	5.85E-02
Glutathione metabolism	26	1.50	4	5.85E-02

RBMEC

Pathway	Total	Expected	Hits	Raw p
Purine metabolism	68	2.72	9	1.06E-03
Sulfur metabolism	5	0.2	2	1.45E-02
D-Glutamine and D-glutamate metabolism	5	0.2	2	1.45E-02
Tyrosine metabolism	42	1.68	5	2.33E-02
Arginine and proline metabolism	44	1.76	5	2.80E-02
Amino sugar and nucleotide sugar metabolism	37	1.48	4	5.66E-02

Figure 3.5: AC and RBMEC exhibit differential activity of metabolic pathways under physiological conditions. Top metabolic pathways up-regulated in AC (upper Table) and RBMEC (lower Table) compared to each other obtained by pathway analysis using MetaboAnalyst software. Total: total number of metabolites involved in pathway, Expected: number of metabolites detected in a pathway by chance, Hits: up-regulated metabolites in sample, Raw p: calculated significance, *P*-value.

Next we selected specific pathways elevated in AC for detailed investigation to answer our major question, which metabolic pathways may account for their higher tolerance in hypoxic and ischemic injury compared to RBMEC. Based on previous literature we selected pathways that are known to be important for normal brain function and survival during O_2 deprivation/OGD and compared their activity between AC and RBMEC. The selected pathways are creatine/phosphocreatine, glutathione and glycogen metabolism.

For tissues with high fluctuating energy requirements, like the brain or muscles, the creatine/phosphocreatine (CR/pCR) system is of particular importance as it is essential for ATP safeguarding and movement, protection against excitotoxicity and has anti-apoptotic and antioxidant actions (Perasso *et al.*, 2013). Under conditions of energy shortage pCR donates its phosphate group to ADP and thus fosters rapid replenishment of ATP pools in absence of glucose or O_2 (Perasso *et al.*, 2013; Tachikawa *et al.*, 2007). We compared the abundance of metabolites involved in CR biosynthesis and CR/pCR cycle (Fig. 3.6). The biosynthesis pathway of CR involves conversion of glycine, L-arginine and S-adenosyl-L-methionine to form CR, L-ornithine and S-adenosyl-homocysteine (Fig. 3.6A, upper panel). Indeed we observed that the levels of glycine, ornithine and S-adenosyl-L-methionine were higher in AC than in RBMEC, suggesting a higher rate of CR biosynthesis (Fig. 3.6A, lower panel)

Presence of ATP favors the reversible conversion of CR to the highly energetic pCR (Beard and Braissant, 2010; Perasso *et al.*, 2013). Supporting the assumption of elevated astrocytic CR biosynthesis, pCR was clearly more abundant in AC compared to RBMEC, whereas we did not observe any difference in CR levels, which is likely due to the rapid conversion of CR to pCR in AC (Fig. 3.6B, lower panel). Interestingly we observed that the ADP levels in RBMEC were much higher than in AC, which may explain the low pCR levels although CR is present in RBMEC. Unfortunately detection of ATP was not reliable in the mass spectrometry measurements preventing this correlation to be established. However, due to its central function in cellular protection, and particularly during insults that impair energy generation like hypoxia or ischemia, the strong expression of the CR/pCR system represents an excellent adaptation of AC to withstand such stress conditions.

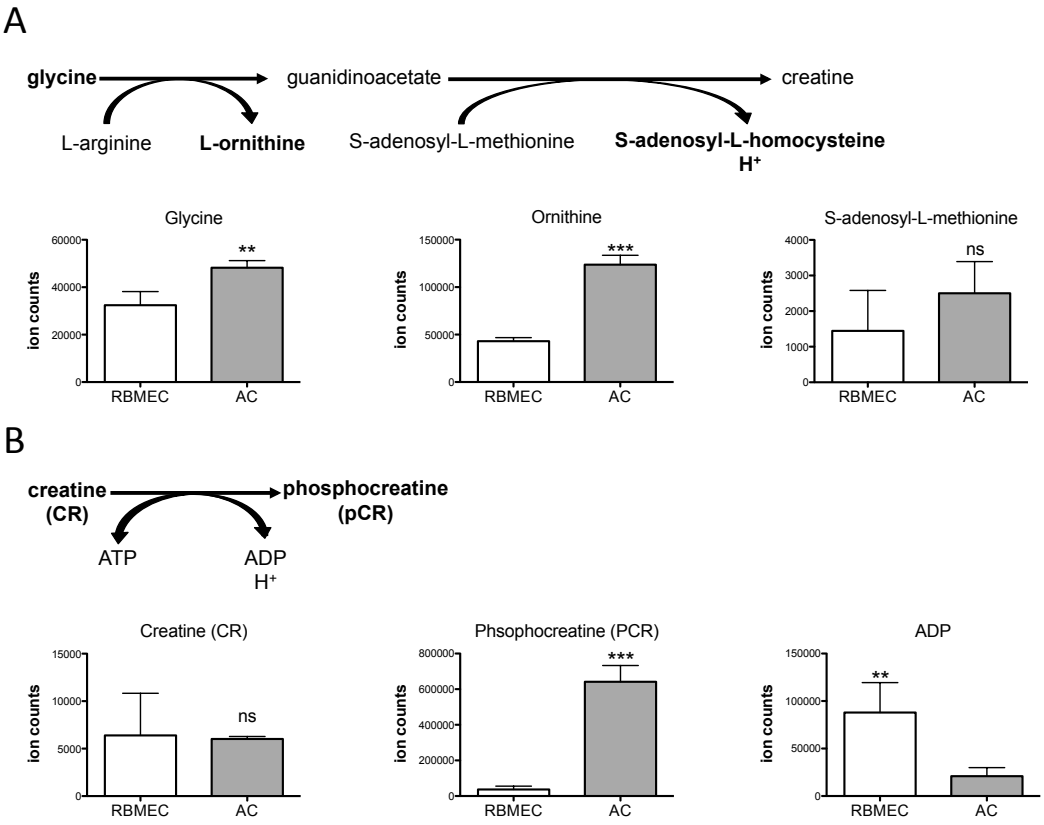

Figure 3.6: The creatine/phosphocreatine system is more prevalent in astrocytes than in RBMEC. The flow charts depict the metabolites involved in creatine biosynthesis **(A)** and creatine/phosphocreatine cycle **(B).** Lower panels show bar graphs of metabolite abundance (in total ion counts) of selected metabolites involved in these pathways comparing between RBMEC and AC under physiological conditions (NX+Glc, 24h). N=4. **P<0.01, ***P<0.001; unpaired student`s t-test.

Glycogen represents the major store of glucose equivalents within the brain and thus similarly to CR/pCR contributes to replenishment of ATP levels (Belanger *et al.*, 2011; Gruetter, 2003). Starch and sucrose metabolism was another major hit in AC pathway analysis and glycogen metabolism is an important branch of it. Since UDP-glucose is a direct precursor of glycogen we investigated metabolites participating in UDP-glucose formation (Fig.3.7A). Interestingly the abundance of hexoses, probably mainly D-glucose, was much higher in AC than in RBMEC (Fig. 3.7A). In addition very high levels of UDP-glucose, the major building block of glycogen, were detected in AC suggesting a high rate of glycogen biosynthesis, whereas RBMEC only showed negligible amounts of UDP-glucose (Fig. 3.7A). Unfortunately glycogen itself cannot be directly detected by mass spectrometry, as it is a polymer of glucose that is indistinguishable from glucose/hexose monomers. However both high levels of hexoses as well as UDP-glucose strongly suggest that AC have more glycogen stores than RBMEC.

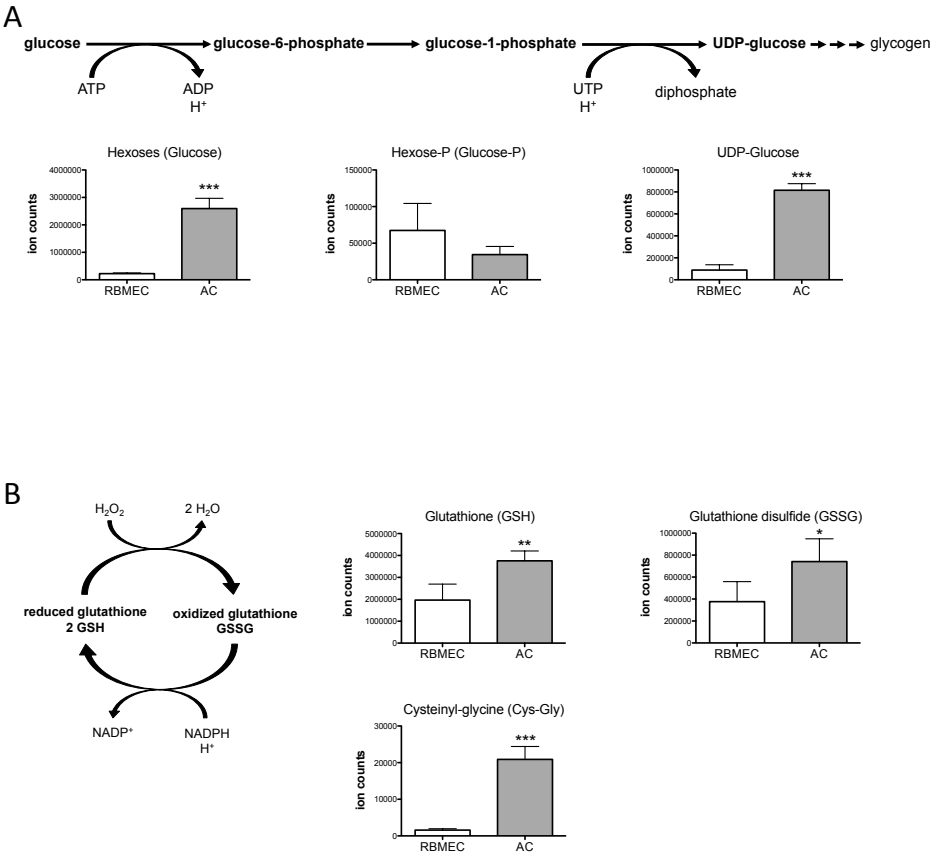

Figure 3.7: High abundance of glycogen- and glutathione-related metabolites in astrocytes. The flow charts depict the metabolites involved in glycogen biosynthesis **(A)** and glutathione redox cycle **(B)** Bar graphs show a comparison of selected metabolites between RBMEC and AC under control conditions (NX+Glc, 24h) for the mentioned pathways. N=4. *P<0.05, **P<0.01, ***P<0.001; unpaired student`s t-test.

In addition to energy equivalents antioxidants crucially contribute to cellular well-being. Glutathione is one of the most important cellular antioxidants that diminishes oxidative stress and plays a central role in cell survival during hypoxic and ischemic injury (Juurlink, 1997). As predicted by pathway analysis AC indeed contained higher levels of reduced glutathione (GSH) and oxidized glutathione (GSSG) than RBMEC (Fig. 3.7B). In addition AC had significantly higher levels of Cysteinyl-glycine (Cys-Gly), a compound used as precursor for glutathione biosynthesis (Dringen *et al.*, 2001), showing a good correlation with the increased glutathione levels.

Next we investigated whether the above-mentioned differences in the discussed pathways could account for the different sensitivities of AC and RBMEC to O_2 deprivation and OGD (Fig. 3.8). Notably for all treatments pCR levels were consistently and significantly higher in AC compared to RBMEC (Fig. 3.8A). The CR/pCR system was modulated in AC in response

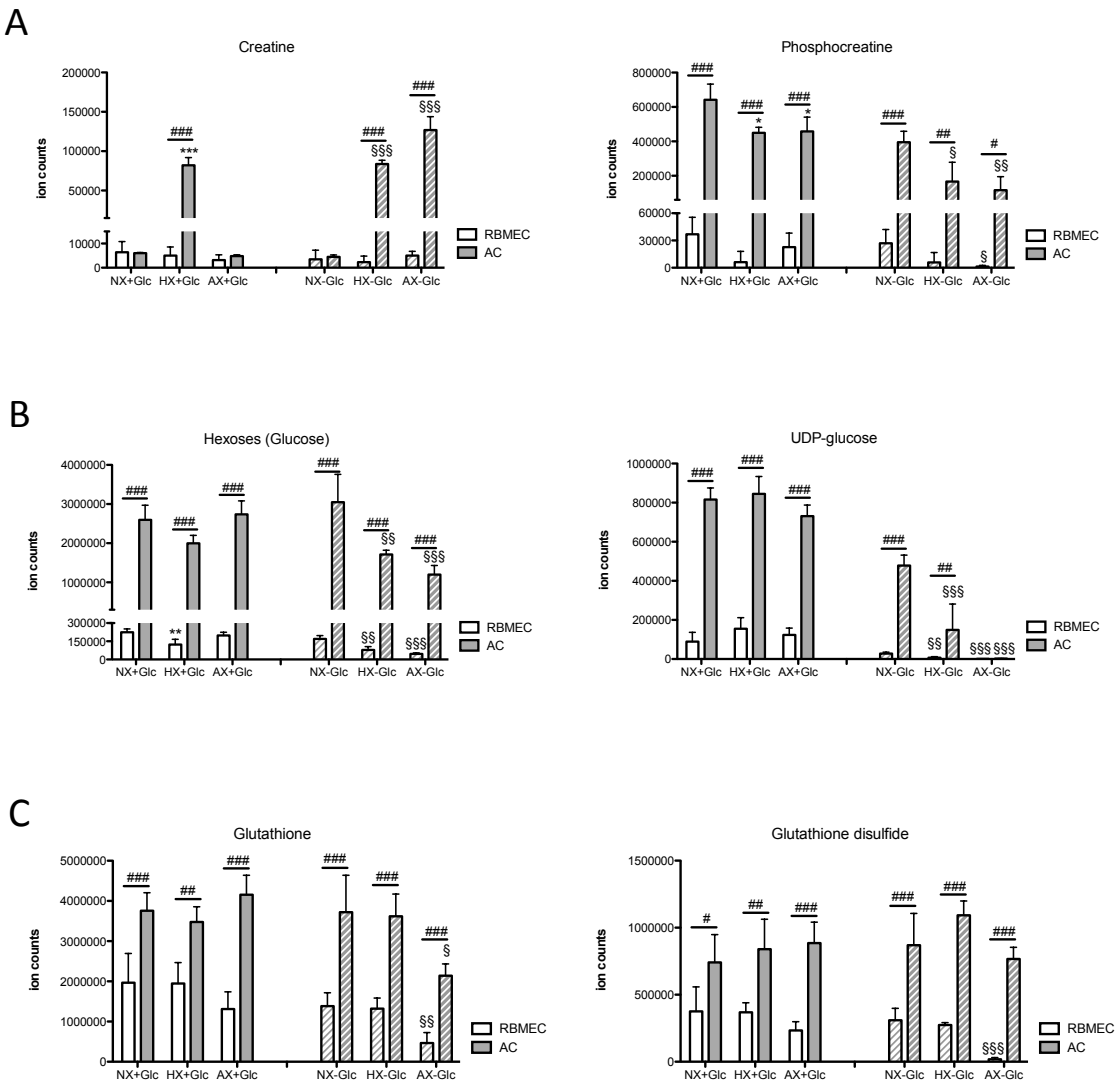

Figure 3.8: O_2 deprivation and ischemia causes changes in phosphocreatine, glycogen and glutathione metabolism. Astrocytes and RBMEC were exposed to normoxia (NX), hypoxia (HX) and near anoxia (AX) with and without glucose (+/-Glc) for 24h. Abundance of metabolites participating in creatine/phosphocreatine cycle (A), glycogen biosynthesis (B) and glutathione turnover (C) were compared. N=4. *P<0.05, **P<0.01, ***P<0.001; 1-way ANOVA compared to NX+Glc. §P<0.05, §§P<0.01, §§§P<0.001; 1-way ANOVA compared to NX-Glc. $^{\#}$P<0.05, $^{\#\#}$P<0.01, $^{\#\#\#}$P<0.001; 2-way ANOVA comparing RBMEC versus AC.

to O_2 deprivation but particularly during OGD. After 24h of HX and AX pCR was reduced by about 30%, in line with this we observed a significant increase of CR under HX. Contrary to our expectations the reduced PCR levels in AX did not results in an increase of CR.

However overall the data indicate that AC use pCR during O_2 deprivation to replenish their ATP pools. OGD led to a further reduction of pCR in AC concomitantly with an increase in CR, highlighting the progressive depletion of the pCR pool to generate ATP. In contrast no significant alteration in CR and pCR was observed in RBMEC during O_2 deprivation, whereas

OGD resulted in a complete exhaustion of pCR during AX. Notably, although we observed universal reduction of pCR levels due to OGD AC were still able to maintain some reserves after 24h of exposure whereas RBMEC were completely depleted.

Regarding glycogen metabolism we observed quite stable hexose and UDP-glucose levels for both AC and RBMEC during O_2 deprivation (Fig 3.8B), suggesting that glycogen synthesis can be maintained as long as glucose is available in the culture media. In contrast during OGD both hexose and UDP-glucose levels decreased in a severity dependent manner for both cell types in line with the fact that glucose becomes a limiting factor. Intriguingly after 24h of AX-Glc AC display a considerable amount of hexoses (probably from their glycogen pool), whereas RBMEC have almost completely depleted their sugar deposits in this condition.

Glutathione levels were, as already observed for normoxic conditions previously (Fig. 3.7B), significantly higher in AC than in RBMEC for all treatments (Fig. 3.8C). O_2 deprivation alone did not alter reduced glutathione levels in AC, whereas in RBMEC a trend for reduction was detected, although not significantly (Fig. 3.8C). OGD caused a significant decrease of GSH in both cell types in AX but not in HX. Again it is important to note that although for both cell types GSH levels declined AC still maintained much higher stores than RBMEC. This indicates that only during AX-Glc treatment both cell types consume considerable amounts of GSH to deactivate ROS, whereas due to the higher levels AC might be able to withstand the oxidative stress longer than RBMEC. Unfortunately we could not make any conclusions on GSSG levels due to the fact that it is likely to be rapidly secreted by cells to maintain a reduced thiol redox potential during oxidative stress and thus intracellular GSSG levels cannot be correlated well to actual GSSG formation (Dringen and Hirrlinger, 2003; Hirrlinger *et al.*, 2001).

A

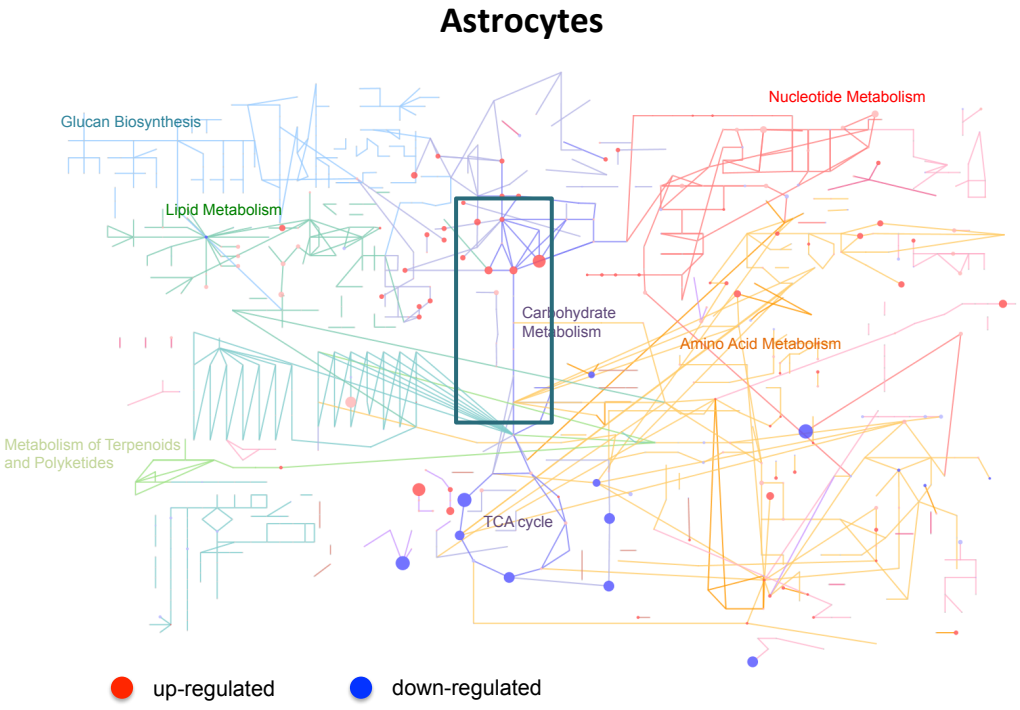

B

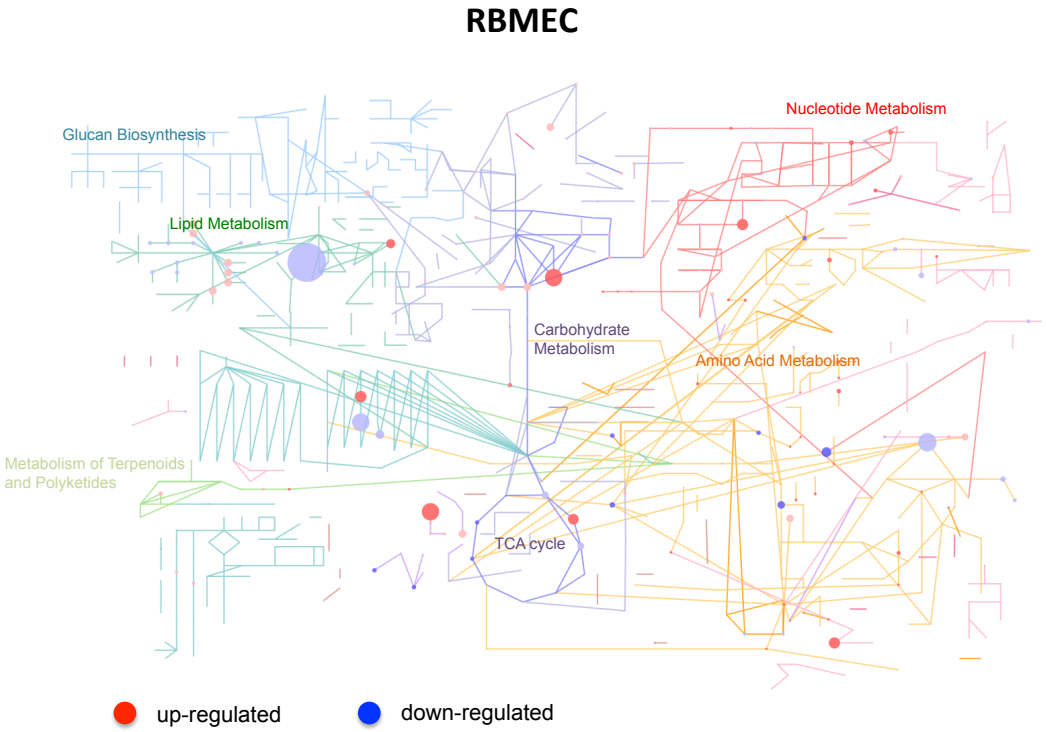

Figure 3.9: O_2 deprivation only minorly affects metabolic pathways in astrocytes and RBMEC. KEGG pathway analysis of changes in metabolite profile after exposure to AX+Glc (0.2% O_2) for 24h in astrocytes **(A)** and RBMEC **(B),** compared to NX+Glc. Red circles depict up-regulated metabolites, blue circles down-regulated metabolites. Circles colored in dark are significantly changed; light colored ones are not significant. Green box: glycolysis pathway, purple lines: carbohydrate metabolism, red lines: nucleotide metabolism, orange lines: amino acid metabolism, dark green lines: lipid metabolism, light green lines: terpenoids and polyketides metabolism, light blue lines: glucan biosynthesis.

A

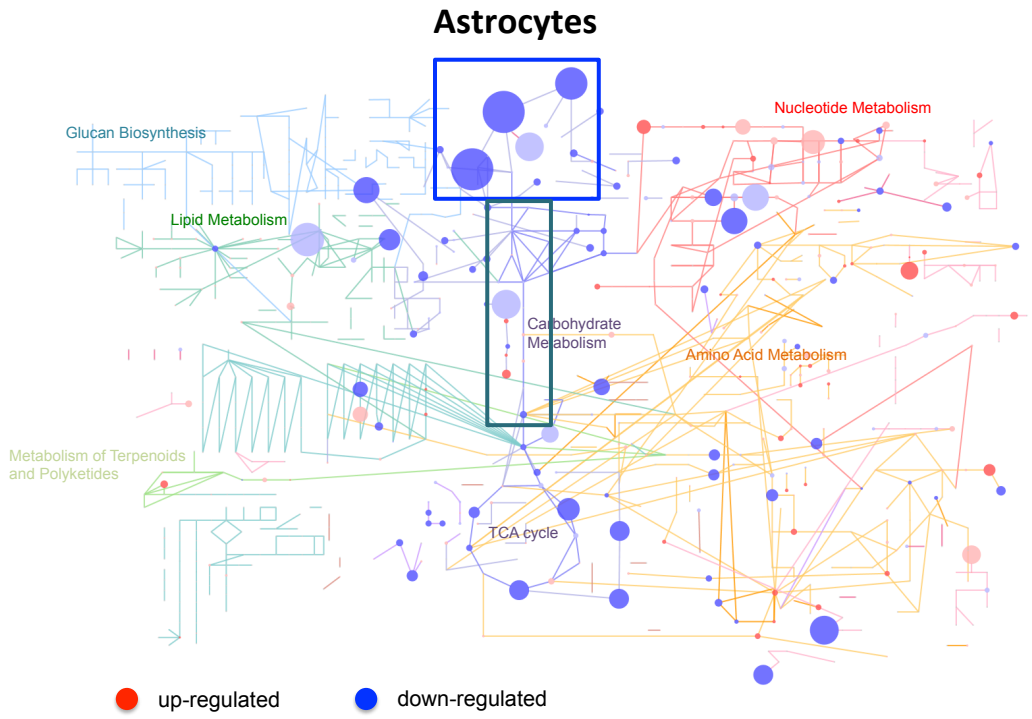

B

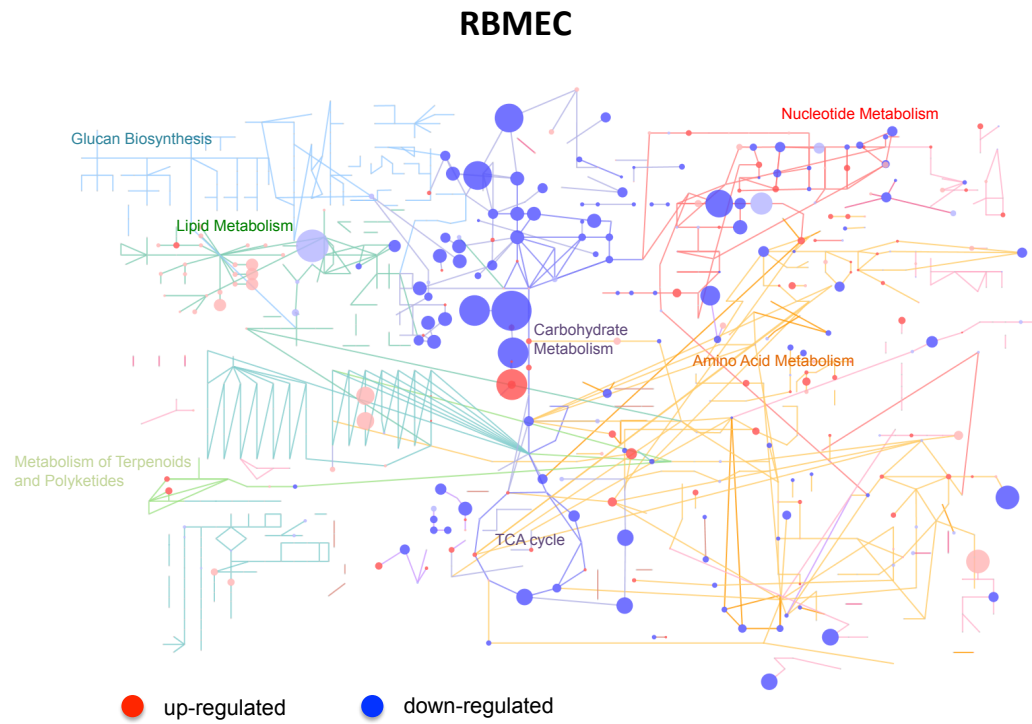

Figure 3.10: OGD in near anoxia results in profound changes of the cellular metabolome. KEGG pathway analysis of changes in metabolite profile after exposure to AX-Glc for 24h in astrocytes (A) and RBMEC (B) compared to NX-Glc. Red circles symbolize up-regulated metabolites, blue circles down-regulated metabolites. Circles colored in dark are significantly changed; light colored ones are not significant. Blue box: UDP-glucose/glycogen metabolism, green box: glycolysis. Purple lines: carbohydrate metabolism, red lines: nucleotide metabolism, orange lines: amino acid metabolism, dark green lines: lipid metabolism, light green lines: terpenoids and polyketides metabolism, light blue lines: glucan biosynthesis.

In order to obtain a more global overview of the metabolic changes occurring in the individual cell types in response to O_2 deprivation and OGD additional pathway analyses were performed. Although overall O_2 deprivation alone did not cause any dramatic metabolome alterations comparing AX+Glc exposure to NX+Glc for both AC (Fig. 3.9A) and RBMEC (Fig. 3.9B) a cell type specific modulation of carbohydrate metabolism was clear from the pathway analysis map. In AC metabolites involved in glycolysis were up-regulated (green box), whereas intermediates of the TCA cycle were down-regulated, suggesting a shift from oxidative metabolism towards a more glycolytic metabolism. In contrast the largely unchanged metabolism pathway observed in RBMEC implied a more rigid and less versatile metabolic profile of RBMEC. Fold changes and statistics of the top altered metabolites presented in the pathway analyses Fig. 3.9 A+B are presented in Appendix Tables A.2 and A.3.

On the other hand glucose deprivation combined with AX caused differential and distinct metabolic changes in both cell types (Fig. 3.10A+B, refer to Appendix Table A.4 and A.5 for fold changes and statistics). The pathway analysis depicts the changes in the metabolic pathways between AX-Glc and NX-Glc after 24h of treatment. Generally a down-regulation of metabolites was observed, rather than an up-regulation, with the amino acid metabolism (orange lines) pathway being the only one showing an accumulation of metabolites. AC showed a marked reduction in metabolites related to UDP-glucose/glycogen metabolism (blue box), whereas the down-stream pathways like glycolysis remained largely unaffected (green box) (Fig. 3.10A). Similarly to AX+Glc we observed a reduction of metabolites related to TCA cycle in AC. In RBMEC the metabolic changes were very profound and many more metabolites were reduced compared to AC, particularly in carbohydrate and nucleotide metabolism (Fig. 3.10B). The reduction of multiple metabolites of carbohydrate metabolism implies that compared to AC the RBMEC are starved of carbohydrates since they do not have as high reserves as AC do.

Finally we compared the metabolic pathways up-regulated during AX-Glc treatment in the two cell types relative to each other, to get an idea which pathways are particularly different in this condition (Fig. 3.11). Interestingly amino acid metabolism pathway-related metabolites were the major elevated ones in AC (highlighted in light red), but again also glutathione metabolism

and starch and sucrose metabolism (including glycogen metabolism) were present in the list (highlighted in dark red) (Fig. 3.11A). As AC clearly tolerate AX-Glc better than RBMEC, this finding again confirms our previous observation that glycogen and glutathione metabolism strongly contribute to the tolerance of AC towards these injury conditions. However the Table also suggests that AC have a much more active amino acid metabolism under severe injury conditions raising the question whether they use amino acid catabolism to feed their energy needs. In RBMEC the citrate cycle as well as amino sugar and nucleotide sugar metabolism and pyruvate metabolism was increased compared to AC (Fig. 3.11B, highlighted in blue). The fact that both TCA cycle as well as pyruvate pathway-related metabolites are accumulated in RBMEC suggests a higher oxidative metabolism than for AC.

A

Astrocytes

Pathway	Total	Expected	Hits	Raw p
Phenylalanine metabolism	9	0.54	5	7.15E-05
Glycine, serine and threonine metabolism	32	1.92	8	3.84E-04
Aminoacyl-tRNA biosynthesis	67	4.01	12	3.89E-04
Glutathione metabolism	26	1.56	7	5.60E-04
Phenylalanine, tyrosine and tryptophan biosynthesis	4	0.24	3	7.95E-04
Valine, leucine and isoleucine biosynthesis	11	0.66	4	2.87E-03
Taurine and hypotaurine metabolism	8	0.48	3	9.34E-03
Alanine, aspartate and glutamate metabolism	24	1.44	5	1.18E-02
Nitrogen metabolism	9	0.54	3	1.34E-02
Cysteine and methionine metabolism	28	1.68	5	2.26E-02
D-Glutamine and D-glutamate metabolism	5	0.30	2	3.15E-02
Pyridine metabolism	41	2.46	6	3.20E-02
Starch and sucrose metabolism	23	1.38	4	4.43E-02

B

RBMEC

Pathway	Total	Expected	Hits	Raw p
Citrate cycle (TCA cycle)	20	0.34	4	2.67E-04
Alanine, aspartate and glutamate metabolism	24	0.41	4	5.59E-04
Amino sugar and nucleotide metabolism	37	0.63	4	2.99E-03
Tyrosine metabolism	42	0.72	3	3.27E-02
Butanoate metabolism	20	0.34	2	4.42E-02
Pyruvate metabolism	22	0.38	2	5.27E-02

Figure 3.11: Severe ischemic injury causes differential pathway activity in astrocytes and RBMEC. Comparison of active metabolic pathways after 24h of AX-Glc exposure in AC (A) and RBMEC (B) compared to each other. Total: total number of metabolites involved in pathway, Expected: number of metabolites detected in a pathway by chance, Hits: up-regulated metabolites in sample, Raw p: calculated significance, *P*-value.

3.3.4 Discussion

Our own studies (Section 3.2, Figure 3.2C) and others (Ceruti *et al.*, 2011; Redzic *et al.*, 2013) have clearly demonstrated that endothelial cells are more susceptible to hypoxic/ischemic injury than AC. Since adequate adaptation of cell metabolism is a crucial parameter for cell survival during such injuries (Ogunshola and Al-Ahmad, 2012), we hypothesized that the capability of the different cell types to adapt their metabolism accordingly might account for the observed differences in their tolerance and subsequently strongly impact barrier integrity. The liquid chromatography-mass spectrometry (LC-MS) approach used in this study allowed us to record global changes in cell metabolism in an untargeted and very sensitive way. Importantly, a great advantage was that the use of a capillary-based system requiring only low amounts of sample material made it possible to conduct this study with primary RBMEC instead of an endothelial cell line. A caveat of this work was that we had to culture cells in similar media to directly compare the treatment effects between the cells. During pilot tests we tested 2 different minimal media (+ and - bFGF) both of which appeared to be tolerated well by both cell types and reiterated the differential sensitivity of AC and RBMEC towards OGD that also has been reported previously. Perplexingly however during the actual experiments the RBMEC were clearly impaired in the minimal media-bFGF under normoxic conditions. Fortunately this problem was solved by using a media that contained supplements similar to the original RBMEC media but only 10% calf serum (MS media) for both AC and RBMEC. To really prove that the MS media shows the same effects on MTT conversion as previously observed for the pilot experiment we plan to repeat these experiment using MS media.

The second challenge for direct comparison of metabolite abundance between the cell types was the normalization of the data. In the metabolomics field a gold standard for robust and reliable normalization of cells has not been established (Silva *et al.*, 2013). In general normalization to total protein amount, cell number and DNA content are discussed (Silva *et al.*, 2013). The study by Silva and co-workers revealed that normalization to protein amount is difficult because the metabolite extraction buffers interfere with conventional protein assays (Silva *et al.*, 2013), moreover hypoxia and ischemia affect protein synthesis (Koritzinsky and Wouters, 2007) and thus might not correlate well to cellular metabolite amounts. Cell number

would probably be the most accurate method but again hypoxic/ischemic treatment alters proliferation (Ogunshola and Al-Ahmad, 2012; Stanimirovic and Friedman, 2012) and thus we could not assume similar cell numbers for the different treatments and would have needed a control plate of each treatment for counting, which is not realizable for the RBMEC. More importantly AC and RBMEC have a very different cell size, thus it seems likely that the large AC would contain more metabolites than the smaller RBMEC, underlining that cell number is not a good normalization factor. Measurement of cellular DNA is another possibility, but again depending of the degree and mode of cell death (apoptosis versus necrosis) DNA content may not be a very reliable measure. The last option, which is widely used in the field and which we finally adopted, is to normalize all metabolites based on the total ion count of the sample (Katajamaa and Oresic, 2007). The total ion count reflects the total amounts of metabolites present in a sample, e.g. comparable to total protein amount in a cell lysate. We consider that for our experiments this method represents the most accurate method as it expresses the abundance of a given metabolite in correlation to the total metabolites within the sample.

Principal component analysis of the data sets revealed that the cell type determined the major difference of the recorded metabolomic profiles suggesting a general difference in the metabolism of AC and RBMEC. Indeed pathway analyses showed fundamental differences in physiological metabolism between the two cell types. Compared to RBMEC AC accumulated large amounts of metabolites involved in sugar and particular glucose metabolism under physiological conditions. However, a weak point of choosing an untargeted study approach was that the different types of metabolite isomers could not be distinguished from each other. This particularly applies for sugar intermediates like hexoses or their phosphorylated derivatives and makes an in depth interpretation of sugar metabolism impossible. Nevertheless this study has revealed important information regarding differences in carbohydrate metabolism between AC and RBMEC and future in depth studies like gas chromatography mass spectrometry can be used to distinguishing such isomers and investigate sugar metabolism pathways in more detail.

The high hexose content in AC however correlates very well with the crucial role in supply of important energy substrates produced from glucose, like lactate or glycogen, for themselves

but also for other brain cells, particularly neurons (Belanger *et al.*, 2011; Prebil *et al.*, 2011; Sickmann *et al.*, 2009; Walls *et al.*, 2009). Since endothelial cells at the BBB in contrast primarily mediate transport of glucose from the blood across into the brain (Abbott *et al.*, 2006; Mann *et al.*, 2003), and no role in supply of energetic fuels to other cells has been discussed like for AC, it seems logical that AC contain higher concentrations of glucose-related metabolites than RBMEC. Indeed AC appeared to have high rates of glycogen and phosphocreatine biosynthesis, two compounds being crucially involved in maintenance of ATP levels under energy demanding conditions (Belanger *et al.*, 2011; Perasso *et al.*, 2013; Prebil *et al.*, 2011; Tachikawa *et al.*, 2007). Indeed strong accumulation of UDP-glucose in AC approximately 8 times higher than in RBMEC supports this hypothesis. This also agrees with studies demonstrating that AC are the major glycogen store within the brain, whereas only minor amounts are detected in capillary endothelial cells, neurons, pericytes and meningeal cells (Cataldo and Broadwell, 1986a; Cataldo and Broadwell, 1986b). Different studies have shown that glycogen is consumed during hypoxia and particularly ischemia by AC and represents a central energy source under such conditions (Kahlert and Reiser, 2004; Niitsu *et al.*, 1999). This correlates with reduced UDP-glucose observed in our model during OGD (Fig. 3.8B and Fig. 3.10A) indicating that glycogen biosynthesis is inhibited. Furthermore the fact that metabolites involved in glycolysis remain largely unaffected during AX-Glc in AC suggests they degrade glycogen stores to feed glycolysis, in complete contrast to RBMEC where a marked reduction of carbohydrate metabolites was observed.

AC also appear to profit from approximately 10 times higher levels of phosphocreatine compared to RBMEC. During O_2 deprivation and OGD AC consume pCR, implying they use it for ATP generation in stress conditions. Interestingly the expression levels of cytosolic brain type creatine kinase, a crucial enzyme for creatine biosynthesis, has been directly correlated to resistance of cell types to acute energy loss, e.g. during hypoxia or hypoglycemia (Tachikawa *et al.*, 2007). Indeed in the brain mainly AC express high levels of brain type creatine kinase, whereas its immunoreactivity was absent in capillaries of the adult mouse cortex (Lowe *et al.*, 2013; Tachikawa *et al.*, 2004; Tachikawa *et al.*, 2007), confirming our hypothesis that endothelial cells do not synthesize considerable amounts of creatine and thus may be protected less during ischemic injuries.

Depletion of ATP stores during hypoxia and ischemia represents one important factor that has deleterious effects on cell survival, another factor crucially determining cell fate under such injury conditions is oxidative stress (Love, 1999; Miyata *et al.*, 2011; Stanimirovic and Friedman, 2012). Reduced glutathione (GSH) is considered the major antioxidant within cells (Hirrlinger and Dringen, 2010; Wang *et al.*, 2013) and in line with this the resistant AC retained about double the amount of GSH than RBMEC. Interestingly GSH slightly decreased in RBMEC during O_2 deprivation whereas the levels remained stable in AC, which may either be due to increased oxidative stress in RBMEC compared to AC or the ability of AC to compensate GSH oxidation via regeneration from GSSG or biosynthesis. In AX-Glc treatment both cell types exhibited a considerable reduction of GSH levels likely due to increased ROS formation under such severe conditions. Overall our data implies that the higher GSH levels help AC to better tolerate severe injury conditions than RBMEC. Indeed depletion of astrocytic glutathione stores has been correlated to their decreased resistance during ischemia (Gabryel and Malecki, 2006; Sims *et al.*, 2004) underlining our hypothesis that the amount of glutathione levels correlates to increased ischemic tolerance.

Overall AC appear to be perfectly equipped for stress conditions of energy depletion and ROS, whereas endothelial cells cannot rely on similar protective mechanisms. The high tolerance of cultured AC to hypoxic/ischemic conditions appears to be largely reliant on a combination of various fine-tuned and versatile metabolic changes including energy generation by either glycolysis or oxidative pathways, efficient metabolism of substrates other than glucose and a high glutathione content – to name only those revealed in this study. However it seems likely that further in-depth analysis of other pathways could reveal additional key metabolic adaptations. This perfect adaptation of AC is likely due to their important protective role for other brain cells, particularly neurons but also endothelial cells at the BBB (Engelhardt *et al.*, 2014b; Schroeter *et al.*, 1999; Turner and Adamson, 2011), during injury conditions. It is well known that AC provide energy substrates, such as lactate derived from glucose or glycogen, to neurons and also secretion of glutathione by AC has been well documented to protect neurons from oxidative stress (Belanger *et al.*, 2011; Bouzier-Sore and Pellerin, 2013; Wiesinger *et al.*, 1997). For this reason it would be very interesting to define whether AC also provide such metabolic support to endothelial cells in order to improve

endothelial function during injury conditions. For example treatment of endothelial cells with AC-conditioned media or co-cultivation of EC and AC could give very interesting information on whether AC alter endothelial metabolism under injury conditions. In addition a study including pericytes and monitoring how their metabolism compares to AC and endothelial adaptations would add to our understanding about cell-specific adaptations to hypoxia and ischemia.

In conclusion this study is the first to compare the global metabolism between AC and endothelial cells. Unfortunately until now brain researchers have largely disregarded the contribution of an intact BBB brain function in disease states. Thus most studies investigating brain metabolism exclusively focus on AC and neurons with the importance of endothelial cells and pericytes being almost completely neglected. However due to their central role in mediating brain homeostasis it is crucial to understand more about the physiological and pathophysiological metabolism of the BBB associated cells. In this regard an important open question in the field is: which cellular parameters regulate cellular resistance to hypoxic and ischemic injury? This study has provided convincing evidence that differences in cellular metabolism contribute hypoxic/ischemic tolerance with particularly highly energetic metabolites like glycogen or phosphocreatine, and antioxidants being important determinants for cellular survival. In the next steps we must assess whether we can take advantage of such mechanisms during injury and disease progression to improve barrier stability and, ultimately, functional recovery.

4 CONCLUSIONS AND PERSPECTIVES

The scope of this work was to improve understanding of the molecular aspects of BBB impairment in response to hypoxic and ischemic injury with a special focus on the specific responses of the individual BBB cells. Thematically the work was subdivided in two major parts. The first part investigated the impact of HIF-1 signaling on hypoxic BBB impairment in endothelial cells with a particular focus on tight and adherens junction regulation.

HIF-1 represents a crucial transcription factor for adaptation to hypoxic/ischemic results. Particularly in neurons HIF-1 signaling has been demonstrated to be crucial for cell survival during hypoxic and ischemic injury (Baranova *et al.*, 2007; Vangeison *et al.*, 2008). Despite the fact that HIF-1 improves cellular adaptation its impact on BBB was only inferred. By initiation of angiogenesis e.g. via VEGF signaling, hypoxic signaling provokes barrier opening causing brain edema, dysregulation of brain homeostasis, oxidative stress and inflammatory events (Ogunshola and Al-Ahmad, 2012; Stanimirovic and Friedman, 2012). Indeed various studies modulating HIF-1 activity using HIF-1 stabilizers and inhibitors suggested a negative impact of HIF-1 signaling on outcome in ischemic models resulting, increased edema formation and infarct volumes, which are both closely related to impaired BBB function (Chen *et al.*, 2008a; Yeh *et al.*, 2007). However these studies did not directly investigate the mechanisms of BBB disruption on a molecular level. Our study (Engelhardt *et al.*, 2014a) showed that normoxic HIF-1α stabilization mimics hypoxic BBB disruption on a temporal and mechanistic level exhibiting similar disturbance of barrier function and tight/adherens junction modulation, thus substantiating our hypothesis that HIF-1 mediates hypoxic BBB disruption.

Indeed this observation discloses some caveats regarding the use of HIF-1 stabilizers in clinical applications. Particularly in stroke and traumatic brain injury research HIF-1 stabilizers are considered for treatment due to their neuroprotective and erythropoiesis-stimulating action (Harten *et al.*, 2010; Nagel *et al.*, 2010). However the adverse action of such drugs on barrier function should not be disregarded. The increased edema formation and penetration of blood-borne molecules that convenes with increased BBB permeability contributes to aggravated cerebral damage. This observation clarifies that HIF-1 exerts different outcomes

on different cell types: improving cell survival in the case of neurons but promoting loss of barrier function in endothelial cells. Therefore the use of HIF-1 stabilizers in therapeutic settings needs to be very well defined and potentially requires a very tight time window in order to achieve neuroprotection without too severe BBB impairment. In this context more knowledge about the action of HIF-1 on different cell types and about the temporal progress of diseases will be required. Another potential solution to combat the adverse effects of HIF-1 on barrier function would be to apply the HIF-1 stabilizers locally into the brain avoiding a systemic administration (either orally or via the blood stream), where the drugs would have to reach the brain across the vasculature.

It is also noteworthy that there is also the potential to exploit the barrier-permeabilizing effect of HIF-1 to selectively open the BBB for drug delivery. However currently there is insufficient information on the mechanistic action of HIF-1 on the endothelial permeability to be able to estimate the consequences of such a treatment.

Importantly we showed in our study that HIF-1 induced displacement of ZO-1, claudin-5 and VE-cadherin from the plasma membrane and tyrosine phosphorylation of occludin appears to play a more important role in BBB opening than down-regulation of tight/adherens junction proteins. In support of this HIF-1 inhibition could partially revert the adverse outcome of hypoxia on barrier function and cellular junction rearrangements although not completely. With this study we obtained a good insight how HIF-1 signaling affects tight junction and BBB modulation. However it seems likely that these effects are not directly exerted by HIF-1 but more c clikely via HIF-1 target genes, therefore in future studies it would be very interesting to investigate the underlying mechanism of tight junction rearrangements in more depth and to identify the players inducing and exerting tight junction displacement. Moreover it would be highly attractive to investigate whether HIF-2 signaling contributes to hypoxic barrier impairment, particularly since the brain endothelium exhibits strong HIF-2α expression and HIF-2 appears to be an important vascular regulator *in vivo* (Skuli *et al.*, 2009). In addition a modulation of HIF-2 signaling by HIF-1 stabilizers and inhibitors is likely because of the similar regulation mechanisms of HIF-α proteins. Due to technical limitations of we could not directly target HIF-1 using overexpression and knock down in RBE4 cells and thus had to use HIF-1 modulating drugs despite the caveat of simultaneously targeting HIF-2α. In addition

HIF-2α expression could not be monitored at that time due to the lack of a reliable antibody on the market. Certainly as improved methodology becomes available the impact of HIF-2 on BBB function needs to be clarified.

We have previously shown that astrocytes and pericytes protect the endothelial barrier during O_2 deprivation (Al Ahmad *et al.*, 2009). For this reason it would be enlightening to include astrocytes and pericytes in the model and investigate whether they are able to revert the negative effects on endothelial HIF-1 signaling. Furthermore investigations of how HIF-1 signaling in astrocytes and pericytes affects endothelial barrier function and tight junction regulation are also required.

The second part of this work focused on the basal responses of endothelial cells, astrocytes and pericytes to hypoxic and ischemic insults. This part of the work did not directly investigate BBB modulation but was performed to improve our fundamental comprehension of barrier changes that occur during hypoxic and ischemic disease settings. At the basic level, better knowledge of individual responsiveness and tolerance of the BBB cells to such insults will help to better define their participation in BBB modulation. As expected the barrier cells differed considerably in their hypoxic/ischemic tolerance. Endothelial cells (RBE4 cells) were very sensitive to O_2 deprivation alone and responded with massive induction of hypoxia-induced gene/protein expression, severe disruption of the actin cytoskeleton and strong impairment in viability, whereas astrocytes and pericytes tolerated prolonged O_2 deprivation without any obvious signs of impairment. Oxygen-glucose deprivation (OGD) in contrast affected astrocytes and pericytes particularly when exposed to near anoxia, but nevertheless both were able to tolerate these severe insults for a limited period of time, with astrocytes being more tolerant than pericytes. Indeed both astrocytes and pericytes were potently able to appropriately modulate crucial responses for survival such as cell cycle and autophagy.

This study aimed to characterize the cell-specific fate and responses in a comprehensive way but clearly a more in depth analysis of some particular parameters e.g. activated cell death and autophagy pathways would give the study more weight. Similarly the use of primary endothelial cells for some crucial experiments would clarify whether RBE4 cells have similar responses to primary ECs and importantly whether the cells exhibit similar sensitivities towards the treatments. Indeed it is a constant point of discussion in the field how well

endothelial cell lines and primary isolated endothelial cells reflect the vascular responses at the BBB *in vivo*. In my point of view, it is desirable to use primary isolated cells over endothelial cell lines as they more closely manifest the physiological setting, but as isolation of primary brain endothelial cells is very time and cost intense, endothelial cell lines represent an appropriate alternative. Indeed depending on the research question endothelial cell lines represent a good model system, for example when mechanistic queries are addressed.

In summary the present study taught us, that particularly endothelial function needs to be improved during hypoxic/ischemic injury conditions as the vasculature endothelium clearly represents a weak link in such conditions and perivascular cells are considerably more tolerant. Our previous study has suggested that at least in terms of barrier function and tight junctions HIF-1 signaling exerts rather negative effects on the vasculature and similarly the current results indicate that endothelial cells are characterized by elevated HIF-1 stabilization compared to the perivascular cells. For this reason it may be worthwhile to investigate whether suppression/reduction of HIF-1 signaling can improve endothelial performance and revert some of the negative effects observed in the comparative study. Based on the findings of the comparative study the reason why some cells are much more resistant to hypoxia/ischemia than others remained to be better elucidated. Considering the importance of metabolic adaptation for cell survival under these circumstances (see introduction, Section 1.2.2 and 1.2.3) the hypothesis that some basal differences in the capability of metabolic adaptation could account for the varying sensitivities amongst the cell types caught my interest. To explore this question in an unbiased and global way an untargeted LC-MS approach was chosen, which allowed detection of about 500 annotated metabolites by accurate mass. To prevent the initiation of a highly complex study we decided to compare only the metabolic footprints of endothelial cells (as rather sensitive cell type) and astrocytes (as very robust cells). In order to reduce artifacts that could be caused by the use of a transformed cell line, primary rat brain microvascular endothelial cells (RBMEC) and astrocytes were isolated and cultured in identical media. In support of our hypothesis we observed that indeed RBMEC and astrocytes significantly differed in their metabolic profiles and modulation. Astrocytes were particularly equipped for conditions of nutrient shortage and oxidative stress as they showed strong glycogen metabolism, high glutathione and high

phosphocreatine levels. All these observations agree well with existing literature and support the current view about astrocytes providing the “emergency supply” of lactate (generated from glycogen) and glutathione for neurons (Belanger *et al.*, 2011; Bouzier-Sore and Pellerin, 2013; Wiesinger *et al.*, 1997). In this case we could hypothesize that astrocytes may also provide substrates to endothelial cells experiencing stressful conditions. Much less is known about the metabolism of endothelial cells. Our study is the first to measure the endothelial metabolome and show that unlike astrocytes endothelial cells do not build major stores of glycogen, glutathione and/or phosphocreatine and thus suffer much more from ischemic conditions, although both tolerate hypoxic and near anoxic exposure well when glucose is present in the culture media. Overall the metabolomics study gave us very interesting insights into metabolic adaptation of endothelial cells and astrocytes and supported our initial hypothesis that differences in cellular metabolism could crucially contribute to their sensitivity to hypoxia/ischemia. However as for all screening approaches some possible pitfalls need to be considered. Although this study gave us important indications about which metabolic pathways might account for the differential sensitivities of astrocytes and endothelial cells, it remains to be fully experimentally proven. Thus the metabolomics study can be seen as a starting point, the initial screen that requires further experimental evidence to really corroborate our hypotheses. In addition the results obtained from the LC-MS approach regarding isomers like hexoses or amino acids need to interpreted with particular caution. To really investigate glycolytic pathways in detail gas chromatography mass spectrometry (GC-MS) that allows separation of isomers would need to be applied. In addition looking at mitochondrial respiration in terms of TCA cycle and electron transport chain activity in the individual cell types would add valuable information to our current study. To go a step ahead it would be highly interesting to investigate how a co-culture with astrocytes or astrocyte-conditioned media would affect the metabolic response of RBMEC and whether factors released from astrocytes like lactate or glutathione would improve RBMEC outcome. Finally, it is apparent that we did not include pericytes in this study, however observing how their metabolism compares to astrocytes and whether they similarly possess protective metabolites conferring tolerance to ischemia, as the comparative study suggested, would be fascinating.

In summary this project addressed various aspects of hypoxic and ischemic responses occurring at the BBB. We substantiated our hypothesis that HIF-1 signaling indeed exerts adverse effects during hypoxic barrier loss and in addition demonstrated that the cells at the BBB are considerably different in their tolerance, responses and metabolic adaptation to hypoxia and ischemia. Overall this project significantly increased our knowledge about the consequences of hypoxia/ischemia on BBB and individual cellular function and opened up various new interesting questions and directions.

5 APPENDIX

Table A.1: Relationship of metabolite abundance between AC and RBMEC under physiological conditions (NX+Glc) expressed as fold changes. Statistics: *p<0.05, **p<0.01, *** p<0.001; 1-way Anova.

Metabolite Name	KEGG ID	Monoisotopic mass	Up in	Significance	Fold change
UDP-glucuronate	C00167	580.0343	AC	***	331.56
N-Acetyl-L-aspartate	C01042	175.0481	EC	*	146.43
N-Carbamoyl-L-aspartate	C00438	176.0433	EC	*	131.54
Allantoate	C00499	176.0546	EC	*	131.54
GDP-mannose	C00096	605.0772	AC	***	57.57
Naphthalene-1,2-diol	C03012	160.0524	AC	***	36.31
AMP	C00020	347.0631	EC	***	31.44
dGMP	C00362	347.0631	EC	***	31.44
Hypotaurine	C00519	109.0197	AC	***	25.66
N-Acetyl-D-glucosamine 6-phosphate	C00357	301.0563	EC	*	23.97
N-Acetyl-D-mannosamine 6-phosphate	C04257	301.0563	EC	*	23.97
N-Acetyl-alpha-D-glucosamine 1-phosphate	C04501	301.0563	EC	*	23.97
Succinyl-CoA	C00091	867.1313	AC	***	23.29
(S)-Methylmalonyl-CoA	C00683	867.1313	AC	***	23.29
(R)-Methylmalonyl-CoA	C01213	867.1313	AC	***	23.29
Malonyl-CoA methyl ester	C19673	867.1313	AC	***	23.29
5-Acetylamino-6-formylamino-3-methyluracil	C16365	226.0702	AC	***	18.44
Phosphocreatine	C02305	211.0358	AC	***	17.21
L-2-Aminoadipate adenylate	C05560	490.1213	AC	***	16.68
Ethanolamine phosphate	C00346	141.0191	EC	**	12.90
Cys-Gly	C01419	178.0412	AC	***	12.75
D-Glucono-1,5-lactone	C00198	178.0477	AC	***	12.75
L-Gulono-1,4-lactone	C01040	178.0477	AC	***	12.75
2-Dehydro-3-deoxy-D-galactonate	C01216	178.0477	AC	***	12.75
1,2-Dihydronaphthalene-1,2-diol	C06205	162.0681	AC	**	11.56
Pyruvate	C00022	88.016	AC	***	11.47
3-Oxopropanoate	C00222	88.016	AC	***	11.47
L-Tyrosine	C00082	181.0739	AC	***	11.29
D-Glucose	C00031	180.0634	AC	***	11.25
D-Fructose	C00095	180.0634	AC	***	11.25
D-Galactose	C00124	180.0634	AC	***	11.25
myo-Inositol	C00137	180.0634	AC	***	11.25
D-Mannose	C00159	180.0634	AC	***	11.25
beta-D-Glucose	C00221	180.0634	AC	***	11.25
alpha-D-Glucose	C00267	180.0634	AC	***	11.25
beta-D-Fructose	C02336	180.0634	AC	***	11.25
D-chiro-Inositol	C19891	180.0634	AC	***	11.25
Theobromine	C07480	180.0647	AC	***	11.25
1,7-Dimethylxanthine	C13747	180.0647	AC	***	11.25
L-erythro-4-Hydroxyglutamate	C05947	163.0481	AC	***	10.99
Homovanillate	C05582	182.0579	AC	***	9.21
3-Methoxy-4-hydroxyphenylglycolaldehyde	C05583	182.0579	AC	***	9.21
UDP-glucose	C00029	566.055	AC	***	9.00
UDP-D-galactose	C00052	566.055	AC	***	9.00
Biotin	C00120	244.0882	AC	***	7.71
Stachyose	C01613	666.2219	AC	**	7.56
Pyridoxamine phosphate	C00647	248.0562	AC	***	7.53
Cytidine	C00475	243.0855	AC	***	7.51
gamma-Glutamyl-beta-cyanoalanine	C05711	243.0855	AC	***	7.51
L-2-Aminoadipate	C00956	161.0688	AC	*	7.25
N-Glycoloyl-neuraminate	C03410	325.1009	AC	***	6.74
sn-glycero-3-Phosphocholine	C00670	258.1106	AC	***	6.10
cis-Aconitate	C00417	174.0164	AC	***	6.03
sn-glycero-3-Phosphoethanolamine	C01233	215.0559	AC	***	5.91
GDP-L-fucose	C00325	589.0822	AC	***	5.83
D-Sorbitol	C00794	182.079	EC	**	5.78
Galactitol	C01697	182.079	EC	**	5.78
3-Methylcrotonyl-CoA	C03069	849.1571	AC	***	5.63
2-Methylbut-2-enoyl-CoA	C03345	849.1571	AC	***	5.63
UMP	C00105	324.0359	EC	*	5.47
3-Methoxy-4-hydroxyphenylethyleneglycol	C05594	184.0736	EC	**	5.45
Choline phosphate	C00588	184.0739	EC	**	5.45
L-Adrenaline	C00788	183.0895	EC	**	5.43
L-Normetanephrine	C05589	183.0895	EC	**	5.43
(S)-3-Hydroxyoctanoyl-CoA	C05266	909.2146	AC	***	5.24
N-Acetyl-L-glutamate	C00624	189.0637	EC	*	4.86

Table A.1 (continued): Relationship of metabolite abundance between AC and RBMEC under physiological conditions (NX+Glc) expressed as fold changes. Statistics: *p<0.05, **p<0.01, *** p<0.001; 1-way Anova.

Metabolite Name	KEGG ID	Monoisotopic mass	Up in	Significance	Fold change
sn-Glycerol 3-phosphate	C00093	172.0137	AC	***	4.61
6-Deoxy-L-galactose	C01019	164.0685	EC	***	4.51
Cinnavalininate	C05640	300.0382	AC	***	4.40
Adenylyl sulfate	C00224	427.0199	EC	**	4.30
ADP	C00008	427.0294	EC	**	4.30
Adenosine 3,5-bisphosphate	C00054	427.0294	EC	**	4.30
dGDP	C00361	427.0294	EC	**	4.30
Sulfate	C00059	97.9674	AC	***	4.28
Orthophosphate	C00009	97.9769	AC	***	4.28
Uridine	C00299	244.0695	EC	*	4.25
N-Acetylneuraminate	C00270	309.106	AC	***	3.89
O-Acetylneuraminic acid	C03525	309.106	AC	***	3.89
7-Methyluric acid	C16355	182.044	AC	*	3.74
1-Methyluric acid	C16359	182.044	AC	*	3.74
NAD+	C00003	664.1169	AC	***	3.71
L-Homocysteine	C00155	135.0354	EC	**	3.58
Protoporphyrin	C02191	562.258	AC	***	3.56
Prunasin	C00844	295.1056	EC	***	3.53
D-Glucono-1,5-lactone 6-phosphate	C01236	258.0141	AC	***	3.44
2-Deoxyinosine 5-phosphate	C06196	332.0522	EC	**	3.27
Sedoheptulose 1,7-bisphosphate	C00447	370.0066	EC	**	3.15
3,4-Dihydroxymandelate	C05580	184.0372	AC	***	2.97
4-Hydroxybenzoate	C00156	138.0317	EC	*	2.86
Gentisate aldehyde	C05585	138.0317	EC	*	2.86
L-Ornithine	C00077	132.0899	AC	***	2.80
D-Ornithine	C00515	132.0899	AC	***	2.80
Nicotinamide D-ribonucleotide	C00455	334.0566	EC	***	2.66
Adenosine	C00212	267.0968	EC	**	2.65
Deoxyguanosine	C00330	267.0968	EC	**	2.65
(1aalpha,2beta,3alpha,11calpha)-1a,2,3,11c-Tetrahydr	C19559	306.1256	AC	**	2.63
CMP-2-aminoethylphosphonate	C05673	430.0655	AC	*	2.60
Calcitriol	C01673	416.329	EC	***	2.59
Secalciferol	C07712	416.329	EC	***	2.59
7alpha,24-Dihydroxy-4-cholesten-3-one	C17331	416.329	EC	***	2.59
7alpha,25-Dihydroxy-4-cholesten-3-one	C17332	416.329	EC	***	2.59
3beta-Hydroxy-5-cholestenoate	C17333	416.329	EC	***	2.59
7alpha,26-Dihydroxy-4-cholesten-3-one	C17336	416.329	EC	***	2.59
4-Cholesten-7alpha,12alpha-diol-3-one	C17339	416.329	EC	***	2.59
(S)-4-Hydroxymandelonitrile	C03742	149.0477	EC	***	2.56
5,6-Dihydroxyindole	C05578	149.0477	EC	***	2.56
L-Methionine	C00073	149.051	EC	***	2.56
CDP	C00112	403.0182	EC	***	2.56
7,8-Dihydroneopterin 3-triphosphate	C04895	494.9957	EC	**	2.56
L-Alanine	C00041	89.0477	AC	***	2.54
beta-Alanine	C00099	89.0477	AC	***	2.54
Sarcosine	C00213	89.0477	AC	***	2.54
5-Phosphoribosylglycinamide	C03838	286.0566	AC	*	2.46
(S)-Malate	C00149	134.0215	EC	**	2.46
Raffinose	C00492	504.169	AC	***	2.42
D-Gal alpha 1->6D-Gal alpha 1->6D-Glucose	C05404	504.169	AC	***	2.42
4-Aminobutanoate	C00334	103.0633	EC	***	2.41
N,N-Dimethylglycine	C01026	103.0633	EC	***	2.41
L-3-Amino-isobutanoate	C03284	103.0633	EC	***	2.41
3-Aminoisobutyric acid	C05145	103.0633	EC	***	2.41
Decanoyl-CoA	C05274	921.251	AC	**	2.38
O-Phospho-L-serine	C01005	185.0089	EC	**	2.31
Glycerol	C00116	92.0473	EC	*	2.31
Ouabain	C01443	584.2833	EC	*	2.31
L-Glutamate	C00025	147.0532	EC	***	2.31
D-Glutamate	C00217	147.0532	EC	***	2.31
L-4-Hydroxyglutamate semialdehyde	C05938	147.0532	EC	***	2.31
Anthranilate	C00108	137.0477	EC	**	2.23
Isoniazid	C07054	137.0589	EC	**	2.23
Pidolic acid	C01879	129.0426	EC	***	2.23
L-1-Pyrroline-3-hydroxy-5-carboxylate	C04281	129.0426	EC	***	2.23
1-Pyrroline-4-hydroxy-2-carboxylate	C04282	129.0426	EC	***	2.23
3-Sulfino-L-alanine	C00606	153.0096	AC	***	2.18

Table A.1 (continued): Relationship of metabolite abundance between AC and RBMEC under physiological conditions (NX+Glc) expressed as fold changes. Statistics: *p<0.05, **p<0.01, *** p<0.001; 1-way Anova.

Metabolite Name	KEGG ID	Monoisotopic mass	Up in	Significance	Fold change
5-Methoxyindoleacetate	C05660	205.0739	AC	*	2.17
Deoxyribose	C01801	134.0579	EC	*	2.17
2-(S-Glutathionyl)acetyl glutathione	C14863	654.1625	EC	***	2.14
Formyl-N-acetyl-5-methoxykynurenamine	C05642	264.111	AC	**	2.11
CDP-choline	C00307	488.1073	EC	*	2.10
Xylitol	C00379	152.0685	EC	*	2.08
L-Arabitol	C00532	152.0685	EC	*	2.08
Pantothenate	C00864	219.1107	AC	*	2.03
Aflatoxin B1exo-8,9-epoxide-GSH	C11278	635.1421	AC	**	2.02

Table A.2: Top altered metabolites in AC upon exposure to AX+Glc compared to normoxic baseline (NX+Glc). Statistics: *p<0.05, **p<0.01, *** p<0.001; 1-way Anova.

Metabolite Name	KEGG ID	Monoisotopic mass	Up in	Significance	Fold change
(-)-Ureidoglycolate	C00603	134.0328	NX	***	6.60
(S)-Malate	C00149	134.0215	NX	*	6.40
Sedoheptulose 7-phosphate	C05382	290.0403	AX	***	5.08
Succinyl-CoA	C00091	867.1313	NX	**	4.19
(S)-Methylmalonyl-CoA	C00683	867.1313	NX	**	4.19
(R)-Methylmalonyl-CoA	C01213	867.1313	NX	**	4.19
Malonyl-CoA methyl ester	C19673	867.1313	NX	**	4.19
Fumarate	C00122	116.011	NX	***	3.63
L-Aspartate	C00049	133.0375	NX	***	2.85
D-Aspartate	C00402	133.0375	NX	***	2.85
Pantetheine	C00831	278.13	AX	***	2.81
Protoporphyrin	C02191	562.258	AX	**	2.78
Ouabain	C01443	584.2833	AX	*	2.76
Glycerone phosphate	C00111	169.998	AX	**	2.69
D-Glyceraldehyde 3-phosphate	C00118	169.998	AX	**	2.69
N-Acetyl-L-glutamate	C00624	189.0637	AX	*	2.65
CMP-2-aminoethylphosphonate	C05673	430.0655	NX	*	2.46
3-Sulfino-L-alanine	C00606	153.0096	AX	***	2.42
D-Sorbitol	C00794	182.079	AX	***	2.26
Galactitol	C01697	182.079	AX	***	2.26
3-Methoxy-4-hydroxyphenylethyleneglycol	C05594	184.0736	AX	**	2.17
Choline phosphate	C00588	184.0739	AX	**	2.17
L-Adrenaline	C00788	183.0895	AX	***	2.11
L-Normetanephrine	C05589	183.0895	AX	***	2.11

Table A.3: Top altered metabolites in RBMEC upon exposure to AX+Glc compared to normoxic baseline (NX+Glc). Statistics: *p<0.05, **p<0.01, *** p<0.001; 1-way Anova.

Metabolite Name	KEGG ID	Monoisotopic mass	Up in	Significance	Fold change
Stachyose	C01613	666.2219	AX	**	14.16
Sedoheptulose 7-phosphate	C05382	290.0403	AX	***	8.64
(S)-3-Hydroxyoctanoyl-CoA	C05266	909.2146	AX	*	4.12
Cytidine	C00475	243.0855	AX	***	4.02
gamma-Glutamyl-beta-cyanoalanine	C05711	243.0855	AX	***	4.02
Biotin	C00120	244.0882	AX	***	4.00
cis-Aconitate	C00417	174.0164	AX	***	3.79
sn-glycero-3-Phosphocholine	C00670	258.1106	AX	***	3.64
(-)-Ureidoglycolate	C00603	134.0328	NX	**	3.53
sn-Glycerol 3-phosphate	C00093	172.0137	AX	***	3.10
sn-glycero-3-Phosphoethanolamine	C01233	215.0559	AX	***	3.04
Raffinose	C00492	504.169	AX	*	2.70
D-Gal alpha 1->6D-Gal alpha 1->6D-Glucose	C05404	504.169	AX	*	2.70
L-Homocysteine	C00155	135.0354	NX	*	2.67
2,5-Dioxopentanoate	C00433	130.0266	AX	***	2.19
2-Oxoglutaramate	C00940	145.0375	AX	***	2.07
L-Aspartate	C00049	133.0375	NX	**	2.04
D-Aspartate	C00402	133.0375	NX	**	2.04
11beta,21-Dihydroxy-5beta-pregnane-3,20-dione	C05475	348.2301	AX	**	2.04
3alpha,21-Dihydroxy-5beta-pregnane-11,20-dione	C05478	348.2301	AX	**	2.04
17alpha,21-Dihydroxypregnenolone	C05487	348.2301	AX	**	2.04

Table A.4: Top altered metabolites in AC upon exposure to AX-Glc compared to NX-Glc. Statistics: *p<0.05, **p<0.01, *** p<0.001; 1-way Anova.

Metabolite Name	KEGG ID	Monoisotopic mass	Up in	Significance	Fold change
UDP-glucose	C00029	566.055	NX	***	236.62
UDP-D-galactose	C00052	566.055	NX	***	236.62
UDP-glucuronate	C00167	580.0343	NX	**	66.28
Biotin	C00120	244.0882	NX	***	42.84
Cytidine	C00475	243.0855	NX	***	30.62
gamma-Glutamyl-beta-cyanoalanine	C05711	243.0855	NX	***	30.62
GDP-mannose	C00096	605.0772	NX	*	29.78
sn-glycero-3-Phosphocholine	C00670	258.1106	NX	***	26.77
cis-Aconitate	C00417	174.0164	NX	***	18.86
sn-glycero-3-Phosphoethanolamine	C01233	215.0559	NX	***	17.67
sn-Glycerol 3-phosphate	C00093	172.0137	NX	***	16.37
Succinyl-CoA	C00091	867.1313	NX	*	13.67
(S)-Methylmalonyl-CoA	C00683	867.1313	NX	*	13.67
(R)-Methylmalonyl-CoA	C01213	867.1313	NX	*	13.67
Malonyl-CoA methyl ester	C19673	867.1313	NX	*	13.67
2-Oxoglutaramate	C00940	145.0375	AX	**	11.24
L-2-Aminoadipate adenylate	C05560	490.1213	NX	***	10.98
UMP	C00105	324.0359	NX	***	9.93
FAD	C00016	785.1571	AX	***	9.56
CMP-2-aminoethylphosphonate	C05673	430.0655	NX	***	8.81
(S)-3-Hydroxyoctanoyl-CoA	C05266	909.2146	NX	**	7.51
5-Phosphoribosylamine	C03090	229.0351	AX	***	5.95
L-Homocysteine	C00155	135.0354	NX	***	4.98
(-)-Ureidoglycolate	C00603	134.0328	NX	***	4.61
6-Thioguanosine monophosphate	C16619	379.0352	NX	***	4.50
(S)-Malate	C00149	134.0215	NX	***	4.43
3-Methylcrotonyl-CoA	C03069	849.1571	NX	***	4.40
2-Methylbut-2-enoyl-CoA	C03345	849.1571	NX	***	4.40
Creatine	C00300	131.0695	AX	**	4.17
GDP-L-fucose	C00325	589.0822	NX	***	3.72
Phosphocreatine	C02305	211.0358	NX	**	3.54
3,5-Cyclic GMP	C00942	345.0474	NX	**	3.48
5-Acetylamino-6-formylamino-3-methyluracil	C16365	226.0702	NX	***	3.42
11beta,21-Dihydroxy-5beta-pregnane-3,20-dione	C05475	348.2301	AX	***	3.36
3alpha,21-Dihydroxy-5beta-pregnane-11,20-dione	C05478	348.2301	AX	***	3.36
17alpha,21-Dihydroxypregnenolone	C05487	348.2301	AX	***	3.36
Decanoyl-CoA	C05274	921.251	NX	***	3.03
N-Acetylneuraminate	C00270	309.106	AX	*	2.96
O-Acetylneuraminic acid	C03525	309.106	AX	*	2.96
Sulfate	C00059	97.9674	NX	***	2.88
Orthophosphate	C00009	97.9769	NX	***	2.88
Cys-Gly	C01419	178.0412	NX	***	2.81
D-Glucono-1,5-lactone	C00198	178.0477	NX	***	2.81
L-Gulono-1,4-lactone	C01040	178.0477	NX	***	2.81
2-Dehydro-3-deoxy-D-galactonate	C01216	178.0477	NX	***	2.81
16-Glucuronide-estriol	C05504	464.2046	AX	**	2.81
Pantetheine	C00831	278.13	AX	**	2.76
L-Tyrosine	C00082	181.0739	NX	***	2.67
D-Glucose	C00031	180.0634	NX	***	2.65
D-Fructose	C00095	180.0634	NX	***	2.65
D-Galactose	C00124	180.0634	NX	***	2.65
myo-Inositol	C00137	180.0634	NX	***	2.65
D-Mannose	C00159	180.0634	NX	***	2.65
beta-D-Glucose	C00221	180.0634	NX	***	2.65
alpha-D-Glucose	C00267	180.0634	NX	***	2.65
beta-D-Fructose	C02336	180.0634	NX	***	2.65
D-chiro-Inositol	C19891	180.0634	NX	***	2.65
Theobromine	C07480	180.0647	NX	***	2.65
1,7-Dimethylxanthine	C13747	180.0647	NX	***	2.65
Protoporphyrin	C02191	562.258	AX	*	2.62
Pyruvate	C00022	88.016	NX	***	2.60
3-Oxopropanoate	C00222	88.016	NX	***	2.60
Homovanillate	C05582	182.0579	NX	***	2.60
3-Methoxy-4-hydroxyphenylglycolaldehyde	C05583	182.0579	NX	***	2.60
Presqualene diphosphate	C03428	586.3188	AX	**	2.55
Ouabain	C01443	584.2833	AX	*	2.54

Table A.4 (continued): Top altered metabolites in AC upon exposure to AX-Glc compared to NX-Glc. Statistics: *p<0.05, **p<0.01, *** p<0.001; 1-way Anova.

Metabolite Name	KEGG ID	Monoisotopic mass	Up in	Significance	Fold change
D-Glucosamine 6-phosphate	C00352	259.0457	NX	**	2.53
GMP	C00144	363.058	NX	**	2.43
Precursor Z	C18239	363.058	NX	**	2.43
Fumarate	C00122	116.011	NX	***	2.40
L-erythro-4-Hydroxyglutamate	C05947	163.0481	NX	***	2.36
Adenosine	C00212	267.0968	NX	*	2.33
Deoxyguanosine	C00330	267.0968	NX	*	2.33
Arachidonate	C00219	304.2402	NX	*	2.30
D-Ribose 5-phosphate	C00117	230.0192	NX	**	2.29
D-Ribulose 5-phosphate	C00199	230.0192	NX	**	2.29
D-Xylulose 5-phosphate	C00231	230.0192	NX	**	2.29
alpha-D-Ribose 1-phosphate	C00620	230.0192	NX	**	2.29
7-Hydroxymethyl-12-methylbenz[a]anthracene sulfate	C19562	352.0769	AX	*	2.29
Acetyl-CoA	C00024	809.1258	NX	**	2.29
S-Adenosyl-L-methionine	C00019	398.1372	AX	**	2.16
4-(2-Aminophenyl)-2,4-dioxobutanoate	C01252	207.0532	NX	**	2.15
1-Nitro-5,6-dihydroxy-dihydronaphthalene	C14801	207.0532	NX	**	2.15
L-Glutamate	C00025	147.0532	AX	***	2.02
D-Glutamate	C00217	147.0532	AX	***	2.02
L-4-Hydroxyglutamate semialdehyde	C05938	147.0532	AX	***	2.02
dADP	C00206	411.0345	AX	**	2.01

Table A.5: Top altered metabolites in RBMEC upon exposure to AX-Glc compared to NX-Glc. Statistics: *p<0.05, **p<0.01, *** p<0.001; 1-way Anova.

Metabolite Name	KEGG ID	Monoisotopic mass	Up in	Significance	Fold change
UDP-N-acetyl-D-glucosamine	C00043	607.0816	NX	*	193.59
UDP-N-acetyl-D-galactosamine	C00203	607.0816	NX	*	193.59
N-Acetyl-D-glucosamine 6-phosphate	C00357	301.0563	NX	**	58.70
N-Acetyl-D-mannosamine 6-phosphate	C04257	301.0563	NX	**	58.70
N-Acetyl-alpha-D-glucosamine 1-phosphate	C04501	301.0563	NX	**	58.70
N-Acetylneuraminate	C00270	309.106	AX	***	46.55
O-Acetylneuraminic acid	C03525	309.106	AX	***	46.55
UDP-glucose	C00029	566.055	NX	***	46.00
UDP-D-galactose	C00052	566.055	NX	***	46.00
UMP	C00105	324.0359	NX	**	40.15
Phosphocreatine	C02305	211.0358	NX	*	24.00
Glutathione disulfide	C00127	612.152	NX	***	19.62
Sulfate	C00059	97.9674	NX	*	14.27
Orthophosphate	C00009	97.9769	NX	*	14.27
N-Glycoloyl-neuraminate	C03410	325.1009	AX	***	12.57
Biotin	C00120	244.0882	NX	***	9.88
Succinyl-CoA	C00091	867.1313	NX	**	9.64
(S)-Methylmalonyl-CoA	C00683	867.1313	NX	**	9.64
(R)-Methylmalonyl-CoA	C01213	867.1313	NX	**	9.64
Malonyl-CoA methyl ester	C19673	867.1313	NX	**	9.64
2-Methyl-1-hydroxypropyl-ThPP	C15976	497.1025	NX	**	8.35
sn-glycero-3-Phosphoethanolamine	C01233	215.0559	NX	***	7.46
Cytidine	C00475	243.0855	NX	***	7.14
gamma-Glutamyl-beta-cyanoalanine	C05711	243.0855	NX	***	7.14
D-Glucono-1,5-lactone 6-phosphate	C01236	258.0141	NX	***	7.08
D-Fructose 6-phosphate	C00085	260.0297	NX	***	6.85
D-Glucose 6-phosphate	C00092	260.0297	NX	***	6.85
D-Glucose 1-phosphate	C00103	260.0297	NX	***	6.85
D-Mannose 6-phosphate	C00275	260.0297	NX	***	6.85
alpha-D-Galactose 1-phosphate	C00446	260.0297	NX	***	6.85
D-Mannose 1-phosphate	C00636	260.0297	NX	***	6.85
alpha-D-Glucose 6-phosphate	C00668	260.0297	NX	***	6.85
D-Fructose 1-phosphate	C01094	260.0297	NX	***	6.85
D-Tagatose 6-phosphate	C01097	260.0297	NX	***	6.85
beta-D-Glucose 6-phosphate	C01172	260.0297	NX	***	6.85
Inositol 1-phosphate	C01177	260.0297	NX	***	6.85
beta-D-Fructose 2-phosphate	C03267	260.0297	NX	***	6.85
myo-Inositol 4-phosphate	C03546	260.0297	NX	***	6.85
1D-myo-Inositol 3-phosphate	C04006	260.0297	NX	***	6.85
beta-D-Fructose 6-phosphate	C05345	260.0297	NX	***	6.85
Nicotinamide D-ribonucleotide	C00455	334.0566	NX	***	6.77
sn-glycero-3-Phosphocholine	C00670	258.1106	NX	***	5.79
(1aalpha,2beta,3alpha,11calpha)-1a,2,3,11c-Tetrahydro-6,11-dimethylbenzo[6,7]phenanthro[3,4-b]oxirene-2,3-diol	C19559	306.1256	AX	***	5.53
3,5-Cyclic GMP	C00942	345.0474	NX	***	5.46
sn-Glycerol 3-phosphate	C00093	172.0137	NX	***	5.45
Porphobilinogen	C00931	226.0954	NX	**	5.08
Uridine	C00299	244.0695	NX	*	5.00
Aflatoxin B1exo-8,9-epoxide-GSH	C11278	635.1421	NX	**	4.98
cis-Aconitate	C00417	174.0164	NX	***	4.96
Sedoheptulose 1,7-bisphosphate	C00447	370.0066	NX	***	4.91
L-Tyrosine	C00082	181.0739	NX	***	4.61
AMP	C00020	347.0631	NX	***	4.29
dGMP	C00362	347.0631	NX	***	4.29
Homovanillate	C05582	182.0579	NX	***	4.24
3-Methoxy-4-hydroxyphenylglycolaldehyde	C05583	182.0579	NX	***	4.24
D-Glucose	C00031	180.0634	NX	***	4.23
D-Fructose	C00095	180.0634	NX	***	4.23
D-Galactose	C00124	180.0634	NX	***	4.23
myo-Inositol	C00137	180.0634	NX	***	4.23
D-Mannose	C00159	180.0634	NX	***	4.23
beta-D-Glucose	C00221	180.0634	NX	***	4.23
alpha-D-Glucose	C00267	180.0634	NX	***	4.23
beta-D-Fructose	C02336	180.0634	NX	***	4.23
D-chiro-Inositol	C19891	180.0634	NX	***	4.23

Table A.5 (continued): Top altered metabolites in RBMEC upon exposure to AX-Glc compared to NX-Glc. Statistics: *p<0.05, **p<0.01, *** p<0.001; 1-way Anova.

Metabolite Name	KEGG ID	Monoisotopic mass	Up in	Significance	Fold change
Theobromine	C07480	180.0647	NX	***	4.23
1,7-Dimethylxanthine	C13747	180.0647	NX	***	4.23
NAD+	C00003	664.1169	NX	***	4.20
Pyruvate	C00022	88.016	NX	***	4.17
3-Oxopropanoate	C00222	88.016	NX	***	4.17
2,5-Dioxopentanoate	C00433	130.0266	NX	***	4.01
(1R,2S)-Naphthalene 1,2-oxide	C14786	144.0575	NX	**	3.73
CMP-2-aminoethylphosphonate	C05673	430.0655	NX	**	3.67
N-Acetyl-L-glutamate	C00624	189.0637	NX	***	3.65
2-Oxoadipate	C00322	160.0372	AX	***	3.63
3-Oxoadipate	C00846	160.0372	AX	***	3.63
2-Oxoglutarate	C00026	146.0215	NX	**	3.53
2-(alpha-Hydroxyethyl)thiamine diphosphate	C05125	469.0712	AX	***	3.52
6-Thioguanosine monophosphate	C16619	379.0352	NX	***	3.42
Glutathione	C00051	307.0838	NX	**	3.41
L-Fucose 1-phosphate	C02985	244.0348	NX	***	3.31
Adenosine	C00212	267.0968	NX	***	3.23
Deoxyguanosine	C00330	267.0968	NX	***	3.23
2-Oxosuccinamate	C02362	131.0219	AX	***	3.20
Pantetheine	C00831	278.13	NX	*	3.19
D-Ribose 5-phosphate	C00117	230.0192	NX	*	3.01
D-Ribulose 5-phosphate	C00199	230.0192	NX	*	3.01
D-Xylulose 5-phosphate	C00231	230.0192	NX	*	3.01
alpha-D-Ribose 1-phosphate	C00620	230.0192	NX	*	3.01
Adenylyl sulfate	C00224	427.0199	NX	*	2.93
ADP	C00008	427.0294	NX	*	2.93
Adenosine 3,5-bisphosphate	C00054	427.0294	NX	*	2.93
dGDP	C00361	427.0294	NX	*	2.93
Linamarin	C01594	247.1056	AX	*	2.91
L-Aspartate	C00049	133.0375	AX	***	2.82
D-Aspartate	C00402	133.0375	AX	***	2.82
D-Xylonolactone	C02266	148.0372	NX	***	2.82
2-Hydroxyglutarate	C02630	148.0372	NX	***	2.82
gamma-L-Glutamyl-L-cysteine	C00669	250.0623	NX	**	2.82
D-Glucosamine 6-phosphate	C00352	259.0457	NX	***	2.73
4-(2-Aminophenyl)-2,4-dioxobutanoate	C01252	207.0532	NX	***	2.68
1-Nitro-5,6-dihydroxy-dihydronaphthalene	C14801	207.0532	NX	***	2.68
Thymidine	C00214	242.0903	AX	**	2.67
Phenylacetaldehyde	C00601	120.0575	NX	**	2.59
Glycerol	C00116	92.0473	NX	***	2.55
Anthranilate	C00108	137.0477	NX	***	2.51
Isoniazid	C07054	137.0589	NX	***	2.51
N-Acetylserotonin	C00978	218.1055	AX	*	2.49
CMP-N-acetylneuraminate	C00128	614.1473	AX	**	2.47
Cys-Gly	C01419	178.0412	NX	**	2.43
D-Glucono-1,5-lactone	C00198	178.0477	NX	**	2.43
L-Gulono-1,4-lactone	C01040	178.0477	NX	**	2.43
2-Dehydro-3-deoxy-D-galactonate	C01216	178.0477	NX	**	2.43
Hypotaurine	C00519	109.0197	NX	*	2.40
GMP	C00144	363.058	NX	***	2.27
Precursor Z	C18239	363.058	NX	***	2.27
L-erythro-4-Hydroxyglutamate	C05947	163.0481	NX	*	2.27
2-Oxobutanoate	C00109	102.0317	NX	**	2.27
Acetoacetate	C00164	102.0317	NX	**	2.27
Succinate semialdehyde	C00232	102.0317	NX	**	2.27
(S)-Methylmalonate semialdehyde	C06002	102.0317	NX	**	2.27
L-Alanine	C00041	89.0477	AX	***	2.24
beta-Alanine	C00099	89.0477	AX	***	2.24
Sarcosine	C00213	89.0477	AX	***	2.24
4-Hydroxybenzoate	C00156	138.0317	AX	*	2.21
Gentisate aldehyde	C05585	138.0317	AX	*	2.21
Presqualene diphosphate	C03428	586.3188	AX	**	2.20
Deoxyribose	C01801	134.0579	NX	**	2.10
5,6-Dihydrothymine	C00906	128.0586	NX	***	2.09
Raffinose	C00492	504.169	AX	**	2.09
D-Gal alpha 1->6D-Gal alpha 1->6D-Glucose	C05404	504.169	AX	**	2.09
Inosine	C00294	268.0808	NX	*	2.08

Table A.5 (continued): Top altered metabolites in RBMEC upon exposure to AX-Glc compared to NX-Glc. Statistics: *p<0.05, **p<0.01, *** p<0.001; 1-way Anova.

Metabolite Name	KEGG ID	Monoisotopic mass	Up in	Significance	Fold change
9-Hydroxybenzo[a]pyrene	C14556	268.0888	NX	*	2.08
Benzo[a]pyrene-7,8-oxide	C14850	268.0888	NX	*	2.08
Benzo[a]pyrene-4,5-oxide	C14851	268.0888	NX	*	2.08
Urocanate	C00785	138.0429	AX	***	2.07
Prunasin	C00844	295.1056	NX	***	2.07
Hydroquinone	C00530	110.0368	NX	***	2.05
Imidazole-4-acetaldehyde	C05130	110.048	NX	***	2.05
Thymine	C00178	126.0429	NX	**	2.05
Imidazole-4-acetate	C02835	126.0429	NX	**	2.05
O-Phospho-L-serine	C01005	185.0089	NX	***	2.04
Adenine	C00147	135.0545	AX	***	2.03
Hypoxanthine	C00262	136.0385	NX	***	2.03
4-Hydroxyphenylacetaldehyde	C03765	136.0524	NX	***	2.03
Phenylacetic acid	C07086	136.0524	NX	***	2.03
(R)-Mevalonate	C00418	148.0736	NX	***	2.03
7,8-Dihydroneopterin 3-triphosphate	C04895	494.9957	NX	*	2.03

6 REFERENCES

Abbott, N. J. 2013. Blood-brain barrier structure and function and the challenges for CNS drug delivery. *J Inherit Metab Dis.* 36:437-449.

Abbott, N. J., A. A. Patabendige, D. E. Dolman, S. R. Yusof and D. J. Begley. 2010. Structure and function of the blood-brain barrier. *Neurobiol Dis.* 37:13-25.

Abbott, N. J., L. Ronnback and E. Hansson. 2006. Astrocyte-endothelial interactions at the blood-brain barrier. *Nat Rev Neurosci.* 7:41-53.

Abbruscato, T. J. and T. P. Davis. 1999a. Combination of hypoxia/aglycemia compromises in vitro blood-brain barrier integrity. *J Pharmacol Exp Ther.* 289:668-675.

Abbruscato, T. J. and T. P. Davis. 1999b. Protein expression of brain endothelial cell E-cadherin after hypoxia/aglycemia: influence of astrocyte contact. *Brain research.* 842:277-286.

Al Ahmad, A., M. Gassmann and O. O. Ogunshola. 2009. Maintaining blood-brain barrier integrity: pericytes perform better than astrocytes during prolonged oxygen deprivation. *J Cell Physiol.* 218:612-622.

Al Ahmad, A., C. B. Taboada, M. Gassmann and O. O. Ogunshola. 2011. Astrocytes and pericytes differentially modulate blood-brain barrier characteristics during development and hypoxic insult. *J Cereb Blood Flow Metab.* 31:693-705.

Allen, N. J. and B. A. Barres. 2009. Neuroscience: Glia - more than just brain glue. *Nature.* 457:675-677.

Altman, B. J. and J. C. Rathmell. 2012. Metabolic stress in autophagy and cell death pathways. *Cold Spring Harb Perspect Biol.* 4:a008763.

Antonelli-Orlidge, A., K. B. Saunders, S. R. Smith and P. A. D'Amore. 1989. An activated form of transforming growth factor beta is produced by cocultures of endothelial cells and pericytes. *Proc Natl Acad Sci U S A.* 86:4544-4548.

Argaw, A. T., L. Asp, J. Zhang, K. Navrazhina, T. Pham, J. N. Mariani, S. Mahase, D. J. Dutta, J. Seto, E. G. Kramer, N. Ferrara, M. V. Sofroniew and G. R. John. 2012. Astrocyte-derived VEGF-A drives blood-brain barrier disruption in CNS inflammatory disease. *J Clin Invest.* 122:2454-2468.

Argaw, A. T., Y. Zhang, B. J. Snyder, M. L. Zhao, N. Kopp, S. C. Lee, C. S. Raine, C. F. Brosnan and G. R. John. 2006. IL-1beta regulates blood-brain barrier permeability via reactivation of the hypoxia-angiogenesis program. *Journal of immunology.* 177:5574-5584.

Armulik, A., G. Genove, M. Mae, M. H. Nisancioglu, E. Wallgard, C. Niaudet, L. He, J. Norlin, P. Lindblom, K. Strittmatter, B. R. Johansson and C. Betsholtz. 2010. Pericytes regulate the blood-brain barrier. *Nature.* 468:557-561.

Arsham, A. M., J. J. Howell and M. C. Simon. 2003. A novel hypoxia-inducible factor-independent hypoxic response regulating mammalian target of rapamycin and its targets. *J Biol Chem.* 278:29655-29660.

Balduini, W., S. Carloni and G. Buonocore. 2012. Autophagy in hypoxia-ischemia induced brain injury. *J Matern Fetal Neonatal Med.* 25 Suppl 1:30-34.

Ballabh, P., A. Braun and M. Nedergaard. 2004. The blood-brain barrier: an overview: structure, regulation, and clinical implications. *Neurobiology of disease.* 16:1-13.

Baranova, O., L. F. Miranda, P. Pichiule, I. Dragatsis, R. S. Johnson and J. C. Chavez. 2007. Neuron-specific inactivation of the hypoxia inducible factor 1 alpha increases brain injury in a mouse model of transient focal cerebral ischemia. *J Neurosci.* 27:6320-6332.

Bauer, A. T., H. F. Burgers, T. Rabie and H. H. Marti. 2010. Matrix metalloproteinase-9 mediates hypoxia-induced vascular leakage in the brain via tight junction rearrangement. *Journal of cerebral blood flow and metabolism : official journal of the International Society of Cerebral Blood Flow and Metabolism.* 30:837-848.

Bauer, H. C., A. Traweger, J. Zweimueller-Mayer, C. Lehner, H. Tempfer, I. Krizbai, I. Wilhelm and H. Bauer. 2011. New aspects of the molecular constituents of tissue barriers. *J Neural Transm.* 118:7-21.

Baum, B. and M. Georgiou. 2011. Dynamics of adherens junctions in epithelial establishment, maintenance, and remodeling. *The Journal of cell biology.* 192:907-917.

Beard, E. and O. Braissant. 2010. Synthesis and transport of creatine in the CNS: importance for cerebral functions. *J Neurochem.* 115:297-313.

Belanger, M., I. Allaman and P. J. Magistretti. 2011. Brain energy metabolism: focus on astrocyte-neuron metabolic cooperation. *Cell Metab.* 14:724-738.

Bell, R. D., E. A. Winkler, A. P. Sagare, I. Singh, B. LaRue, R. Deane and B. V. Zlokovic. 2010. Pericytes control key neurovascular functions and neuronal phenotype in the adult brain and during brain aging. *Neuron.* 68:409-427.

Bellot, G., R. Garcia-Medina, P. Gounon, J. Chiche, D. Roux, J. Pouyssegur and N. M. Mazure. 2009. Hypoxia-induced autophagy is mediated through hypoxia-inducible factor induction of BNIP3 and BNIP3L via their BH3 domains. *Mol Cell Biol.* 29:2570-2581.

Ben-Zvi, A., B. Lacoste, E. Kur, B. J. Andreone, Y. Mayshar, H. Yan and C. Gu. 2014. Mfsd2a is critical for the formation and function of the blood-brain barrier. *Nature.* 509:507-511.

Berezowski, V., C. Landry, M. P. Dehouck, R. Cecchelli and L. Fenart. 2004. Contribution of glial cells and pericytes to the mRNA profiles of P-glycoprotein and multidrug resistance-associated proteins in an in vitro model of the blood-brain barrier. *Brain Res.* 1018:1-9.

Bi, M., C. Naczki, M. Koritzinsky, D. Fels, J. Blais, N. Hu, H. Harding, I. Novoa, M. Varia, J. Raleigh, D. Scheuner, R. J. Kaufman, J. Bell, D. Ron, B. G. Wouters and C. Koumenis. 2005. ER stress-regulated translation increases tolerance to extreme hypoxia and promotes tumor growth. *EMBO J.* 24:3470-3481.

Bouzier-Sore, A. K. and L. Pellerin. 2013. Unraveling the complex metabolic nature of astrocytes. *Front Cell Neurosci.* 7:179.

Bouzier-Sore, A. K., P. Voisin, V. Bouchaud, E. Bezancon, J. M. Franconi and L. Pellerin. 2006. Competition between glucose and lactate as oxidative energy substrates in both neurons and astrocytes: a comparative NMR study. *Eur J Neurosci.* 24:1687-1694.

Brown, R. C., K. S. Mark, R. D. Egleton, J. D. Huber, A. R. Burroughs and T. P. Davis. 2003. Protection against hypoxia-induced increase in blood-brain barrier permeability: role of tight junction proteins and NFkappaB. *Journal of cell science.* 116:693-700.

Cambier, S., S. Gline, D. Mu, R. Collins, J. Araya, G. Dolganov, S. Einheber, N. Boudreau and S. L. Nishimura. 2005. Integrin alpha(v)beta8-mediated activation of transforming growth factor-beta by perivascular astrocytes: an angiogenic control switch. *Am J Pathol.* 166:1883-1894.

Candelario-Jalil, E., Y. Yang and G. A. Rosenberg. 2009. Diverse roles of matrix metalloproteinases and tissue inhibitors of metalloproteinases in neuroinflammation and cerebral ischemia. *Neuroscience.* 158:983-994.

Carmeliet, P., Y. Dor, J. M. Herbert, D. Fukumura, K. Brusselmans, M. Dewerchin, M. Neeman, F. Bono, R. Abramovitch, P. Maxwell, C. J. Koch, P. Ratcliffe, L. Moons, R. K. Jain, D. Collen and E. Keshert. 1998. Role of HIF-1alpha in hypoxia-mediated apoptosis, cell proliferation and tumour angiogenesis. *Nature.* 394:485-490.

Cataldo, A. M. and R. D. Broadwell. 1986a. Cytochemical identification of cerebral glycogen and glucose-6-phosphatase activity under normal and experimental conditions: I. Neurons and glia. *Journal of Electron Microscopy Technique.* 3:413-437.

Cataldo, A. M. and R. D. Broadwell. 1986b. Cytochemical identification of cerebral glycogen and glucose-6-phosphatase activity under normal and experimental conditions. II. Choroid plexus and ependymal epithelia, endothelia and pericytes. *J Neurocytol.* 15:511-524.

Ceruti, S., L. Colombo, G. Magni, F. Vigano, M. Boccazzi, M. A. Deli, B. Sperlagh, M. P. Abbracchio and A. Kittel. 2011. Oxygen-glucose deprivation increases the enzymatic activity and the microvesicle-mediated release of ectonucleotidases in the cells composing the blood-brain barrier. *Neurochemistry international.*

Chandel, N. S., D. S. McClintock, C. E. Feliciano, T. M. Wood, J. A. Melendez, A. M. Rodriguez and P. T. Schumacker. 2000. Reactive oxygen species generated at mitochondrial complex III stabilize hypoxia-inducible factor-1alpha during hypoxia: a mechanism of O2 sensing. *J Biol Chem.* 275:25130-25138.

Chen, C., Q. Hu, J. Yan, X. Yang, X. Shi, J. Lei, L. Chen, H. Huang, J. Han, J. H. Zhang and C. Zhou. 2009. Early inhibition of HIF-1alpha with small interfering RNA reduces ischemic-reperfused brain injury in rats. *Neurobiol Dis.* 33:509-517.

Chen, W., V. Jadhav, J. Tang and J. H. Zhang. 2008a. HIF-1 alpha inhibition ameliorates neonatal brain damage after hypoxic-ischemic injury. *Acta Neurochir Suppl.* 102:395-399.

Chen, W., V. Jadhav, J. Tang and J. H. Zhang. 2008b. HIF-1alpha inhibition ameliorates neonatal brain injury in a rat pup hypoxic-ischemic model. *Neurobiol Dis.* 31:433-441.

Chong, Z. Z., F. Li and K. Maiese. 2005. Oxidative stress in the brain: novel cellular targets that govern survival during neurodegenerative disease. *Prog Neurobiol.* 75:207-246.

Chow, J., O. Ogunshola, S. Y. Fan, Y. Li, L. R. Ment and J. A. Madri. 2001. Astrocyte-derived VEGF mediates survival and tube stabilization of hypoxic brain microvascular endothelial cells in vitro. *Brain research. Developmental brain research.* 130:123-132.

Cipolla, M. J., R. Crete, L. Vitullo and R. D. Rix. 2004. Transcellular transport as a mechanism of blood-brain barrier disruption during stroke. *Front Biosci.* 9:777-785.

Coisne, C., L. Dehouck, C. Faveeuw, Y. Delplace, F. Miller, C. Landry, C. Morissette, L. Fenart, R. Cecchelli, P. Tremblay and B. Dehouck. 2005. Mouse syngenic in vitro blood-brain barrier model: a new tool to examine inflammatory events in cerebral endothelium. *Lab Invest.* 85:734-746.

Colgan, O. C., N. T. Collins, G. Ferguson, R. P. Murphy, Y. A. Birney, P. A. Cahill and P. M. Cummins. 2008. Influence of basolateral condition on the regulation of brain microvascular endothelial tight junction properties and barrier function. *Brain Res.* 1193:84-92.

Compernolle, V., K. Brusselmans, T. Acker, P. Hoet, M. Tjwa, H. Beck, S. Plaisance, Y. Dor, E. Keshet, F. Lupu, B. Nemery, M. Dewerchin, P. Van Veldhoven, K. Plate, L. Moons, D. Collen and P. Carmeliet. 2002. Loss of HIF-2alpha and inhibition of VEGF impair fetal lung maturation, whereas treatment with VEGF prevents fatal respiratory distress in premature mice. *Nat Med.* 8:702-710.

Cummins, P. M. 2012. Occludin: one protein, many forms. *Molecular and cellular biology.* 32:242-250.

Daneman, R., L. Zhou, A. A. Kebede and B. A. Barres. 2010. Pericytes are required for blood-brain barrier integrity during embryogenesis. *Nature.* 468:562-566.

Davson, H. and W. H. Oldendorf. 1967. Symposium on membrane transport. Transport in the central nervous system. *Proceedings of the Royal Society of Medicine.* 60:326-329.

Dehouck, M. P., S. Meresse, P. Delorme, J. C. Fruchart and R. Cecchelli. 1990. An easier, reproducible, and mass-production method to study the blood-brain barrier in vitro. *Journal of neurochemistry.* 54:1798-1801.

Deli, M. A., C. S. Abraham, Y. Kataoka and M. Niwa. 2005. Permeability studies on in vitro blood-brain barrier models: physiology, pathology, and pharmacology. *Cellular and molecular neurobiology.* 25:59-127.

Dienel, G. A. 2012. Brain lactate metabolism: the discoveries and the controversies. *J Cereb Blood Flow Metab.* 32:1107-1138.

Dohgu, S., F. Takata, A. Yamauchi, S. Nakagawa, T. Egawa, M. Naito, T. Tsuruo, Y. Sawada, M. Niwa and Y. Kataoka. 2005. Brain pericytes contribute to the induction and up-regulation of blood-brain barrier functions through transforming growth factor-beta production. *Brain Res.* 1038:208-215.

Dohgu, S., A. Yamauchi, F. Takata, M. Naito, T. Tsuruo, S. Higuchi, Y. Sawada and Y. Kataoka. 2004. Transforming growth factor-beta1 upregulates the tight junction and P-glycoprotein of brain microvascular endothelial cells. *Cell Mol Neurobiol.* 24:491-497.

Dore-Duffy, P. and J. C. LaManna. 2007. Physiologic angiodynamics in the brain. *Antioxidants & redox signaling.* 9:1363-1371.

Dore-Duffy, P., C. Owen, R. Balabanov, S. Murphy, T. Beaumont and J. A. Rafols. 2000. Pericyte migration from the vascular wall in response to traumatic brain injury. *Microvasc Res.* 60:55-69.

Dringen, R., J. M. Gutterer, C. Gros and J. Hirrlinger. 2001. Aminopeptidase N mediates the utilization of the GSH precursor CysGly by cultured neurons. *J Neurosci Res.* 66:1003-1008.

Dringen, R. and J. Hirrlinger. 2003. Glutathione pathways in the brain. *Biol Chem.* 384:505-516.
Duelli, R. and W. Kuschinsky. 2001. Brain glucose transporters: relationship to local energy demand. *News Physiol Sci.* 16:71-76.
Ehrlich, P. 1885. Das Sauerstoffbedürfnis des Organismus. Eine farbenanalytische Studie *Habilitation thesis.*
el Hafny, B., J. M. Bourre and F. Roux. 1996. Synergistic stimulation of gamma-glutamyl transpeptidase and alkaline phosphatase activities by retinoic acid and astroglial factors in immortalized rat brain microvessel endothelial cells. *J Cell Physiol.* 167:451-460.
Engelhardt, S., A. J. Al-Ahmad, M. Gassmann and O. O. Ogunshola. 2014a. Hypoxia selectively disrupts brain microvascular endothelial tight junction complexes through a hypoxia-inducible factor-1 (HIF-1) dependent mechanism. *J Cell Physiol.* 229:1096-1105.
Engelhardt, S., S. Patkar and O. O. Ogunshola. 2014b. Cell-specific blood-brain barrier regulation in health and disease: a focus on hypoxia. *Br J Pharmacol.* 171:1210-1230.
Erecinska, M. and I. A. Silver. 2001. Tissue oxygen tension and brain sensitivity to hypoxia. *Respir Physiol.* 128:263-276.
Fan, X., C. J. Heijnen, M. A. van der Kooij, F. Groenendaal and F. van Bel. 2009. The role and regulation of hypoxia-inducible factor-1alpha expression in brain development and neonatal hypoxic-ischemic brain injury. *Brain Res Rev.* 62:99-108.
Fandrey, J. and M. Gassmann. 2009. Oxygen sensing and the activation of the hypoxia inducible factor 1 (HIF-1)--invited article. *Adv Exp Med Biol.* 648:197-206.
Fischer, D., C. Panse and E. Laczko. 2014. Cosmiq - COmbining Single Masses Into Quantities. *R package version 0.99.3.* http://fgcz-data.uzh.ch/~cpanse/cosmiq.
Fischer, S., M. Clauss, M. Wiesnet, D. Renz, W. Schaper and G. F. Karliczek. 1999. Hypoxia induces permeability in brain microvessel endothelial cells via VEGF and NO. *Am J Physiol.* 276:C812-820.
Fischer, S., M. Wobben, J. Kleinstuck, D. Renz and W. Schaper. 2000. Effect of astroglial cells on hypoxia-induced permeability in PBMEC cells. *American journal of physiology. Cell physiology.* 279:C935-944.
Fischer, S., M. Wobben, H. H. Marti, D. Renz and W. Schaper. 2002. Hypoxia-induced hyperpermeability in brain microvessel endothelial cells involves VEGF-mediated changes in the expression of zonula occludens-1. *Microvasc Res.* 63:70-80.
Fleegal, M. A., S. Hom, L. K. Borg and T. P. Davis. 2005. Activation of PKC modulates blood-brain barrier endothelial cell permeability changes induced by hypoxia and posthypoxic reoxygenation. *Am J Physiol Heart Circ Physiol.* 289:H2012-2019.
Gabryel, B. and A. Malecki. 2006. Ebselen attenuates oxidative stress in ischemic astrocytes depleted of glutathione. Comparison with glutathione precursors. *Pharmacol Rep.* 58:381-392.
Goda, N., H. E. Ryan, B. Khadivi, W. McNulty, R. C. Rickert and R. S. Johnson. 2003. Hypoxia-inducible factor 1alpha is essential for cell cycle arrest during hypoxia. *Mol Cell Biol.* 23:359-369.
Goncalves, A., A. F. Ambrosio and R. Fernandes. 2013. Regulation of claudins in blood-tissue barriers under physiological and pathological states. *Tissue Barriers.* 1:e24782.
Gonul, E., B. Duz, S. Kahraman, H. Kayali, A. Kubar and E. Timurkaynak. 2002. Early pericyte response to brain hypoxia in cats: an ultrastructural study. *Microvascular research.* 64:116-119.
Gonzalez-Mariscal, L., A. Betanzos, P. Nava and B. E. Jaramillo. 2003. Tight junction proteins. *Progress in biophysics and molecular biology.* 81:1-44.
Gonzalez-Mariscal, L., R. Tapia and D. Chamorro. 2008. Crosstalk of tight junction components with signaling pathways. *Biochimica et biophysica acta.* 1778:729-756.
Greijer, A. E. and E. van der Wall. 2004. The role of hypoxia inducible factor 1 (HIF-1) in hypoxia induced apoptosis. *Journal of clinical pathology.* 57:1009-1014.
Gruetter, R. 2003. Glycogen: the forgotten cerebral energy store. *Journal of neuroscience research.* 74:179-183.
Gulino-Debrac, D. 2013. Mechanotransduction at the basis of endothelial barrier function. *Tissue Barriers.* 1:e24180.

Gusarova, G. A., L. A. Dada, A. M. Kelly, C. Brodie, L. A. Witters, N. S. Chandel and J. I. Sznajder. 2009. Alpha1-AMP-activated protein kinase regulates hypoxia-induced Na,K-ATPase endocytosis via direct phosphorylation of protein kinase C zeta. *Mol Cell Biol.* 29:3455-3464.

Guzy, R. D., B. Hoyos, E. Robin, H. Chen, L. Liu, K. D. Mansfield, M. C. Simon, U. Hammerling and P. T. Schumacker. 2005. Mitochondrial complex III is required for hypoxia-induced ROS production and cellular oxygen sensing. *Cell Metab.* 1:401-408.

Hamanaka, R. B. and N. S. Chandel. 2010. Mitochondrial reactive oxygen species regulate cellular signaling and dictate biological outcomes. *Trends Biochem Sci.* 35:505-513.

Harjes, U., K. Bensaad and A. L. Harris. 2012. Endothelial cell metabolism and implications for cancer therapy. *Br J Cancer.* 107:1207-1212.

Harten, S. K., M. Ashcroft and P. H. Maxwell. 2010. Prolyl hydroxylase domain inhibitors: a route to HIF activation and neuroprotection. *Antioxidants & redox signaling.* 12:459-480.

Hawkins, B. T. and T. P. Davis. 2005. The blood-brain barrier/neurovascular unit in health and disease. *Pharmacol Rev.* 57:173-185.

Hayashi, K., S. Nakao, R. Nakaoke, S. Nakagawa, N. Kitagawa and M. Niwa. 2004. Effects of hypoxia on endothelial/pericytic co-culture model of the blood-brain barrier. *Regulatory peptides.* 123:77-83.

Hayashi, Y., M. Nomura, S. Yamagishi, S. Harada, J. Yamashita and H. Yamamoto. 1997. Induction of various blood-brain barrier properties in non-neural endothelial cells by close apposition to co-cultured astrocytes. *Glia.* 19:13-26.

Hellstrom, M., H. Gerhardt, M. Kalen, X. Li, U. Eriksson, H. Wolburg and C. Betsholtz. 2001. Lack of pericytes leads to endothelial hyperplasia and abnormal vascular morphogenesis. *The Journal of cell biology.* 153:543-553.

Helton, R., J. Cui, J. R. Scheel, J. A. Ellison, C. Ames, C. Gibson, B. Blouw, L. Ouyang, I. Dragatsis, S. Zeitlin, R. S. Johnson, S. A. Lipton and C. Barlow. 2005. Brain-specific knock-out of hypoxia-inducible factor-1alpha reduces rather than increases hypoxic-ischemic damage. *J Neurosci.* 25:4099-4107.

Hertz, L. 2008. Bioenergetics of cerebral ischemia: a cellular perspective. *Neuropharmacology.* 55:289-309.

Hertz, L., L. Peng and G. A. Dienel. 2007. Energy metabolism in astrocytes: high rate of oxidative metabolism and spatiotemporal dependence on glycolysis/glycogenolysis. *J Cereb Blood Flow Metab.* 27:219-249.

Hirrlinger, J. and R. Dringen. 2010. The cytosolic redox state of astrocytes: Maintenance, regulation and functional implications for metabolite trafficking. *Brain Res Rev.* 63:177-188.

Hirrlinger, J., J. Konig, D. Keppler, J. Lindenau, J. B. Schulz and R. Dringen. 2001. The multidrug resistance protein MRP1 mediates the release of glutathione disulfide from rat astrocytes during oxidative stress. *J Neurochem.* 76:627-636.

Hori, S., S. Ohtsuki, K. Hosoya, E. Nakashima and T. Terasaki. 2004. A pericyte-derived angiopoietin-1 multimeric complex induces occludin gene expression in brain capillary endothelial cells through Tie-2 activation in vitro. *Journal of neurochemistry.* 89:503-513.

Hubbi, M. E., W. Luo, J. H. Baek and G. L. Semenza. 2011. MCM proteins are negative regulators of hypoxia-inducible factor 1. *Mol Cell.* 42:700-712.

Iadecola, C. and M. Nedergaard. 2007. Glial regulation of the cerebral microvasculature. *Nat Neurosci.* 10:1369-1376.

Igarashi, Y., H. Utsumi, H. Chiba, Y. Yamada-Sasamori, H. Tobioka, Y. Kamimura, K. Furuuchi, Y. Kokai, T. Nakagawa, M. Mori and N. Sawada. 1999. Glial cell line-derived neurotrophic factor induces barrier function of endothelial cells forming the blood-brain barrier. *Biochem Biophys Res Commun.* 261:108-112.

Ilan, N. and J. A. Madri. 2003. PECAM-1: old friend, new partners. *Curr Opin Cell Biol.* 15:515-524.

Itoh, M., A. Nagafuchi, S. Moroi and S. Tsukita. 1997. Involvement of ZO-1 in cadherin-based cell adhesion through its direct binding to alpha catenin and actin filaments. *J Cell Biol.* 138:181-192.

Iyer, N. V., L. E. Kotch, F. Agani, S. W. Leung, E. Laughner, R. H. Wenger, M. Gassmann, J. D. Gearhart, A. M. Lawler, A. Y. Yu and G. L. Semenza. 1998.

Cellular and developmental control of O2 homeostasis by hypoxia-inducible factor 1 alpha. *Genes Dev.* 12:149-162.
Janzer, R. C. and M. C. Raff. 1987. Astrocytes induce blood-brain barrier properties in endothelial cells. *Nature.* 325:253-257.
Juurlink, B. H. 1997. Response of glial cells to ischemia: roles of reactive oxygen species and glutathione. *Neurosci Biobehav Rev.* 21:151-166.
Kahlert, S. and G. Reiser. 2004. Glial perspectives of metabolic states during cerebral hypoxia—calcium regulation and metabolic energy. *Cell Calcium.* 36:295-302.
Katajamaa, M. and M. Oresic. 2007. Data processing for mass spectrometry-based metabolomics. *J Chromatogr A.* 1158:318-328.
Kaur, C., V. Sivakumar, Y. Zhang and E. A. Ling. 2006. Hypoxia-induced astrocytic reaction and increased vascular permeability in the rat cerebellum. *Glia.* 54:826-839.
Kim, J. W., I. Tchernyshyov, G. L. Semenza and C. V. Dang. 2006. HIF-1-mediated expression of pyruvate dehydrogenase kinase: a metabolic switch required for cellular adaptation to hypoxia. *Cell Metab.* 3:177-185.
Koh, M. Y. and G. Powis. 2012. Passing the baton: the HIF switch. *Trends Biochem Sci.* 37:364-372.
Koritzinsky, M., M. G. Magagnin, T. van den Beucken, R. Seigneuric, K. Savelkouls, J. Dostie, S. Pyronnet, R. J. Kaufman, S. A. Weppler, J. W. Voncken, P. Lambin, C. Koumenis, N. Sonenberg and B. G. Wouters. 2006. Gene expression during acute and prolonged hypoxia is regulated by distinct mechanisms of translational control. *EMBO J.* 25:1114-1125.
Koritzinsky, M. and B. G. Wouters. 2007. Hypoxia and regulation of messenger RNA translation. *Methods Enzymol.* 435:247-273.
Koshiji, M., Y. Kageyama, E. A. Pete, I. Horikawa, J. C. Barrett and L. E. Huang. 2004. HIF-1alpha induces cell cycle arrest by functionally counteracting Myc. *EMBO J.* 23:1949-1956.
Koto, T., K. Takubo, S. Ishida, H. Shinoda, M. Inoue, K. Tsubota, Y. Okada and E. Ikeda. 2007. Hypoxia disrupts the barrier function of neural blood vessels through changes in the expression of claudin-5 in endothelial cells. *Am J Pathol.* 170:1389-1397.
Krause, G., L. Winkler, S. L. Mueller, R. F. Haseloff, J. Piontek and I. E. Blasig. 2008. Structure and function of claudins. *Biochimica et biophysica acta.* 1778:631-645.
Kubli, D. A., J. E. Ycaza and A. B. Gustafsson. 2007. Bnip3 mediates mitochondrial dysfunction and cell death through Bax and Bak. *Biochem J.* 405:407-415.
Kuhlmann, C. R., R. Tamaki, M. Gamerdinger, V. Lessmann, C. Behl, O. S. Kempski and H. J. Luhmann. 2007. Inhibition of the myosin light chain kinase prevents hypoxia-induced blood-brain barrier disruption. *J Neurochem.* 102:501-507.
Kunz, M., S. Ibrahim, D. Koczan, H. J. Thiesen, H. J. Kohler, T. Acker, K. H. Plate, S. Ludwig, U. R. Rapp, E. B. Brocker, G. N. van Muijen, E. Flory and G. Gross. 2001. Activation of c-Jun NH2-terminal kinase/stress-activated protein kinase (JNK/SAPK) is critical for hypoxia-induced apoptosis of human malignant melanoma. *Cell Growth Differ.* 12:137-145.
Ladomery, M. R., S. J. Harper and D. O. Bates. 2007. Alternative splicing in angiogenesis: the vascular endothelial growth factor paradigm. *Cancer Lett.* 249:133-142.
Lee, S. W., W. J. Kim, Y. K. Choi, H. S. Song, M. J. Son, I. H. Gelman, Y. J. Kim and K. W. Kim. 2003. SSeCKS regulates angiogenesis and tight junction formation in blood-brain barrier. *Nat Med.* 9:900-906.
Lenihan, C. R. and C. T. Taylor. 2013. The impact of hypoxia on cell death pathways. *Biochem Soc Trans.* 41:657-663.
Lewandowsky, M. 1900. Zur Lehre von Cerebrospinalflüssigkeit. *Z. Klin. Med.* 40:480-494.
Li, M. M., L. Y. Wu, T. Zhao, K. W. Wu, L. Xiong, L. L. Zhu and M. Fan. 2011. The protective role of 5-hydroxymethyl-2-furfural (5-HMF) against acute hypobaric hypoxia. *Cell Stress Chaperones.* 16:529-537.
Liebner, S., M. Corada, T. Bangsow, J. Babbage, A. Taddei, C. J. Czupalla, M. Reis, A. Felici, H. Wolburg, M. Fruttiger, M. M. Taketo, H. von Melchner, K. H. Plate, H. Gerhardt and E. Dejana. 2008. Wnt/beta-catenin signaling controls development of the blood-brain barrier. *J Cell Biol.* 183:409-417.
Lindahl, P., B. R. Johansson, P. Leveen and C. Betsholtz. 1997. Pericyte loss and microaneurysm formation in PDGF-B-deficient mice. *Science.* 277:242-245.

Loboda, A., A. Jozkowicz and J. Dulak. 2010. HIF-1 and HIF-2 transcription factors--similar but not identical. *Mol Cells.* 29:435-442.

Lochhead, J. J., G. McCaffrey, C. E. Quigley, J. Finch, K. M. DeMarco, N. Nametz and T. P. Davis. 2010. Oxidative stress increases blood-brain barrier permeability and induces alterations in occludin during hypoxia-reoxygenation. *J Cereb Blood Flow Metab.* 30:1625-1636.

Love, S. 1999. Oxidative stress in brain ischemia. *Brain Pathol.* 9:119-131.

Lowe, M. T., E. H. Kim, R. L. Faull, D. L. Christie and H. J. Waldvogel. 2013. Dissociated expression of mitochondrial and cytosolic creatine kinases in the human brain: a new perspective on the role of creatine in brain energy metabolism. *J Cereb Blood Flow Metab.* 33:1295-1306.

Lu, D. Y., W. H. Yu, W. L. Yeh, C. H. Tang, Y. M. Leung, K. L. Wong, Y. F. Chen, C. H. Lai and W. M. Fu. 2009. Hypoxia-induced matrix metalloproteinase-13 expression in astrocytes enhances permeability of brain endothelial cells. *Journal of cellular physiology.* 220:163-173.

Luissint, A. C., C. Artus, F. Glacial, K. Ganeshamoorthy and P. O. Couraud. 2012. Tight junctions at the blood brain barrier: physiological architecture and disease-associated dysregulation. *Fluids and barriers of the CNS.* 9:23.

Majmundar, A. J., W. J. Wong and M. C. Simon. 2010. Hypoxia-inducible factors and the response to hypoxic stress. *Mol Cell.* 40:294-309.

Malthankar-Phatak, G. H., A. B. Patel, Y. Xia, S. Hong, G. M. Chowdhury, K. L. Behar, I. A. Orina and J. C. Lai. 2008. Effects of continuous hypoxia on energy metabolism in cultured cerebro-cortical neurons. *Brain Res.* 1229:147-154.

Mann, G. E., D. L. Yudilevich and L. Sobrevia. 2003. Regulation of amino acid and glucose transporters in endothelial and smooth muscle cells. *Physiol Rev.* 83:183-252.

Mark, K. S. and T. P. Davis. 2002. Cerebral microvascular changes in permeability and tight junctions induced by hypoxia-reoxygenation. *American journal of physiology. Heart and circulatory physiology.* 282:H1485-1494.

Meng, W. and M. Takeichi. 2009. Adherens junction: molecular architecture and regulation. *Cold Spring Harb Perspect Biol.* 1:a002899.

Mense, S. M., A. Sengupta, M. Zhou, C. Lan, G. Bentsman, D. J. Volsky and L. Zhang. 2006. Gene expression profiling reveals the profound upregulation of hypoxia-responsive genes in primary human astrocytes. *Physiological genomics.* 25:435-449.

Meyer, J., J. Rauh and H. J. Galla. 1991. The susceptibility of cerebral endothelial cells to astroglial induction of blood-brain barrier enzymes depends on their proliferative state. *J Neurochem.* 57:1971-1977.

Miyata, T., S. Takizawa and C. van Ypersele de Strihou. 2011. Hypoxia. 1. Intracellular sensors for oxygen and oxidative stress: novel therapeutic targets. *American journal of physiology. Cell physiology.* 300:C226-231.

Mojsilovic-Petrovic, J., D. Callaghan, H. Cui, C. Dean, D. B. Stanimirovic and W. Zhang. 2007. Hypoxia-inducible factor-1 (HIF-1) is involved in the regulation of hypoxia-stimulated expression of monocyte chemoattractant protein-1 (MCP-1/CCL2) and MCP-5 (Ccl12) in astrocytes. *Journal of neuroinflammation.* 4:12.

Murphy, M. J. and S. G. Crewther. 2013. Ouabain inhibition of Na/K-ATPase across the retina prevents signed refractive compensation to lens-induced defocus, but not default ocular growth in young chicks *F1000Research 2013.* 2:

Nagel, S., N. P. Talbot, J. Mecinovic, T. G. Smith, A. M. Buchan and C. J. Schofield. 2010. Therapeutic manipulation of the HIF hydroxylases. *Antioxidants & redox signaling.* 12:481-501.

Nakagawa, S., M. A. Deli, S. Nakao, M. Honda, K. Hayashi, R. Nakaoke, Y. Kataoka and M. Niwa. 2007. Pericytes from brain microvessels strengthen the barrier integrity in primary cultures of rat brain endothelial cells. *Cellular and molecular neurobiology.* 27:687-694.

Nakayama, M. and P. Berger. 2013. Coordination of VEGF receptor trafficking and signaling by coreceptors. *Exp Cell Res.* 319:1340-1347.

Neuwelt, E. A., B. Bauer, C. Fahlke, G. Fricker, C. Iadecola, D. Janigro, L. Leybaert, Z. Molnar, M. E. O'Donnell, J. T. Povlishock, N. R. Saunders, F. Sharp, D. Stanimirovic, R. J. Watts and L. R. Drewes. 2011. Engaging neuroscience to advance translational research in brain barrier biology. *Nat Rev Neurosci.* 12:169-182.

Nico, B. and D. Ribatti. 2012. Morphofunctional aspects of the blood-brain barrier. *Current drug metabolism.* 13:50-60.
Niessen, C. M. 2007. Tight junctions/adherens junctions: basic structure and function. *J Invest Dermatol.* 127:2525-2532.
Niitsu, Y., O. Hori, A. Yamaguchi, Y. Bando, K. Ozawa, M. Tamatani, S. Ogawa and M. Tohyama. 1999. Exposure of cultured primary rat astrocytes to hypoxia results in intracellular glucose depletion and induction of glycolytic enzymes. *Brain Res Mol Brain Res.* 74:26-34.
Niquet, J., R. A. Baldwin, S. G. Allen, D. G. Fujikawa and C. G. Wasterlain. 2003. Hypoxic neuronal necrosis: protein synthesis-independent activation of a cell death program. *Proc Natl Acad Sci U S A.* 100:2825-2830.
Nitta, T., M. Hata, S. Gotoh, Y. Seo, H. Sasaki, N. Hashimoto, M. Furuse and S. Tsukita. 2003. Size-selective loosening of the blood-brain barrier in claudin-5-deficient mice. *J Cell Biol.* 161:653-660.
Nowak, D. G., J. Woolard, E. M. Amin, O. Konopatskaya, M. A. Saleem, A. J. Churchill, M. R. Ladomery, S. J. Harper and D. O. Bates. 2008. Expression of pro- and anti-angiogenic isoforms of VEGF is differentially regulated by splicing and growth factors. *J Cell Sci.* 121:3487-3495.
Ogata, H., S. Goto, K. Sato, W. Fujibuchi, H. Bono and M. Kanehisa. 1999. KEGG: Kyoto Encyclopedia of Genes and Genomes. *Nucleic Acids Res.* 27:29-34.
Ogunshola, O. O. 2011. In vitro modeling of the blood-brain barrier: simplicity versus complexity. *Curr Pharm Des.* 17:2755-2761.
Ogunshola, O. O. and A. Al-Ahmad. 2012. HIF-1 at the blood-brain barrier: a mediator of permeability? *High altitude medicine & biology.* 13:153-161.
Papandreou, I., R. A. Cairns, L. Fontana, A. L. Lim and N. C. Denko. 2006. HIF-1 mediates adaptation to hypoxia by actively downregulating mitochondrial oxygen consumption. *Cell Metab.* 3:187-197.
Park, Y. S., N. H. Kim and I. Jo. 2003. Hypoxia and vascular endothelial growth factor acutely up-regulate angiopoietin-1 and Tie2 mRNA in bovine retinal pericytes. *Microvasc Res.* 65:125-131.
Pellerin, L. 2010. Food for thought: the importance of glucose and other energy substrates for sustaining brain function under varying levels of activity. *Diabetes & Metabolism.* 36:S59-S63.
Perasso, L., P. Spallarossa, C. Gandolfo, P. Ruggeri and M. Balestrino. 2013. Therapeutic use of creatine in brain or heart ischemia: available data and future perspectives. *Med Res Rev.* 33:336-363.
Persidsky, Y., D. Heilman, J. Haorah, M. Zelivyanskaya, R. Persidsky, G. A. Weber, H. Shimokawa, K. Kaibuchi and T. Ikezu. 2006. Rho-mediated regulation of tight junctions during monocyte migration across the blood-brain barrier in HIV-1 encephalitis (HIVE). *Blood.* 107:4770-4780.
Plateel, M., E. Teissier and R. Cecchelli. 1997. Hypoxia dramatically increases the nonspecific transport of blood-borne proteins to the brain. *J Neurochem.* 68:874-877.
Prebil, M., J. Jensen, R. Zorec and M. Kreft. 2011. Astrocytes and energy metabolism. *Arch Physiol Biochem.* 117:64-69.
Raub, T. J., S. L. Kuentzel and G. A. Sawada. 1992. Permeability of bovine brain microvessel endothelial cells in vitro: barrier tightening by a factor released from astroglioma cells. *Experimental cell research.* 199:330-340.
Redzic, Z. B., T. Rabie, B. A. Sutherland and A. M. Buchan. 2013. Differential effects of paracrine factors on the survival of cells of the neurovascular unit during oxygen glucose deprivation. *International journal of stroke : official journal of the International Stroke Society.*
Renault, T. T. and S. Manon. 2011. Bax: Addressed to kill. *Biochimie.* 93:1379-1391.
Reuss, B., R. Dono and K. Unsicker. 2003. Functions of fibroblast growth factor (FGF)-2 and FGF-5 in astroglial differentiation and blood-brain barrier permeability: evidence from mouse mutants. *J Neurosci.* 23:6404-6412.
Rist, R. J., I. A. Romero, M. W. Chan, P. O. Couraud, F. Roux and N. J. Abbott. 1997. F-actin cytoskeleton and sucrose permeability of immortalised rat brain microvascular endothelial cell monolayers: effects of cyclic AMP and astrocytic factors. *Brain research.* 768:10-18.

Rubin, L. L., D. E. Hall, S. Porter, K. Barbu, C. Cannon, H. C. Horner, M. Janatpour, C. W. Liaw, K. Manning, J. Morales and et al. 1991. A cell culture model of the blood-brain barrier. *The Journal of cell biology.* 115:1725-1735.

Ryan, H. E., J. Lo and R. S. Johnson. 1998. HIF-1 alpha is required for solid tumor formation and embryonic vascularization. *EMBO J.* 17:3005-3015.

Sa-Pereira, I., D. Brites and M. A. Brito. 2012. Neurovascular unit: a focus on pericytes. *Molecular neurobiology.* 45:327-347.

Saitou, M., M. Furuse, H. Sasaki, J. D. Schulzke, M. Fromm, H. Takano, T. Noda and S. Tsukita. 2000. Complex phenotype of mice lacking occludin, a component of tight junction strands. *Mol Biol Cell.* 11:4131-4142.

Sakakibara, A., M. Furuse, M. Saitou, Y. Ando-Akatsuka and S. Tsukita. 1997. Possible involvement of phosphorylation of occludin in tight junction formation. *J Cell Biol.* 137:1393-1401.

Sanchez-Pulido, L., F. Martin-Belmonte, A. Valencia and M. A. Alonso. 2002. MARVEL: a conserved domain involved in membrane apposition events. *Trends Biochem Sci.* 27:599-601.

Schmid-Brunclik, N., C. Burgi-Taboada, X. Antoniou, M. Gassmann and O. O. Ogunshola. 2008. Astrocyte responses to injury: VEGF simultaneously modulates cell death and proliferation. *Am J Physiol Regul Integr Comp Physiol.* 295:R864-873.

Schoch, H. J., S. Fischer and H. H. Marti. 2002. Hypoxia-induced vascular endothelial growth factor expression causes vascular leakage in the brain. *Brain.* 125:2549-2557.

Schroeter, M. L., K. Mertsch, H. Giese, S. Muller, A. Sporbert, B. Hickel and I. E. Blasig. 1999. Astrocytes enhance radical defence in capillary endothelial cells constituting the blood-brain barrier. *FEBS Lett.* 449:241-244.

Semenza, G. L. 2003. Targeting HIF-1 for cancer therapy. *Nat Rev Cancer.* 3:721-732.

Semenza, G. L. 2011. Hypoxia. Cross talk between oxygen sensing and the cell cycle machinery. *Am J Physiol Cell Physiol.* 301:C550-552.

Shannon, P., A. Markiel, O. Ozier, N. S. Baliga, J. T. Wang, D. Ramage, N. Amin, B. Schwikowski and T. Ideker. 2003. Cytoscape: a software environment for integrated models of biomolecular interaction networks. *Genome Res.* 13:2498-2504.

Shen, L., C. R. Weber and J. R. Turner. 2008. The tight junction protein complex undergoes rapid and continuous molecular remodeling at steady state. *J Cell Biol.* 181:683-695.

Shen, W., S. Li, S. H. Chung, L. Zhu, J. Stayt, T. Su, P. O. Couraud, I. A. Romero, B. Weksler and M. C. Gillies. 2011. Tyrosine phosphorylation of VE-cadherin and claudin-5 is associated with TGF-beta1-induced permeability of centrally derived vascular endothelium. *Eur J Cell Biol.* 90:323-332.

Shimizu, F., Y. Sano, M. A. Abe, T. Maeda, S. Ohtsuki, T. Terasaki and T. Kanda. 2011. Peripheral nerve pericytes modify the blood-nerve barrier function and tight junctional molecules through the secretion of various soluble factors. *J Cell Physiol.* 226:255-266.

Shimizu, F., Y. Sano, K. Saito, M. A. Abe, T. Maeda, H. Haruki and T. Kanda. 2012. Pericyte-derived glial cell line-derived neurotrophic factor increase the expression of claudin-5 in the blood-brain barrier and the blood-nerve barrier. *Neurochem Res.* 37:401-409.

Sickmann, H. M., A. B. Walls, A. Schousboe, S. D. Bouman and H. S. Waagepetersen. 2009. Functional significance of brain glycogen in sustaining glutamatergic neurotransmission. *J Neurochem.* 109 Suppl 1:80-86.

Siddharthan, V., Y. V. Kim, S. Liu and K. S. Kim. 2007. Human astrocytes/astrocyte-conditioned medium and shear stress enhance the barrier properties of human brain microvascular endothelial cells. *Brain Res.* 1147:39-50.

Silva, L. P., P. L. Lorenzi, P. Purwaha, V. Yong, D. H. Hawke and J. N. Weinstein. 2013. Measurement of DNA concentration as a normalization strategy for metabolomic data from adherent cell lines. *Analytical chemistry.* 85:9536-9542.

Sims, N. R., M. Nilsson and H. Muyderman. 2004. Mitochondrial glutathione: a modulator of brain cell death. *J Bioenerg Biomembr.* 36:329-333.

Singh, N., G. Sharma, V. Mishra and R. Raghubir. 2012. Hypoxia Inducible Factor-1: Its Potential Role In Cerebral Ischemia. *Cellular and Molecular Neurobiology.* 32:491-507.

Skuli, N., L. Liu, A. Runge, T. Wang, L. Yuan, S. Patel, L. Iruela-Arispe, M. C. Simon and B. Keith. 2009. Endothelial deletion of hypoxia-inducible factor-2alpha (HIF-2alpha) alters vascular function and tumor angiogenesis. *Blood.* 114:469-477.

Sobue, K., N. Yamamoto, K. Yoneda, M. E. Hodgson, K. Yamashiro, N. Tsuruoka, T. Tsuda, H. Katsuya, Y. Miura, K. Asai and T. Kato. 1999. Induction of blood-brain barrier properties in immortalized bovine brain endothelial cells by astrocytic factors. *Neurosci Res.* 35:155-164.

Song, H. S., M. J. Son, Y. M. Lee, W. J. Kim, S. W. Lee, C. W. Kim and K. W. Kim. 2002. Oxygen tension regulates the maturation of the blood-brain barrier. *Biochem Biophys Res Commun.* 290:325-331.

Stamatovic, S. M., R. F. Keep, S. L. Kunkel and A. V. Andjelkovic. 2003. Potential role of MCP-1 in endothelial cell tight junction 'opening': signaling via Rho and Rho kinase. *J Cell Sci.* 116:4615-4628.

Stamatovic, S. M., P. Shakui, R. F. Keep, B. B. Moore, S. L. Kunkel, N. Van Rooijen and A. V. Andjelkovic. 2005. Monocyte chemoattractant protein-1 regulation of blood-brain barrier permeability. *J Cereb Blood Flow Metab.* 25:593-606.

Stanimirovic, D. B. and A. Friedman. 2012. Pathophysiology of the neurovascular unit: disease cause or consequence? *Journal of cerebral blood flow and metabolism : official journal of the International Society of Cerebral Blood Flow and Metabolism.* 32:1207-1221.

Steed, E., M. S. Balda and K. Matter. 2010. Dynamics and functions of tight junctions. *Trends Cell Biol.* 20:142-149.

Steinbach, J. P., H. Wolburg, A. Klumpp, H. Probst and M. Weller. 2003. Hypoxia-induced cell death in human malignant glioma cells: energy deprivation promotes decoupling of mitochondrial cytochrome c release from caspase processing and necrotic cell death. *Cell Death Differ.* 10:823-832.

Stenman, J. M., J. Rajagopal, T. J. Carroll, M. Ishibashi, J. McMahon and A. P. McMahon. 2008. Canonical Wnt signaling regulates organ-specific assembly and differentiation of CNS vasculature. *Science.* 322:1247-1250.

Stewart, P. A. and M. J. Wiley. 1981. Developing nervous tissue induces formation of blood-brain barrier characteristics in invading endothelial cells: a study using quail--chick transplantation chimeras. *Developmental biology.* 84:183-192.

Tachikawa, M., M. Fukaya, T. Terasaki, S. Ohtsuki and M. Watanabe. 2004. Distinct cellular expressions of creatine synthetic enzyme GAMT and creatine kinases uCK-Mi and CK-B suggest a novel neuron-glial relationship for brain energy homeostasis. *Eur J Neurosci.* 20:144-160.

Tachikawa, M., K. Hosoya, S. Ohtsuki and T. Terasaki. 2007. A novel relationship between creatine transport at the blood-brain and blood-retinal barriers, creatine biosynthesis, and its use for brain and retinal energy homeostasis. *Subcell Biochem.* 46:83-98.

Taddei, A., C. Giampietro, A. Conti, F. Orsenigo, F. Breviario, V. Pirazzoli, M. Potente, C. Daly, S. Dimmeler and E. Dejana. 2008. Endothelial adherens junctions control tight junctions by VE-cadherin-mediated upregulation of claudin-5. *Nature cell biology.* 10:923-934.

Takai, Y., K. Irie, K. Shimizu, T. Sakisaka and W. Ikeda. 2003. Nectins and nectin-like molecules: roles in cell adhesion, migration, and polarization. *Cancer Sci.* 94:655-667.

Takai, Y. and H. Nakanishi. 2003. Nectin and afadin: novel organizers of intercellular junctions. *J Cell Sci.* 116:17-27.

Takano, T., G. F. Tian, W. Peng, N. Lou, W. Libionka, X. Han and M. Nedergaard. 2006. Astrocyte-mediated control of cerebral blood flow. *Nat Neurosci.* 9:260-267.

Takata, F., S. Dohgu, J. Matsumoto, H. Takahashi, T. Machida, T. Wakigawa, E. Harada, H. Miyaji, M. Koga, T. Nishioku, A. Yamauchi and Y. Kataoka. 2011. Brain pericytes among cells constituting the blood-brain barrier are highly sensitive to tumor necrosis factor-alpha, releasing matrix metalloproteinase-9 and migrating in vitro. *J Neuroinflammation.* 8:106.

Tao-Cheng, J. H., Z. Nagy and M. W. Brightman. 1987. Tight junctions of brain endothelium in vitro are enhanced by astroglia. *J Neurosci.* 7:3293-3299.

Thanabalasundaram, G., C. Pieper, M. Lischper and H. J. Galla. 2010. Regulation of the blood-brain barrier integrity by pericytes via matrix metalloproteinases mediated activation of vascular endothelial growth factor in vitro. *Brain research.* 1347:1-10.

Thanabalasundaram, G., J. Schneidewind, C. Pieper and H. J. Galla. 2011. The impact of pericytes on the blood-brain barrier integrity depends critically on the pericyte differentiation stage. *The international journal of biochemistry & cell biology.*
Tian, H., R. E. Hammer, A. M. Matsumoto, D. W. Russell and S. L. McKnight. 1998. The hypoxia-responsive transcription factor EPAS1 is essential for catecholamine homeostasis and protection against heart failure during embryonic development. *Genes Dev.* 12:3320-3324.
Tracy, K. and K. F. Macleod. 2007. Regulation of mitochondrial integrity, autophagy and cell survival by BNIP3. *Autophagy.* 3:616-619.
Trendelenburg, G. and U. Dirnagl. 2005. Neuroprotective role of astrocytes in cerebral ischemia: focus on ischemic preconditioning. *Glia.* 50:307-320.
Turner, D. A. and D. C. Adamson. 2011. Neuronal-Astrocyte Metabolic Interactions. *Journal of Neuropathology and Experimental Neurology.* 70:167-176.
van Patot, M. C. and M. Gassmann. 2011. Hypoxia: adapting to high altitude by mutating EPAS-1, the gene encoding HIF-2alpha. *High Alt Med Biol.* 12:157-167.
Vangeison, G., D. Carr, H. J. Federoff and D. A. Rempe. 2008. The good, the bad, and the cell type-specific roles of hypoxia inducible factor-1 alpha in neurons and astrocytes. *The Journal of neuroscience : the official journal of the Society for Neuroscience.* 28:1988-1993.
Vangeison, G. and D. A. Rempe. 2009. The Janus-faced effects of hypoxia on astrocyte function. *The Neuroscientist : a review journal bringing neurobiology, neurology and psychiatry.* 15:579-588.
Vestweber, D. 2008. VE-cadherin: the major endothelial adhesion molecule controlling cellular junctions and blood vessel formation. *Arterioscler Thromb Vasc Biol.* 28:223-232.
Vogel, C., A. Bauer, M. Wiesnet, K. T. Preissner, W. Schaper, H. H. Marti and S. Fischer. 2007. Flt-1, but not Flk-1 mediates hyperpermeability through activation of the PI3-K/Akt pathway. *J Cell Physiol.* 212:236-243.
Walls, A. B., C. M. Heimburger, S. D. Bouman, A. Schousboe and H. S. Waagepetersen. 2009. Robust glycogen shunt activity in astrocytes: Effects of glutamatergic and adrenergic agents. *Neuroscience.* 158:284-292.
Walsh, T. G., R. P. Murphy, P. Fitzpatrick, K. D. Rochfort, A. F. Guinan, A. Murphy and P. M. Cummins. 2011. Stabilization of brain microvascular endothelial barrier function by shear stress involves VE-cadherin signaling leading to modulation of pTyr-occludin levels. *Journal of cellular physiology.* 226:3053-3063.
Walshe, T. E., M. Saint-Geniez, A. S. Maharaj, E. Sekiyama, A. E. Maldonado and P. A. D'Amore. 2009. TGF-beta is required for vascular barrier function, endothelial survival and homeostasis of the adult microvasculature. *PLoS One.* 4:e5149.
Wamelink, M. M., E. A. Struys and C. Jakobs. 2008. The biochemistry, metabolism and inherited defects of the pentose phosphate pathway: a review. *J Inherit Metab Dis.* 31:703-717.
Wang, W., Z. Wu, Z. Dai, Y. Yang, J. Wang and G. Wu. 2013. Glycine metabolism in animals and humans: implications for nutrition and health. *Amino Acids.* 45:463-477.
Wang, Y. L., Y. N. Hui, B. Guo and J. X. Ma. 2007. Strengthening tight junctions of retinal microvascular endothelial cells by pericytes under normoxia and hypoxia involving angiopoietin-1 signal way. *Eye (Lond).* 21:1501-1510.
Warner, D. S., H. Sheng and I. Batinic-Haberle. 2004. Oxidants, antioxidants and the ischemic brain. *J Exp Biol.* 207:3221-3231.
Wei, M. C., W. X. Zong, E. H. Cheng, T. Lindsten, V. Panoutsakopoulou, A. J. Ross, K. A. Roth, G. R. MacGregor, C. B. Thompson and S. J. Korsmeyer. 2001. Proapoptotic BAX and BAK: a requisite gateway to mitochondrial dysfunction and death. *Science.* 292:727-730.
Wenger, R. H., D. P. Stiehl and G. Camenisch. 2005. Integration of oxygen signaling at the consensus HRE. *Science's STKE : signal transduction knowledge environment.* 2005:re12.
Wheaton, W. W. and N. S. Chandel. 2011. Hypoxia. 2. Hypoxia regulates cellular metabolism. *Am J Physiol Cell Physiol.* 300:C385-393.
Wiesinger, H., B. Hamprecht and R. Dringen. 1997. Metabolic pathways for glucose in astrocytes. *Glia.* 21:22-34.

Willis, C. L. 2011. Glia-induced reversible disruption of blood-brain barrier integrity and neuropathological response of the neurovascular unit. *Toxicol Pathol.* 39:172-185.

Willis, C. L., L. Leach, G. J. Clarke, C. C. Nolan and D. E. Ray. 2004a. Reversible disruption of tight junction complexes in the rat blood-brain barrier, following transitory focal astrocyte loss. *Glia.* 48:1-13.

Willis, C. L., D. S. Meske and T. P. Davis. 2010. Protein kinase C activation modulates reversible increase in cortical blood-brain barrier permeability and tight junction protein expression during hypoxia and posthypoxic reoxygenation. *Journal of cerebral blood flow and metabolism : official journal of the International Society of Cerebral Blood Flow and Metabolism.* 30:1847-1859.

Willis, C. L., C. C. Nolan, S. N. Reith, T. Lister, M. J. Prior, C. J. Guerin, G. Mavroudis and D. E. Ray. 2004b. Focal astrocyte loss is followed by microvascular damage, with subsequent repair of the blood-brain barrier in the apparent absence of direct astrocytic contact. *Glia.* 45:325-337.

Witt, K. A., K. S. Mark, K. E. Sandoval and T. P. Davis. 2008. Reoxygenation stress on blood-brain barrier paracellular permeability and edema in the rat. *Microvasc Res.* 75:91-96.

Xia, J., R. Mandal, I. V. Sinelnikov, D. Broadhurst and D. S. Wishart. 2012. MetaboAnalyst 2.0--a comprehensive server for metabolomic data analysis. *Nucleic Acids Res.* 40:W127-133.

Xia, J. and D. S. Wishart. 2010. MetPA: a web-based metabolomics tool for pathway analysis and visualization. *Bioinformatics.* 26:2342-2344.

Yamagata, K., M. Tagami, F. Takenaga, Y. Yamori and S. Itoh. 2004. Hypoxia-induced changes in tight junction permeability of brain capillary endothelial cells are associated with IL-1beta and nitric oxide. *Neurobiol Dis.* 17:491-499.

Yan, J., B. Zhou, S. Taheri and H. Shi. 2011. Differential effects of HIF-1 inhibition by YC-1 on the overall outcome and blood-brain barrier damage in a rat model of ischemic stroke. *PLoS One.* 6:e27798.

Yeh, W. L., D. Y. Lu, C. J. Lin, H. C. Liou and W. M. Fu. 2007. Inhibition of hypoxia-induced increase of blood-brain barrier permeability by YC-1 through the antagonism of HIF-1alpha accumulation and VEGF expression. *Mol Pharmacol.* 72:440-449.

Zehendner, C. M., L. Librizzi, M. de Curtis, C. R. Kuhlmann and H. J. Luhmann. 2011. Caspase-3 contributes to ZO-1 and Cl-5 tight-junction disruption in rapid anoxic neurovascular unit damage. *PloS one.* 6:e16760.

Zepeda, A. B., A. Pessoa, Jr., R. L. Castillo, C. A. Figueroa, V. M. Pulgar and J. G. Farias. 2013. Cellular and molecular mechanisms in the hypoxic tissue: role of HIF-1 and ROS. *Cell Biochem Funct.* 31:451-459.

Zhang, H., M. Bosch-Marce, L. A. Shimoda, Y. S. Tan, J. H. Baek, J. B. Wesley, F. J. Gonzalez and G. L. Semenza. 2008. Mitochondrial autophagy is an HIF-1-dependent adaptive metabolic response to hypoxia. *J Biol Chem.* 283:10892-10903.

Zhang, W., J. M. Petrovic, D. Callaghan, A. Jones, H. Cui, C. Howlett and D. Stanimirovic. 2006. Evidence that hypoxia-inducible factor-1 (HIF-1) mediates transcriptional activation of interleukin-1beta (IL-1beta) in astrocyte cultures. *J Neuroimmunol.* 174:63-73.

Zhou, G., L. A. Dada, N. S. Chandel, K. Iwai, E. Lecuona, A. Ciechanover and J. I. Sznajder. 2008. Hypoxia-mediated Na-K-ATPase degradation requires von Hippel Lindau protein. *FASEB J.* 22:1335-1342.

Zong, W. X. and C. B. Thompson. 2006. Necrotic death as a cell fate. *Genes Dev.* 20:1-15.

Zoppo, G. J. and J. M. Hallenbeck. 2000. Advances in the vascular pathophysiology of ischemic stroke. *Thrombosis research.* 98:73-81.

Zozulya, A., C. Weidenfeller and H. J. Galla. 2008. Pericyte-endothelial cell interaction increases MMP-9 secretion at the blood-brain barrier in vitro. *Brain research.* 1189:1-11.

7 REVIEW ARTICLE

Cell-specific blood-brain barrier regulation in health and disease: a focus on hypoxia

S. Engelhardt, S.Patkar and O.O. Ogunshola

British Journal of Pharmacology, Volume 171, Issue 5, Pages 1210-1230

BJP British Journal of Pharmacology

DOI:10.1111/bph.12489
www.brjpharmacol.org

REVIEW

Cell-specific blood–brain barrier regulation in health and disease: a focus on hypoxia

S Engelhardt, S Patkar and O O Ogunshola

Institute of Veterinary Physiology, University of Zurich, Zurich, Switzerland

Correspondence
O.O. Ogunshola, Institute of Veterinary Physiology, University of Zurich, Winterthurerstrasse 260, Zurich, Switzerland. E-mail: Larao@access.uzh.ch

Keywords
BBB cell-specific response; endothelial cells; astrocytes; pericytes; hypoxia; HIF-1; neurodegenerative diseases

Received
12 August 2013
Revised
2 October 2013
Accepted
16 October 2013

The blood–brain barrier (BBB) is a complex vascular structure consisting of microvascular endothelial cells that line the vessel wall, astrocyte end-feet, pericytes, as well as the basal lamina. BBB cells act in concert to maintain the characteristic impermeable and low paracellular flux of the brain vascular network, thus ensuring a homeostatic neuronal environment. Alterations in BBB stability that occur during injury have dire consequences on disease progression and it is clear that BBB cell-specific responses, positive or negative, must make a significant contribution to injury outcome. Reduced oxygenation, or hypoxia, is a characteristic of many brain diseases that significantly increases barrier permeability. Recent data suggest that hypoxia-inducible factor (HIF-1), the master regulator of the hypoxic response, probably mediates many hypoxic effects either directly or indirectly via its target genes. This review discusses current knowledge of physiological cell-specific regulation of barrier function, their responses to hypoxia as well as consequences of hypoxic- and HIF-1-mediated mechanisms on barrier integrity during select brain diseases. In the final sections, the potential of current advances in targeting HIF-1 as a therapeutic strategy will be overviewed.

Abbreviations

BBB, blood–brain barrier; HIF-1, hypoxia-inducible factor-1; TJ, tight junction; ECs, endothelial cells; TEER, transendothelial electrical resistance

The maintenance of CNS homeostasis is performed largely by the blood–brain barrier (BBB), which together with neurons and microglia form an organization referred to as the neurovascular unit (NVU). The BBB is dynamic performing both passive and active features of the brain endothelium essentially acting as a vascular gatekeeper that controls movement of substances from the circulating blood into the brain parenchyma – a role crucial for neuronal, and therefore CNS, homeostasis. Accumulating experimental evidence supports the hypothesis that opening of the BBB triggers a chain of events leading to neuronal dysfunction and damage resulting in neurological disease, and when coupled with previous insults BBB disruption could have serious detrimental consequences for patient outcome. Despite this knowledge, our understanding of physiological barrier function, as well as during disease, is very limited. In addition, the contribution of the perivascular cells that modulate barrier characteristics and their individual responses to injury is poorly characterized. This review will discuss the mechanisms through which hypoxia, a characteristic state of many brain diseases, disrupts barrier function and the importance of BBB cell-specific responses to barrier integrity. Additionally, consequences of hypoxia-mediated barrier modulation during brain disease and future therapeutic use of hypoxia-inducible factor-1 (HIF-1) modulators in the clinics will be reviewed.

Physiology

BBB organization and cell-specific function

The BBB is a complex structure consisting of microvascular endothelial cells (ECs) that line the vessel wall, astrocyte end-feet, pericytes, as well as the basal lamina (see Figure 1), which together with neurons and microglia form an organization referred to as the NVU. The basal lamina is an essential part of the BBB that surrounds the capillaries thereby anchoring the cells in place and providing a link with the resident

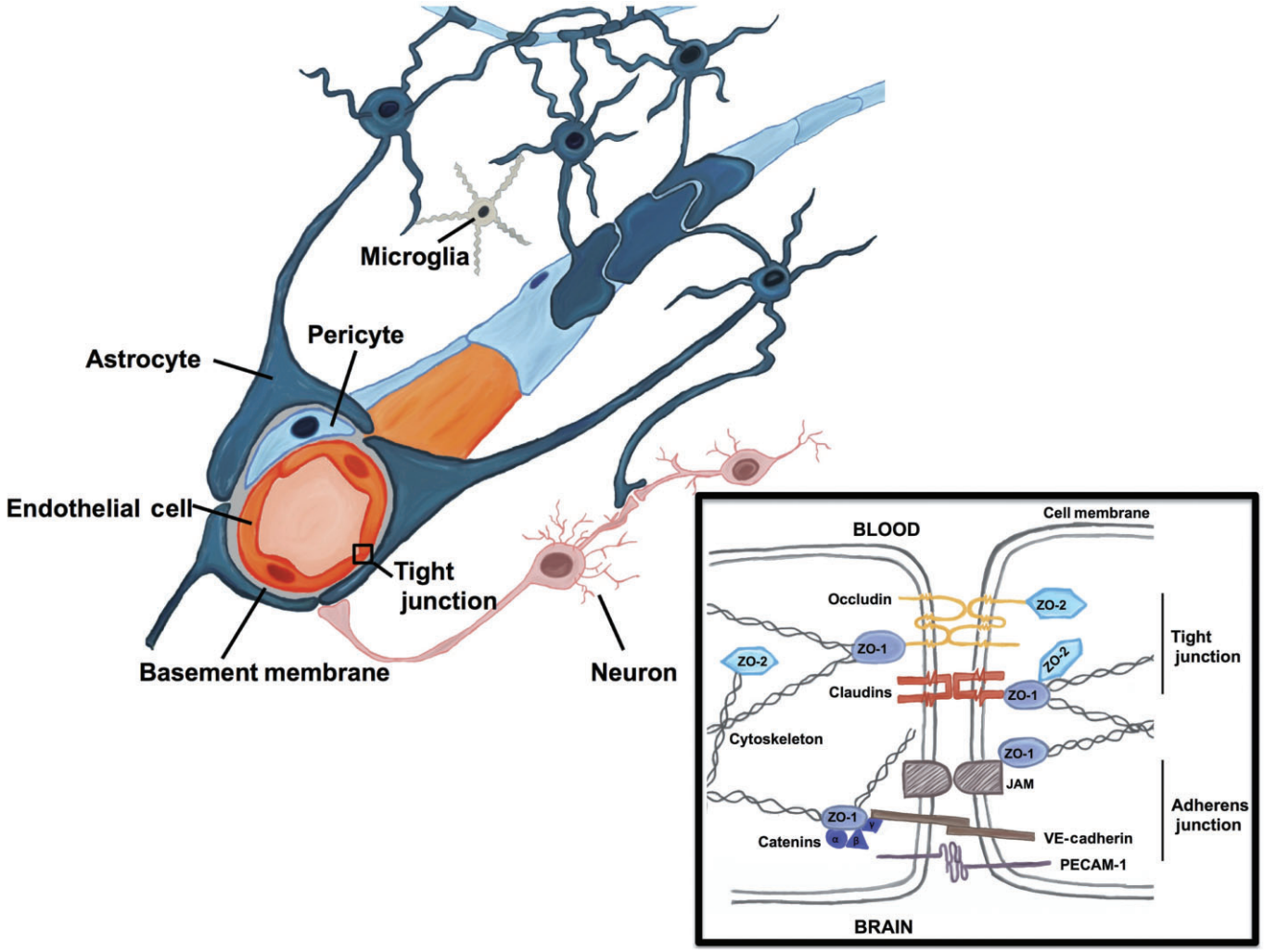

Figure 1

The BBB protects neurons and glial cells from systemically circulating agents as brain microvessels form a very tight barrier clearly distinct from vessels in other organs. The barrier is formed by ECs (red), which line the blood vessels, surrounded by pericytes (light blue), BM (grey) and astrocytic (dark blue) end-feet. Astrocytes provide the cellular link to the adjacent neurons (pink). The illustration also shows microglial cells (grey) in contact with astrocytes. Inset (black box) shows the cell–cell contact that takes place between two adjacent ECs at the BBB and demonstrates the basic organization of the BBB tight and adherens junctional proteins. Note the interactions of the junctional proteins with the cytoskeleton.

brain cells. The brain ECs are in direct contact with brain pericytes (Abbott *et al.*, 2010; Ogunshola and Al-Ahmad, 2012) and separated from the brain parenchyma by two layers of extracellular matrices (ECM). The inner layer is formed by the vascular basement membrane (BM) localized at the EC basolateral side and is shared with neighbouring pericytes (Hallmann *et al.*, 2005). The outer layer is formed by the glia limitans as a result of glial end-feet processes that surrounds or ensheaths the cerebral vascular tree (Paolinelli *et al.*, 2011). Perivascular glial end-feet form a direct interface between the vascular compartment and the brain parenchyma (see Figure 1) and are therefore thought to represent key checkpoints of brain metabolism and function (Wolburg *et al.*, 2009a).

BBB cells act in concert to maintain the characteristic impermeable and low paracellular flux of the vascular network that is chiefly mediated via high expression levels and localization of tight junction (TJ) proteins, namely, occludins, claudins, junctional adhesion molecules and their adaptor protein zonula occludens-1 (ZO-1; reviewed in Förster, 2008; Abbott *et al.*, 2010). TJs are elaborate structures that function as both a 'zipper' that separates the apical and basolateral cell membranes thus enabling asymmetric distribution of membrane constituents, and a 'fence' that limits paracellular permeability (see Figure 1 inset). Thus, stringent regulation of CNS homeostasis by severe restriction of the paracellular diffusional pathway between the ECs and substances and/or cells within the circulating blood is ensured. TJs are highly dynamic structures that rapidly undergo subcellular redistribution, expression level alterations as well as post-translational modifications, all of which affect protein–protein interactions (reviewed in Förster, 2008; Ogunshola, 2011). Cellular interactions and local release of factors (discussed in detail later), in addition to signals from circulating

substances, have marked effects on TJ expression and therefore barrier integrity. Brain ECs do not seem to spontaneously express high TJ levels but are induced by the surrounding perivascular cells, astrocytes and pericytes (Ballabh *et al.*, 2004; Abbott *et al.*, 2006; Ogunshola, 2011). Astrocytes are the most abundant cell in the brain and their long filamentous end-foot processes extend towards and envelope the vascular network. Astrocytes have long been known to play a central role in inducing expression of TJ proteins in microvascular ECs (Abbott, 2002; Ogunshola, 2011). Although pericytes have very close contact with ECs, lying juxtaposed to the capillary and sharing a BM, for a long time, the function of this cell in barrier maintenance was largely unknown. Scientific advances in tools and methodologies, however, have provided recent evidence from both *in vitro* and *in vivo* studies that pericytes also significantly contribute to barrier stability during development and adulthood.

Barrier effectiveness is directly related to the ability of the perivascular cells to maintain their normal functional activities. As such, alterations or modifications of perivascular cell properties *per se*, as a result of disease progression or signalling pathway activation, will compromise barrier integrity and increase permeability. Despite this fact, the highly coordinated signalling mechanisms and dynamic interactions that exist between individual cells of the BBB remain largely unknown. Such knowledge is key to better understand barrier function under physiological as well as pathological conditions. This implies possible future development of cell-specific therapies and targeted treatments that could indeed represent an important way to stabilize barrier function during injury. The following sections deal with some of the cell-specific responses that occur particularly during oxygen deprivation and diseases characterized by hypoxia in more detail. Notably, because of the complexity related to studying BBB *in vivo*, much of the data comes from *in vitro* model systems, however, where possible reference to *in vivo* studies will also be given.

Astrocytes at the BBB

Similar to neurons and other glial cells astrocytes originate from the neuroectoderm (Allen and Barres, 2009). To date, 11 different types of astrocytes are known of which eight are specifically associated with blood vessels (Abbott *et al.*, 2006). Astrocytes are crucially involved in control of neuronal function through regulation of brain homeostasis, supply of neurons with energy and substrates for neurotransmission and recycling of neurotransmitters. Furthermore, they represent the connection between neurons and the brain vasculature, which they cover with their end-feet. Almost 50 years ago, the close proximity of the astrocytic end-feet to the brain endothelium raised the hypothesis that astrocytes contribute to BBB regulation (Davson and Oldendorf, 1967). Since then, a number of *in vivo* (Stewart and Wiley, 1981; Janzer and Raff, 1987; Willis *et al.*, 2004) and particularly *in vitro* studies have demonstrated the importance of astrocytes to BBB induction and regulation. Model systems using astrocyte-endothelial co-cultures (Dehouck *et al.*, 1990; Rist *et al.*, 1997; Fischer *et al.*, 2000; Al Ahmad *et al.*, 2009) as well as astrocyte-conditioned media (ACM) (Rubin *et al.*, 1991; Raub *et al.*, 1992) demonstrated the inductive potential of astrocytes on barrier tightness by increased transendothelial electrical resistance (TEER) and reduced permeability to low molecular weight tracers (for detailed review, refer to the excellent article by Deli *et al.*, 2005). There is now good evidence that barrier induction through astrocytes is mainly mediated via changes in the number, length and complexity of endothelial TJs (Tao-Cheng *et al.*, 1987), expression levels of TJ and associated-proteins like occludin and ZO-1, respectively (Siddharthan *et al.*, 2007; Colgan *et al.*, 2008), and the redistribution of junctional proteins such as platelet endothelial cell adhesion molecule-1, ZO-1 and claudin-5 at endothelial junctions (Colgan *et al.*, 2008; Al Ahmad *et al.*, 2011). In addition, astrocytes modulate expression and polarized localization of endothelial transporters, such as P-glycoprotein (P-gp) or multi-drug resistance protein (MRP) (Berezowski *et al.*, 2004; Al Ahmad *et al.*, 2011) as well as BBB-specific enzyme-systems such as γ-glutamyl transpeptidase (Meyer *et al.*, 1991; Hayashi *et al.*, 1997) and thus crucially regulate EC function.

Major efforts have been made to unravel how astrocytes modulate TJs, transporters and enzyme systems. Astrocytes are known to secrete a large number of substances including peptides, growth factors and chemokines (Nico and Ribatti, 2012) several of which modulate barrier function, such as basic fibroblast growth factor (bFGF), TGF-β1, glial cell-derived neurotrophic factor and src-suppressed C-kinase substrate (SSeCKS) (Igarashi *et al.*, 1999; Sobue *et al.*, 1999; Lee *et al.*, 2003; Reuss *et al.*, 2003; Dohgu *et al.*, 2004; Walshe *et al.*, 2009; Shimizu *et al.*, 2012). For instance, bFGF has demonstrated barrier-tightening effects *in vitro* by reducing barrier permeability (Sobue *et al.*, 1999) and increasing endothelial γ-glutamyl-transpeptidase and alkaline phosphatase activity (Hafny *et al.*, 1996). *In vivo* bFGF knockout increases BBB permeability to albumin and reduces the expression of ZO-1 and occludin, and coincides with reduced astrocyte differentiation (Reuss *et al.*, 2003). The effect of astrocyte-secreted TGF-β1 on barrier function is controversial. While some studies observed reduced BBB permeability and increased TJ expression in the presence of TGF-β1/TGF-β (Dohgu *et al.*, 2004; 2005; Walshe *et al.*, 2009), others reported adverse effects (Shen *et al.*, 2011). This discrepancy may be explained by the fact that TGF-β effects on the endothelium are highly dependent on the endothelial activation state and the tissue environment, especially the ECM as it mediates TGF-β activation (Cambier *et al.*, 2005).

Over the past 20 years, our understanding of the importance of astrocytes as regulators of BBB physiology and how they modulate barrier characteristics has dramatically increased but, realistically, unravelling of the complex pathways has just begun.

Pericytes at the BBB

The origin of CNS pericytes remains unclear with derivation from the mesoderm and neuroectoderm as well as from the monocyte lineage under general discussion (Sa-Pereira *et al.*, 2012). Diverse functions within the brain have been attributed to pericytes including regulation of brain homeostasis, angiogenesis, blood flow, immune and phagocytic activity, as well as being a source of pluripotent stem cells (Sa-Pereira *et al.*, 2012). The effect of pericytes on BBB induction and maintenance is less well characterized than astrocyte-induced responses. During development pericytes fulfil central roles in vessel stabilization through inhibition of EC proliferation

and migration as well as regulation of vessel maturation (Antonelli-Orlidge *et al.*, 1989; Hellström *et al.*, 2001; Al Ahmad *et al.*, 2011; Sa-Pereira *et al.*, 2012). Recent *in vivo* studies using platelet-derived growth factor (PDGF) receptor β (PDGFRβ) knockout mice have significantly improved our understanding. During embryonic angiogenesis, pericytes are recruited to the vessels via EC-derived PDGF-β. The impaired recruitment of pericytes to the brain microvasculature caused by inhibition of PDGF-β signalling, induced either by PDGF-β or PDGFRβ knockout, resulted in severe vascular consequences such as increased vessel diameter, formation of microaneurysms, endothelial hyperplasia and increased vessel permeability (Lindahl *et al.*, 1997; Hellström *et al.*, 2001; Daneman *et al.*, 2010). These alterations in vessel tightness were attributed to enhanced caveolae formation and transcytosis, abnormal TJ alignment and increased expression of permeability inducing factors like VEGF and angiopoietins (ANG) –2 (Hellström *et al.*, 2001; Daneman *et al.*, 2010). Corresponding studies in adult mice revealed that pericytes are also crucial for adult BBB maintenance, as reduced pericytic vessel coverage resulted in increased BBB permeability, altered endothelial gene expression and loss of astrocyte end-feet polarization (Armulik *et al.*, 2010). Age-dependent pericyte loss in PDGFRβ$^{+/-}$ mice elevated parenchymal accumulation of blood proteins and leakage of neurotoxic and vasculotoxic substances into the brain parenchyma and a reduction in the expression of ZO-1 and occludin protein (Bell *et al.*, 2010). *In vitro* studies using cells of human, murine, bovine and porcine origin further underlined the positive effect of pericytes on BBB tightness (Hayashi *et al.*, 2004; Dohgu *et al.*, 2005; Nakagawa *et al.*, 2007; Al Ahmad *et al.*, 2009; Daneman *et al.*, 2010). Similar to astrocytes, pericytes are capable of secreting factors that modulate BBB permeability under normal conditions, like ANG-1 (Hori *et al.*, 2004; Wang *et al.*, 2007), TGF-β1 (Dohgu *et al.*, 2005) and GDNF (Shimizu *et al.*, 2012) that increase ZO-1, claudin-5 or occludin *in vitro* (Hori *et al.*, 2004; Wang *et al.*, 2007; Shimizu *et al.*, 2011). Therefore, similar to astrocytes, pericytes seem capable of modulating TJs. In contrast, a few *in vitro* studies report that co-culture of ECs with pericytes reduces TEER via induction of matrix metalloproteinases (MMP)-2 and -9 activity and activation of VEGF-mediated signalling (Zozulya *et al.*, 2008; Thanabalasundaram *et al.*, 2010). Interestingly, this negative effect of pericytes seems to be dependent on their differentiation state (Thanabalasundaram *et al.*, 2011).

Tricellular interactions – ECs, pericytes, astrocytes

How ECs, astrocytes and pericytes influence each other and concertedly modulate barrier function is a highly interesting but challenging question. Due to the complexity of the BBB *in vivo* data on this topic is limited, but some *in vitro* studies have investigated the effect of simultaneous astrocyte and pericyte co-culture on ECs. The majority of these studies report increased TEER in triple cultures compared with co-culture or monoculture models (Nakagawa *et al.*, 2007; 2009; Al Ahmad *et al.*, 2009); however, decreased TEER in triple cultures due to the presence of pericytes was also reported (Hatherell *et al.*, 2011). Interestingly, only Hatherell *et al.* used human ECs. Importantly, the permeability to sodium-fluorescein, sucrose or 40 kDa FITC-dextran was not significantly altered in triple cultures compared with contact astrocyte co-cultures (Al Ahmad *et al.*, 2009; Nakagawa *et al.*, 2009). Nakagawa *et al.* indeed observed that claudin-5 and ZO-1 protein expression is increased and more restricted to cell–cell borders in triple cultures compared with endothelial monocultures (Nakagawa *et al.*, 2009). Using a novel three-dimensional culture model, our group showed that co-culture of ECs with astrocytes and pericytes also induces polarized, luminal localization of the ABC transporters P-gp and MRP-2 and that astrocytes and pericytes are indispensable for P-gp activity (Al Ahmad *et al.*, 2011). However, it is patently evident that many more studies and wider use of triple culture model systems is invaluable for understanding the multicellular crosstalk at the BBB.

Basement membrane

The BM represents an important but often neglected component of the BBB. Although the BM does not act as a diffusion barrier *per se*, it fulfils important functions for the BBB by providing structural support for the cells by anchoring them in place. Moreover, the BM provides an important platform for mediating signalling events that regulate cell differentiation, proliferation, migration and adhesion (Baeten and Akassoglou, 2011) and thus BBB function. The BM consists of structural matrix proteins that are secreted by the BBB cells with cell-specific differences (a detailed list is presented in Baeten and Akassoglou, 2011). BBB cells are anchored to the BM via ECM receptors, of which the best understood ones are the integrins and dystroglycan (Baeten and Akassoglou, 2011). More than just providing a physical link between the BM and the cells, the matrix receptors represent important modulators of signalling pathways that allow cellular adaptation to environmental changes. Perlecan, the dominating proteoglycan in the endothelial BM (Engelhardt and Sorokin, 2009), has been shown to interact with a number of different growth factors like VEGF, PDGF or TGF-β and retain them in the ECM thereby regulating cellular signal transduction to control cell responses and BBB maintenance (Roberts *et al.*, 2012).

Composition of the BM can also regulate BBB tightness (Tilling *et al.*, 1998). P-gp expression is increased when ECs are cultured on brain-derived ECM (Tatsuta *et al.*, 1994). ECMs derived from pericytes or astrocytes exhibit differential effects on EC impedance *in vitro* compared with controls grown on their endogenous ECMs (Hartmann *et al.*, 2007). Interestingly, ECs cultured on astrocyte-derived ECM displayed a higher resistance than those cultured on pericyte-derived ECM. Astrocyte-derived ECM has been shown to up-regulate the expression of endothelial-specific γ-glutamyl-transpeptidase and activity (Mizuguchi *et al.*, 1994; Hayashi *et al.*, 1997). Several BM-associated proteins have been shown to be important for BBB maintenance *in vivo*. Depletion of perlecan *in vivo* is lethal due to deterioration of brain vesicles and myocardial BM (Baeten and Akassoglou, 2011), whereas specific depletion of perlecan in the endothelial BM results in microvessel bleeding and endothelial dilations (Hallmann *et al.*, 2005). Agrin, another proteoglycan, accumulates at brain microvessels at the time of BBB tightening (Wolburg *et al.*, 2009b) and its depletion results in TJ disruption (Rascher *et al.*, 2002) and depolarization of astrocytic end-feet mainly through redistribution of aquaporin 4 (AQP4;

Wolburg *et al.*, 2009b). Osada *et al.* showed that blocking of β1-integrin using a neutralizing antibody results in altered claudin-5 localization and increased endothelial permeability *in vitro* and *in vivo* (Osada *et al.*, 2011).

Taken together, these data indicate that the BM composition participates in BBB regulation; however, the mechanisms are only poorly understood and need to be better addressed.

Hypoxia and the BBB

Mechanisms of hypoxic BBB disruption

Hypoxia, when the oxygen demand of tissues is not met, acts as an initial trigger for pathophysiological changes at the BBB such as altered distribution of water and ions, inflammatory events and oxidative stress, oedema formation, infiltration of peripheral immune cells and leakage of blood proteins into the brain. In addition, hypoxia induces major alterations in vessel structure as it stimulates proliferation of ECs leading to formation of new blood vessels and furthermore promotes activation and proliferation of astrocytes (reviewed by Ogunshola and Al-Ahmad, 2012; Stanimirovic and Friedman, 2012). A large number of *in vivo* and *in vitro* studies have demonstrated that hypoxia is a major stress factor inducing BBB disruption (Schoch *et al.*, 2002; Kaur *et al.*, 2006; Al Ahmad *et al.*, 2009; Lochhead *et al.*, 2010). Regarding the temporal course of hypoxic barrier opening, detailed *in vivo* studies are rare. Increased BBB permeability to Evans blue was observed in mice 6 h after onset of hypoxia (7% O_2; Li *et al.*, 2011). After 24 and 48 h of hypoxic exposure to 8% O_2, increased BBB leakage to sodium fluorescein was demonstrated in mice (Schoch *et al.*, 2002; Bauer *et al.*, 2010). Another study by Witt and colleagues demonstrated that exposure to 6% O_2 for 1 h with subsequent re-oxygenation in a rat model resulted in a biphasic opening of the BBB within the first hour and again after 6–24 h of re-oxygenation (Witt *et al.*, 2008). For *in vitro* models, a generalized statement about the course of barrier opening is almost impossible due to different culture systems, cell sources, oxygen concentrations and read-outs. However, decreased endothelial tightness has been observed from the first 30 min of hypoxic exposure for up to 48 h (Abbruscato and Davis, 1999a; Fischer *et al.*, 1999; Yamagata *et al.*, 2004; Fleegal *et al.*, 2005; Kuhlmann *et al.*, 2007; Al Ahmad *et al.*, 2009).

The mechanisms of hypoxic barrier disruption have been studied intensively and it is evident that disruption of the BBB occurs on many different molecular levels. TJ complexes are major targets of hypoxic BBB disruption. At the molecular level, hypoxia modulates protein expression levels and subcellular redistribution of occludin, ZO-1 and claudin-5 (Fischer *et al.*, 2002; Mark and Davis, 2002; Koto *et al.*, 2007; Bauer *et al.*, 2010; Willis *et al.*, 2010). The redistribution critically regulates TJ integrity and is probably mediated via phosphorylation changes at serine, threonine and tyrosine residues and by caveolae-mediated endocytosis that determines their localization at the plasma membrane and interaction with other proteins at the TJ (Luissint *et al.*, 2012). PKC enzymes, myosin light chain kinase, and RhoA regulate TJ protein phosphorylation and contribute to hypoxic or inflammatory barrier disruption (for review, refer to Luissint *et al.*, 2012). Increased transcellular and pinocytic activity of brain ECs represent additional events contributing to augmented barrier permeability during hypoxia (Plateel *et al.*, 1997; Cipolla *et al.*, 2004). Hypoxia-mediated alterations and breakdown of the BM also aggravate BBB opening and are particularly important during ischaemic events (Candelario-Jalil *et al.*, 2009; Stanimirovic and Friedman, 2012). Direct and indirect contribution of pericytes and astrocytes to hypoxic-mediated BBB permeability is discussed below.

HIFs as mediators of the hypoxic response

Hypoxia requires an immediate response of the affected tissues/cells to sustain their function and prevent cell death. The most important tasks of the adaptation process are to decrease energy consumption and increase oxygenation. This is mainly achieved through metabolic adaptation and temporal cell cycle arrest as well as induction of angiogenic and erythropoietic genes to increase oxygen delivery to the hypoxic tissues (Wenger *et al.*, 2005). Different signalling pathways are involved in these events including the unfolded protein response, mammalian target of rapamycin signalling, and HIF-mediated gene regulation (Majmundar *et al.*, 2010). HIFs are considered master regulators of the hypoxic response and are heterodimeric transcription factors composed of an oxygen-sensitive α-subunit and a constitutively expressed β-subunit. Under normoxia, the HIFα subunits are constitutively transcribed but constantly targeted for proteasomal degradation through a cascade of hydroxylation of conserved proline residues via prolyl hydroxylases (PHDs), subsequent recognition by the Von Hippel–Lindau (VHL) protein, ubiquitination and degradation by the proteasome. As oxygen tension drops, the PHD enzymes are inhibited and the lack of hydroxylation results in cytoplasmic stabilization of the α-subunits. After phosphorylation, HIFαs translocate to the nucleus and dimerize with ARNT (also known as HIF-β) and co-activators forming a functional HIF transcription factor (Wenger *et al.*, 2005; Fandrey and Gassmann, 2009). By binding to hypoxia-responsive elements in promoter regions, HIFs induce the expression of target genes involved in cellular adaptation to hypoxic stress-regulating erythropoiesis, angiogenesis, proliferation and cellular metabolism (Ogunshola and Al-Ahmad, 2012; see Figure 2).

Three different HIFs have been identified, namely, HIF-1, -2 and -3 of which HIF-1 is the most widely studied. More than 100 HIF-1 target genes are known to date (Semenza, 2003). HIF-1 signalling is considered essential for cellular adaptation and survival during hypoxia. Several HIF-1 target genes are neuroprotective and act as pro-survival factors such as erythropoietin and VEGF. Moreover, HIF-1 signalling regulates the expression of several proteins implicated in glycolysis such as phosphofructokinase or enolase-1 and glucose transporter 1 (GLUT1), thus regulating metabolic adaptation to low oxygenation. Besides its positive effects, HIF-1 also accounts for detrimental effects observed during hypoxia/ischaemia by activation of prodeath genes, such as BNIP3, COX2 or p53 stabilization (reviewed in Singh *et al.*, 2012). At present, it is not clear what determines whether the initiated HIF-1-mediated response is protective or detrimental. However, it is likely that the severity of the insult and its duration, as well as cell type-specific differences and paracrine

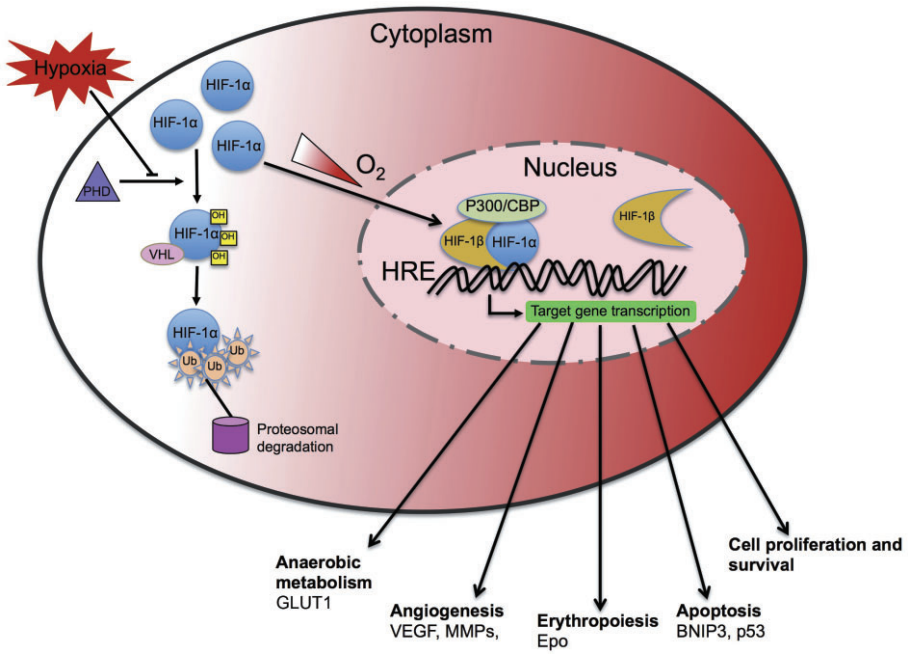

Figure 2

Schematic diagram illustrating the mechanism of HIF-1 regulation under normoxic and hypoxic conditions. HIFs are heterodimeric transcription factors composed of an oxygen-sensitive α-subunit and a constitutively expressed β-subunit. Under normoxia (white gradient), the HIF-1α subunit is constitutively transcribed but constantly targeted degradation through hydroxylation of conserved proline residues by PHDs leading to recognition by VHL protein, ubiquitination and subsequent degradation by proteasome. As oxygen tension drops (red gradient), the PHD enzymes are inhibited and the lack of hydroxylation results in cytoplasmic stabilization of the α-subunits. After phosphorylation, HIF-1α translocates to the nucleus and dimerizes with HIF-1β (also known as ARNT) and co-activators such as p300/CBP forming a functional HIF-1 transcription factor. HIF-1 then binds to hypoxia-responsive elements (HREs) in the promoter regions of its many targets inducing expression of genes involved in cellular adaptation to hypoxic stress by regulating erythropoiesis, angiogenesis, proliferation and cellular metabolism in order to reduce O_2 consumption and increase O_2 delivery to tissues.

signalling play a critical role. Thus, HIF-1 signalling is a key determinant of functional outcome.

HIF-1 regulates BBB permeability

Growing evidence suggests that HIF-1 could play a pivotal role in the changes that occur at the BBB during hypoxia. Good insights have been obtained from cerebral ischaemia and reperfusion studies as well as *in vitro* work (reviewed by Ogunshola and Al-Ahmad, 2012). The HIF-1 inhibitors 2-methoxyestradiol and YC-1 reduce oedema formation (directly correlating to BBB permeability) and infarct volumes after ischaemia or ischaemia reperfusion (Yeh *et al.*, 2007; Chen *et al.*, 2008a), whereas rapid DMOG (dimethyloxalylglycine)-induced HIF-1α stabilization increased oedema formation. In both studies, these effects were attributed to modulation of VEGF production (Chen *et al.*, 2008a). Our own *in vitro* work using brain ECs also suggest that HIF-1 stabilization is directly linked to barrier disruption and that inhibition of HIF-1 can significantly improve barrier stability (Engelhardt *et al.* unpubl. data). Likewise, HIF-1 inhibition using siRNA in a rat focal ischaemia model showed less BBB disruption and a better outcome for the animals and is correlated with decreased VEGF levels, as well as reduction of caspase-3 and p53 expression (Chen *et al.*, 2009). These studies suggest that HIF-1 stabilization is likely to trigger increased BBB permeability through activation of its multiple target genes and signalling cascade.

Contribution of astrocytes and pericytes to hypoxic BBB regulation

The importance of non-neuronal cells in brain diseases associated with hypoxia has long been neglected. The next section discusses the response of BBB cells to hypoxia/ischaemia and their subsequent effect on BBB function.

Astrocytes

Information on the basal responses of astrocytes to reduced oxygenation is limited and far from complete. We know that astrocytes are more resistant to hypoxia and ischaemia than neurons, which is probably due to their higher capacity to metabolically adapt to hypoxia/ischaemia by using alternative energy sources and switching to anaerobic glycolysis thereby ensuring maintenance of the ATP levels (Schmid-Brunclik *et al.*, 2008; Turner and Adamson, 2011). Astrocytes are activated *in vivo* (Kaur *et al.*, 2006) and *in vitro* (Schmid-Brunclik *et al.*, 2008) following hypoxic/ischaemic injury and secrete elevated levels of a large number of factors that can be neurotoxic as well as neuroprotective (reviewed in Trendelenburg and Dirnagl, 2005; Vangeison and Rempe, 2009). Modulation of a variety of proteins suggests a highly

complex tempering of barrier status. Indeed, a microarray study recorded more than 1100 hypoxia-responsive genes in human astrocytes with five times more genes up-regulated than suppressed. Notably, many of the up-regulated genes were glycolytic enzymes and angiogenic molecules (Mense *et al.*, 2006). Astrocytes co-cultured with ECs results in mutual up-regulation and preservation of antioxidant enzymatic activity and reduced radical-induced EC injury (lipid peroxidation) compared with endothelial monocultures (Schroeter *et al.*, 1999; Ogunshola and Al-Ahmad, 2012).

Different *in vitro* studies have shown that astrocyte co-culture or treatment of ECs with ACM improves EC performance and maintenance of barrier function during hypoxic insults (Fischer *et al.*, 2000; Brown *et al.*, 2003; Al Ahmad *et al.*, 2009). Consistent with these observations astrocytes/ACM preserve the junctional localization of TJ proteins, like ZO-1 or claudin-5 (Fischer *et al.*, 2000; Al Ahmad *et al.*, 2011) and hypoxia/glycaemia-dependent down-regulation of the adherens junction protein E-cadherin is partially reversed in the presence of astrocytes (Abbruscato and Davis, 1999b). Media from hypoxic and re-oxygenated astrocytes contain ANG-1 that increases occludin expression and reduces endothelial proliferation thereby stabilizing the vasculature (Song *et al.*, 2002). In addition, co-culture with astrocytes attenuates endothelial caspase-3 activation during hypoxia (Al Ahmad *et al.*, 2009) thereby reducing cell death and caspase-3-mediated TJ disruption (Zehendner *et al.*, 2011).

Astrocytes are the major source of VEGF in the brain and respond to hypoxic stimuli with increased induction and secretion of VEGF that acts as an endothelial survival factor (Chow *et al.*, 2001; Kaur *et al.*, 2006; Mense *et al.*, 2006; Schmid-Brunclik *et al.*, 2008). However, VEGF is also a prominent angiogenic molecule and thus a strong inducer of vascular permeability *in vitro* and *in vivo* (Fischer *et al.*, 1999; Schoch *et al.*, 2002). Our group has shown that despite a beneficial effect of astrocyte co-cultures on hypoxic barrier maintenance, inhibition of VEGF signalling (with the VEGF receptor inhibitor SU1498) further improved maintenance of barrier characteristics (Al Ahmad *et al.*, 2011). In agreement with this result, astrocyte-derived VEGF was also shown to drive BBB disruption after hypoxic exposure (Kaur *et al.*, 2006) and in CNS inflammatory disease (Argaw *et al.*, 2012). Thus, the effect of VEGF secretion during insult is multifaceted. VEGF binds and activates two TK receptors, namely, VEGFR1 (also known as FLT1) and VEGFR2 (also known as KDR or FLK1). Hypoxia-induced endothelial hyperpermeability seems to be mediated predominantly by activation of VEGFR1 (Vogel *et al.*, 2007), in agreement with the finding that hypoxia up-regulates both the expression of VEGFR1 and the binding of VEGF to VEGFR1 (Fischer *et al.*, 1999). Excellent reviews on hypoxia- and HIF-1-mediated VEGF permeability have been published (Fan *et al.*, 2009; Nakayama and Berger, 2013). However, it has also been shown that VEGF splicing in the terminal exon results in variants, termed $VEGF_{xxx}b$ ($VEGF_{165}b$), that act as anti-angiogenic dominant negative splice isoforms (Ladomery *et al.*, 2007; Nowak *et al.*, 2008). Notably, high homology means these anti-angiogenic isoforms may have been mistakenly identified as the more canonical species in many studies. Although the ratio of the b-isoforms to the canonical species could be highly relevant, investigations on the effects of stimuli such as hypoxia on these splice variants are yet to be performed. Astrocytic secretion of MMPs during hypoxia also causes BM reorganization and weakens barrier function. Increased activity of MMP-2, MMP-9 and MMP-13 was detected in hypoxic astrocyte supernatants and treatment of ECs with those supernatants led to MMP-13-dependent delocalization and proteolysis of ZO-1 and disruption of VE-cadherin (Lu *et al.*, 2009).

Astrocytes additionally express various cytokines in response to hypoxic stimulation. For example, IL-1β is a HIF-1 target gene (Zhang *et al.*, 2006) that can activate HIF-1α and VEGF expression in a NFκB-dependent manner in astrocytes and cause down-regulation of the vessel-stabilizing factor SSeCKs (Argaw *et al.*, 2006). Also, large amounts of the monocyte chemoattractant proteins (MCP) MCP-1 and MCP-5 are produced by hypoxic astrocytes in a HIF-1-dependent manner (Mojsilovic-Petrovic *et al.*, 2007). Apart from its main function of recruiting leukocytes at sites of inflammation, MCP-1 was shown to increase the paracellular permeability of endothelial monolayers via TJ redistribution mediated by Rho signalling (Stamatovic *et al.*, 2003) and is involved in formation of vasogenic oedema *in vivo* (Stamatovic *et al.*, 2005). Clearly, hypoxic responses of astrocytes are critical during injury and disease and particularly affect the stability of the BBB.

Pericytes in hypoxic BBB regulation

Only a few studies have investigated the survival of pericytes after hypoxic and ischaemic insults. Our *in vitro* data suggest that pericytes have comparable sensitivity to astrocytes. We did not observe any impairment of mitochondrial activity in pericytes exposed for up to 48 h in 0.2% oxygen reflecting no loss of viability, whereas ischaemic conditions reduced mitochondrial function only after 24 h of exposure (Engelhardt *et al.*, unpubl. obs.). Likewise, it was shown that ECs are much more susceptible to ischaemia than astrocytes and pericytes *in vitro* (Ceruti *et al.*, 2011). *In vivo* pericytes were observed to migrate away from microvessels in response to traumatic brain injury (TBI; Dore-Duffy *et al.*, 2000) and hypoxic stimuli already 2 h after onset of the insult and preceding any changes in vessel structure (Gonul *et al.*, 2002). Furthermore, a reduction of pericyte-to-EC ratio was reported after 1 week of hypobaric hypoxia (Dore-Duffy *et al.*, 2007). Although the cell status during these events remains unclear, the changes occurring during pathologies associated with increased BBB permeability suggest that pericyte loss *per se* could contribute to augmented barrier leakage. Indeed, *in vitro* models have shown that the presence of pericytes protects endothelial monolayers from hypoxic barrier disruption (Hayashi *et al.*, 2004; Al Ahmad *et al.*, 2009), particularly during prolonged and severe oxygen deprivation, by maintaining TJ protein localization and reducing endothelial caspase-3 activation (Al Ahmad *et al.*, 2009; 2011). Interestingly, under severe conditions, co-culture of pericytes with ECs maintained TEER and reduced paracellular flux of labelled substances better than astrocyte co-cultures (Al Ahmad *et al.*, 2009).

Like astrocytes, pericytes respond to hypoxia by up-regulating various growth factors. Park *et al.* demonstrated that in retinal pericytes ANG-1, but not ANG-2, mRNA is significantly elevated (Park *et al.*, 2003) again suggesting a

vessel-stabilizing effect. Interestingly, the induction of ANG-1 could be mimicked through treatment of the pericytes with recombinant VEGF (Park *et al.*, 2003). An *in vivo* study suggested that hypoxic pericytes rapidly increase VEGF levels within 24 h, whereas astrocytic VEGF production was observed after 4 days (Dore-Duffy *et al.*, 2007). In our studies, we observed different outcomes when inhibiting VEGF signalling using SU1498; inhibition was only beneficial in EC pericyte co-cultures during 1% O_2 but not during more severe oxygen deprivation (0.1% O_2; Al Ahmad *et al.*, 2009). Although temporal-spatial VEGF-mediated induction of ANG-1 may be a plausible explanation for some of the barrier-stabilizing effects of pericytes during hypoxia, it is unlikely that elevated VEGF expression does not largely contribute to hypoxic barrier disruption, indeed VEGF signalling by other brain cells may also have an effect. Like astrocytes, pericytes also secrete MMPs and their expression is augmented through pro-inflammatory cytokines like TNF-α (Takata *et al.*, 2011). Additionally, pericytes can induce MMP expression in ECs, although the link between pericyte MMP expression and hypoxic barrier disruption is still to be properly demonstrated. Taken together, however, the data indicate that timing, severity and cellular crosstalk is likely to be very complex.

Overall, despite limited information, similar to astrocytes, pericytes appear to fulfil important barrier-stabilizing functions but in response to stress also secrete molecules that can cause BBB remodelling and increased permeability. Thus, more studies are required to understand the multiple roles of this elusive perivascular cell.

Pathophysiology

Hypoxia-mediated BBB dysfunction is associated with many neurological diseases such as stroke, TBI and Alzheimer's disease (AD) (Ballabh *et al.*, 2004). As discussed earlier, paracrine interactions between brain ECs, astrocytes and pericytes play a crucial role in maintaining the BBB. However, their contribution to various brain diseases by secreting factors that modulate the barrier during injury is frequently overlooked. The next section of this review will focus on direct or indirect influences of hypoxic, and particularly HIF-1-mediated BBB cell-specific responses to progression of select diseases namely stroke, TBI and AD (see Figure 3).

Stroke/cerebral ischaemia

Stroke is a major cause of morbidity and mortality across all industrialized countries. The most commonly occurring type of stroke is ischaemic (Bamford *et al.*, 1990), which accounts for approximately 80% of the total incidences. Ischaemic stroke results from occlusion of a major cerebral artery either by thrombosis or an embolus. In either case, this restricts the delivery of substrates to the tissue, particularly oxygen and glucose, which leads to a cascade of ischaemic events (Dirnagl *et al.*, 1999). Within the core of the ischaemic region, deficits in blood flow, decreased energy stores (ATP levels), metabolic failure and ionic imbalance are severe and cell death progresses within minutes. The region surrounding the compromised area, called the ischaemic penumbra, suffers milder insults and is salvageable if blood flow is restored quickly. However, the reperfusion of ischaemic tissue can also lead to

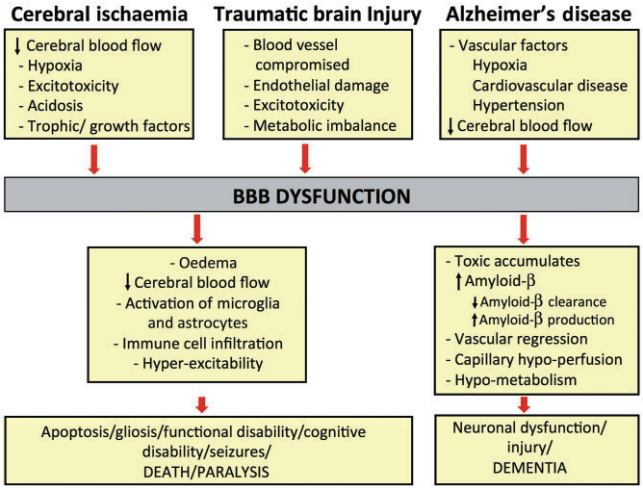

Figure 3

Flow chart of the events leading to BBB disruption and the following events occurring later in stroke, TBI and AD.

secondary damage caused by the rapid re-exposure to oxygen and inflammatory responses in the damaged tissue. Restoration of blood flow also increases the pressure on the damaged ECs and their TJs (Sandoval and Witt, 2008). Additionally, reperfusion results in a fresh supply of leukocytes that translocate into the parenchyma triggering a cascade of cytokine release (Dirnagl *et al.*, 1999). Activated astrocytes and pericytes modulate blood flow, maintain ion homeostasis and contribute to water homeostasis, as well as participate in the inflammatory cascade and release a number of substances that may be either neuroprotective or harmful during ischaemia. This wide variety of responses results in a number of effects including loss of TJ expression and localization, increase in permeability, degradation of BM, loss of integrins, oedema and further inflammation (Sandoval and Witt, 2008; Kwon *et al.*, 2009), all of which contribute to BBB disruption (see Figure 3). Although the trigger for the pathological changes is hard to establish they are probably interdependent. Cerebral ischaemia induced by transient occlusion of middle cerebral artery evokes a marked biphasic opening of the BBB. Early opening of the BBB takes place within the first half hour of reperfusion and is followed by partial closing. This initial acute opening is described as a 'haemodynamic' BBB opening resulting in cytotoxic oedema (reviewed by Nagy *et al.*, 1979; Kuroiwa *et al.*, 1985). Subsequently, a second delayed, but progressive, opening occurs between 24 and 48 h post-reperfusion and results in vasogenic oedema (Huang *et al.*, 1999). Notably, taking advantage of this later progressive BBB opening may aid the delivery of low permeability neuroprotective therapeutic agents.

Brain ECs maintain impermeability of the BBB largely through their TJs. Notably, ZO-1 and occludin expression were reduced in a microsphere-induced cerebral embolism model of cerebral ischaemia (Kago *et al.*, 2003). Although not many studies have evaluated TJ changes post-ischaemia, some reports have demonstrated changes in BBB cell contacts partly due to BM degradation. Astrocyte end-feet are well known to swell post-ischaemia (Kimelberg, 2005) and degra-

dation of BM also causes their detachment from the vessel wall leading to increased permeability (Kwon *et al.*, 2009). In addition to swelling, surviving astrocytes in the vicinity of the ischaemic damage also undergo a process of hypertrophy referred to as reactive astrogliosis. Similarly, pericytes have also been shown to migrate away from vessels in animal models of ischaemia by breaking through the BM that ensheaths them (Dore-Duffy *et al.*, 2000; Melgar *et al.*, 2006). This indicates that in addition to changes in BBB permeability induced by TJ alterations, contact with BBB-supportive cells is also modified and probably enhances BBB disruption. It is reported that ischaemia followed by reperfusion in rats results in BBB disruption and breakdown of BM collagen IV (Hamann *et al.*, 2002; Scholler *et al.*, 2007). Likewise, ischaemic/reperfusion injury also results in a decrease in laminin and fibronectin (Hamann *et al.*, 1995). Other BM proteins, such as agrin and perlecan are also degraded after ischaemia (Fukuda *et al.*, 2004; Baumann *et al.*, 2009). Fukuda and group were the first to provide direct evidence that active proteases, which are known to degrade the BM are generated in ischaemic cerebral tissue (Fukuda *et al.*, 2004). The most widely studied proteases, MMPs, are released by astrocytes (Zhang *et al.*, 2004) and microglia (Del Zoppo *et al.*, 2007) post-ischaemic injury. MMP-9 and -2, in particular, are major contributors of ischaemic pathology. Many groups have demonstrated the detrimental role of MMP-9 in ischaemic models by using inhibitors of MMP-9 or MMP-9 knockout animals and reported reduction in BBB damage, brain water content, infarct size and neurological deficit (Romanic *et al.*, 1998; Asahi *et al.*, 2001; Jiang *et al.*, 2001; Park *et al.*, 2009; Cui *et al.*, 2012). Therefore, inhibiting MMPs may be highly beneficial for treating cerebral ischaemia, as reviewed elsewhere (Cunningham *et al.*, 2005; Morancho *et al.*, 2010).

BBB disruption after ischaemia increases permeability to macromolecules allowing fluid movement from intravascular to extravascular spaces and leading to vasogenic oedema (Sandoval and Witt, 2008). Aquaporins (AQPs) are highly permeable water channels that play a crucial role in fluid balance. AQP4 in particular participates in the maintenance of brain water homeostasis and is highly concentrated on astrocyte end-feet (Nielsen *et al.*, 1997). The role of AQP4 has been explored in various models of ischaemic stroke where it contributes to the formation of cerebral oedema. In disease models, such as acute cerebral ischaemia and water intoxication (Manley *et al.*, 2000), water moves into the cell resulting in cytotoxic brain oedema. Deletion of AQP4 was shown to prevent cellular water uptake in these models, as demonstrated by reduced brain water content, lower intracranial pressure values, infarct size and lesion volume (Manley *et al.*, 2000; Zeng *et al.*, 2012). In chronic ischaemia or TBI models that result in vasogenic oedema due to BBB disruption, deletion of AQP4 exacerbated cerebral oedema formation assessed by water content measurements and intracranial pressure (Papadopoulos *et al.*, 2004). Based on these findings it can be concluded that AQP4 plays a differential role in modulating brain water homeostasis and is dependent on the duration and type of insult.

VEGF, one of the most important factors induced by hypoxia, performs a major role in driving BBB disruption leading to oedema formation in the acute phase following ischaemia (Zhang *et al.*, 2000; Chi *et al.*, 2007; 2008). Elevated VEGF expression appears as early as 1 h after the onset of cerebral ischaemia (Abumiya *et al.*, 1999; Plate *et al.*, 1999b). Indeed, early administration of VEGF increases BBB permeability, increases infarct size and worsens neurological outcome following an ischaemic insult (Zhang *et al.*, 2000). Similarly, inhibition of endogenous VEGF in the acute phase reduces BBB permeability (Mayhan, 1999; Valable *et al.*, 2005; Yeh *et al.*, 2007). This is in line with findings that suggest VEGF is not only an angiogenic factor but also a permeability factor (Plate, 1999a). Apart from its role at the vasculature, there are several studies that have also examined the effect of VEGF on cerebral infarct size. Van Bruggen *et al.* reported that antagonism of VEGF reduces ischaemia reperfusion-related brain oedema and injury in mice (van Bruggen *et al.*, 1999). Similarly, VEGF administered i.v. increased infarct size when given early after ischaemia in rats but, in contrast, improved neurological function when given at later stages 2 days post-ischaemia (Zhang *et al.*, 2000). These studies suggest that despite enhancing angiogenesis and reducing neurological deficits during late-stage stroke recovery, inhibition of VEGF at the acute stage of injury may reduce BBB compromise. The negative side of VEGF could perhaps be achieved partly by counteracting its permeabilizing effect in the acute phase of ischaemia. Indeed, systemic adenoviral gene delivery of ANG-1, a known anti-permeability factor that maintains and stabilizes mature vessels by promoting interaction between ECs and surrounding support cells (Hori *et al.*, 2004), causes resistance to vascular leakage induced by VEGF in the brain after cerebral ischaemia (Zhang *et al.*, 2002). Conversely, ANG-2 that leads to de-stabilization of vessels and dissociation of pericytes, is up-regulated by hypoxia and cytokines including VEGF (Mandriota and Pepper, 1998; Valable *et al.*, 2005). Thus, the co-ordination of VEGF and the ANG is crucial for maintaining the integrity of existing vessels and modulating growing vessels for better outcome following ischaemia.

In summary, the exact mechanisms causing brain vascular disruption are hard to establish but factors like VEGF and MMPs released from BBB-supportive cells are likely to play an instrumental role. Further confirmation of these conclusions using cell-specific conditional knockout animal experiments is necessary for better understanding of the role of these cells at the BBB post-ischaemia.

Traumatic brain injury

TBI results from an outside force causing instant mechanical disruption of brain tissue and delayed pathogenic events that collectively mediate widespread neurodegeneration (reviewed by Gaetz, 2004). Subsequently, the traumatized brain is highly susceptible to secondary brain injuries, which can be caused by hypoxia (Hellewell *et al.*, 2010) and seizures (Bao *et al.*, 2011). Reports from animal model studies and significant clinical data both suggest a central role for vascular integrity in TBI outcome, especially BBB breakdown which can last from minutes to several days to weeks, or even years after the acute event (Unterberg *et al.*, 2004; Hawkins and Davis, 2005; Abbott *et al.*, 2006; Tomkins *et al.*, 2008). This kind of disruption might also influence the progression of long-term TBI complications, such as AD, which include delayed neuronal dysfunction and cell death (see Figure 3).

Studies of animal models of TBI have also demonstrated a biphasic increase in BBB permeability to albumin and other high molecular weight proteins peaking at 4 to 6 h as well as 2–3 days after injury (Başkaya *et al.*, 1997; Hicks *et al.*, 1997). The first peak in BBB permeability generally overlaps with increased production of a number of secretory factors that include chemokines, cytokines, MMPs and VEGF, which contribute to BBB dysfunction and also invasion of neutrophils. A thorough review on molecular pathogenesis of BBB breakdown in TBI has been recently published (Nag *et al.*, 2011).

Chemokines not only play a key role in post-traumatic recruitment of leukocytes, but may also modify the permeability of the BBB. After injury recruitment of leukocytes into the brain parenchyma releases a number of inflammatory cytokines that worsen the outcome of the disease state. For example, as stated earlier MCP-1 is up-regulated post-hypoxia and very recently, Semple *et al*. reported its important role in reducing lesion size and secondary damage and improving functional outcome in mice following TBI (Semple *et al.*, 2010). This improvement may be attributed to decreased leukocyte accumulation resulting in an environment more advantageous for neuronal survival. Increased levels of cytokines are correlated to poorer clinical outcomes. TNF-α mRNA and protein is elevated acutely after experimental TBI (Bermpohl *et al.*, 2007) as well as in clinical settings (Csuka *et al.*, 1999) and is known to exacerbate BBB disruption post-TBI (Bermpohl *et al.*, 2007). Similarly, a rapid increase of IL-1β is observed early enough after experimental TBI (Wang and Shuaib, 2002). Patel *et al.*, using intracerebral or intraventricular administration of exogenous IL-1β, demonstrated significant exacerbation of injury (Patel *et al.*, 2003). In addition, transgenic mice, in which the IL-1β is overexpressed in astrocytes alone, were observed to have a leaky BBB (Shaftel *et al.*, 2007). Thus, BBB dysfunction mediated via cytokines released from BBB cells can worsen injury outcome in the acute stages and may be hypoxia-dependent. In contrast, the mechanisms involved in the delayed (second phase) opening of the BBB are presently unclear and require further investigation.

Although the role of VEGF and its receptors has been studied extensively in ischaemia over the last years, only a few groups have performed studies elucidating the role of this molecule post-TBI. Using different models of TBI, it was reported that astrocytes as well as inflammatory cells react to injury by increasing VEGF expression (Papavassiliou *et al.*, 1997; Sköld *et al.*, 2002). In contrast, pericytes were shown to undergo cell death post-TBI using TUNEL assay (Dore-Duffy *et al.*, 2007). Morgan *et al*. demonstrated a substantial increase in angiogenesis, based on BrdU-positive nuclei within the endothelium post-TBI via increased expression of VEGF and its receptor (Morgan *et al.*, 2007). This induction of angiogenesis could be mediated by the up-regulation of astrocytic VEGF, which in turn increases both astrocyte proliferation and facilitates the expression of other growth factors, which support late-stage recovery (Krum *et al.*, 2008). Corticosteroids that are usually used for treating early vasogenic oedema after acute BBB compromise have been demonstrated to stabilize the BBB by decreasing the expression of VEGF (Kim *et al.*, 2008). Again, the data suggest that during disease early VEGF release from glial cells can be harmful to BBB function and further worsen the outcome post-TBI. Similarly, MMPs, in particular MMP-2, MMP-3 and MMP-9, are up-regulated following TBI (Shigemori *et al.*, 2006; Vilalta *et al.*, 2008; Hayashi *et al.*, 2010). As found in cerebral ischaemia, genetic deletion of MMP-9 or pharmacological inhibition of the activity of MMPs using TIMPs significantly reduced the extent of tissue damage and improved functional outcome in murine models of TBI (Wang *et al.*, 2000). In addition, mice overexpressing the human TIMP1 gene subjected to TBI showed reduced levels of MMP-9 synthesis and a less leaky vasculature accompanied by decreased brain tissue damage compared with control animals (Tejima *et al.*, 2009). All these observations indicate that secretion of VEGF and MMPs by BBB cells could indeed represent a potential target for pharmacological intervention in TBI and ischaemia. Nonetheless, it should be emphasized that as these factors also play an important role in the repair process at later stages, delayed inhibition of their activity may actually have adverse therapeutic effects (Nag *et al.*, 1997; Zhao *et al.*, 2006).

AQP4 expression is markedly modified in both experimental and clinical TBI (Manley *et al.*, 2000; Papadopoulos and Verkman, 2007; Tang *et al.*, 2010; Fukuda and Badaut, 2012). Initial studies implied that induction of AQPs in a model of TBI promoted oedema formation (Manley *et al.*, 2000) and that therapeutic inhibition of AQP4 could be beneficial in controlling oedema (Taya *et al.*, 2008). Indeed, Fukuda *et al*. used siRNA against AQP4 to demonstrate improvements that were associated with decreased oedema formation, increased microglial activation and decreased BBB disruption post-TBI (Fukuda *et al.*, 2013). However, it subsequently became apparent that the modifications in AQP4 expression are dependent on the type of oedema and its regional distinction (Sun *et al.*, 2003; Papadopoulos *et al.*, 2004). For instance, in an ischaemic model that results in cytotoxic oedema, inhibition of AQP4 expression was associated with decreased oedema, reduced infarct area and an improvement in functional outcome (Fazzina *et al.*, 2010). In contrast, in a cold lesion injury model of vasogenic brain oedema, AQP4-deficient mice had a markedly worse clinical outcome (Papadopoulos *et al.*, 2004). These findings suggest that AQP4 is mainly essential for the clearance of vasogenic oedema but its other effects depend on the type of injury and the time point being measured.

Finally, BBB disruption also triggers a chain of events that not only affects vascular cells but also neuronal cells by causing epilepsy (Tomkins *et al.*, 2007; 2008). This theory seems plausible since the studies cited suggest that damage to the microvasculature might result in the extravasation of serum proteins such as albumin, which leads to the activation of astrocytes as the first step in the epileptogenic process. This interaction suggests a key functional role of activated astrocytes in neuronal excitability. Hardly any work has been performed on the specific role of pericytes in TBI, although endothelin-1-induced pericyte-mediated vasoconstriction was recently reported (Dore-Duffy *et al.*, 2011). Many more studies on cell-specific responses to TBI are surely warranted.

Alzheimer's disease

AD is a progressive and irreversible neurodegenerative disorder characterized by the accumulation of amyloid β-peptide (Aβ) in the CNS, the presence of hyper-phosphorylated tau

filaments and cerebrovascular changes that lead to cerebral amyloid angiopathy (Greenberg *et al.*, 2004). AD is another neurodegenerative disease that is characterized by hypoxia, a state that is believed to only aggravate disease progression (Ogunshola and Antoniou, 2009; Peers *et al.*, 2009; Figure 3).

At present, the cellular and molecular basis by which systemic hypoxia influences AD are not completely understood. However, the emerging evidence indicates that prolonged hypoxia induces formation of Aβ that accumulates over years and probably contributes to vascular alterations (Selkoe, 2001). Hypoxia induces Aβ processing through mechanisms that increase the activity of two enzymes crucial for Aβ formation, β-secretase and γ-secretase (Sun *et al.*, 2006; Zhang *et al.*, 2007; Li *et al.*, 2009). HIF-1α mediates a transcriptional increase in β-secretase expression (Zhang *et al.*, 2007) and presenilin-1 levels – presenilin being the major protein of the γ-secretase complex (Pluta, 2007). In addition, hypoxia also promotes down-regulation of neprilysin, an Aβ-degrading enzyme (Nalivaevaa *et al.*, 2004), which can lead to alterations in the expression of vascular-specific genes in brain ECs (Wu *et al.*, 2005). All of these effects can be considered pro-amyloidogenic, that is, would predispose to increased Aβ levels either through increased production or reduced degradation. Recently, Wilcock and colleagues used a transgenic mouse model to demonstrate that during progression of an AD-related pathology the numbers of astrocytic processes in apparent contact with cerebral vasculature were reduced. Furthermore, amyloid accumulation caused significant reductions in AQP4 and potassium channels associated with cerebral vessels in both the mouse model and individuals with AD (Wilcock *et al.*, 2009). This observation seems to agree with studies performed in cerebral ischaemia or TBI models during the vasogenic phase suggesting that the presence of AQP4 is beneficial for functional outcome. Clearly, AQ4 plays a significant role in controlling brain water homeostasis; however, many more studies are required to define how its modulation will affect functional outcome of disease progression in different pathologies. An excellent review on aquaporins and AD has been published (Foglio and Rodella, 2010). Emerging evidence suggests that the Aβ accumulation that causes vascular alterations ultimately leads to hypo-perfusion (Sagare *et al.*, 2012). Pericytes could probably influence this hypo-perfusion in conditions of severe ischaemia and oxidative stress, as they contract not only during the hypoxic insult but remain contracted even after reperfusion (Yemisci *et al.*, 2009). Hypoxia also promotes phosphorylation of tau through the MAPK pathway (Fang *et al.*, 2010). Tau is a microtubule-associated protein that plays a major role in stabilizing microtubules, found mainly in neurons but has also been shown in low levels in astrocytes (Lee *et al.*, 2001). Aβ and/or hypo-perfusion can induce hyperphosphorylation of tau, leading to the protein structural changes found in AD patients, which affects its binding with tubulin and causes destabilization of the cytoskeleton (Michaelis *et al.*, 2002). This leads to formation of neurofibrillary tangles and suggests that tau pathology develops secondary to Aβ injury and can be modulated via hypoxia-mediated signalling.

Alterations in vascular permeability and BBB disruption are detected in the brains of AD patients (Claudio, 1996). However, deposition of Aβ aggregates in cerebrovasculature and the brain is less understood and the mechanisms that cause changes in permeability are not clear. The BBB regulates the entry of plasma-derived Aβ into the brain and clears brain-derived Aβ through the receptor for advanced glycation end-products (RAGE) and low-density lipoprotein receptor-related protein respectively (Shibata *et al.*, 2000; Deane *et al.*, 2003). Previous reports showed increased levels of free Aβ in plasma of AD patients or mouse models (Kawarabayashi *et al.*, 2001; Zhou *et al.*, 2012). Through these studies, one can speculate that Aβ may disrupt the TJs of BBB via interaction with RAGE as a specific mediator. In agreement with this hypothesis, a recent study performed by Kook *et al.* using cultured ECs showed Aβ-induced structural alterations and reduction in protein levels of ZO-1 as well as increased permeability. Furthermore, a neutralizing antibody against the extracellular domain of RAGE effectively blocked Aβ-induced alterations in ZO-1 distribution suggesting that Aβ–RAGE interactions are critical for TJ integrity (Kook *et al.*, 2012). It is well known that calcium influx is induced by Aβ in the cells (Kawahara *et al.*, 2000) and increased intracellular calcium also leads to TJ alterations as well as inducing MMP expression (Stuart *et al.*, 1996; Rosenberg, 2009; Kook *et al.*, 2012). Thus, MMP activation could further accelerate degradation of the BM as observed post-ischaemia and worsen the outcome of AD.

Thus, although the amyloid hypothesis for the pathogenesis of AD suggests this peptide initiates a cascade of events leading to neuronal injury and loss and eventually dementia, from the studies mentioned above, vascular alteration may significantly contribute to the disease as well. Recently, Zlokovic presented an alternative, two-step vascular hypothesis as discussed in the review (Zlokovic, 2011). The hypothesis suggests that in the first step, the primary damage to brain vasculature initiates a non-amyloidogenic pathway of neuronal dysfunction and injury, which is mediated by BBB dysfunction. This is correlated with leakage and secretion of multiple toxic molecules and/or reduced blood flow, which causes multiple focal ischaemic or hypoxic injuries. In the second step, BBB dysfunction also leads to increased Aβ generation and impairment of Aβ clearance. Both these processes contribute to accumulation of Aβ species in the brain and toxicity. It is clear from this hypothesis that phenomena like vascular regression and hypo-metabolism occur secondary to vascular and/or Aβ injury but also that BBB alterations probably make a sizeable contribution to disease progression. Temporal-spatial BBB disruption in senescence-accelerated mouse prone 8 mice, considered by some researchers as a model of AD, was recently reported (Del Valle *et al.*, 2009). However, the role of the perivascular cells, astrocytes and pericytes, and the mechanisms that caused the changes in permeability are not clear and require further investigation.

Vascular regression is a phenomenon observed in AD patients (Zlokovic, 2005; Grammas, 2011) as well as in APP transgenic mice – a model for late-stage AD (Paris *et al.*, 2004). For example, reduction in brain capillary length in the hippocampus correlated well with increased clinical dementia rating scores in AD patients (Bouras *et al.*, 2006). The reason for this phenomenon is unclear but could be explained partly by the anti-angiogenic activity of Aβ (Thomas *et al.*, 1996). Aβ counteracts the pro-angiogenic effects of VEGF and bFGF in ECs by sequestering VEGF in the plaques (Yang *et al.*, 2004).

Reduced angiogenic effects in AD are also caused by TGF-β1 (Tesseur and Wyss-Coray, 2006). Transgenic overexpression of TGF-β1 in astrocytes stimulates Aβ deposition in brain vessels, along with alterations in regional cerebral blood flow and AD-like vascular degeneration and brain metabolic activity. Furthermore, elevated levels of TGF-β1 in human AD correlate with increased Aβ deposition in brain vessels (Wyss-Coray *et al.*, 2001). However, it is noteworthy that TGF-β1 can also be neuroprotective and promote Aβ clearance as shown in microglia (Wyss-Coray *et al.*, 2001). These findings raise an interesting question of whether vascular regression and/or degeneration in AD results from unsuccessful vascular repair and/or remodelling.

Another phenomenon that occurs during AD progression that may be modulated by BBB cells is hypo-metabolism. Neurons are incapable of synthesizing or storing glucose and are dependent on glucose transport across the BBB, a process that is mediated by glucose transporters (GLUTs). GLUT1 is also located on cerebrovascular ECs and astrocytes (Vannucci *et al.*, 1997). In AD, dysfunctional cerebral ECs express less GLUT1 as well as HIF-1, a major regulator of GLUT1, thereby reducing glucose uptake in the brain (Liu *et al.*, 2008). Furthermore, studies using 18F-fluorodeoxyglucose PET have identified reductions in glucose uptake in individuals with a high risk of dementia (Herholz, 2010). Decreased glucose uptake across the BBB, as seen by PET, may also precede brain atrophy (Herholz, 2010). This suggests that hypo-metabolism due to BBB dysfunction is a contributing factor for disease progression and occurs at a later stage after vascular and/or Aβ injury. Whether swelling and retraction of astrocyte endfeet inhibits glucose transport to neurons and thereby facilitates neuronal hypo-metabolism needs further study.

It is clear that many more studies are needed to fully understand the effect of hypoxia-mediated changes on neurodegenerative pathologies with respect to BBB function and contribution of astrocytes and pericytes. And the question remains, are we missing important mechanistic roles of the BBB under pathophysiological conditions by studying the nervous system in isolation from the influence of the vascular system? The likely answer is yes. Thus, more research based on the BBB and the NVU as a whole is warranted to provide important insights in the future.

Pharmacology

HIF modulators as therapeutic targets

The important role for HIF-1 in the mediation of the adaptive processes to hypoxia means that it could potentially represent an important target to prevent cellular damage during disease progression. Targeting HIF-1 now represents a potential therapeutic strategy in numerous physiological including myocardial ischaemia and cerebrovascular diseases. In this regard, a wide variety of PHD inhibitors that cause stabilization of HIF-1 have been developed as erythropoiesis stimulating agents and neuroprotective drugs. Additionally, activity relating to development of HIF-1 inhibitors to prevent solid tumour angiogenesis has also exponentially increased in the last years but may also be useful to prevent BBB alterations during injury conditions. Some promising advances in these areas are discussed below.

HIF stabilizers

The therapeutic potential of development and use of small molecule HIF stabilizers to improve cell survival after injury is gaining popularity in many different fields. In particular PHDs, the enzymes that regulate HIF-1 stabilization, are now being recognized as important targets for future medical intervention. PHD enzymes require iron and 2-oxyglutarate (2-OG) in order to catalyse HIF prolyl hydroxylation (Jaakkola *et al.*, 2001). hus iron chelators and competitive inhibitors impair the activity of PHD enzymes and other iron-dependent enzymes. deferoxamine, an iron chelator, and cobalt chloride ($CoCl_2$), a competitive inhibitor of iron, are routinely used both *in vitro* and *in vivo* to inhibit PHD enzyme activity and thus stabilize HIF. Both seem to be protective in preconditioning preclinical models of cerebral ischaemia (Prass *et al.*, 2002; Siddiq *et al.*, 2005; Aminova *et al.*, 2008; Jones *et al.*, 2008). Indeed, *in vivo* high concentrations of iron, stored in the cytoplasmic protein ferritin, are released during ischaemia (Harten *et al.*, 2010) and could lead to radical-mediated damage of cellular components (Sorond and Ratan, 2000). Thus, sequestration of iron in general may be beneficial in certain injuries as well as making a major contribution to the neuroprotective action of iron chelators such as $CoCl_2$. The 2-OG analogues L-mimosine, DMOG and 3,4-dihydroxybenzoate can also be used to inhibit PHD enzymes (reviewed by Harten *et al.*, 2010). Some small-molecule activators have also been identified. A potent and effective activator of the HIF pathway is tilorone. Tilorone appears to be able to cross the BBB, stabilize HIF-1α protein and confer significant resistance to stroke and spinal cord injury by an as yet unknown mechanism (Ratan *et al.*, 2008). However, as its use is associated with the accumulation glycosaminoglycans, its future use in humans is debatable (Harten *et al.*, 2010). Finally, the race is on for development of novel PHD inhibitors, particularly for the treatment of ischaemic diseases such as stroke, and a number of compounds has been developed by Fibrogen (reviewed by Harten *et al.*, 2010). A selection of the most promising PHD inhibitors currently being considered for therapeutic strategies has recently been reviewed (Nagel *et al.*, 2010; Karuppagounder and Ratan, 2012). However, it must be emphasized that, although HIF stabilizers mimic the neuroprotective effects of preconditioning in both *in vitro* and *in vivo* ischaemic models, the use of PHD inhibition as a post-injury treatment remains somewhat controversial. In mice, post-ischaemic PHD inhibition offered less protection than pre-ischaemic treatments (Baranova *et al.*, 2007) and early activation of HIF-1α using DMOG accentuated brain oedema and BBB disruption compared with ischaemia alone (Chen *et al.*, 2008b). Importantly, in both cases, these effects were attributed to increased VEGF levels with astrocytes being the most likely culprits (Vangeison *et al.*, 2008).

HIF inhibitors

Although identification of agents that specifically increase hydroxylation activity of PHDs – and thus HIF-1 degradation – is relatively unexplored, the fact that HIF-1 induction is closely linked to BBB permeability means putative inhibitors may have a relevant application preventing barrier changes associated with hypoxic and/or ischaemic-induced injury progression. Indeed, in the cancer field, targeting of HIF-1 in

hypoxic cells is an attractive therapeutic strategy that is already being actively pursued, since HIF-1 is tightly linked to the metastatic potential of many tumours, treatment resistance and poor prognosis (Hu *et al.*, 2012; Meijer *et al.*, 2012; Xia *et al.*, 2012). To date, a number of molecules that inhibit the HIF-1 pathway have been identified predominantly using cell-based screening systems and research of HIF-1 activity in cancer cell lines. Supraphysiological supplementation of iron and ascorbate enhances PHD activity and results in HIF-1 degradation (Harten *et al.*, 2010) and has already been used in the clinics. In addition, both are considered relatively safe, inexpensive and readily available. 2-OG and its derivatives, the rate-limiting co-substrate for PHDs, stimulate PHD activity and reduce basal HIF-1α protein levels suggesting they may also have a therapeutic role (Ban *et al.*, 2011). Moreover, targeted screening recently identified a compound, KRH102053, as a PHD2 activator and showed it reduced levels of HIF-1 and its downstream target genes, leading to inhibition of hypoxia-induced responses including metastasis and glucose metabolism *in vitro* (Choi *et al.*, 2008). A number of other inhibitors have also been developed – for excellent overviews of putative HIF-1 inhibitors in development as well as clinical and preclinical trials see Ban *et al.* (2011); Xia *et al.* (2012). Although various small molecules have been developed as HIF-1 inhibitors, the mechanisms by which they work are still unclear in many cases. The fact that none of them seem to exclusively target HIF-1α signalling suggests they can also have multiple off-target effects. Perhaps an exception is EZN-2968, an RNA antagonist that targets HIF-1α mRNA and thereby directly inhibits HIF-1α expression (Greenberger *et al.*, 2008). Tumour reduction was found in nude mice implanted with DU145 human prostate cancer cells treated with EZN-2968 and a phase I clinical study in patients with advanced malignancies revealed that EZN-2968 was well tolerated (Ban *et al.*, 2011). EZN-2968 is currently discussed as the best potential for specific HIF-1α inhibition and promising results of the clinical studies are expected (Ban *et al.*, 2011).

In conclusion, the future looks bright for the use of HIF inhibitors as therapeutics, but overall, it is apparent that future design of more specific agents is required for better drugs to be developed. Perhaps such drugs will also be useful to prevent BBB disruption particularly during the acute phase after injury in the future.

Targeted BBB cell-specific treatment

The major focus of therapeutic targets has always been neuronal mechanisms of injury. Notably, attention to dysfunction or loss of non-neuronal cell types, that is, the cells that maintain the neuronal homeostatic environment, are avenues not well explored even though they may significantly increase the chances of success. As discussed above, HIF stabilization, and/or PHD inhibition, compromises barrier stability and as such targeting HIF-1 may be a way to maintain barrier stability during injury. Using therapeutic targets that activate a broad programme of genes in different cell types, as discussed above, may stimulate biological effects better than the separate application of growth factors or other repair proteins (reviewed by (Ratan *et al.*, 2007), especially in this case as an endogenous programme of adaptation is augmented. However, the wide range of HIF targets could have the caveat that modulation of multiple processes could potentially have a negative outcome on whole body physiology. For example, clinical syndromes associated with excessive activation of the HIF pathway exist (Gassmann *et al.*, 2003) and whereas some studies indicate that HIF-1 is neuroprotective, others demonstrate negative outcomes. Clearly, the effects on the NVU in particular must be better understood to ascertain the general widespread application of such therapeutics. Since different cell types of the BBB and CNS show diverse and sometimes opposing responses to HIF-1 modulation, targeting the pathway in a cell-specific manner will circumvent adverse side effects that can be expected of general HIF-1 modulators. Cell-specific therapeutics (e.g. endothelial-, astrocyte- or pericyte-specific drugs) may also result in more efficacious treatment and better tailoring to the injury in question. Targeting and augmenting vascular EC function directly will provide the significant advantage that such drugs would not be required to cross the BBB, that is, be easier targets than current neuron-directed research. Thus, detailed knowledge of cell-specific responses during injury is required to support development of more specific therapeutic agents. Additionally, in-depth knowledge of the side effects of long-term or high-dose treatments must be well defined prior to their clinical implementation. It must also be emphasized that the consequence of increased levels of HIF-1 in different cell types is highly divergent and dependent on the type of injury. Indeed, it is now becoming clear that the PHDs may also have specific endogenous substrates as well as divergent cell-specific roles (Smirnova *et al.*, 2012). Thus, an additional challenge will be whether development of isoform-specific inhibitors will be more efficacious and safe than a more global approach. Clearly, BBB cell-specific responses and their contribution to injury progression are instrumental factors that need to be carefully considered, and the balance of HIF-1 neuroprotective effects with the putative negative outcome on BBB function must be weighed before implementing any treatment strategy.

Conclusion

Overall, hypoxia and HIF-1 significantly contribute to BBB dysfunction in various neurological diseases. The influence of BBB cell specificity to outcome remains very unclear but deserves significantly more investigation since this knowledge will enable development of more effective therapeutic strategies to combat disease progression. Clearly, balancing HIF-1 beneficial and deleterious effects with cell-specific responses, disease profiles, and windows of opportunity will be very difficult.

Conflict of interest

No conflict of interest.

References

Abbott NJ (2002). Astrocyte-endothelial interactions and blood-brain barrier permeability. J Anat 200: 629–638.

Abbott NJ, Ronnback L, Hansson E (2006). Astrocyte-endothelial interactions at the blood-brain barrier. Nat Rev Neurosci 7: 41–53.

Abbott NJ, Patabendige AAK, Dolman DEM, Yusof SR, Begley DJ (2010). Structure and function of the blood-brain barrier. Neurobiol Dis 37: 13–25.

Abbruscato TJ, Davis TP (1999a). Combination of hypoxia/aglycemia compromises in vitro blood-brain barrier integrity. J Pharmacol Exp Ther 289: 668–675.

Abbruscato TJ, Davis TP (1999b). Protein expression of brain endothelial cell E-cadherin after hypoxia/aglycemia: influence of astrocyte contact. Brain Res 842: 277–286.

Abumiya T, Lucero J, Heo JH, Tagaya M, Koziol JA, Copeland BR *et al.* (1999). Activated microvessels express vascular endothelial growth factor and integrin alpha(v)beta3 during focal cerebral ischemia. J Cereb Blood Flow Metab 19: 1038–1050.

Al Ahmad A, Gassmann M, Ogunshola OO (2009). Maintaining blood-brain barrier integrity: pericytes perform better than astrocytes during prolonged oxygen deprivation. J Cell Physiol 218: 612–622.

Al Ahmad A, Taboada CB, Gassmann M, Ogunshola OO (2011). Astrocytes and pericytes differentially modulate blood-brain barrier characteristics during development and hypoxic insult. J Cereb Blood Flow Metab 31: 693–705.

Allen NJ, Barres BA (2009). Neuroscience: glia –more than just brain glue. Nature 457: 675–677.

Aminova LR, Siddiq A, Ratan RR (2008). Antioxidants, HIF prolyl hydroxylase inhibitors or short interfering RNAs to BNIP3 or PUMA, can prevent prodeath effects of the transcriptional activator, HIF-1alpha, in a mouse hippocampal neuronal line. Antioxid Redox Signal 10: 1989–1998.

Antonelli-Orlidge A, Saunders KB, Smith SR, D'Amore PA (1989). An activated form of transforming growth factor beta is produced by cocultures of endothelial cells and pericytes. Proc Natl Acad Sci U S A 86: 4544–4548.

Argaw AT, Zhang Y, Snyder BJ, Zhao ML, Kopp N, Lee SC *et al.* (2006). IL-1beta regulates blood-brain barrier permeability via reactivation of the hypoxia-angiogenesis program. J Immunol 177: 5574–5584.

Argaw AT, Asp L, Zhang J, Navrazhina K, Pham T, Mariani JN *et al.* (2012). Astrocyte-derived VEGF-A drives blood-brain barrier disruption in CNS inflammatory disease. J Clin Invest 122: 2454–2468.

Armulik A, Genove G, Mae M, Nisancioglu MH, Wallgard E, Niaudet C *et al.* (2010). Pericytes regulate the blood-brain barrier. Nature 468: 557–561.

Asahi M, Wang X, Mori T, Sumii T, Jung JC, Moskowitz MA *et al.* (2001). Effects of matrix metalloproteinase-9 gene knock-out on the proteolysis of blood-brain barrier and white matter components after cerebral ischemia. J Neurosci 21: 7724–7732.

Baeten KM, Akassoglou K (2011). Extracellular matrix and matrix receptors in blood-brain barrier formation and stroke. Dev Neurobiol 71: 1018–1039.

Ballabh P, Braun A, Nedergaard M (2004). The blood-brain barrier: an overview: structure, regulation, and clinical implications. Neurobiol Dis 16: 1–13.

Bamford J, Sandercock P, Dennis M, Burn J, Warlow C (1990). A prospective study of acute cerebrovascular disease in the community: the Oxfordshire Community Stroke Project – 1981–86. 2. Incidence, case fatality rates and overall outcome at one year of cerebral infarction, primary intracerebral and subarachnoid haem. J Neurol Neurosurg Psychiatry 53: 16–22.

Ban HS, Uto Y, Nakamura H (2011). Hypoxia-inducible factor inhibitors: a survey of recent patented compounds (2004–2010). Expert Opin Ther Pat 21: 131–146.

Bao Y, Bramlett HM, Atkins CM, Truettner JS, Lotocki G, Alonso OF *et al.* (2011). Post-traumatic seizures exacerbate histopathological damage after fluid-percussion brain injury. J Neurotrauma 28: 35–42.

Baranova O, Miranda LF, Pichiule P, Dragatsis I, Johnson RS, Chavez JC (2007). Neuron-specific inactivation of the hypoxia inducible factor 1 alpha increases brain injury in a mouse model of transient focal cerebral ischemia. J Neurosci 27: 6320–6332.

Başkaya MK, Rao AM, Doğan A, Donaldson D, Dempsey RJ (1997). The biphasic opening of the blood-brain barrier in the cortex and hippocampus after traumatic brain injury in rats. Neurosci Lett 226: 33–36.

Bauer AT, Burgers HF, Rabie T, Marti HH (2010). Matrix metalloproteinase-9 mediates hypoxia-induced vascular leakage in the brain via tight junction rearrangement. J Cereb Blood Flow Metab 30: 837–848.

Baumann E, Preston E, Slinn J, Stanimirovic D (2009). Post-ischemic hypothermia attenuates loss of the vascular basement membrane proteins, agrin and SPARC, and the blood-brain barrier disruption after global cerebral ischemia. Brain Res 1269: 185–197.

Bell RD, Winkler EA, Sagare AP, Singh I, LaRue B, Deane R *et al.* (2010). Pericytes control key neurovascular functions and neuronal phenotype in the adult brain and during brain aging. Neuron 68: 409–427.

Berezowski V, Landry C, Dehouck MP, Cecchelli R, Fenart L (2004). Contribution of glial cells and pericytes to the mRNA profiles of P-glycoprotein and multidrug resistance-associated proteins in an in vitro model of the blood-brain barrier. Brain Res 1018: 1–9.

Bermpohl D, You Z, Lo EH, Kim H-H, Whalen MJ (2007). TNF alpha and Fas mediate tissue damage and functional outcome after traumatic brain injury in mice. J Cereb Blood Flow Metab 27: 1806–1818.

Bouras C, Kövari E, Herrmann FR, Rivara C-B, Bailey TL, Gunten AV *et al.* (2006). Stereologic analysis of microvascular morphology in the elderly: Alzheimer disease pathology and cognitive status. J Neuropathol Exp Neurol 65: 235–244.

Brown RC, Mark KS, Egleton RD, Huber JD, Burroughs AR, Davis TP (2003). Protection against hypoxia-induced increase in blood-brain barrier permeability: role of tight junction proteins and NFkappaB. J Cell Sci 116: 693–700.

Bruggen N, Thibodeaux H, Palmer JT, Lee WP, Fu L, Cairns B *et al.* (1999). VEGF antagonism reduces edema formation and tissue damage after ischemia/reperfusion injury in the mouse brain. J Clin Invest 104: 1613–1620.

Cambier S, Gline S, Mu D, Collins R, Araya J, Dolganov G *et al.* (2005). Integrin alpha(v)beta8-mediated activation of transforming growth factor-beta by perivascular astrocytes: an angiogenic control switch. Am J Pathol 166: 1883–1894.

Candelario-Jalil E, Yang Y, Rosenberg GA (2009). Diverse roles of matrix metalloproteinases and tissue inhibitors of metalloproteinases in neuroinflammation and cerebral ischemia. Neuroscience 158: 983–994.

Ceruti S, Colombo L, Magni G, Viganò F, Boccazzi M, Deli MA *et al.* (2011). Oxygen-glucose deprivation increases the enzymatic activity

and the microvesicle-mediated release of ectonucleotidases in the cells composing the blood-brain barrier. Neurochem Int 59: 259–271.

Chen C, Hu Q, Yan J, Yang X, Shi X, Lei J *et al.* (2009). Early inhibition of HIF-1alpha with small interfering RNA reduces ischemic-reperfused brain injury in rats. Neurobiol Dis 33: 509–517.

Chen W, Jadhav V, Tang J, Zhang JH (2008a). HIF-1 alpha inhibition ameliorates neonatal brain damage after hypoxic-ischemic injury. Acta Neurochir Suppl 102: 395–399.

Chen W, Jadhav V, Tang J, Zhang JH (2008b). HIF-1alpha inhibition ameliorates neonatal brain injury in a rat pup hypoxic-ischemic model. Neurobiol Dis 31: 433–441.

Chi OZ, Hunter C, Liu X, Weiss HR (2007). Effects of anti-VEGF antibody on blood-brain barrier disruption in focal cerebral ischemia. Exp Neurol 204: 283–287.

Chi OZ, Hunter C, Liu X, Weiss HR (2008). Effects of deferoxamine on blood–brain barrier disruption and VEGF in focal cerebral ischemia. Neurol Res 30: 288–293.

Choi HJ, Song B-J, Gong Y-D, Gwak WJ, Soh Y (2008). Rapid degradation of hypoxia-inducible factor-1alpha by KRH102053, a new activator of prolyl hydroxylase 2. Br J Pharmacol 154: 114–125.

Chow J, Ogunshola O, Fan SY, Li Y, Ment LR, Madri JA (2001). Astrocyte-derived VEGF mediates survival and tube stabilization of hypoxic brain microvascular endothelial cells in vitro. Brain Res Dev Brain Res 130: 123–132.

Cipolla MJ, Crete R, Vitullo L, Rix RD (2004). Transcellular transport as a mechanism of blood-brain barrier disruption during stroke. Front Biosci 9: 777–785.

Claudio L (1996). Ultrastructural features of the blood-brain barrier in biopsy tissue from Alzheimer's disease patients. Acta Neuropathol 91: 6–14.

Colgan OC, Collins NT, Ferguson G, Murphy RP, Birney YA, Cahill PA *et al.* (2008). Influence of basolateral condition on the regulation of brain microvascular endothelial tight junction properties and barrier function. Brain Res 1193: 84–92.

Csuka E, Morganti-Kossmann MC, Lenzlinger PM, Joller H, Trentz O, Kossmann T (1999). IL-10 levels in cerebrospinal fluid and serum of patients with severe traumatic brain injury: relationship to IL-6, TNF-alpha, TGF-beta1 and blood-brain barrier function. J Neuroimmunol 101: 211–221.

Cui J, Chen S, Zhang C, Meng F, Wu W, Hu R *et al.* (2012). Inhibition of MMP-9 by a selective gelatinase inhibitor protects neurovasculature from embolic focal cerebral ischemia. Mol Neurodegener 7: 21.

Cunningham LA, Wetzel M, Rosenberg GA (2005). Multiple roles for MMPs and TIMPs in cerebral ischemia. Glia 50: 329–339.

Daneman R, Zhou L, Kebede AA, Barres BA (2010). Pericytes are required for blood-brain barrier integrity during embryogenesis. Nature 468: 562–566.

Davson H, Oldendorf WH (1967). Symposium on membrane transport. Transport in the central nervous system.Proc R Soc Med 60: 326–329.

Deane R, Yan SD, Submamaryan RK, LaRue B, Jovanovic S, Hogg E *et al.* (2003). RAGE mediates amyloid-beta peptide transport across the blood-brain barrier and accumulation in brain. Nat Med 9: 907–913.

Dehouck MP, Meresse S, Delorme P, Fruchart JC, Cecchelli R (1990). An easier, reproducible, and mass-production method to study the blood-brain barrier in vitro. J Neurochem 54: 1798–1801.

Del Valle J, Duran-Vilaregut J, Manich G, Camins A, Pallàs M, Vilaplana J *et al.* (2009). Time-course of blood-brain barrier disruption in senescence-accelerated mouse prone 8 (SAMP8) mice. Int J Dev Neurosci 27: 47–52.

Deli MA, Abraham CS, Kataoka Y, Niwa M (2005). Permeability studies on in vitro blood-brain barrier models: physiology, pathology, and pharmacology. Cell Mol Neurobiol 25: 59–127.

Dirnagl U, Iadecola C, Moskowitz MA (1999). Pathobiology of ischaemic stroke: an integrated view. Trends Neurosci 22: 391–397.

Dohgu S, Yamauchi A, Takata F, Naito M, Tsuruo T, Higuchi S *et al.* (2004). Transforming growth factor-beta1 upregulates the tight junction and P-glycoprotein of brain microvascular endothelial cells. Cell Mol Neurobiol 24: 491–497.

Dohgu S, Takata F, Yamauchi A, Nakagawa S, Egawa T, Naito M *et al.* (2005). Brain pericytes contribute to the induction and up-regulation of blood-brain barrier functions through transforming growth factor-beta production. Brain Res 1038: 208–215.

Dore-Duffy P, Owen C, Balabanov R, Murphy S, Beaumont T, Rafols JA (2000). Pericyte migration from the vascular wall in response to traumatic brain injury. Microvasc Res 60: 55–69.

Dore-Duffy P, Wang X, Mehedi A, Kreipke CW, Rafols JA (2007). Differential expression of capillary VEGF isoforms following traumatic brain injury. Neurol Res 29: 395–403.

Dore-Duffy P, Wang S, Mehedi A, Katyshev V, Cleary K, Tapper A *et al.* (2011). Pericyte-mediated vasoconstriction underlies TBI-induced hypoperfusion. Neurol Res 33: 176–186.

Engelhardt B, Sorokin L (2009). The blood-brain and the blood-cerebrospinal fluid barriers: function and dysfunction. Semin Immunopathol 31: 497–511.

Fan X, Heijnen CJ, van der Kooij MA, Groenendaal F, Van Bel F (2009). The role and regulation of hypoxia-inducible factor-1alpha expression in brain development and neonatal hypoxic-ischemic brain injury. Brain Res Rev 62: 99–108.

Fandrey J, Gassmann M (2009). Oxygen sensing and the activation of the hypoxia inducible factor 1 (HIF-1) – invited article. Adv Exp Med Biol 648: 197–206.

Fang H, Zhang L-F, Meng F-T, Du X, Zhou J-N (2010). Acute hypoxia promote the phosphorylation of tau via ERK pathway. Neurosci Lett 474: 173–177.

Fazzina G, Amorini AM, Marmarou CR, Fukui S, Okuno K, Dunbar JG *et al.* (2010). The protein kinase C activator phorbol myristate acetate decreases brain edema by aquaporin 4 downregulation after middle cerebral artery occlusion in the rat. J Neurotrauma 27: 453–461.

Fischer S, Clauss M, Wiesnet M, Renz D, Schaper W, Karliczek GF (1999). Hypoxia induces permeability in brain microvessel endothelial cells via VEGF and NO. Am J Physiol 276: C812–C820.

Fischer S, Wobben M, Kleinstuck J, Renz D, Schaper W (2000). Effect of astroglial cells on hypoxia-induced permeability in PBMEC cells. Am J Physiol Cell Physiol 279: C935–C944.

Fischer S, Wobben M, Marti HH, Renz D, Schaper W (2002). Hypoxia-induced hyperpermeability in brain microvessel endothelial cells involves VEGF-mediated changes in the expression of zonula occludens-1. Microvasc Res 63: 70–80.

Fleegal MA, Hom S, Borg LK, Davis TP (2005). Activation of PKC modulates blood-brain barrier endothelial cell permeability changes induced by hypoxia and posthypoxic reoxygenation. Am J Physiol Heart Circ Physiol 289: H2012–H2019.

Foglio E, Rodella LF (2010). Aquaporins and neurodegenerative diseases. Curr Neuropharmacol 8: 112–121.

Förster C (2008). Tight junctions and the modulation of barrier function in disease. Histochem Cell Biol 130: 55–70.

Fukuda AM, Badaut J (2012). Aquaporin 4: a player in cerebral edema and neuroinflammation. J Neuroinflammation 9: 279.

Fukuda AM, Adami A, Pop V, Bellone JA, Coats JS, Hartman RE *et al*. (2013). Posttraumatic reduction of edema with aquaporin-4 RNA interference improves acute and chronic functional recovery. J Cereb Blood Flow Metab 33: 1–12.

Fukuda S, Fini CA, Mabuchi T, Koziol JA, Eggleston Jr LL, Zoppo G (2004). Focal cerebral ischemia induces active proteases that degrade microvascular matrix. Stroke 35: 998–1004.

Gaetz M (2004). The neurophysiology of brain injury. Clin Neurophysiol 115: 4–18.

Gassmann M, Heinicke K, Soliz J, Ogunshola OO (2003). Non-erythroid functions of erythropoietin. Adv Exp Med Biol 543: 323–330.

Gonul E, Duz B, Kahraman S, Kayali H, Kubar A, Timurkaynak E (2002). Early pericyte response to brain hypoxia in cats: an ultrastructural study. Microvasc Res 64: 116–119.

Grammas P (2011). Neurovascular dysfunction, inflammation and endothelial activation: implications for the pathogenesis of Alzheimer's disease. J Neuroinflammation 8: 26.

Greenberg SM, Gurol ME, Rosand J, Smith EE (2004). Amyloid angiopathy-related vascular cognitive impairment. Stroke 35: 2616–2619.

Greenberger LM, Horak ID, Filpula D, Sapra P, Westergaard M, Frydenlund HF *et al*. (2008). A RNA antagonist of hypoxia-inducible factor-1alpha, EZN-2968, inhibits tumor cell growth. Mol Cancer Ther 7: 3598–3608.

Hafny B, Bourre JM, Roux F (1996). Synergistic stimulation of gamma-glutamyl transpeptidase and alkaline phosphatase activities by retinoic acid and astroglial factors in immortalized rat brain microvessel endothelial cells. J Cell Physiol 167: 451–460.

Hallmann R, Horn N, Selg M, Wendler O, Pausch F, Sorokin LM (2005). Expression and function of laminins in the embryonic and mature vasculature. Physiol Rev 85: 979–1000.

Hamann GF, Okada Y, Fitridge R, Zoppo GJ (1995). Microvascular basal lamina antigens disappear during cerebral ischemia and reperfusion. Stroke 26: 2120–2126.

Hamann GF, Liebetrau M, Martens H, Burggraf D, Kloss CUA, Bültemeier G *et al*. (2002). Microvascular basal lamina injury after experimental focal cerebral ischemia and reperfusion in the rat. J Cereb Blood Flow Metab 22: 526–533.

Harten SK, Ashcroft M, Maxwell PH (2010). Prolyl hydroxylase domain inhibitors: a route to HIF activation and neuroprotection. Antioxid Redox Signal 12: 459–480.

Hartmann C, Zozulya A, Wegener J, Galla HJ (2007). The impact of glia-derived extracellular matrices on the barrier function of cerebral endothelial cells: an in vitro study. Exp Cell Res 313: 1318–1325.

Hatherell K, Couraud PO, Romero IA, Weksler B, Pilkington GJ (2011). Development of a three-dimensional, all-human in vitro model of the blood-brain barrier using mono-, co-, and tri-cultivation Transwell models. J Neurosci Methods 199: 223–229.

Hawkins BT, Davis TP (2005). The blood-brain barrier/neurovascular unit in health and disease. Pharmacol Rev 57: 173–185.

Hayashi K, Nakao S, Nakaoke R, Nakagawa S, Kitagawa N, Niwa M (2004). Effects of hypoxia on endothelial/pericytic co-culture model of the blood-brain barrier. Regul Pept 123: 77–83.

Hayashi T, Kaneko Y, Yu S, Bae E, Stahl CE, Kawase T *et al*. (2010). Quantitative analyses of matrix metalloproteinase activity after traumatic brain injury in adult rats. Brain Res 1280: 177–192.

Hayashi Y, Nomura M, Yamagishi S, Harada S, Yamashita J, Yamamoto H (1997). Induction of various blood-brain barrier properties in non-neural endothelial cells by close apposition to co-cultured astrocytes. Glia 19: 13–26.

Hellewell SC, Yan EB, Agyapomaa DA, Bye N, Morganti-Kossmann MC (2010). Post-traumatic hypoxia exacerbates brain tissue damage: analysis of axonal injury and glial responses. J Neurotrauma 27: 1997–2010.

Hellström M, Gerhardt H, Kalén M, Li X, Eriksson U, Wolburg H *et al*. (2001). Lack of pericytes leads to endothelial hyperplasia and abnormal vascular morphogenesis. J Cell Biol 153: 543–553.

Herholz K (2010). Cerebral glucose metabolism in preclinical and prodromal Alzheimer's disease. Expert Rev Neurother 10: 1667–1673.

Hicks RR, Baldwin SA, Scheff SW (1997). Serum extravasation and cytoskeletal alterations following traumatic brain injury in rats. Comparison of lateral fluid percussion and cortical impact models. Mol Chem Neuropathol 32: 1–16.

Hori S, Ohtsuki S, Hosoya K, Nakashima E, Terasaki T (2004). A pericyte-derived angiopoietin-1 multimeric complex induces occludin gene expression in brain capillary endothelial cells through Tie-2 activation in vitro. J Neurochem 89: 503–513.

Hu Y, Liu J, Huang H (2012). Recent agents targeting HIF-1α for cancer therapy. J Cell Biochem 114: 1–28.

Huang ZG, Xue D, Preston E, Karbalai H, Buchan AM (1999). Biphasic opening of the blood-brain barrier following transient focal ischemia: effects of hypothermia. Can J Neurol Sci 26: 298–304.

Igarashi Y, Utsumi H, Chiba H, Yamada-Sasamori Y, Tobioka H, Kamimura Y *et al*. (1999). Glial cell line-derived neurotrophic factor induces barrier function of endothelial cells forming the blood-brain barrier. Biochem Biophys Res Commun 261: 108–112.

Jaakkola P, Mole DR, Tian YM, Wilson MI, Gielbert J, Gaskell SJ *et al*. (2001). Targeting of HIF-alpha to the von Hippel-Lindau ubiquitylation complex by O2-regulated prolyl hydroxylation. Science 292: 468–472.

Janzer RC, Raff MC (1987). Astrocytes induce blood-brain barrier properties in endothelial cells. Nature 325: 253–257.

Jiang X, Namura S, Nagata I (2001). Matrix metalloproteinase inhibitor KB-R7785 attenuates brain damage resulting from permanent focal cerebral ischemia in mice. Neurosci Lett 305: 41–44.

Jones NM, Kardashyan L, Callaway JK, Lee EM, Beart PM (2008). Long-term functional and protective actions of preconditioning with hypoxia, cobalt chloride, and desferrioxamine against hypoxic-ischemic injury in neonatal rats. Pediatr Res 63: 620–624.

Kago T, Takagi N, Date I, Takenaga Y, Takagi K, Takeo S (2003). Cerebral ischemia enhances tyrosine phosphorylation of occludin in brain capillaries. Biochem Biophys Res Commun 339: 341–346.

Karuppagounder SS, Ratan RR (2012). Hypoxia-inducible factor prolyl hydroxylase inhibition: robust new target or another big bust for stroke therapeutics? J Cereb Blood Flow Metab 32: 1347–1361.

Kaur C, Sivakumar V, Zhang Y, Ling EA (2006). Hypoxia-induced astrocytic reaction and increased vascular permeability in the rat cerebellum. Glia 54: 826–839.

Kawahara M, Kuroda Y, Arispe N, Rojas E (2000). Alzheimer's beta-amyloid, human islet amylin, and prion protein fragment evoke intracellular free calcium elevations by a common mechanism in a hypothalamic GnRH neuronal cell line. J Biol Chem 275: 14077–14083.

Kawarabayashi T, Younkin LH, Saido TC, Shoji M, Ashe KH, Younkin SG (2001). Age-dependent changes in brain, CSF, and plasma amyloid (beta) protein in the Tg2576 transgenic mouse model of Alzheimer's disease. J Neurosci 21: 372–381.

Kim H, Lee JM, Park JS, Jo SA, Kim Y-O, Kim C-W *et al.* (2008). Dexamethasone coordinately regulates angiopoietin-1 and VEGF: a mechanism of glucocorticoid-induced stabilization of blood-brain barrier. Biochem Biophys Res Commun 372: 243–248.

Kimelberg HK (2005). Astrocytic swelling in cerebral ischemia as a possible cause of injury and target for therapy. Glia 50: 389–397.

Kook S-Y, Hong HS, Moon M, Ha CM, Chang S, Mook-Jung I (2012). Aβ1-42-RAGE interaction disrupts tight junctions of the blood-brain barrier via Ca2+-calcineurin signaling. J Neurosci 32: 8845–8854.

Koto T, Takubo K, Ishida S, Shinoda H, Inoue M, Tsubota K *et al.* (2007). Hypoxia disrupts the barrier function of neural blood vessels through changes in the expression of claudin-5 in endothelial cells. Am J Pathol 170: 1389–1397.

Krum JM, Mani N, Rosenstein JM (2008). Roles of the endogenous VEGF receptors flt-1 and flk-1 in astroglial and vascular remodeling after brain injury. Exp Neurol 212: 108–117.

Kuhlmann CRW, Tamaki R, Gamerdinger M, Lessmann V, Behl C, Kempski OS *et al.* (2007). Inhibition of the myosin light chain kinase prevents hypoxia-induced blood-brain barrier disruption. J Neurochem 102: 501–507.

Kuroiwa T, Ting P, Martinez H, Klatzo I (1985). The biphasic opening of the blood-brain barrier to proteins following temporary middle cerebral artery occlusion. Acta Neuropathol 68: 122–129.

Kwon I, Kim EH, Del Zoppo GJ, Heo JH (2009). Ultrastructural and temporal changes of the microvascular basement membrane and astrocyte interface following focal cerebral ischemia. J Neurosci Res 87: 668–676.

Ladomery MR, Harper SJ, Bates DO (2007). Alternative splicing in angiogenesis: the vascular endothelial growth factor paradigm. Cancer Lett 249: 133–142.

Lee SW, Kim WJ, Choi YK, Song HS, Son MJ, Gelman IH *et al.* (2003). SSeCKS regulates angiogenesis and tight junction formation in blood-brain barrier. Nat Med 9: 900–906.

Lee VM, Goedert M, Trojanowski JQ (2001). Neurodegenerative tauopathies. Annu Rev Neurosci 24: 1121–1159.

Li L, Zhang X, Yang D, Luo G, Chen S, Le W (2009). Hypoxia increases Abeta generation by altering beta- and gamma-cleavage of APP. Neurobiol Aging 30: 1091–1098.

Li M-M, Wu L-Y, Zhao T, Wu K-W, Xiong L, Zhu L-L *et al.* (2011). The protective role of 5-hydroxymethyl-2-furfural (5-HMF) against acute hypobaric hypoxia. Cell Stress Chaperones 16: 529–537.

Lindahl P, Johansson BR, Leveen P, Betsholtz C (1997). Pericyte loss and microaneurysm formation in PDGF-B-deficient mice. Science 277: 242–245.

Liu Y, Liu F, Iqbal K, Grundke-Iqbal I, Gong C-X (2008). Decreased glucose transporters correlate to abnormal hyperphosphorylation of tau in Alzheimer disease. FEBS Lett 582: 359–364.

Lochhead JJ, McCaffrey G, Quigley CE, Finch J, DeMarco KM, Nametz N *et al.* (2010). Oxidative stress increases blood-brain barrier permeability and induces alterations in occludin during hypoxia-reoxygenation. J Cereb Blood Flow Metab 30: 1625–1636.

Lu D-YY, Yu W-HH, Yeh W-LL, Tang C-HH, Leung Y-MM, Wong K-LL *et al.* (2009). Hypoxia-induced matrix metalloproteinase-13 expression in astrocytes enhances permeability of brain endothelial cells. J Cell Physiol 220: 163–173.

Luissint AC, Artus C, Glacial F, Ganeshamoorthy K, Couraud PO (2012). Tight junctions at the blood brain barrier: physiological architecture and disease-associated dysregulation. Fluids Barriers CNS 9: 23.

Majmundar AJ, Wong WJ, Simon MC (2010). Hypoxia-inducible factors and the response to hypoxic stress. Mol Cell 40: 294–309.

Mandriota SJ, Pepper MS (1998). Regulation of angiopoietin-2 mRNA levels in bovine microvascular endothelial cells by cytokines and hypoxia. Circ Res 83: 852–859.

Manley GT, Fujimura M, Ma T, Noshita N, Filiz F, Bollen AW *et al.* (2000). Aquaporin-4 deletion in mice reduces brain edema after acute water intoxication and ischemic stroke. Nat Med 6: 159–163.

Mark KS, Davis TP (2002). Cerebral microvascular changes in permeability and tight junctions induced by hypoxia-reoxygenation. Am J Physiol Heart Circ Physiol 282: H1485–H1494.

Mayhan WG (1999). VEGF increases permeability of the blood-brain barrier via a nitric oxide synthase/cGMP-dependent pathway. Am J Physiol 276: C1148–C1153.

Meijer TWH, Kaanders JHAM, Span PN, Bussink J (2012). Targeting hypoxia, HIF-1, and tumor glucose metabolism to improve radiotherapy efficacy. Clin Cancer Res 18: 5585–5594.

Melgar MA, Rafols J, Gloss D, Diaz FG (2006). Postischemic reperfusion: ultrastructural blood-brain barrier and hemodynamic correlative changes in an awake model of transient forebrain ischemia. Neurosurgery 59: E1152.

Mense SM, Sengupta A, Zhou M, Lan C, Bentsman G, Volsky DJ *et al.* (2006). Gene expression profiling reveals the profound upregulation of hypoxia-responsive genes in primary human astrocytes. Physiol Genomics 25: 435–449.

Meyer J, Rauh J, Galla HJ (1991). The susceptibility of cerebral endothelial cells to astroglial induction of blood-brain barrier enzymes depends on their proliferative state. J Neurochem 57: 1971–1977.

Michaelis ML, Dobrowsky RT, Li G (2002). Tau neurofibrillary pathology and microtubule stability. J Mol Neurosci 19: 289–293.

Mizuguchi H, Hashioka Y, Fujii A, Utoguchi N, Kubo K, Nakagawa S *et al.* (1994). Glial extracellular matrix modulates gamma-glutamyl transpeptidase activity in cultured bovine brain capillary and bovine aortic endothelial cells. Brain Res 651: 155–159.

Mojsilovic-Petrovic J, Callaghan D, Cui H, Dean C, Stanimirovic DB, Zhang W (2007). Hypoxia-inducible factor-1 (HIF-1) is involved in the regulation of hypoxia-stimulated expression of monocyte chemoattractant protein-1 (MCP-1/CCL2) and MCP-5 (Ccl12) in astrocytes. J Neuroinflammation 4: 12.

Morancho A, Rosell A, Garcia-Bonilla L, Montaner J, García-Bonilla L (2010). Metalloproteinase and stroke infarct size: role for anti-inflammatory treatment? Ann N Y Acad Sci 1207: 123–133.

Morgan R, Kreipke CW, Roberts G, Bagchi M, Rafols JA (2007). Neovascularization following traumatic brain injury: possible evidence for both angiogenesis and vasculogenesis. Neurol Res 29: 375–381.

Nag S, Takahashi JL, Kilty DW (1997). Role of vascular endothelial growth factor in blood-brain barrier breakdown and angiogenesis in brain trauma. J Neuropathol Exp Neurol 56: 912–921.

Nag S, Kapadia A, Stewart DJ (2011). Review: molecular pathogenesis of blood-brain barrier breakdown in acute brain injury. Neuropathol Appl Neurobiol 37: 3–23.

Nagel S, Talbot NP, Mecinovic J, Smith TG, Buchan AM, Schofield CJ (2010). Therapeutic manipulation of the HIF hydroxylases. Antioxid Redox Signal 12: 481–501.

Nagy Z, Mathieson G, Hüttner I (1979). Blood-brain barrier opening to horseradish peroxidase in acute arterial hypertension. Acta Neuropathol 48: 45–53.

Nakagawa S, Deli MA, Nakao S, Honda M, Hayashi K, Nakaoke R *et al.* (2007). Pericytes from brain microvessels strengthen the barrier integrity in primary cultures of rat brain endothelial cells. Cell Mol Neurobiol 27: 687–694.

Nakagawa S, Deli M, Kawaguchi H, Shimizudani T, Shimono T, Kittel A *et al.* (2009). A new blood-brain barrier model using primary rat brain endothelial cells, pericytes and astrocytes. Neurochem Int 54: 253–263.

Nakayama M, Berger P (2013). Coordination of VEGF receptor trafficking and signaling by coreceptors. Exp Cell Res 319: 1340–1347.

Nalivaevaa NN, Fisk L, Kochkina EG, Plesneva SA, Zhuravin IA, Babusikova E *et al.* (2004). Effect of hypoxia/ischemia and hypoxic preconditioning/reperfusion on expression of some amyloid-degrading enzymes. Ann N Y Acad Sci 1035: 21–33.

Nico B, Ribatti D (2012). Morphofunctional aspects of the blood-brain barrier. Curr Drug Metab 13: 50–60.

Nielsen S, Nagelhus EA, Amiry-Moghaddam M, Bourque C, Agre P, Ottersen OP (1997). Specialized membrane domains for water transport in glial cells: high-resolution immunogold cytochemistry of aquaporin-4 in rat brain. J Neurosci 17: 171–180.

Nowak DG, Woolard J, Amin EM, Konopatskaya O, Saleem MA, Churchill AJ *et al.* (2008). Expression of pro- and anti-angiogenic isoforms of VEGF is differentially regulated by splicing and growth factors. J Cell Sci 121: 3487–3495.

Ogunshola OO (2011). In vitro modeling of the blood-brain barrier: simplicity versus complexity. Curr Pharm Des 17: 2755–2761.

Ogunshola OO, Al-Ahmad A (2012). HIF-1 at the blood-brain barrier: a mediator of permeability? High Alt Med Biol 13: 153–161.

Ogunshola OO, Antoniou X (2009). Contribution of hypoxia to Alzheimer's disease: is HIF-1alpha a mediator of neurodegeneration? Cell Mol Life Sci 66: 3555–3563.

Osada T, Gu YH, Kanazawa M, Tsubota Y, Hawkins BT, Spatz M *et al.* (2011). Interendothelial claudin-5 expression depends on cerebral endothelial cell-matrix adhesion by beta(1)-integrins. J Cereb Blood Flow Metab 31: 1972–1985.

Paolinelli R, Corada M, Orsenigo F, Dejana E (2011). The molecular basis of the blood brain barrier differentiation and maintenance. Is it still a mystery? Pharmacol Res 63: 165–171.

Papadopoulos MC, Verkman AS (2007). Aquaporin-4 and brain edema. Pediatr Nephrol 22: 778–784.

Papadopoulos MC, Manley GT, Krishna S, Verkman AS (2004). Aquaporin-4 facilitates reabsorption of excess fluid in vasogenic brain edema. FASEB J 18: 1291–1293.

Papavassiliou E, Gogate N, Proescholdt M, Heiss JD, Walbridge S, Edwards NA *et al.* (1997). Vascular endothelial growth factor (vascular permeability factor) expression in injured rat brain. J Neurosci Res 49: 451–460.

Paris D, Patel N, DelleDonne A, Quadros A, Smeed R, Mullan M (2004). Impaired angiogenesis in a transgenic mouse model of cerebral amyloidosis. Neurosci Lett 366: 80–85.

Park K, Rosell A, Foerch C, Xing C, Kim WJ, Lee S *et al.* (2009). Plasma and brain matrix metalloproteinase-9 after acute focal cerebral ischemia in rats. Stroke 40: 2836–2842.

Park YS, Kim NH, Jo I (2003). Hypoxia and vascular endothelial growth factor acutely up-regulate angiopoietin-1 and Tie2 mRNA in bovine retinal pericytes. Microvasc Res 65: 125–131.

Patel HC, Boutin H, Allan SM (2003). Interleukin-1 in the brain: mechanisms of action in acute neurodegeneration. Ann N Y Acad Sci 992: 39–47.

Peers C, Dallas ML, Boycott HE, Scragg JL, Pearson H, Boyle JP (2009). Hypoxia and neurodegeneration. Ann N Y Acad Sci 1177: 169–177.

Plate KH (1999a). Mechanisms of angiogenesis in the brain. J Neuropathol Exp Neurol 58: 313–320.

Plate KH, Beck H, Danner S, Allegrini PR, Wiessner C (1999b). Cell type specific upregulation of vascular endothelial growth factor in an MCA-occlusion model of cerebral infarct. J Neuropathol Exp Neurol 58: 654–666.

Plateel M, Teissier E, Cecchelli R (1997). Hypoxia dramatically increases the nonspecific transport of blood-borne proteins to the brain. J Neurochem 68: 874–877.

Pluta R (2007). Role of ischemic blood-brain barrier on amyloid plaques development in Alzheimer's disease brain. Curr Neurovasc Res 4: 121–129.

Prass K, Ruscher K, Karsch M, Isaev N, Megow D, Priller J *et al.* (2002). Desferrioxamine induces delayed tolerance against cerebral ischemia in vivo and in vitro. J Cereb Blood Flow Metab 22: 520–525.

Rascher G, Fischmann A, Kroger S, Duffner F, Grote EH, Wolburg H (2002). Extracellular matrix and the blood-brain barrier in glioblastoma multiforme: spatial segregation of tenascin and agrin. Acta Neuropathol 104: 85–91.

Ratan RR, Siddiq A, Smirnova N, Karpisheva K, Haskew-Layton R, McConoughey S *et al.* (2007). Harnessing hypoxic adaptation to prevent, treat, and repair stroke. J Mol Med 85: 1331–1338.

Ratan RR, Siddiq A, Aminova L, Langley B, McConoughey S, Karpisheva K *et al.* (2008). Small molecule activation of adaptive gene expression: tilorone or its analogs are novel potent activators of hypoxia inducible factor-1 that provide prophylaxis against stroke and spinal cord injury. Ann N Y Acad Sci 1147: 383–394.

Raub TJ, Kuentzel SL, Sawada GA (1992). Permeability of bovine brain microvessel endothelial cells in vitro: barrier tightening by a factor released from astroglioma cells. Exp Cell Res 199: 330–340.

Reuss B, Dono R, Unsicker K (2003). Functions of fibroblast growth factor (FGF)-2 and FGF-5 in astroglial differentiation and blood-brain barrier permeability: evidence from mouse mutants. J Neurosci 23: 6404–6412.

Rist RJ, Romero IA, Chan MW, Couraud PO, Roux F, Abbott NJ (1997). F-actin cytoskeleton and sucrose permeability of immortalised rat brain microvascular endothelial cell monolayers: effects of cyclic AMP and astrocytic factors. Brain Res 768: 10–18.

Roberts J, Kahle MP, Bix GJ (2012). Perlecan and the blood-brain barrier: beneficial proteolysis? Front Pharmacol 3: 155.

Romanic AM, White RF, Arleth AJ, Ohlstein EH, Barone FC (1998). Matrix metalloproteinase expression increases after cerebral focal ischemia in rats: inhibition of matrix metalloproteinase-9 reduces infarct size. Stroke 29: 1020–1030.

Rosenberg GA (2009). Matrix metalloproteinases and their multiple roles in neurodegenerative diseases. Lancet 8: 205–216.

Rubin LL, Hall DE, Porter S, Barbu K, Cannon C, Horner HC *et al.* (1991). A cell culture model of the blood-brain barrier. J Cell Biol 115: 1725–1735.

Sagare AP, Bell RD, Zlokovic BV (2012). Neurovascular dysfunction and faulty amyloid β-peptide clearance in Alzheimer disease. Cold Spring Harb Perspect Med 2: pii: a011452.

Sandoval KE, Witt KA (2008). Blood-brain barrier tight junction permeability and ischemic stroke. Neurobiol Dis 32: 200–219.

Sa-Pereira I, Brites D, Brito MA, Sá-Pereira I (2012). Neurovascular unit: a focus on pericytes. Mol Neurobiol 45: 327–347.

Schmid-Brunclik N, Burgi-Taboada C, Antoniou X, Gassmann M, Ogunshola OO, Bürgi-Taboada C (2008). Astrocyte responses to injury: VEGF simultaneously modulates cell death and proliferation. Am J Physiol Regul Integr Comp Physiol 295: R864–R873.

Schoch HJ, Fischer S, Marti HH (2002). Hypoxia-induced vascular endothelial growth factor expression causes vascular leakage in the brain. Brain 125: 2549–2557.

Scholler K, Trinkl A, Klopotowski M, Thal SC, Plesnila N, Trabold R *et al.* (2007). Characterization of microvascular basal lamina damage and blood-brain barrier dysfunction following subarachnoid hemorrhage in rats. Brain Res 1142: 237–246.

Schroeter ML, Mertsch K, Giese H, Muller S, Sporbert A, Hickel B *et al.* (1999). Astrocytes enhance radical defence in capillary endothelial cells constituting the blood-brain barrier. FEBS Lett 449: 241–244.

Selkoe DJ (2001). Alzheimer's disease?: genes, proteins, and therapy. Perspective 81: 741–767.

Semenza GL (2003). Targeting HIF-1 for cancer therapy. Nat Rev Cancer 3: 721–732.

Semple BD, Bye N, Rancan M, Ziebell JM, Morganti-Kossmann MC (2010). Role of CCL2 (MCP-1) in traumatic brain injury (TBI): evidence from severe TBI patients and CCL2–/– mice. J Cereb Blood Flow Metab 30: 769–782.

Shaftel SS, Carlson TJ, Olschowka JA, Kyrkanides S, Matousek SB, O'Banion MK (2007). Chronic interleukin-1beta expression in mouse brain leads to leukocyte infiltration and neutrophil-independent blood brain barrier permeability without overt neurodegeneration. J Neurosci 27: 9301–9309.

Shen W, Li S, Chung SH, Zhu L, Stayt J, Su T *et al.* (2011). Tyrosine phosphorylation of VE-cadherin and claudin-5 is associated with TGF-beta1-induced permeability of centrally derived vascular endothelium. Eur J Cell Biol 90: 323–332.

Shibata M, Yamada S, Kumar SR, Calero M, Bading J, Frangione B *et al.* (2000). Clearance of Alzheimer's amyloid-ss(1-40) peptide from brain by LDL receptor-related protein-1 at the blood-brain barrier. J Clin Invest 106: 1489–1499.

Shigemori Y, Katayama Y, Mori T, Maeda T, Kawamata T (2006). Matrix metalloproteinase-9 is associated with blood-brain barrier opening and brain edema formation after cortical contusion in rats. Acta Neurochir Suppl 96: 130–133.

Shimizu F, Sano Y, Abe MA, Maeda T, Ohtsuki S, Terasaki T *et al.* (2011). Peripheral nerve pericytes modify the blood-nerve barrier function and tight junctional molecules through the secretion of various soluble factors. J Cell Physiol 226: 255–266.

Shimizu F, Sano Y, Saito K, Abe MA, Maeda T, Haruki H *et al.* (2012). Pericyte-derived glial cell line-derived neurotrophic factor increase the expression of claudin-5 in the blood-brain barrier and the blood-nerve barrier. Neurochem Res 37: 401–409.

Siddharthan V, Kim YV, Liu S, Kim KS (2007). Human astrocytes/astrocyte-conditioned medium and shear stress enhance the barrier properties of human brain microvascular endothelial cells. Brain Res 1147: 39–50.

Siddiq A, Ayoub IA, Chavez JC, Aminova L, Shah S, LaManna JC *et al.* (2005). Hypoxia-inducible factor prolyl 4-hydroxylase inhibition. A target for neuroprotection in the central nervous system. J Biol Chem 280: 41732–41743.

Singh N, Sharma G, Mishra V, Raghubir R (2012). Hypoxia inducible factor-1: its potential role in cerebral ischemia. Cell Mol Neurobiol 32: 491–507.

Sköld MK, Gertten CV, Sandberg-Nordqvist A-C, Mathiesen T, Holmin S (2002). VEGF and VEGF receptor expression after experimental brain contusion in rat. J Neurotrauma 19: 353–367.

Smirnova NA, Hushpulian DM, Speer RE, Gaisina IN, Ratan RR, Gazaryan IG (2012). Catalytic mechanism and substrate specificity of HIF prolyl hydroxylases. Biochemistry 77: 1108–1119.

Sobue K, Yamamoto N, Yoneda K, Hodgson ME, Yamashiro K, Tsuruoka N *et al.* (1999). Induction of blood-brain barrier properties in immortalized bovine brain endothelial cells by astrocytic factors. Neurosci Res 35: 155–164.

Song HS, Son MJ, Lee YM, Kim WJ, Lee S-W, Kim CW *et al.* (2002). Oxygen tension regulates the maturation of the blood-brain barrier. Biochem Biophys Res Commun 290: 325–331.

Sorond FA, Ratan RR (2000). Ironing-out mechanisms of neuronal injury under hypoxic-ischemic conditions and potential role of iron chelators as neuroprotective agents. Antioxid Redox Signal 2: 421–436.

Stamatovic SM, Keep RF, Kunkel SL, Andjelkovic AV (2003). Potential role of MCP-1 in endothelial cell tight junction 'opening': signaling via Rho and Rho kinase. J Cell Sci 116: 4615–4628.

Stamatovic SM, Shakui P, Keep RF, Moore BB, Kunkel SL, Rooijen NV *et al.* (2005). Monocyte chemoattractant protein-1 regulation of blood-brain barrier permeability. J Cereb Blood Flow Metab 25: 593–606.

Stanimirovic DB, Friedman A (2012). Pathophysiology of the neurovascular unit: disease cause or consequence? J Cereb Blood Flow Metab 32: 1207–1221.

Stewart PA, Wiley MJ (1981). Developing nervous tissue induces formation of blood-brain barrier characteristics in invading endothelial cells: a study using quail – chick transplantation chimeras. Dev Biol 84: 183–192.

Stuart RO, Sun A, Bush KT, Nigam SK (1996). Dependence of epithelial intercellular junction biogenesis on thapsigargin-sensitive intracellular calcium stores. J Biol Chem 271: 13636–13641.

Sun M-C, Honey CR, Berk C, Wong NLM, Tsui JKC (2003). Regulation of aquaporin-4 in a traumatic brain injury model in rats. J Neurosurg 98: 9–20.

Sun X, He G, Qing H, Zhou W, Dobie F, Cai F *et al.* (2006). Hypoxia facilitates Alzheimer's disease pathogenesis by up-regulating BACE1 gene expression. Proc Natl Acad Sci U S A 103: 18727–18732.

Takata F, Dohgu S, Matsumoto J, Takahashi H, Machida T, Wakigawa T *et al.* (2011). Brain pericytes among cells constituting the blood-brain barrier are highly sensitive to tumor necrosis factor-α, releasing matrix metalloproteinase-9 and migrating in vitro. J Neuroinflammation 8: 106.

Tang Y, Wu P, Su J, Xiang J, Cai D, Dong Q (2010). Effects of Aquaporin-4 on edema formation following intracerebral hemorrhage. Exp Neurol 223: 485–495.

Tao-Cheng JH, Nagy Z, Brightman MW (1987). Tight junctions of brain endothelium in vitro are enhanced by astroglia. J Neurosci 7: 3293–3299.

Tatsuta T, Naito M, Mikami K, Tsuruo T (1994). Enhanced expression by the brain matrix of P-glycoprotein in brain capillary endothelial cells. Cell Growth Differ 5: 1145–1152.

Taya K, Gulsen S, Okuno K, Prieto R, Marmarou CR, Marmarou A (2008). Modulation of AQP4 expression by the selective V1a receptor antagonist, SR49059, decreases trauma-induced brain edema. Acta Neurochir Suppl 102: 425–429.

Tejima E, Guo S, Murata Y, Arai K, Lok J, Van Leyen K *et al.* (2009). Neuroprotective effects of overexpressing tissue inhibitor of metalloproteinase TIMP-1. J Neurotrauma 26: 1935–1941.

Tesseur I, Wyss-Coray T (2006). A role for TGF-beta signaling in neurodegeneration: evidence from genetically engineered models. Curr Alzheimer Res 3: 505–513.

Thanabalasundaram G, Pieper C, Lischper M, Galla H-J (2010). Regulation of the blood-brain barrier integrity by pericytes via matrix metalloproteinases mediated activation of vascular endothelial growth factor in vitro. Brain Res 1347: 1–10.

Thanabalasundaram G, Schneidewind J, Pieper C, Galla H-J (2011). The impact of pericytes on the blood-brain barrier integrity depends critically on the pericyte differentiation stage. Int J Biochem Cell Biol 43: 1284–1293.

Thomas T, Thomas G, McLendon C, Sutton T, Mullan M (1996). beta-Amyloid-mediated vasoactivity and vascular endothelial damage. Nature 380: 168–171.

Tilling T, Korte D, Hoheisel D, Galla HJ (1998). Basement membrane proteins influence brain capillary endothelial barrier function in vitro. J Neurochem 71: 1151–1157.

Tomkins O, Friedman O, Ivens S, Reiffurth C, Major S, Dreier JP *et al.* (2007). Blood-brain barrier disruption results in delayed functional and structural alterations in the rat neocortex. Neurobiol Dis 25: 367–377.

Tomkins O, Shelef I, Kaizerman I, Eliushin A, Afawi Z, Misk A *et al.* (2008). Blood-brain barrier disruption in post-traumatic epilepsy. J Neurol Neurosurg Psychiatry 79: 774–777.

Trendelenburg G, Dirnagl U (2005). Neuroprotective role of astrocytes in cerebral ischemia: focus on ischemic preconditioning. Glia 50: 307–320.

Turner DA, Adamson DC (2011). Neuronal-astrocyte metabolic interactions. J Neuropathol Exp Neurol 70: 167–176.

Unterberg AW, Stover J, Kress B, Kiening KL (2004). Edema and brain trauma. Neuroscience 129: 1021–1029.

Valable S, Montaner J, Bellail A, Berezowski V, Brillault J, Cecchelli R *et al.* (2005). VEGF-induced BBB permeability is associated with an MMP-9 activity increase in cerebral ischemia: both effects decreased by Ang-1. J Cereb Blood Flow Metab 25: 1491–1504.

Vangeison G, Rempe DA (2009). The Janus-faced effects of hypoxia on astrocyte function. Neuroscientist 15: 579–588.

Vangeison G, Carr D, Federoff HJ, Rempe DA (2008). The good, the bad, and the cell type-specific roles of hypoxia inducible factor-1 alpha in neurons and astrocytes. J Neurosci 28: 1988–1993.

Vannucci SJ, Maher F, Simpson IA (1997). Glucose transporter proteins in brain: delivery of glucose to neurons and glia. Glia 21: 2–21.

Vilalta A, Sahuquillo J, Poca MA, De Los Rios J, Cuadrado E, Ortega-Aznar A *et al.* (2008). Brain contusions induce a strong local overexpression of MMP-9. Results of a pilot study. Acta Neurochir Suppl 102: 415–419.

Vogel C, Bauer A, Wiesnet M, Preissner KT, Schaper W, Marti HH *et al.* (2007). Flt-1, but not Flk-1 mediates hyperpermeability through activation of the PI3-K / Akt pathway. J Cell Physiol 212: 236–243.

Walshe TE, Saint-Geniez M, Maharaj AS, Sekiyama E, Maldonado AE, D'Amore PA (2009). TGF-beta is required for vascular barrier function, endothelial survival and homeostasis of the adult microvasculature. PLoS ONE 4: e5149.

Wang CX, Shuaib A (2002). Involvement of inflammatory cytokines in central nervous system injury. Prog Neurobiol 67: 161–172.

Wang X, Jung J, Asahi M, Chwang W, Russo L, Moskowitz MA *et al.* (2000). Effects of matrix metalloproteinase-9 gene knock-out on morphological and motor outcomes after traumatic brain injury. J Neurosci 20: 7037–7042.

Wang YL, Hui YN, Guo B, Ma JX (2007). Strengthening tight junctions of retinal microvascular endothelial cells by pericytes under normoxia and hypoxia involving angiopoietin-1 signal way. Eye 21: 1501–1510.

Wenger RH, Stiehl DP, Camenisch G (2005). Integration of oxygen signaling at the consensus HRE. Sci STKE 2005: re12.

Wilcock DM, Vitek MP, Colton CA (2009). Vascular amyloid alters astrocytic water and potassium channels in mouse models and humans with Alzheimer's disease. Neuroscience 159: 1055–1069.

Willis CL, Nolan CC, Reith SN, Lister T, Prior MJ, Guerin CJ *et al.* (2004). Focal astrocyte loss is followed by microvascular damage, with subsequent repair of the blood-brain barrier in the apparent absence of direct astrocytic contact. Glia 45: 325–337.

Willis CL, Meske DS, Davis TP (2010). Protein kinase C activation modulates reversible increase in cortical blood-brain barrier permeability and tight junction protein expression during hypoxia and posthypoxic reoxygenation. J Cereb Blood Flow Metab 30: 1847–1859.

Witt KA, Mark KS, Sandoval KE, Davis TP (2008). Reoxygenation stress on blood-brain barrier paracellular permeability and edema in the rat. Microvasc Res 75: 91–96.

Wolburg H, Noell S, Mack A, Wolburg-Buchholz K, Fallier-Becker P (2009a). Brain endothelial cells and the glio-vascular complex. Cell Tissue Res 335: 75–96.

Wolburg H, Noell S, Wolburg-Buchholz K, Mack A, Fallier-Becker P (2009b). Agrin, aquaporin-4, and astrocyte polarity as an important feature of the blood-brain barrier. Neuroscientist 15: 180–193.

Wu Z, Guo H, Chow N, Sallstrom J, Bell RD, Deane R *et al.* (2005). Role of the MEOX2 homeobox gene in neurovascular dysfunction in Alzheimer disease. Nat Med 11: 959–965.

Wyss-Coray T, Lin C, Yan F, Yu GQ, Rohde M, McConlogue L *et al.* (2001). TGF-beta1 promotes microglial amyloid-beta clearance and reduces plaque burden in transgenic mice. Nat Med 7: 612–618.

Xia Y, Choi H-K, Lee K (2012). Recent advances in hypoxia-inducible factor (HIF)-1 inhibitors. Eur J Med Chem 49C: 24–40.

Yamagata K, Tagami M, Takenaga F, Yamori Y, Itoh S (2004). Hypoxia-induced changes in tight junction permeability of brain capillary endothelial cells are associated with IL-1beta and nitric oxide. Neurobiol Dis 17: 491–499.

Yang S-P, Bae D-G, Kang HJ, Gwag BJ, Gho YS, Chae C-B (2004). Co-accumulation of vascular endothelial growth factor with beta-amyloid in the brain of patients with Alzheimer's disease. Neurobiol Aging 25: 283–290.

Yeh W-L, Lu D-Y, Lin C-J, Liou H-C, Fu W-M (2007). Inhibition of hypoxia-induced increase of blood-brain barrier permeability by YC-1 through the antagonism of HIF-1alpha accumulation and VEGF expression. Mol Pharmacol 72: 440–449.

Yemisci M, Gursoy-Ozdemir Y, Vural A, Can A, Topalkara K, Dalkara T (2009). Pericyte contraction induced by oxidative-nitrative stress impairs capillary reflow despite successful opening of an occluded cerebral artery. Nat Med 15: 1031–1037.

Zehendner CM, Librizzi L, de Curtis M, Kuhlmann CR, Luhmann HJ (2011). Caspase-3 contributes to ZO-1 and Cl-5 tight-junction disruption in rapid anoxic neurovascular unit damage. PLoS ONE 6: e16760.

Zeng XN, Xie LL, Liang R, Sun XL, Fan Y, Hu G (2012). AQP4 knockout aggravates ischemia/reperfusion injury in mice. CNS Neurosci Ther 18: 388–394.

Zhang W, Petrovic JM, Callaghan D, Jones A, Cui H, Howlett C *et al*. (2006). Evidence that hypoxia-inducible factor-1 (HIF-1) mediates transcriptional activation of interleukin-1beta (IL-1beta) in astrocyte cultures. J Neuroimmunol 174: 63–73.

Zhang X, Cheng M, Chintala SK (2004). Optic nerve ligation leads to astrocyte-associated matrix metalloproteinase-9 induction in the mouse retina. Neurosci Lett 356: 140–144.

Zhang X, Zhou K, Wang R, Cui J, Lipton SA, Liao F-F *et al*. (2007). Hypoxia-inducible factor 1alpha (HIF-1alpha)-mediated hypoxia increases BACE1 expression and beta-amyloid generation. J Biol Chem 282: 10873–10880.

Zhang ZG, Zhang L, Jiang Q, Zhang R, Davies K, Powers C *et al*. (2000). VEGF enhances angiogenesis and promotes blood-brain barrier leakage in the ischemic brain. J Clin Invest 106: 829–838.

Zhang ZG, Zhang L, Croll SD, Chopp M (2002). Angiopoietin-1 reduces cerebral blood vessel leakage and ischemic lesion volume after focal cerebral embolic ischemia in mice. Neuroscience 113: 683–687.

Zhao B-QQ, Wang S, Kim H-YY, Storrie H, Rosen BR, Mooney DJ *et al*. (2006). Role of matrix metalloproteinases in delayed cortical responses after stroke. Nat Med 12: 441–445.

Zhou L, Chan KH, Chu LW, Kwan JSC, Song YQ, Chen LH *et al*. (2012). Plasma amyloid-β oligomers level is a biomarker for Alzheimer's disease diagnosis. Biochem Biophys Res 423: 697–702.

Zlokovic BV (2005). Neurovascular mechanisms of Alzheimer's neurodegeneration. Trends Neurosci 28: 202–208.

Zlokovic BV (2011). Neurovascular pathways to neurodegeneration in Alzheimer's disease and other disorders. Nat Rev Neurosci 12: 723–738.

Del Zoppo GJ, Milner R, Mabuchi T, Hung S, Wang X, Berg GI *et al*. (2007). Microglial activation and matrix protease generation during focal cerebral ischemia. Stroke 38: 646–651.

Zozulya A, Weidenfeller C, Galla HJ (2008). Pericyte-endothelial cell interaction increases MMP-9 secretion at the blood-brain barrier in vitro. Brain Res 1189: 1–11.

8 ABBREVIATIONS

2ME2	2-Methoxyestradiol
α-SMA	α-smooth muscle actin
AC	Astrocyte
acetyl-CoA	Acetyl coenzyme A
AF-6	Afadin
AJ	Adherens junction
ANG	Angiopoietin
ARNT	Aryl hydrocarbon receptor nuclear translocator
ATP	Adenosine triphosphate
AX	Near anoxia
BBB	Blood-brain barrier
bFGF	Basic fibroblast growth factor
BHS	Bluthirnschranke
BNIP3	BCL2/adenovirus E1B 19 kDa protein-interacting protein 3
BrdU	Bromodeoxyuridine
CNS	Central nervous system
$CoCl_2$	Cobalt chloride
CR	Creatine
DFO	Deferoxamine mesylate salt
DMOG	Dimethyloxalylglycine
DNA	Deoxyribonucleic acid
EC	Endothelial cell
ELISA	Enzyme-linked immunosorbent assay
$FADH_2$	Flavin adenine dinucleotide
GFAP	Glial fibrillary acidic protein
GLUT	Glucose transporter
GSH	Glutathione
GSSG	Glutathione disulfide
HIF	Hypoxia-inducible factor
HX	Hypoxia
LC-MS	Liquid chromatography-mass spectrometry
LC3	Microtubule-associated protein light chain 3
MMP	Matrix metalloproteinase
MS	Mass spectrometry
MTT	3-(4,5-dimethylthiazol-2-yl)-2,5-diphenyltetrazolium bromide
NADH	Nicotinamide adenine dinucleotide
NX	Normoxia
OGD	Oxygen-glucose deprivation
PC	Pericyte
PCA	Principal component analysis
pCR	Phosphocreatine
PCR	Polymerase chain reaction
PDGF	Platelet-derived growth factor
PHD	Prolyl hydroxylase
RBE4	Rat brain endothelial 4
RBMEC	Rat brain microvascular endothelial cell
ROS	Reactive oxygen species
TCA	Tricarboxylic acid
TEER	Transendothelial electrical resistance
TJ	Tight junction
UDP-glucose	Uridindiphosphate-glucose
VEGF	Vascular endothelial growth factor
YC-1	3-(5'-hydroxymethyl-2'-furyl)-1-benzylindazole
ZO-1	Zonula occludens 1

9 ACKNOWLEDGEMENTS

The last four years were an exciting and enriching experience, but surely also demanding and as such a constant learning process on professional but also on a personal level.
Without help it would not have been possible to realize this thesis and therefore I thank everyone who contributed in one or the other way to this work:

I would like to thank Prof. Max Gassmann for the opportunity to do my PhD in his group and for his support.

A special thank goes to Dr. `Lara Ogunshola for the supervision of this thesis and her constant input, support and motivation within the last four years, but also her open ear for new ideas as well as problems.

In addition I thank my committee members Prof. Pierre-Olivier Couraud and Prof. François Verrey for their constant and valuable input.

Thanks to Dr. Ignacio Romero for agreeing to function as external reviewer for this thesis.

I further want to acknowledge Dr. Endre Laczko and David Fischer from the Functional Genomics Center, University of Zurich, who performed the mass spectrometry measurements and the data analysis.

A very big thank goes to all the girls of the Ogunshola group, particularly Shalu for her professional help in the lab, who always gave her helping when it was needed and who has become a good friend in the last years.
Sheng-Fu and Daniela G. supported me a lot during the last weeks to finish the labwork - thanks for all your efforts.
Tanja and Daniela N., who accompanied me almost during my entire PhD, without you it would not have been the same, thanks for the good and not so good times we shared.
Furthermore I thank all the other members of the Gassmann and Lutz group.

Ein ganz spezieller Dank geht allerdings an meine Familie, die mir immer bedingungslos Rückhalt gegeben hat und mir eine wichtige Stütze ist.
David danke ich im ganz Besonderen, zum einen für die große Mühe, die er in unser Metabolomics Projekt gesteckt hat und die zahlreichen Wochenenden die er dafür geopfert hat, aber mehr noch, dass er immer für mich und unsere kleine Familie da ist.

10 CURRICULUM VITAE

PERSONAL DETAILS

Sabrina Engelhardt, Diplom Biologin
Winzerstrasse 7
CH-8049 Zürich

Telephone: 043-5347680, E-mail: Sabrina.Engelhardt@gmx.de
Date of birth: 11th of January 1984, Mühlacker, Germany

EDUCATION

July 2010 to July 2014

Member of the Integrative Molecular Medicine PhD program, Zurich

Doctoral studies in the group of Dr. O. Ogunshola, Institute of Veterinary Physiology, University of Zurich, Switzerland

Title: Facing hypoxia and ischemia - cell-specific signaling and metabolism at the blood-brain barrier.

May 2009 to April 2010

Member of the Microbiology and Immunology PhD program, Zurich

Doctoral studies in the group of PD Dr. H. Hilbi at the Institute of Zoology, University of Zurich, Switzerland

Title: Modulation of phosphoinositide (PI) metabolism by *L. pneumophila:* characterization of the PI phosphatase LppA

October 2008

Diploma in Biology, University of Konstanz

Diploma thesis at the Chair of Immunology, University of Constance, Germany.

Title: Investigating the cross-presentation of cellular and particulate antigen *in vitro* and *in vivo*.

November 2005 to December 2007

Advanced studies at the University of Konstanz

Study focus: Cellular Biochemistry, Plant Physiology, Alternative *in vitro* Methods, Microbiology.

October 2003 to October 2005

Basic studies of Biology, University of Konstanz

September 1994 to May 2003

Progymnasium Maulbronn, Germany and High school, Bretten, Germany

September 1990 to July 1994

Primary school, Sternenfels, Germany

INTERNSHIPS & JOB EXPERIENCE

March 2008 to March 2009

Temporary job at GATC Biotech AG, Constance, Germany in the area of custom sequencing

November 2008 to December 2008

Student assistant at the Chair of Immunology, University of Constance, Germany

October 2007

Student assistant at the Biotechnology Institute Thurgau, Kreuzlingen, Switzerland

August to September 2007

Internship at the Biotechnology Institute Thurgau, Kreuzlingen, Switzerland

February to March 2007

Internship at the Paul-Ehrlich-Institute, Langen, Germany

August to September 2006

Volunteer at a biological station in Bilsa, Ecuador

July 2006

Student assistant at the Chair of Microbiology, University of Constance, Germany

GRANTS AND AWARDS

May 2014

Grant for PhD salary, the University of Zurich. Forschungskredit, 6 months.

October 2013

Travel grant from the Swiss Society for Neuroscience to attend the "Signal transduction in the blood-brain barriers conference 2013", Sümeg, Hungary.

May 2013

Best poster award at the students retreat of the Integrative Molecular Medicine PhD program, Mariastein, Switzerland

June 2012

Travel grant from the Swiss Physiological Society to attend the Gordon Conference "Barriers of the CNS - bridging barriers to treat CNS disease", New London, USA.

August 2011

Best poster award at the 7th Symposium of the ZHIP, Zurich, Switzerland

ARTICLES

Cell-specific blood-brain barrier regulation in health and disease: a focus on hypoxia. Review article.
Engelhardt S., Patkar S., and Ogunshola O.O.. *Br. J. Pharmacol. 2014; 171(5):1210-1230.*

Hypoxia selectively disrupts brain microvascular endothelial tight junction complexes through a hypoxia-inducible factor-1 (HIF-1) dependent mechanism.
Engelhardt S., Al Ahmad AJ., Gassmann M., Ogunshola O.O.. *J. Cell. Physiol. 2013; 229(8):1096-1105.*

CD8- dendritic cells and macrophages cross-present poly(D,L-lactate-co-glycolate)acid microsphere-encapsulated antigen in vivo.
Schliehe C., Redaelli C., **Engelhardt S.**, Fehlings M., Mueller M., van Rooijen N., Thiry M., Hildner K., Weller H., Groettrup M.. *J. Immunol. 2011;187(5):2112-21.*